Bulletin
of
The Geological Society of America

VOLUME 69 November 1958 NUMBER 11

CONTENTS

Pages

Metadolerite dike swarm in Bakersville-Roan Mountain area, North Carolina. By Ronald E. Wilcox and Arie Poldervaart 1323–1368

Progressive metamorphism and granitization of the major paragneiss, northwest Adirondack Mountains, New York. Part I. Total rock. By A. E. J. Engel and Celeste G. Engel 1369–1414

Mineralization in the intrusive rocks in Little Cottonwood Canyon, Utah. By Byron J. Sharp 1415–1430

Fault patterns in southeastern Alaska. By William S. Twenhofel and C. L. Sainsbury 1431–1442

Plastic deformation of quartz in nature. By S. W. Bailey, R. A. Bell, and C. J. Peng 1443–1466

Short Notes

Three-dimensional Liesegang rings by diffusion in a colloidal matrix, and their significance for the interpretation of geological phenomena. By James D. Carl and G. C. Amstutz 1467–1468

Ages of minerals from the Baltimore gneiss near Baltimore, Maryland. By G. R. Tilton, G. W. Wetherill, G. L. Davis, and C. A. Hopson 1469–1474

Subscription $15.00 per year.

Printing Office: Mt. Royal & Guilford Aves., Baltimore 2, Md.

Communications for publications should be addressed to The Geological Society of America, Dr. H. R. Aldrich, Secretary, 419 West 117 Street, New York, N. Y.

Please give notice of change of address 4 weeks in advance. Claims for nonreceipt of the Bulletin of a given month must be sent to the Secretary of the Society before the end of the second succeeding month.

Entered as second-class matter at the Post Office at Baltimore, Md., under the Act of Congress of July, 16, 1894.
Accepted for mailing at special rate of postage provided for in Section 1103 Act of October 3, 1917, authorized on July 8, 1918.

PAPERS IN PRESS FOR FORTHCOMING ISSUES

Older Precambrian Rocks of the Diamond Butte Quadrangle, Gila County, Arizona. By Gordon Gastil

Analytical and Experimental Study of Simple Geologic Structures. By A. R. Sanford

Deccan Basalts of the Bombay Area, India. By Ratan N. Sukheswala and Arie Poldervaart

Athabasca Formation of Western Canada. By W. C. Gussow

Geometry of Superposed Folding. By L. G. Weiss

Hydrothermal Alteration in the Front Range, Colorado. By Félix Gonzalez Bonorino

Strawn-Canyon (Pennsylvanian) Boundary in North-Central Texas. By John W. Shelton

BULLETIN OF THE GEOLOGICAL SOCIETY OF AMERICA
VOL. 69, PP. 1323-1368, 17 FIGS., 3 PLS. NOVEMBER 1958

METADOLERITE DIKE SWARM IN BAKERSVILLE-ROAN MOUNTAIN AREA, NORTH CAROLINA

BY RONALD E. WILCOX AND ARIE POLDERVAART

ABSTRACT

A Precambrian metadolerite dike swarm, emplaced in Cranberry gneiss, extends from Roan Mountain toward Bakersville, North Carolina, but loses its identity in the hornblendic Roan gneiss and schist. Ortho-amphibolites exposed near Toecane in the boundary zone between the Cranberry and Roan formations are equivalents of the metadolerites exposed in Cranberry gneiss. Age relationships of the region indicate that the country rocks have been affected by at least two, and probably three, plutonic cycles.

Magnetic, petrographic, mineralogical, chemical, and spectrographic data of the dike rocks are given. The metamorphic origin of the rocks is established by textural and mineralogical criteria. Chemically the dike rocks are typical olivine dolerites belonging to the middle- and late-stage basalts of Wager. The ortho- and para-amphibolites cannot be distinguished by their bulk chemical compositions. Comparisons of contents of copper, gallium, barium, nickel, cobalt, and chromium lead to the same conclusion, but it is believed possible that ortho- and para-amphibolites can be differentiated by their strontium contents.

Metamorphism was of amphibolite facies; temperatures were probably about 450°–500° C. Differences between subophitic plagioclase-pyroxene and granoblastic plagioclase-hornblende dike rocks are attributed to differences in water content during recrystallization at essentially the same temperatures and total pressures. The abnormal granulitic trend of metamorphic recrystallization of basaltic rocks is due to water-deficient conditions. This type of recrystallization can occur both in the granulite and the amphibolite facies of metamorphism. Four stages of metamorphism, each of different water content, are detailed. Amphibolite problems are reviewed briefly.

CONTENTS

TEXT

	Page
Introduction	1324
General statement	1324
Geologic setting	1324
Acknowledgments	1327
Field characters	1327
Exposures	1327
Thickness and trend	1329
Country rocks and xenoliths	1330
Textures	1330
Multiple dikes	1331
Ortho-amphibolites	1331
Relationships to pegmatites	1332
Age relationships	1333
Magnetic properties	1333
General statement	1333
Remanent magnetic polarization	1334
Magnetic susceptibility	1335
Petrography	1335
Introduction	1335
Description of thin sections	1336
Mineralogy	1341
General statement	1341
Methods of study	1341
Plagioclase	1341
Pyroxenes	1344
Hornblende	1346
Biotite	1346
Garnet	1346
Other minerals	1347
Chemical data	1348
Major elements	1348
Selected minor elements	1352
Petrology	1354
Metamorphic clouding	1354
Metamorphic facies	1357
Role of water	1358
Stages of recrystallization	1361
Amphibolite problems	1362
Summary and conclusions	1363
References cited	1365

ILLUSTRATIONS

Figure	Page
1. Index map of the Bakersville-Roan Mountain area and adjacent regional geology	1325
2. Geologic sketch map of Bakersville-Roan Mountain area	1326
3. Stereographic projections of dike contacts	1328
4. Stereographic projection of thermoremanent magnetic vectors	1334

Figure — Page
5. Susceptibility anisotropy ... 1336
6. Optical data for plagioclases ... 1343
7. Optical data for hornblendes ... 1344
8. Refractive indices of hornblende and coexisting biotite ... 1346
9. Refractive index of garnet with composition of coexisting plagioclase ... 1347
10. Silica-alkalies diagram for Bakersville-Roan Mountain rocks ... 1350
11. Differentiation diagram after Wager ... 1352
12. Differentiation diagram after Thornton and Tuttle ... 1353
13. Differentiation diagram after Simpson ... 1354
14. Superimposed ternary diagrams of Fe_{total}-Mg-(Na + K) and Na-Ca-K (atomic weight per cent) ... 1355
15. Spectrographic data for selected minor elements ... 1357
16. ACF diagram showing metadolerites and amphibolites in relation to selected minerals of the amphibolite facies ... 1360
17. Stability field of pargasite ... 1360

Plate — Following page
1. Dikes crosscutting gneiss and brecciated gneiss ... 1330
2. Garnet "trails", banded amphibolite, and metadolerite textures ... 1330
3. Metadolerite textures ... 1330

TABLES

Table — Page
1. Remanent magnetization ... 1334
2. Modes (weight per cent) ... 1337
3. Optical data ... 1342
4. Hornblende analyses ... 1345
5. Chemical analyses ... 1349
6. Averages: basalts and amphibolites ... 1351
7. Standards for spectrographic analyses ... 1355
8. Spectrographic data for selected minor elements ... 1356
9. Spectrographic data for analyzed rocks ... 1357
10. Strontium analyses ... 1358
11. Analyses of clouded plagioclase ... 1358
12. Plagioclase analyses ... 1359

Introduction

General Statement

Basaltic rocks are especially suited to studies of fundamental processes of regional metamorphism because of their relatively simple and well-known chemical and mineralogical compositions and their characteristic textures (Poldervaart, 1953, p. 259). The initial water content of intrusive basaltic rocks is low, hence these rocks are ideal for a study of the role of water in metamorphism. Moreover, basaltic rocks respond differently to metamorphism than sedimentary rocks; in the metamorphism of basaltic rocks, high-temperature mineral assemblages are recrystallized to lower-temperature metamorphic mineral assemblages, the opposite of what happens when a sedimentary rock is metamorphosed. Examples have also been found (Poldervaart, 1953, p. 260–261) of contact and regional metamorphism of basaltic rocks in which the grain size has decreased instead of increasing, as is more common upon metamorphic recrystallization.

Difficulties have been experienced in distinguishing metamorphosed from unmetamorphosed basaltic rocks. For example, the Baltimore gabbro is metamorphosed according to Cohen (1937), unmetamorphosed according to Herz (1951). There are also problems in differentiating between ortho- and para-amphibolites (*e.g.*, Engel, 1956, p. 84–85), the metamorphic equivalents of basaltic rocks and sediments respectively. H. S. Yoder, Jr. (personal communication, 1957) finds "... little difference between the amphibolite and the granite problem. Under equilibrium conditions ortho- and para-amphibolites would be indistinguishable if held at the same P and T."

These problems are not only of petrologic interest; their eventual solution will find many wider geologic applications, extending even to the search for oil, in which the distinction between metamorphosed and unmetamorphosed rocks is in many cases vital.

This study aims at clearer understanding of the metamorphism of basaltic rocks. It traces in detail the mineralogical and petrological changes induced by regional metamorphism in the Bakersville-Roan Mountain dolerite dikes. The writers believe that metamorphosed basaltic rocks can be identified as such, not only by their mineral assemblages and the compositions of their mineral phases, but also by the textural relationships of the constituent minerals. Accordingly both the quantitative and descriptive aspects of the rocks are emphasized.

Geologic Setting

Metabasaltic dikes in central Mitchell County extend from Roan Mountain on the North Carolina-Tennessee state line about 20 miles southwestward. The dike swarm is not more than 5 miles wide. The northernmost dikes are on the north side of Roan Mountain in Carter County, Tennessee; the southernmost dikes crop out in Yancy County, North Carolina (Figs. 1 and 2).

The area is 10 miles northwest of Spruce Pine, North Carolina, famous as a pegmatite and alaskite mining district. Physiographically, it is in the western portion of the Blue Ridge, rarely can be traced more than a few tens of feet along strike.

The dike swarm is emplaced on the northwest limb of a large southwestward-plunging syn-

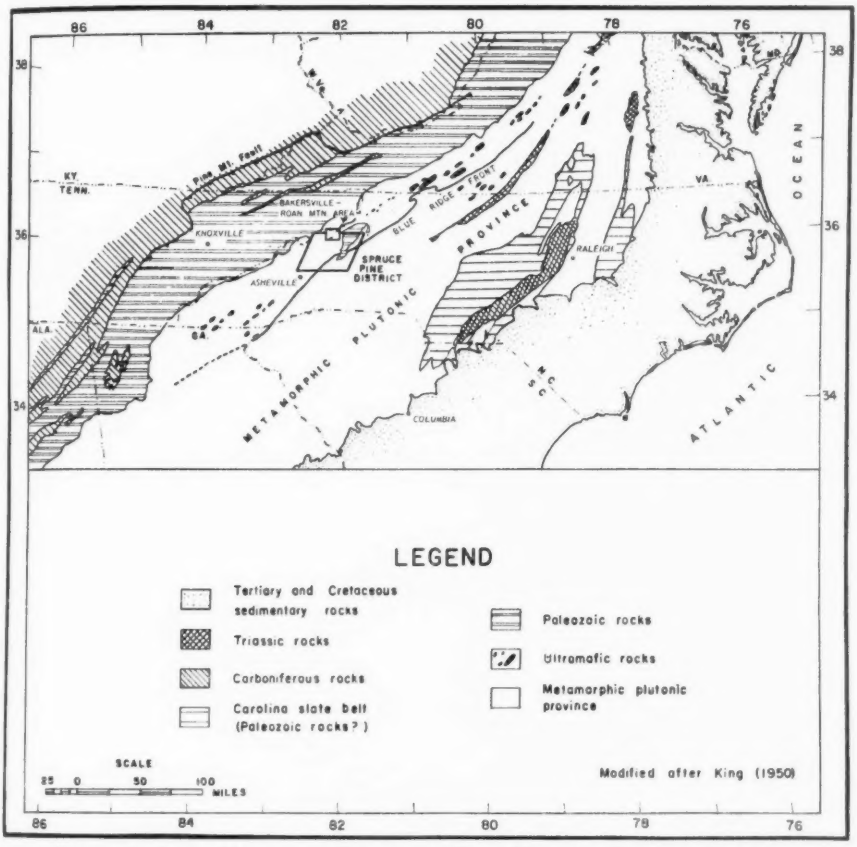

FIGURE 1.—INDEX MAP OF THE BAKERSVILLE-ROAN MOUNTAIN AREA AND ADJACENT REGIONAL GEOLOGY

in which elevations range from 2500 feet to more than 6000 feet at Roan Mountain. Vegetation is dense, and soils are deep, except on a few ridges and on the upper slopes of Roan Mountain, where there are large grassy "balds". Outcrops are rare except along road cuts, especially along the new highway on Roan Mountain, Tennessee, Route 143, and Route 26 west of Bakersville, North Carolina. Other outcrops are found locally along county roads, the Toe River, and Cane Creek. The other outcrops in the area are weathered. Lack of outcrops prevents detailed mapping of the area. Dikes

clinorium (Fig. 2), mapped by Brobst and Kulp (in press). Keith (1903; 1905; 1907), the first to recognize these rocks, named them the Bakersville gabbro. The dike swarm lies across the boundary of two 30-minute quadrangles mapped by him: the Roan Mountain and Mount Mitchell. Keith shows Bakersville gabbro on the Mount Mitchell quadrangle, but this rock type has not been mapped on the Roan Mountain quadrangle, although it is described in the Folio text.

The lowest-exposed unit of the synclinorium is the Cranberry-Henderson gneiss. Keith has

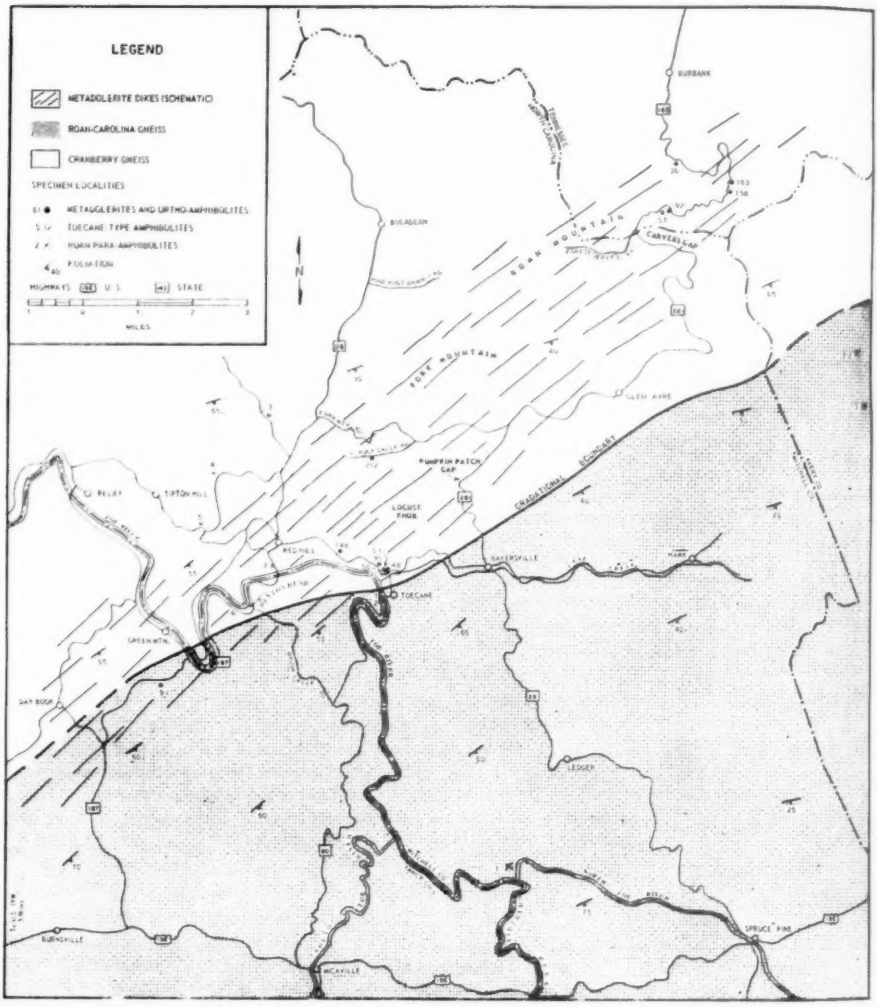

FIGURE 2.—GEOLOGIC SKETCH MAP OF BAKERSVILLE-ROAN MOUNTAIN AREA

differentiated Cranberry gneiss on the northwest limb from Henderson gneiss on the southeast limb. Eckelmann and Kulp (1956, p. 302–304) have shown that the Cranberry gneiss is continuous around the nose of the structure with the Henderson gneiss. The rocks are predominantly quartzofeldspathic gneiss with minor hornblende and pyroxene gneiss. Foliation is well developed and commonly shows complex folding, with folds ranging from microscopic to several tens of feet from trough to crest.

Roan hornblende gneiss overlies the Cranberry-Henderson gneiss and is in turn overlain by the Carolina mica gneiss and schist. The Roan-Carolina gneiss is also intricately folded. The boundary zone between the two major units is about 1 mile wide and is marked by interlayering of Cranberry-type quartzofeldspathic gneiss, Roan-type hornblende gneiss, and Carolina-type mica gneiss. Individual layers of each rock type range up to a few tens of feet in thickness and in all places are parallel to foliation. Interlayering is also common through-

out the Roan-Carolina gneiss, with hornblendic and micaceous layers merging laterally and vertically. Mica gneiss and schist become the dominant lithology upward and form the core of the synclinorium. Brobst and Kulp (in press) have interpreted the hornblende and mica gneisses as, respectively, metamorphosed ferruginous and calcareous argillites, and calcarenites; and metamorphosed argillites and arenites. Eckelmann and Kulp (1956, p. 314) conclude that the Cranberry-Henderson gneiss is also of sedimentary origin.

Large pegmatites which are mined are found only within the Roan-Carolina schist and gneiss in the central portion of the synclinorium. Small pegmatitic veins and lenses are common throughout the area.

Small ultramafic bodies in the area are probably related to similar rocks which are found in a narrow belt extending from Alabama northeastward to Maryland, New Jersey, Vermont, and Quebec (Benson, 1926, p. 56). Near Day Book in Yancy County, an ultramafic body is cut by a pegmatite dike. One of the resulting alteration products, vermiculite, is mined on a small scale (Kulp and Brobst, 1954).

The Beech granite in the northwest portion of the area has been distinguished by Keith (1907) from the Cranberry and Henderson gneisses. Small homogeneous areas of granite in the Cranberry-Henderson gneiss in the northeast part of the area are probably intrusive (Eckelmann and Kulp, 1956, p. 314–315).

King and his co-workers (1952; 1955, p. 727–729) have studied the Great Smoky Mountain region, about 50 miles southwest of the Spruce Pine district. They have shown that the Bakersville-Roan Mountain area and adjoining Spruce Pine district are portions of the Blue Ridge which have been thrust westward onto early Paleozoic rocks. Subsequently the thrust plates were folded and cut by cross faults. From structural evidence King concludes that the older rocks of the region are polymetamorphic.

Acknowledgments

Grateful acknowledgment is made to the following for aid in this study: Drs. J. Laurence Kulp, Donald A. Brobst, and F. Donald Eckelmann introduced the writers to the Spruce Pine district in 1953 and made their maps, samples, thin sections, and unpublished data available. Prof. Walter H. Bucher accompanied the writers in the field for 3 days in 1953 and contributed much in discussions. Drs. S. K. Runcorn and J. C. Belshé determined thermoremanent magnetization directions in 10 samples. Dr. John W. Graham aided Wilcox in magnetic susceptibility measurements. Dr. Karl K. Turekian and Miss Irene Scribny did the spectrographic work. Mr. Leon A. Long made the biotite K/A age determinations. Dr. Hugo B. Wiik, Mr. R. H. Stokes, and Miss L. M. Kehl did the chemical analyses. Dr. J. R. Smith made available his data and technique for optical study of low-temperature plagioclase. Drs. Paul F. Kerr and Ralph J. Holmes gave much helpful advice in the X-ray studies. The manuscript was critically read by Drs. C. H. Behre, A. F. Buddington, P. F. Kerr, and H. S. Yoder, who made many helpful suggestions. Dr. C. Milton and Mr. J. A. Denson of the U. S. Geological Survey took several of the photomicrographs.

The work was supported by a generous grant from the Penrose Bequest of The Geological Society of America and the Kemp and Higgins funds of Columbia University. This support is here also gratefully acknowledged. Wilcox also acknowledges the tenure of a Boese Fellowship during 1954 and a National Science Foundation Fellowship during 1955.

Field Characters

Exposures

The dikes are best exposed for about 3 miles along Tennessee Route 143 on the north side of Roan Mountain below Carvers Gap. The road crosses minor spurs and gulleys along the descent into Tennessee. On spurs, outcrops are fresh, but across gulleys the roadbed does not reach bedrock in most places. Continuous exposures are not more than 300 feet long and become shorter as the road descends. These are the northernmost dike exposures in the area. Similar dikes crop out along the Forest Service Road above Carvers Gap to the top of Roan Mountain (Fig. 2).

On the south side of Roan Mountain along North Carolina Route 261, bedrock exposures are few and poor because of deep soils. Over 180 dikes are well exposed on the north side, but less than 10 dikes are exposed on the south side along the road into Bakersville. In the vicinity of Pumpkin Patch Gap, on Route 261, roadcuts have been graded to smooth surfaces which show outlines of altered dikes in weathered gneiss.

A second series of fresh exposures extends about 10 miles along North Carolina Route 26

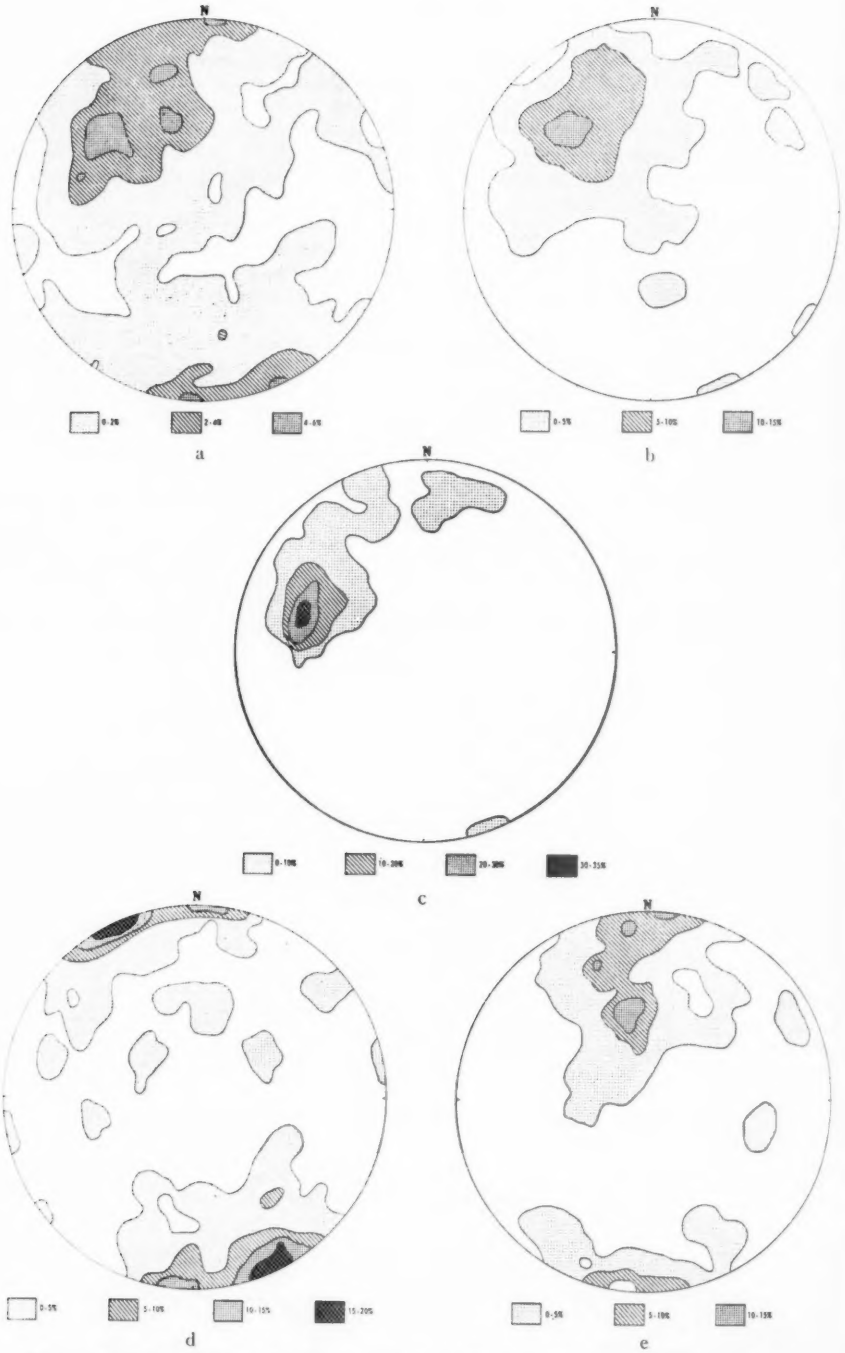

FIGURE 3.—STEREOGRAPHIC PROJECTIONS OF DIKE CONTACTS (LOWER HEMISPHERE EQUAL-AREA PROJECTIONS)

(Caption continued at foot of page 1329)

west of Bakersville. Here, too, outcrops are intermittent and not more than 200 feet long. Relationships between dikes and country rocks are not as well displayed as on Roan Mountain.

The highway follows the valley of Cane Creek from Bakersville to its confluence with the Toe River, 3 miles distant. Along the lower quarter mile of Cane Creek, dikes and country rocks are well exposed on stream-polished surfaces which discourage sampling. At Red Hill, 6 miles west of Bakersville, Route 26 is intersected by North Carolina Route 197, and a quarter mile farther it intersects Tipton Hill Road. Along Route 197 outcrops are intermittently good from Red Hill south to the Toe River and along this route as it follows the river to Green Mountain. The area between Red Hill and Green Mountain is within the boundary zone between the Cranberry-Henderson gneiss to the northwest and the Roan-Carolina gneiss to the southeast. Tipton Hill Road has a few cuts containing dikes but soon passes out of the dike area. Four miles north of Red Hill, Route 26 is intersected by Fork Mountain Road, which connects with Route 261, just north of Pumpkin Patch Gap, 5 miles to the east. Midway between the two highways, Little Rock Creek Road branches off to the southwest from Fork Mountain Road. These two side roads offer few exposures but cross the strike of the dike swarm in the Cranberry-Henderson gneiss and provide the deepest outcrops in the area. The extreme southwestern dike exposure in the area is along U. S. Route 19W, 2 miles from the junction with U. S. Route 19E west of Burnsville in Yancy County, North Carolina. Occasional dikes crop out in numerous other side roads and in a few ridges and stream valleys. Metadolerite float along the upper reaches of Pineroot Branch 1 mile south of Buladean, North Carolina, below the west side of Roan Mountain, suggests that dikes are present, but no outcrops have been found.

Sufficient outcrops are present, even though badly weathered, to establish that dikes are numerous throughout the area. This indicates a dike swarm rather than a single intrusive plug or stock with radiating dikes. Locally in the region from Locust Knob to Fork Mountain and Roan Mountain, metabasaltic rocks predominate, as indicated by Brobst and Kulp (in press).

Thickness and Trend

Dikes range in thickness from less than 1 inch up to 60 feet. Greater apparent thicknesses in a few roadcuts are multiple dikes. Most contacts between dikes and country rocks are sharp and undeformed; a few contacts have been affected by later shearing. In most cases on Roan Mountain the two contacts remain approximately parallel, with only minor curves or bulges. Four miles west of Bakersville on Route 26, a landslide scar shows several dikes 5–20 feet thick which have irregular courses through the country rock.

As the dikes cannot be mapped areally, all available dike contacts have been measured in an attempt to determine the trend of the dike swarm. About 450 measurements are plotted on lower-hemisphere, equal-area stereographic projections. Figure 3*a* shows poles of all contacts for the Bakersville-Roan Mountain area. Strikes are concentrated between N.45°E. and N.100°E., whereas dips range from 75°N. through vertical to 30°S. The maxima represent a relatively small percentage of the poles. Contacts have therefore been divided into four geographical groups. Figure 3*b* shows 160 poles of dike contacts west of Bakersville, with a maximum at N.40°E.-50°S. and a broad area of scatter. Projected southward, this strike for the dike swarm crosses the boundary zone between the Cranberry-Henderson and Roan-Carolina gneiss which trends N.45°-50°E Figures 3*c*–3*e* are dike contacts from Roan Mountain at different elevations. Figure 3*c* shows 56 contacts above Carvers Gap along the Forest Service Road. Figures 3*d* and 3*e* have 116 contacts each, along, respectively, the upper and lower portions of Route 143. The division is arbitrary. A trend is evident, with a northeast strike at the top of Roan Mountain (similar to the strike west of Bakersville), changing to east-west lower down, and northeastward into Tennessee. Dip maxima also change, from about 65°S. at the top of Roan Mountain, to vertical on the upper slope, and 90° to 40°S. on the lower slopes. The dikes approach conformity to the over-all structure of the synclinorium, but in detail each dike is crosscutting, although the angle between dike and foliation in country rocks is in many cases low enough to admit the term "sheet". No regular relationship exists between contacts and foliation. Some dikes sharply crosscut uniformly foliated gneiss (Pl. 1, figs. 1, 2), others cut intensely crenulated foliation and gneiss

Figure 3*a* shows poles of 448 metadolerite dike contacts in the Bakersville-Roan Mountain area; 3*b*—poles of 160 metadolerite dike contacts west of Bakersville; 3*c*—poles of 56 dike contacts southwest of Carvers Gap on Roan Mountain: 3*d*—poles of 116 metadolerite dike contacts along the upper portion of Tennessee Route 143 on Roan Mountain; 3*e*—poles of 116 metadolerite dike contacts along the lower portion of Tennessee Route 143 on Roan Mountain.

folded into sharp recumbent folds or gentle open folds. In a few cases foliation has been dragged out parallel to the dike contacts, probably due to the dike filling a fracture developed when foliation was deformed, or perhaps resulting from later (Appalachian?) deformation.

Country Rocks and Xenoliths

Apparently the country rocks were relatively rigid and brittle when the dikes were emplaced. Dikelets a few inches thick branch off from larger dikes and sharply crosscut foliation (Pl. 1, fig. 3). The dikelets which reach up to 10 feet in length are not deformed, and some cut across intricately folded gneiss. Thin screens of country rocks are enclosed in or protrude into dikes and are also undeformed. The screens range in thickness from less than an inch to a few feet, and in nearly every case foliation in the screen is distinct. Where the screen is still attached at one end, the foliation may be projected to connect with that in the wall rocks. Offset foliation on either side of many dikes indicates that the wall rocks dilated when the dikes were emplaced.

Further evidence that the country rocks were brittle when the dikes intruded is found along Route 143, about 0.9 mile below Carvers Gap. Here a breccia zone 2–6 feet wide in Cranberry-Henderson gneiss is sharply crosscut by a 2-foot dike (Pl. 1, fig. 4). Within the breccia zone are unoriented segments of well-foliated feldspathic gneiss. There is clear evidence of extensive shearing and granulation, and the breccia matrix is dark and has recrystallized to a hard, garnetiferous rock.

In the bed of Cane Creek about 500 yards northeast from the Toe River, numerous xenoliths are enclosed in several dikes. A few xenoliths show evidence of recrystallization and rheomorphism. Quartzofeldspathic xenoliths have lost most of the foliation characteristic of the country rocks, but more mafic inclusions (hornblende gneiss) maintain a distinct foliation. One dike is cut by a quartzofeldspathic vein which appears to represent mobilized wall rock.

At several outcrops in the area mafic lenses of Cranberry gneiss have recrystalliized so that they resemble the metadolerites. A coarse-grained rock with dominant plagioclase and pyroxene crops out along Route 143, 2.8 miles from Carvers Gap. This rock was at first regarded as a metadolerite. It contains irregular, vague bands but is not foliated. Fine-grained dikes cut across the rock which is now known to be a mafic country rock.

Textures

The dike rocks show various textures and grain sizes. Typical or modified subophitic textures are common, the grain size ranging from gabbroic to near-basaltic. The next most common texture is granoblastic and is associated with a greenish-black color, whereas the subophitic rocks are purplish black. A well-defined dike rarely shows foliation or schistose texture in hand specimens; some amphibolites, however, are foliated and may represent metamorphosed dikes. The areal distribution of the various textural types does not form any obvious pattern; this is true also of grain sizes. Side by side or actually in contact, dike rocks may be coarse- or fine-grained. Similarly, a subophitic metadolerite may be next to a granoblastic rock. The areal change of textural type is somewhat more gradual than changes in grain size. The dikes in general have finer-grained margins.

Few of the dikes are porphyroblastic. On Route 26, above the mouth of Cane Creek, a rock with plagioclase up to 1 inch across is exposed. The groundmass is homogeneous and granoblastic. This rock is in contact with several fine-grained dikes less than 1 foot thick and a large dike 30 feet thick, which is chilled against the porphyroblastic rock. Two hundred feet northwest of this outcrop a fine-grained dike contains a few sharply defined

---

PLATE 1.—DIKES CROSSCUTTING GNEISS AND BRECCIATED GNEISS

FIGURE 1.—Metadolerite dike (right) sharply crosscutting well-foliated Cranberry gneiss (left) 0.9 mile from Carvers Gap on Route 143.

FIGURE 2.—Polished slab from locality shown in Figure 1. Note garnet "trails" and spots in dike and thin slivers of dike and gneiss along contact.

FIGURE 3.—Metadolerite dikelets in well-foliated Cranberry gneiss. Note lack of deformation in dikelets and small offsets in foliation; 0.9 mile below Carvers Gap on Route 143.

FIGURE 4.—Breccia zone in Cranberry gneiss (0.9 mile from Carvers Gap on Route 143).

FIGURE 2

FIGURE 4

FIGURE 1

FIGURE 3

DIKES CROSSCUTTING GNEISS AND BRECCIATED GNEISS

FIGURE 1

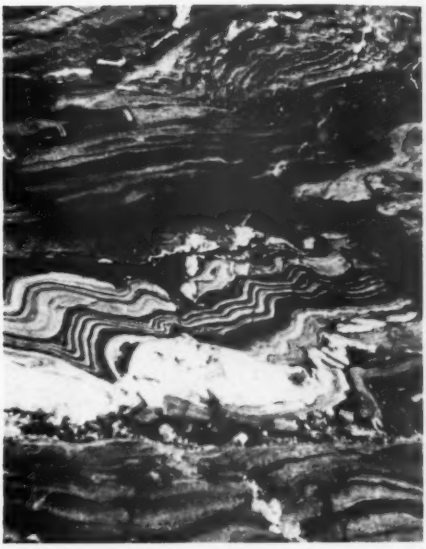

FIGURE 2

FIGURE 3

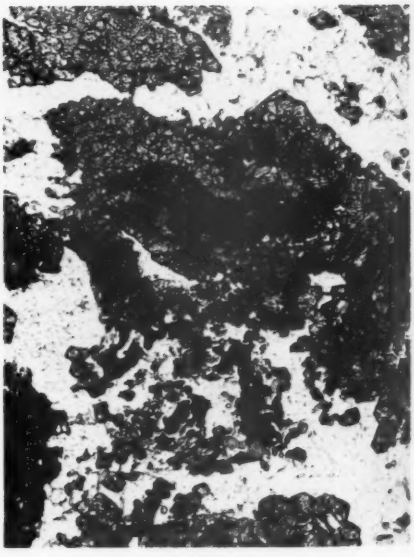

FIGURE 4

GARNET "TRAILS", BANDED AMPHIBOLITE, AND METADOLERITE TEXTURES

FIGURE 1

FIGURE 2

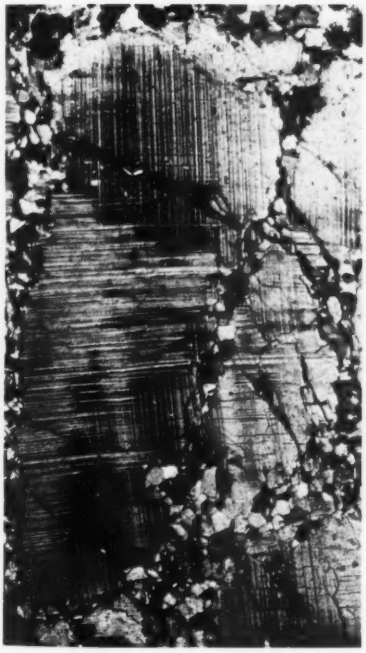

FIGURE 3

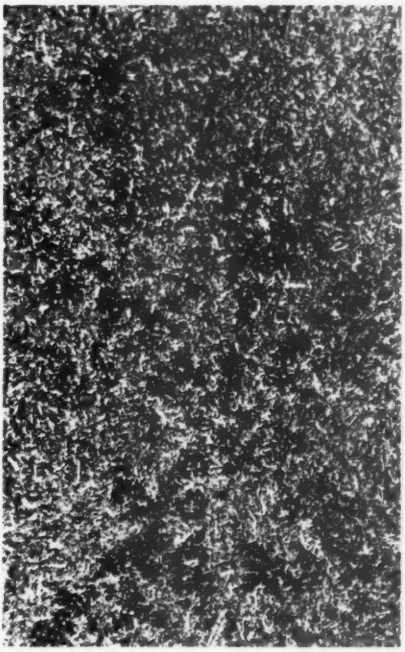

FIGURE 4

METADOLERITE TEXTURES

plagioclase porphyroblasts up to 2 by 4 inches in size. These are not found elsewhere.

One dike along Route 143, about 2.5 miles below Carvers Gap, contains ovoidal crystal segregates up to 5 mm across which may well represent recrystallized amygdules. Both the breccia zone and the presumed amygdules are taken to indicate a shallow depth for the emplacement of the dikes at Carvers Gap.

Most of the metadolerite dikes contain garnet. The mineral may be uniformly clustered, but some dikes show a striking distribution of garnet as clusters up to an inch across or "trails" of small clusters (Pl. 1, fig. 2; Pl. 2, fig. 1). This gives the rock surface a spotted or streaked appearance. Garnet trails may be several inches long and may be subparallel to dike walls or in an irregular criss-cross pattern. Patterns of garnet trails suggest localization of garnet along fractures, healed during metamorphism. The development of a pre-metamorphic fracture system in the dikes at Carvers Gap also indicates shallow emplacement of these intrusions.

Multiple Dikes

Multiple dikes are found mainly where the total thickness of dike rocks is large (200 feet), as along Route 143, 2 miles below Carvers Gap. Along Route 26, 4 miles west of Bakersville, a multiple dike 40 feet thick cuts quartzofeldspathic gneiss. The contact with country rock is fine-grained; it is badly weathered and poorly exposed. The first solid rock in the outcrop is coarse-grained, subophitic metagabbro. About 2 feet from this, a dark, fine-grained rock cuts sharply across the metagabbro. This second dike becomes coarser-grained toward the center, where the rock resembles the metagabbro of the first dike. A third, dark, very fine-grained dike, 2 feet thick, cuts the second dike and has a texture nearly like the fine-grained margin of the second dike. All four contacts have about the same attitude.

Ortho-Amphibolites

In the southwestern part of the area the country rock is dominantly Roan para-amphibolite and hornblende gneiss. Here less than 10 outcrops have been found which contain typical subophitic or dense granoblastic metadolerite dikes. Fewer good exposures in this area may contribute to the apparent lack of typical dikes. If dikes are present and have been metamorphosed to amphibolites similar in appearance to Roan amphibolite, they would be difficult to distinguish from country rocks.

The area where the dike swarm strikes across

PLATE 2.—GARNET "TRAILS", BANDED AMPHIBOLITE, AND METADOLERITE TEXTURES

FIGURE 1.—Garnet "trails" and clusters (light streaks and spots) in metadolerite dike (locality 158; see also Pl. 3, fig. 4).

FIGURE 2.—Quartzofeldspathic and amphibolite layers parallel to foliation in Roan para-amphibolite (Crabtree Creek 3 miles east of Micaville).

FIGURE 3.—Subophitic metadolerite containing plagioclase laths, augite, hornblende, garnet, and magnetite (×15, crossed nicols; No. 16, near locality 149, shown in Figure 2). Courtesy U. S. Geol. Survey.

FIGURE 4.—Equigranular metadolerite containing plagioclase, pyroxene, hornblende, garnet, and magnetite. Note coronas of garnet and hornblende surrounding granular pyroxene; garnet euhedral against plagioclase, anhedral against hornblende and pyroxene (×20, plain light; BK-57, near locality 56). Courtesy U. S. Geol. Survey.

PLATE 3.—METADOLERITE TEXTURES

FIGURE 1.—Equigranular metadolerite containing hornblende, plagioclase, and magnetite rimmed with sphene (×20, plain light; No. 15, 1.5 miles west of Bakersville on Route 26). Courtesy U. S. Geol. Survey.

FIGURE 2.—Fine-grained metadolerite containing plagioclase, pyroxene, garnet, biotite, magnetite, and minor hornblende. Biotite used for age determination (×25, plain light; BK-61).

FIGURE 3.—Broken plagioclase porphyroblast in metadolerite. Note small plagioclase crystals in cracks which cement porphyroblast (×15, crossed nicols; BK-45, near locality 48). Courtesy U. S. Geol. Survey.

FIGURE 4.—Garnet "trails" in fine-grained metadolerite dike. Note alignment which may reflect fracture control. Garnets are black. (×4, crossed nicols; R-98, 0.9 mile from Carvers Gap on Route 143).

the boundary zone between the Cranberry-Henderson and Roan-Caroline gneiss is exposed along the Toe River and Route 197. Here amphibolites possibly related to the dike swarm are well exposed. Most of them are dense, black, homogeneous rocks with well-developed foliation, in many cases with a spotted or streaked appearance due to segregation of salic minerals. These rocks are called Toecane-type amphibolites, as they were first noted on the west side of the Toe River across from Toecane Village, 3 miles west of Bakersville (Fig. 2).

Similar rocks are well exposed along Route 197 between Red Hill and Toe River, and along the Toe River, especially southwest of Deyton Bend. A particularly significant exposure is found along Brush Creek road east of Deyton Bend.

The exposure at the west end of the bridge near Toecane contains a coarse-grained, spotted amphibolite and a fine-grained, black schistose amphibolite in sharp but irregular contact, similar to contacts of coarse- and fine-grained phases of the dike swarm. No contact is exposed between the amphibolite and quartzofeldspathic country rock which crops out 20 yards away. The Toecane amphibolites differ markedly from typical Roan amphibolites, most of which are compositionally banded parallel to foliation, as in figure 2 of Plate 2 (Brobst and Kulp, in press). Toecane-type amphibolites are also exposed in close proximity to the dike swarm. Hence, they may be metamorphosed equivalents of the Bakersville-Roan Mountain dike swarm, but field evidence at Toecane is inconclusive.

Between Red Hill and Toe River on Route 197 a larger exposure (several hundred feet) contains coarse- and fine-grained, spotted, streaked or uniformly black, schistose amphibolites. Relationships between these rock types are clearly exposed here. The amphibolites are in contact with Cranberry gneiss, and contacts are of various types. In one place compositional bands and foliation of the gneiss are sharply cut by amphibolite with foliation parallel to the contact. Another contact is parallel to the foliation of both gneiss and amphibolite, and there is a textural and compositional gradation between gneiss and amphibolite identical with that found throughout the boundary zone between Cranberry-Henderson and Roan-Carolina gneiss. In this same outcrop a metadolerite dike 12 feet thick cuts Cranberry gneiss, but the dike is not in contact with amphibolite, which is about 20 feet away. This dense, fine-grained dike is slightly foliated near one margin at the lower part of the outcrop, and in this respect resembles the Toecane-type amphibolite. Otherwise the two rock types differ in texture, structure, color, and mineralogy.

The first two outcrops southwest of Deyton Bend along Route 197 contain sheetlike amphibolite masses 10–25 feet thick which are well foliated, coarse-grained, and uniformly dark. The enclosing rock is banded Cranberry gneiss with minor hornblende-rich layers. Contacts between sheet-amphibolite and gneiss may parallel foliation in both rocks, and in gross aspect the sheetlike masses are nearly conformable with the gneiss structure. The rocks have been both sheared and folded. Folds a few feet across may be traced through gneiss and amphibolite, and ptygmatic folds with axial planes approximately parallel to those of folds in the foliation are locally well developed in the amphibolite. No unquestionable metadolerite dikes crop out at this locality. Field evidence is again inconclusive as to whether these amphibolites are metamorphosed dikes of the Bakersville-Roan Mountain swarm or part of the country rocks.

At the Brush Creek Road exposure, which is 75 feet long and 0.7 mile from Route 197 at Deyton Bend, Toecane-type amphibolites crop out. They are more streaked and spotted than at Toecane, but are similar in other respects. In other outcrops along Brush Creek Road, relationships between amphibolites and feldspathic gneiss are as inconclusive as at localities already described. However, at this one outcrop a clue to the origin of the amphibolites is found. In the center of the outcrop (south side of road), 50 feet east of the Toecane-type amphibolite, a core of metagabbro crops out. The large plagioclase laths, pyroxene plates, and subophitic texture are easily seen in hand specimens. Between metagabbro and Toecane-type amphibolite a continuous textural and mineralogical gradation is exposed. No contact with country rock is exposed.

Clearly, the amphibolite at the Brush Creek Road exposure is a metamorphosed gabbro, and it is likely that all Toecane-type rocks are of similar origin. The Brush Creek Road exposure is the only example found of direct correlation between Toecane amphibolites and Bakersville-Roan Mountain dikes. However, no metadolerite dikes or amphibolites of Toecane-type have been described from other areas of Cranberry-Henderson gneiss or Roan-Carolina gneiss (Brobst and Kulp, in press), which suggests that a genetic relationship between Toecane amphibolites and Bakersville-Roan Mountain dikes exists.

Relationships to Pegmatites

No metadolerite dikes have been found in contact with Spruce Pine pegmatite. At several localities, pegmatite dikelets 3 inches or less in width cut metabasaltic dikes and country rocks. Along Route 197 and Toe River, 1.2 miles northeast of Deyton Bend, a pegmatite lens (about 20 feet by 45 feet), is enclosed by Toe-

cane-type amphibolite, altered to friable biotite schist along the pegmatite contact. If this pegmatite is the same as the Spruce Pine pegmatites (15 miles distant), and if Toecane-type amphibolites are equivalent to the metadolerite dikes, the dikes are older than the Spruce Pine pegmatites. This is the only field evidence of the age relationship between dikes and pegmatites, accurately dated as Ordovician-Silurian (340 m. y.; Kulp and Poldervaart, 1956, p. 400).

Age Relationships

Age relationships of rocks in the Spruce Pine district and the Bakersville-Roan Mountain area have been discussed by Kulp and Poldervaart (1956, p. 400–402). They gave the following sequence of events:

(1) Deposition of a thick sedimentary sequence in the Appalachian geosyncline, perhaps 800–1000 m. y. ago.

(2) Regional metamorphism and deformation of sediments to form the Cranberry-Henderson and Roan-Carolina complexes, probably about 700 m. y. ago; intrusion of local pods of synkinematic granite (Beech granite); emplacement of ultramafic bodies early in this cycle.

(3) Crustal tension; local brecciation of the metasedimentary rocks; intrusion of the Bakersville-Roan Mountain dike swarm.

(4) Second cycle of regional metamorphism, resulting in recrystallization of the Bakersville-Roan Mountain dikes and breccia matrix and emplacement of Spruce Pine pegmatites and alaskites along the keel of the Roan-Carolina synclinorium; partial recrystallization and tectonic displacement of ultramafic bodies. This cycle of regional metamorphism climaxed about 340 m. y. ago, at about the Ordovician-Silurian boundary (see material to follow).

(5) Development of shear zones, perhaps related to the late Paleozoic Appalachian deformation to the northwest. Younger dolerite dikes in the eastern portion of the Spruce Pine district are unmetamorphosed and probably pre-Cretaceous (perhaps Triassic).

More recent potassium-argon age determinations using metamorphic biotite separated from two metadolerites (BK-61 and BK-149) establish the date of the dike metamorphism as 450 m. y. ago. This work of L. A. Long and J. L. Kulp (personal communication, 1957) shows a continuous progression in ages of the rocks of the region, from about 860 m. y. in the west just below the Paleozoic cover at Pardee Point to 350 m. y. at Spruce Pine (and east of Spruce Pine), a distance of less than 40 miles. The data indicate two plutonic cycles, an older cycle probably in excess of 900 m. y. and perhaps of Grenville age, and a younger Ordovician-Silurian cycle, with focus east of Spruce Pine and showing super-position effects in the area between Spruce Pine and Pardee Point. However, the present writers do not exclude the possibility of yet another cycle of metamorphism, probably late Precambrian or early Paleozoic in age. Reasons are given in following pages why the biotite of the metadolerites used for the age determinations is considered to be metamorphic in origin rather than the product of magmatic crystallization. Field evidence which has been detailed indicates that the dikes were emplaced at relatively shallow depths. Hence the writers believe that considerable time elapsed between the original metamorphism of the country rocks (*ca.* 1 b. y.) and the emplacement of the dikes. The age for the biotite is regarded as an approximate age of the second cycle of metamorphism; the biotite was probably somewhat modified by the youngest plutonic cycle with a 350 m. y. age. Evidence in the Bakersville-Roan Mountain area is not wholly conclusive, but it is possible that detailed work in adjacent regions to the south will disprove or establish the existence of a late Precambrian or early Paleozoic metamorphic cycle.

Much has been written in the last decade of the "younging" of continents seaward. This may be real or only apparent. The Spruce Pine area shows only apparent younging of basement rocks seaward, but it is evident from the geology of the area that the crystalline rocks at and east of Spruce Pine, with 350 m. y. ages, were originally contemporaneous with those west of Spruce Pine, with much greater ages. In this case the younging results from a shift of younger plutonic cycles seaward, rather than the development of younger basement formations seaward. Whether the same also applies elsewhere remains to be established.

Magnetic Properties

General Statement

Five pairs of oriented specimens, each pair consisting of a dike sample and a specimen of country rock about 10 feet from the dike contact, were collected. Thermoremanent magnetic

polarization measurements have been made on the 10 specimens, and magnetic susceptibility anisotropy has been determined in three pairs of rocks.

TABLE 1.—REMANENT MAGNETIZATION

Sample number	Locality Fig. 2	No. of samples measured	Magnetite-ilmenite ratio*	Direction of magnetization
W-1	95	2	1:9	S. 67 W. (+) 62°
W-2	95	2	1:1	S. 86 E. (−) 27°
W-3	48	6	1:9	S. 43 W. (+) 58°
W-4	48	3	1:9	S. 26 W. (−) 7°
W-5	158	2	1:4	S. 18 E. (+) 27°
W-6	158	2	1:9	S. 14 E. (+) 8°
W-7	92	2	1:9	S. 65 W. (−) 40°
W-8	92	4	1:9	S. 35 E. (+) 82°
W-9	8	4	1:1	S. 48 E. (−) 18°
W-10	8	6	9:1	N. 62 E. (+) 65°

* Visual estimate.

Remanent Magnetic Polarization

Nicholls (1955), Néel (1955), and Runcorn (1955) have reviewed, respectively, the magnetic properties of minerals, theoretical considerations, and geophysical aspects of rock magnetism, and Blackett (1956) has considered some of the current complexities of interpreting paleomagnetic data. Runcorn details recent applications of studies of remanent magnetism in lava flows and fine-grained, red sedimentary rocks to the paleomagnetic field of the earth. Evidence indicates that the position of the earth's magnetic poles may have shifted during past geological periods. Data for American rocks show that the north pole was located as follows: Precambrian, in southwestern North America or northeast central Pacific Ocean; early Paleozoic, northwest Pacific Ocean; late Paleozoic and Mesozoic, northeastern Asia; Cenozoic, present position (Runcorn, 1955, p. 285).

Magnetite and other ferromagnetic minerals acquire a magnetization direction parallel to an imposed field when cooled from high temperatures. The temperature at which magnetization takes place, known as the Curie point, is about 575°C. for magnetite and 150°C. for ilmenite (Nicholls, 1955, p. 131, 140). The orientation of this magnetic direction relative to the specimen is fixed and may be measured as a thermoremanent magnetization (T.R.M.) direction subsequent to removal of the original field, provided there are no chemical or physical changes and the rocks are not reheated above the Curie point (Blackett, 1956, p. 9). In such cases the rocks will exhibit the T.R.M. direction characteristic of the field present during the second cooling.

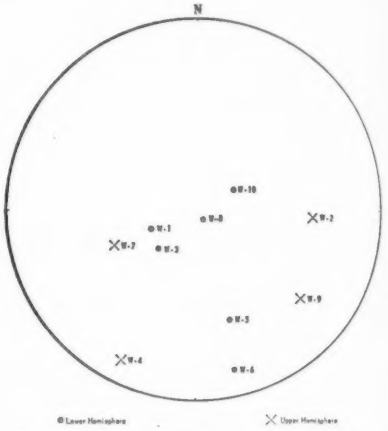

FIGURE 4.—STEREOGRAPHIC PROJECTION OF THERMOREMANENT MAGNETIC VECTORS (North poles; see Table 1 for localities.)

Other factors may also influence the apparent T.R.M. of a rock. Important among these are the chemical histories of the minerals and the variety and distribution of magnetic minerals throughout the rock (Asami, 1956, p. 152–155; Balsley and Buddington, 1954, p. 176–181). These and other problems are discussed in the papers cited.

The metabasaltic dikes and country rocks contain sufficient magnetic opaque minerals (up to 11 per cent by weight) to make T.R.M. and susceptibility measurements possible. It was hoped that T.R.M. studies would yield information regarding: (1) age of the dikes, (2) temperature of metamorphism, and (3) age of metamorphism. As metamorphic rocks have received little attention in magnetic studies, results must be used with caution (Runcorn, 1955, p. 247; Blackett, 1956, p. 13).

Results of T.R.M. measurements are given in Table 1 and Figure 4. Odd numbers are dikes, even numbers country rocks, and members of a pair are consecutively numbered.

If all vectors were parallel, it might be concluded that the rocks have been heated above the Curie point during the second regional

metamorphism and received their T.R.M. at that time. This is not the case, hence temperatures were less than 575°C. during metamorphism of the dikes.

The scatter of T.R.M. poles in Figure 4 precludes use of these data for age interpretations. It further reflects probable compositional complexity of the opaque minerals suggested by comparison of the estimated magnetite-ilmenite ratio (Table 1), modal opaques (*cf.* magnetite, Table 2), and normative opaques (*cf.* chemical analyses, Table 5).

Some degree of regularity is suggested in that W-1 and W-3 have the same polarization. W-7 is a dike 10 miles from the other two, and its vector is about parallel to W-1 and W-3, but opposite in direction. This phenomenon of parallel but reverse direction is common in lava flows, in which there are rapid reversals over short distances (Blackett, 1956, p. 89; Graham, 1953, p. 256–257). Near-parallelism of W-5 and W-6 may be due to contact effects of a larger dike from which the smaller dike sampled branches.

Magnetic Susceptibility

Graham (1954, p. 1257) states that non-equidimensional magnetite particles in a rock have a preferred susceptibility to magnetization parallel to the long dimensions when placed in a magnetic field. If the grains are not randomly oriented, a susceptibility anisotropy results, which may be represented by a triaxial ellipsoid in which the three axes correspond to the maximum (*M*), intermediate (*I*), and least (*L*) susceptibility directions in the rock. No detailed work has been done relating magnetic susceptibility directions to the mineral fabric of a rock. Preliminary work indicates that the *L* axis of susceptibility is normal to dike contacts; the *MI* plane lies in the plane of foliation of schists and gneisses; and the *M* axis parallels lineation.

Poles of axes of susceptibility for three pairs of samples are plotted in Figures 5*a*–5*c* (lower hemisphere projections). For each rock two samples have been measured, and in one case (W-7), one of the two samples has been remeasured to test reproducibility, which is good (Fig. 5*b*). W-5 shows the greatest difference between the two measured samples taken 2 inches apart from the same specimen. The *MI* plane is subparallel to the dike contact. The low inclination of *M* in W-6 makes the two plots appear more different than they are. This country rock is not foliated. The contact and susceptibility axes in dike W-7 are apparently not related, but the *MI* plane in the adjacent gneiss (W-8) is about parallel to foliation. The two country rocks, W-6 and W-8, have nearly identical anisotropy, although they are differ ent rock types and crop out 1.5 miles apart.

Samples W-9 and W-10 are, respectively, a Toecane-type amphibolite and adjacent gneiss. Foliation in both rocks nearly parallels the contact. The *MI* plane of susceptibility is also nearly parallel to the contact, but in the two rocks the *M* and *I* axes are reversed. Their relative magnitudes are similar, hence a small change in orientation may cause reversal. This may indicate that the sheetlike amphibolite is derived from a different source rock (perhaps a dike) than the quartzofeldspathic gneiss. Anisotropy in this gneiss has an orientation different from that in the two country rocks 10 miles away on Roan Mountain.

Petrography

Introduction

About 500 slices have been prepared from metabasaltic rocks and amphibolites collected in the Bakersville-Roan Mountain area. Typical samples were selected on the basis of textural and mineralogical variations. All gradations between the type rocks have been observed. Locations of the rocks described are shown in Figure 2.

Modes have been determined by the point-counter method for each type rock and are presented in Table 2. Several difficulties in mineral identification affect the accuracy of the modes. Although quartz is present up to a few per cent in some rocks, it has not been possible to distinguish quartz from untwinned plagioclase during counting. The only certain method of identifying these minerals is with the universal stage. The mineral counted as diopside in most of the rocks is in minute granules, too small for optical determinations. Aggregates of these granules, intimately mixed with minute crystals of garnet, hornblende, and in some cases biotite, make counting difficult. For this reason modal values for diopside, garnet, and biotite should be viewed with caution.

Ten of the rocks described are metadolerites; eight are Toecane-type amphibolites; and one (R-158) is country rock previously thought to be a special type of dike rock.

Textures characteristic of the rock types are shown in Plates 2 and 3.

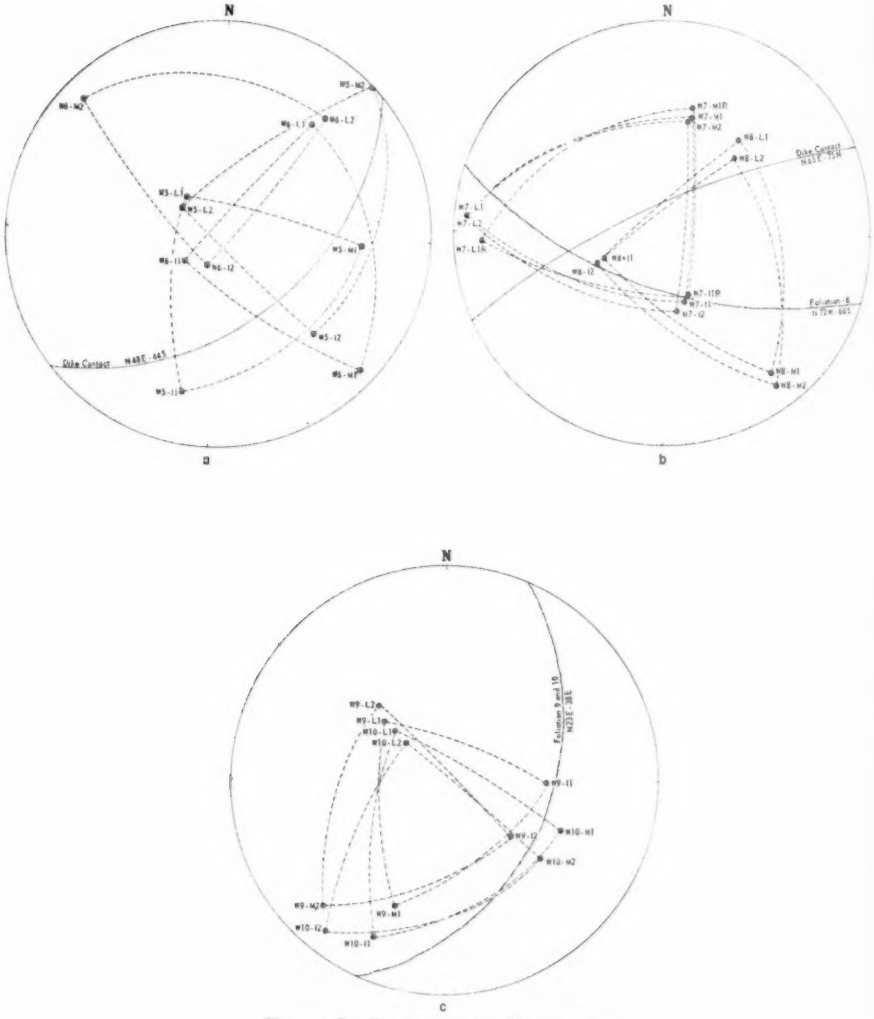

FIGURE 5.—SUSCEPTIBILITY ANISOTROPY
Figure 5*a*—samples W5 and W6; 5*b*—samples W7 and W8; 5*c*—samples W9 and W10.

Description of Thin Sections

BK-48, PORPHYROBLASTIC METADOLERITE: The average grain size of the groundmass is 0.3 mm, whereas porphyroblasts range from 5 mm to 20 mm. Minerals include plagioclase (in groundmass and as porphyroblasts), hornblende, biotite, garnet, and magnetite.[1] The texture of the groundmass is equigranular with a tendency for aggregation of felsic versus mafic minerals. Minerals tend to be elongated, but no foliation is apparent. Boundaries between porphyroblasts and groundmass vary in sharpness. Where the groundmass is dominantly plagioclase and biotite with some hornblende adjacent to porphyroblasts, boundaries are poorly defined. Where dominant groundmass minerals are garnet and minor magnetite, biotite, and hornblende, boundaries are relatively sharp, with garnet forming disconnected rims along the porphyroblasts. Porphyroblasts are crowded with inclusions of biotite, hornblende, and garnet, and

[1] In the following descriptions magnetite includes also ilmenite and titano-magnetite.

TABLE 2.—MODES (WEIGHT PER CENT)

Index	BK-48	BK-56	BK-61	BK-95	BK-149	BK-262	R-36	R-57	R-92	R-158	R-163	TO-1	TO-2	TO-3	TO-4	TO-5	TO-7	TO-8	TO-9
olivine	....	....	....	....	....	....	13.4	....	....	....	....	....	....	....	....	....	....	....	....
plagioclase	46.9	30.0	25.2	21.0	37.0	23.5	30.2	19.8	30.7	42.6	19.9	21.8	21.9	23.0	21.6	19.3	17.4	24.7	51.3
orthoclase	....	....	....	....	0.6	....	....	....	....	....	....	....	....	....	....	....	....	....	....
augite	....	7.8	15.0	0.3	17.2	24.5	9.0	tr.	7.1	17.5	19.9	....	....	....	....	....	....	....	....
diopside	tr.	6.8	7.7	....	6.5	12.3	....	6.5	7.2	....	....	....	....	....	....	....	....	....	....
orthopyroxene	....	....	....	....	0.5	0.1	17.6	....	1.2	13.1	6.1	....	....	....	....	....	....	....	....
hornblende	26.8	26.3	0.2	46.5	2.3	16.7	20.4	54.2	33.4	4.4	46.5	67.0	69.5	70.3	75.8	71.5	73.2	60.8	22.4
garnet	11.1	23.7	26.5	14.8	14.2	11.9	....	9.2	6.7	9.3	tr.	0.4	....	....	....	....	....	....	1.1
biotite	10.9	2.1	16.5	6.7	10.3	1.8	4.0	0.2	1.8	tr.	tr.	3.3	2.5	1.5	....	3.3	1.3	6.5	17.6
zoisite	....	0.2	....	....	....	....	....	....	....	....	....	....	....	....	....	....	....	2.1	0.1
magnetite	4.3	2.9	8.4	9.4	10.1	8.7	5.0	9.7	11.2	11.5	7.4	5.2	5.7	....	1.6	5.8	7.7	....	....
sphene	tr.	....	....	....	....	....	....	....	....	....	....	1.7	tr.	4.9	....	....	0.2	5.5	1.2
pyrite	....	....	....	....	....	....	....	....	....	....	....	....	....	....	....	....	....	tr.	2.8
apatite	....	0.1	0.5	0.6	1.3	0.5	0.4	0.4	0.7	1.6	....	0.6	0.4	0.3	0.4	0.1	0.2	0.4	2.3
calcite	....	0.1	....	0.7	tr.	....	....	....	tr.	....	....	....	....	....	....	....	....	....	1.2
hematite	....	....	....	....	....	....	....	....	....	....	....	....	....	....	0.6	....	....	....	....
Specific gravity																			
experimental	3.00	3.16	3.18	3.16	3.15	3.18	3.27	3.16	3.25	3.11	3.09	3.06	3.11	3.04	3.01	3.12	3.07	3.03	2.94
calculated	3.04	3.23	3.30	3.31	3.19	3.29	3.14	3.32	3.24	3.16	3.24	3.20	3.20	3.15	3.17	3.22	3.26	3.12	2.91

show irregular clouding. Hornblende and biotite inclusions tend to be oriented parallel to cleavage or twin composition planes. Nearly submicroscopic inclusions are aligned parallel to large elongated inclusions. Groundmass plagioclase contains minute scattered inclusions but is not clouded. Many porphyroblasts are broken, and cracks are filled with minute plagioclase crystals (Pl. 3, fig. 3), but fracturing is irregular. Plagioclase filling fractures in porphyroblasts shows twinning and sharp extinction, in contrast with the irregular extinction in porphyroblasts. Ground-mass plagioclase is equigranular and untwinned or shows simple or multiple twinning.

Brownish-green to olive-green hornblende is elongated but of irregular shape. Some large hornblende crystals surround smaller plagioclase units; the result resembles sieve structure, but true sieve structure is rare. Isolated hornblendes or those included in porphyroblasts tend to be equidimensional. Brown to reddish-brown biotite builds irregular basal plates. For distances of a few millimeters biotite and hornblende may be parallel, but general parallelism is absent. Biotite is not preferentially associated with any one mineral. Garnet is pale pink and anhedral to subhedral. Subhedral crystals along edges of porphyroblasts are euhedral toward plagioclase and anhedral toward other minerals. Individual garnets may be clear or contain abundant inclusions of biotite and/or nearly submicroscopic particles which disturb the isotropic character. Throughout a thin section, garnet shows parallel fractures. Some fractures may be traced from garnet into adjoining plagioclase or hornblende. Garnet enclosed in plagioclase porphyroblasts is more nearly euhedral and somewhat elongated but not oriented. Magnetite is scattered irregularly throughout the rock and forms anhedral, in some cases skeletal, crystals. Most individuals are surrounded by hornblende, biotite, or garnet; some are partly rimmed by minute sphene. Pyroxene granules are rarely associated with hornblende, and occasional clusters 1–2 mm in diameter, consisting of minute pyroxenes, are found in the groundmass.

BK-56, EQUIGRANULAR METADOLERITE: This rock is composed of pale-brown, relict augite up to 1 mm in diameter, equigranular plagioclase, hornblende, garnet, magnetite, and scattered biotite, and granules of pale-green pyroxene which average 0.1 mm. The texture is subophitic. Plagioclase is equigranular and shows varying degrees of twinning. Crystals are unclouded but are outlined by small inclusions concentrated along and between grain boundaries. Augite is slightly to intensely clouded. A few crystals show clouding in hourglass pattern. Different portions of an individual are clouded in varying degrees. Crystals are in general irregular because of alteration to hornblende. Brownish-green to olive-green hornblende is associated with or replaces pyroxene. Individual hornblende crystals are equigranular and show poor cleavage. Commonly hornblende rims relict augite, but it is also found scattered in plagioclase. Garnet is pale pink and anhedral or subhedral. It is scattered throughout the rock but is locally aligned to form rims around hornblende, which in turn rims or replaces pyroxene. Most central portions of garnet crystals are isotropic, but marginal inclusions impart a low birefringence to the edges. Scattered skeletal magnetite is associated with clusters of hornblende, garnet, and pyroxene. Rare sphene is present as minute single crystals and does not rim magnetite. Reddish-brown biotite is associated with magnetite or hornblende. Clusters of pale-green pyroxene granules are associated with hornblende and garnet. Relict clouded augite may grade into an aggregate of hornblende and pyroxene granules, and this in turn grades into garnet, crowded with inclusions.

BK-61, FINE-GRAINED METADOLERITE: This rock contains relict plagioclase and pyroxene, recrystallized plagioclase and pyroxene, and biotite, garnet, and magnetite. Hornblende is present only in trace amounts. Relict plagioclase is slightly clouded and forms laths up to 1 mm long with ragged edges. Recrystallized plagioclase builds irregular, equidimensional crystals about 0.1 mm in diameter. A few plagioclase porphyroblasts up to 2 mm in diameter are slightly clouded and contain abundant inclusions. All plagioclase contains minute inclusions of biotite, pyroxene, and hornblende. Relict augite forms irregular, moderately clouded crystals. Clouding is concentrated along cleavage cracks. Recrystallized pyroxene granules may be associated with relict augite, or they may build granules and clusters of granules which are scattered throughout the rock. Light to dark-brown biotite averages about 0.05 mm in diameter. Biotite flakes are mounted on magnetite, garnet, and recrystallized granoblastic pyroxene, and the mineral is therefore clearly of metamorphic origin (Pl. 3, fig. 2). Garnet is pale pink, averages 0.1 mm in diameter, and is in general anhedral, although subhedral crystals are found in contact with plagioclase. It commonly surrounds magnetite and relict augite. Most garnets are choked with inclusions and appear anisotropic. Inclusions are principally minute pyroxene, magnetite, and biotite, along with abundant submicroscopic particles. Skeletal magnetite is scattered throughout the rock and in many places is surrounded by garnet. Scattered sparsely throughout the rock are tiny hornblende granules associated with recrystallized plagioclase, pyroxene, biotite, and magnetite. The association garnet-hornblende is not common in this rock.

BK-95, FINE-GRAINED, EQUIGRANULAR METADOLERITE: The average grain size is 0.1 mm. Major constituents, hornblende and plagioclase, are equally distributed and form a homogeneous texture. Smaller amounts of reddish-brown biotite and skeletal magnetite are scattered throughout the rock. Pink garnet forms loose clusters up to 5 mm in diameter, occasionally rimming magnetite, but garnet is also associated with other minerals. Traces of clouded relict augite are associated with horn-

blende. Plagioclase is unclouded but contains scattered inclusions of hornblende, magnetite, and biotite. Twinning is absent or indistinct. Hornblende is greenish brown, equidimensional, and shows poor cleavage. Submicroscopic, apparently opaque inclusions are present in hornblende and more abundantly in garnet, which appears anisotropic.

BK-149, COARSE-GRAINED METADOLERITE: The average grain size of this subophitic rock is 2.0 mm. Dominant minerals include slightly clouded, lath-shaped plagioclase, in general twinned and with indistinct boundaries, and equidimensional augite, also slightly clouded and with irregular outlines. Degree of clouding in both augite and plagioclase varies in different crystals and within one individual. In plain light, "channel-ways" apparently separate adjacent areas of clouding in a crystal. Subhedral to anhedral, pale-pink, anisotropic garnet, crowded with inclusions, is associated with, and may rim augite. Subhedral, isotropic garnet is in contact with plagioclase. Skeletal magnetite is scattered throughout the rock and in most cases is rimmed by garnet. Reddish-brown biotite is associated with magnetite or distributed throughout the rock. The few orthopyroxenes present follow the habit of augite. Tiny granules of greenish-brown hornblende rim some augite.

BK-262, COARSE-GRAINED METADOLERITE: This rock is similar to BK-149, but slightly coarser-grained, averaging 3.0 mm. Subophitic texture is better developed, and both plagioclase and pyroxene are clouded. Orthopyroxene is strongly pleochroic. Magnetite is larger, more regular in shape, and less widely scattered. Reddish-brown biotite is associated almost exclusively with magnetite. Hornblende varies from green brown to pale greenish blue, and consistently rims augite. Pale-pink, isotropic, subhedral garnets (euhedral against plagioclase) rim masses of finely crystalline material composed of garnet, pyroxene, and minor amounts of biotite, hornblende, and magnetite. These masses may grade imperceptibly into isotropic garnet or microcrystalline aggregates (chiefly pyroxene) surrounded by a rim of garnet crowded with inclusions, in turn surrounded by subhedral, isotropic garnet. In addition to clouding, plagioclase and augite contain scattered larger inclusions which may be aligned parallel to indistinct twinning or cleavage directions. Extinction in plagioclase is rarely sharp and in all places is variable in direction throughout any one crystal.

R-36, OLIVINE METADOLERITE: Average grain size is 2.0 mm, and the texture is relict subophitic. Lath-shaped plagioclase is complexly twinned and shows irregular extinction. Moderate to heavy clouding of plagioclase gives crystals a brownish coloration in plain light. Clouding is irregular in density in different crystals and throughout each individual. Both augite and orthopyroxene commonly surround olivine. Orthopyroxene shows intense pleochroism. Clouding of both pyroxenes may result in near-opacity. Olivine is characteristically cracked, but little is altered to serpentine. It commonly shows a corona of fibrous enstatite, followed by a second corona of fibrous, greenish-brown to greenish-blue hornblende. A few skeletal magnetites are scattered throughout the rock, commonly with associated reddish-brown biotite and traces of green spinel. All minerals have scattered inclusions. Under high magnification, clouding particles in both pyroxene and plagioclase show excellent alignment.

R-57, FINE-GRAINED METADOLERITE: Average grain size is 0.2 mm, and the texture is uniformly equigranular. Dominant minerals include plagioclase and hornblende, whereas relict augite, scattered irregular magnetite, and clusters of garnet are subordinate. Plagioclase is unclouded and contains few inclusions. Most of it is untwinned and shows undulatory extinction. Twinning is indistinct. Relict augite is slightly clouded. Pale-green pyroxene granules are scattered throughout the rock as single crystals and clusters of crystals. Garnet is pale pink, anhedral to subhedral, and forms compact clusters up to 5 mm in diameter. Crystals are invariably choked with inclusions. Clusters of garnet and hornblende may be aligned, suggesting faint foliation. Small flakes of pale reddish-brown biotite are scattered throughout the rock.

R-92, COARSE-GRAINED METADOLERITE: This rock is similar to BK-149 and BK-262, has subophitic texture, and an average grain size of 2 mm. Plagioclase laths show simple and complex twinning and irregular extinction. Both augite and plagioclase are clouded, the degree of clouding ranging from slight to intense. In addition to clouding, plagioclase laths contain abundant inclusions of hornblende, pyroxene, biotite, and magnetite. Greenish-brown, equidimensional, small hornblendes rim augite and in some cases are present along boundaries between augite and plagioclase. New pyroxene granules have replaced some augite, and the granular masses are surrounded by hornblende aggregates which may include magnetite and biotite. Large irregular magnetite and reddish-brown biotite are scattered throughout the rock. Pink, anhedral to subhedral garnet forms small clusters which may grade into aggregates of pyroxene granules. Garnets are invariably choked with inclusions when associated with femic minerals, but commonly are clear adjacent to plagioclase. A few scattered orthopyroxenes are associated with augite or pyroxene granules.

R-158, PLAGIOCLASE-PYROXENE GRANULITE: Equidimensional plagioclase, augite and orthopyroxene form an equigranular rock. Plagioclase is unclouded and in most cases complexly twinned. Subhedral to anhedral garnet, commonly choked with submicroscopic inclusions, rims pyroxene and magnetite. Tiny crystals of brownish-green hornblende rim pyroxene. Hornblende and garnet rims are not associated, but a magnetite or pyroxene crystal may be rimmed by garnet on one side and by hornblende on the other. Pyroxene is slightly

clouded and shows excellent schiller structure. Augite is pale green, and orthopyroxene is pleochroic from pale green to pink. Magnetite and relatively abundant apatite are scattered throughout the rock. This mafic sample is part of the Cranberry and not a Bakersville-Roan Mountain metadolerite.

R-163, FINE-GRAINED METADOLERITE: Grain size is about 0.1 mm, and texture is relict subophitic. Plagioclase laths are long and slender, in most cases complexly twinned, and have undulatory extinction. They are slightly clouded and have few inclusions. Relict augite (up to 1 mm across) is slightly to intensely clouded and invariably associated with, or rimmed by brownish-green hornblende. Scattered radial clusters of orthopyroxene are surrounded by thick rims of closely packed hornblende granules. Small skeletal magnetite is scattered throughout the rock. Highest magnification shows that areas and rims of hornblende are composed of minute granules without cleavage or crystal form.

TO-1, COARSE-GRAINED, TOECANE-TYPE AMPHIBOLITE: The grain size of this rock is 2 mm. Principal minerals are hornblende and plagioclase with minor magnetite, biotite, sphene, garnet, and quartz. The minerals are segregated into distinct patches, dominantly composed of plagioclase or hornblende. Magnetite is commonly rimmed by sphene and is only found associated with hornblende and biotite. The biotite is associated both with hornblende and plagioclase. Garnet is euhedral to anhedral and found only with plagioclase. It is pale pink, isotropic, and contains few inclusions. The hornblende patches can be subdivided into areas of large hornblende crystals with few other minerals and areas of smaller hornblendes, intimately associated with small plagioclase crystals and a little quartz. In hand specimen and on outcrop, elongation and flattening of light and dark areas, in a ratio of approximately 1:3, results in indistinct foliation and a spotted rock surface.

TO-2, FINE-GRAINED AMPHIBOLITE: Average grain size is 0.15 mm. Dominant minerals are hornblende and plagioclase, which form an even-grained, schistose texture. Tiny magnetite and irregular biotite are scattered throughout the rock. Plagioclase is unclouded but contains scattered inclusions. It may be untwinned or twinned; twinning may be simple or complex. Hornblende is brownish green with moderately well-developed cleavage. No garnet is present. This rock is in sharp contact with TO-1, and foliation in the two rocks is parallel to the contact.

TO-3, AMPHIBOLITE: Average grain size is 0.2 mm. Dominant minerals are hornblende and plagioclase; accessories are scattered sphene, quartz, and a few biotite flakes. The rock is foliated and has a uniform texture. Hornblende is brownish green and prismatic. Most of the plagioclase is untwinned and shows undulatory extinction. A little quartz is scattered throughout the rock. Biotite flakes are brown and poorly developed.

TO-4, AMPHIBOLITE: Average grain size is 0.15 mm, and the rock is foliated and of uniform texture. Essential minerals include hornblende and plagioclase with a few ragged crystals of magnetite and associated clusters of dark-brown sphene. Scattered quartz and biotite flakes are also present. Plagioclase is both twinned and untwinned and has irregular extinction patterns, rarely suggesting zoning. Hornblende is pale green and forms moderately to well-developed prisms with good cleavage.

TO-5, AMPHIBOLITE: Average grain size is 0.5 mm. The rock is foliated and contains dominant hornblende (up to 5 mm) and plagioclase, with minor magnetite and scattered reddish-brown biotite. Hornblende is brownish green to bluish green and forms both well-developed prisms and irregular crystals. Magnetite is skeletal and is commonly aligned or elongated parallel to foliation. Plagioclase has poorly developed cleavage and twinning and undulatory extinction. Some crystals are elongated parallel to foliation.

TO-7, AMPHIBOLITE: Average grain size is 0.1 mm. This foliated rock contains abundant hornblende and plagioclase and much scattered magnetite and biotite. A little sphene and quartz is also present. Hornblende is pale brownish green to bluish green and prismatic. Twinning in plagioclase is indistinct or absent; extinction is generally sharp but may be undulatory with a slight suggestion of zoning. Biotite is pale reddish brown. This rock is in sharp contact with a coarse-grained amphibolite, and foliation in the two rocks is parallel to the contact.

TO-8, AMPHIBOLITE: Average grain size is 1 mm. Essential minerals include hornblende, plagioclase, biotite, and sphene, in some cases as well-developed crystals. Hornblende is pale brownish green to dark bluish green and forms elongated crystals, which together with brown biotite define the foliation. Plagioclase is extensively altered to sericite. There are untwinned plagioclase crystals as well as laths showing indistinct, simple twinning and well-developed complex twinning. Extinction is undulatory in some crystals, suggestive of zoning in others, and well defined in still others. Minor clinozoisite, apatite, magnetite, and quartz are scattered throughout the rock. Magnetite is not associated with sphene.

TO-9, SPOTTED AMPHIBOLITE: Average grain size is 0.3 mm. Plagioclase is the main mineral, with about equal amounts of hornblende and biotite. Irregular patches of calcite, magnetite, sphene, and a little quartz are scattered throughout the rock. Anhedral clusters of pink, clear garnet are locally present. Plagioclase is equidimensional and shows a variety of twinning and extinction. Hornblende is brownish green to bluish green and in most cases is irregular. Biotite is pale to dark brown and elongated parallel to foliation, as is elongated hornblende. The "spots" are concentrations of plagioclase with few dark minerals except for garnet, clinozoisite, and a little biotite. Garnets form anhedral clusters within or at the edges of the spots. Foliation bends around the spots, some of which are flattened parallel to foliation.

Mineralogy

General Statement

The principal silicate minerals in the Bakersville-Roan Mountain metadolerites and amphibolites are plagioclase, hornblende, pyroxene, garnet, biotite, and olivine. Selected properties of these minerals have been studied in detail. Limiting factors in these studies are the small size of most crystals and the abundant inclusions in nearly all minerals.

Optic axial angles and refractive indices have been chosen as properties which can be determined most precisely for these minerals. Data are given in Table 3. Attempts to separate pure minerals for chemical analyses or specific gravity determinations have been unsuccessful, except for plagioclase, because all minerals are intimately associated and because inclusions are ubiquitous. Two plagioclase samples have been analyzed chemically (Table 11).

Methods of Study

Optic axial angles have been determined with a 4- or 5-axis Leitz universal stage. Wherever possible, measurements have been made between the two optic axes by rotation on a single axis. Where both optic axes could not be reached by rotation about one axis, measurement has been made from one axis to a bisectrix position; this value has been doubled to give the optic axial angle.

The precision in measuring 2V directly on plagioclase with sharp extinction is $\pm 0.5°$. Because of less well-defined extinction in hornblende, pyroxene, and olivine, precision for these minerals is $\pm 1°$. In highly colored hornblende, precision may be as poor as $\pm 3°$. For each mineral the precision has been ascertained by computing the standard error of the mean of several determinations, both of the same crystal and of different crystals of the same mineral in each thin section. Depending on the optical characteristics of the mineral measured (color density, amount of internal reflection, and color and birefringence of surrounding minerals), measurements have been made with sodium light, white light with the gypsum plate inserted, or plain white light. With experience, comparable precision may be attained with all three lighting arrangements.

Refractive-index determinations on plagioclase have been made using the method of Emmons (1943, p. 70–76), as modified by Smith (1954, unpub. Ph.D. thesis, Princeton Univ.). The lowest refractive index for a sample is determined approximately by the immersion method, after which the sample is mounted on a universal stage equipped with a constant-temperature cell between the hemispheres. Using white light, a grain is oriented so that the fast ray is nearly vertical when all universal stage axes are in zero position. With an index liquid close to, but slightly higher than the α index, the grain is rotated first towards β and then towards γ, until the index of the grain equals that of the liquid. The angles of rotation are noted, another liquid with a slightly higher index is placed around the grain, and the procedure is repeated. Knowing the original orientation of α and the rotations towards β and γ, respectively, the α, β, and γ indices are determined by solving for the axes of the $\alpha\beta$ and the $\alpha\gamma$ ellipses, using the graphical method of Emmons (1943, Pl. 10). If properly oriented grains are used, and corrections are made for temperature variations and angles of tilt, the precision of the method for plagioclase is ± 0.0005. Inclusions in the host mineral and complex twinning lower the precision. In Bakersville-Roan Mountain plagioclase the average precision is ± 0.001. For each grain replicate determinations have been made in sodium light. Index liquids have been checked after each measurement on a temperature-controlled Abbe refractometer with sodium light.

Refractive indices for mafic minerals have been determined by the immersion method using a constant-temperature stage. Sodium light has been used for all determinations, and index liquids have been checked on the Abbe refractometer. For augite, γ has been determined by the method of Tomita (1934). The index of the slow ray (γ') on (110) cleavage fragments is determined, and 0.004 is added to give the true γ index. For orthopyroxene γ is parallel to cleavage, hence direct measurement is possible. Minute pale-green pyroxene granules present in many Bakersville-Roan Mountain rocks have not been determined. R-57 contains only traces of relict augite, and the pale-green pyroxene for which γ has been determined is assumed to be the same as the minute granules present in the other rocks. For hornblende, the slow ray (γ') has been determined on cleavage fragments. This value is close to the true value of γ, which is only 15° removed from the c-axis. In biotite flakes the slow ray (γ) has been determined, and this is also the same as β, since biotite has a small optic angle. For these determinations, the accuracy is probably not better than ± 0.002, principally because of lack of precise orientation.

Extinction angles have not been measured. Emmons *et al.* (1953, p. 23–40) have found that extinction angles are less reliable in characterizing plagioclase than refractive indices. Similarly, Hess (1949, p. 630) states that extinction angles for pyroxene cannot be determined with sufficient precision for meaningful comparison between crystals, because variation of extinction angles with composition is relatively small.

Plagioclase

The three refractive indices and the optic axial angle about the slow ray (γ) have been measured for the plagioclase. Figure 6 shows the data superimposed on a graph determined by

TABLE 3.—OPTICAL DATA

(Leaders indicate mineral is present, but optics were not determined. Blank boxes indicate mineral is absent.)

Index	BK-48	BK-56	BK-61	BK-95	BK-149	BK-262	R-36	R-57	R-92	R-158	R-163	TO-1	TO-2	TO-3	TO-4	TO-5	TO-7	TO-8	TO-9
Plagioclase	*																		
2V(+)	97	97	102	101	91	81	82	99	87	92	88	95	95	96	92	97	93	96	98
α	1.5382	1.5440	1.5397	1.5402	1.5464	1.5522	1.5538	1.5403	1.5425	1.5459	1.5541	1.5421	1.5424	1.5387	1.5435	1.5402	1.5412	1.5398	1.5404
β	1.5424	1.5475	1.5439	1.5444	1.5499	1.5551	1.5568	1.5443	1.5460	1.5492	1.5574	1.5456	1.5461	1.5428	1.5471	1.5442	1.5449	1.5440	1.5444
γ	1.5463	1.5514	1.5477	1.5480	1.5535	1.5596	1.5613	1.5481	1.5502	1.5529	1.5611	1.5495	1.5497	1.5466	1.5510	1.5479	1.5487	1.5479	1.5480
An	18	30	21	22	35	45	50	24	27	34	50	27	27	19	29	22	25	21	24
Clinopyroxene																			
2V(+)	..	56	57	..	59	58	48	..	54	60	51								
γ	..	1.706	1.719	..	1.715	1.707	1.702	1.708	1.718	1.724	1.712								
composition																			
Ca		48	48		48	48	40	48	43	48	43								
Mg		43	33		36	41	51	41	37	29	42								
Fe		9	19		16	11	9	11	20	23	15								
Hornblende																			
2V(−)	72	77	62	70	63	79	77	62	72	63	79	69	74	73	81	76	77	69	71
γ	1.683	1.676	..	1.683	1.691	1.675	1.674	1.693	1.682	1.691	1.676	1.685	1.681	1.676	1.669	1.680	1.676	1.677	1.689
Biotite																			
γ	1.646	1.643	1.650	1.642	1.648	1.642	1.641	..	1.641	1.649	..	1.644	1.644	1.642	..	1.645	1.641	1.631	1.651
Garnet																			
n	1.779	1.786	1.788	1.775	1.785	1.780	..	1.771	1.786	1.763	..	1.785							1.791
a_0(Å)	..	11.576	11.578	..	11.590	..	..	11.608	..	..	..	..							..

* Plagioclase prophyroblasts; 2V(+) 80°, α 1.5513, β 1.5544, γ 1.5585; An 42.

Smith (1956; 1957) to correlate optical properties and chemical composition of low-temperature plagioclase. Refractive-index curves are most useful in determining compositions of rounded by hornblende (R-163). Coarse-grained metadolerites with relict subophitic texture contain andesine, whereas thoroughly recrystallized granoblastic rocks, whether am-

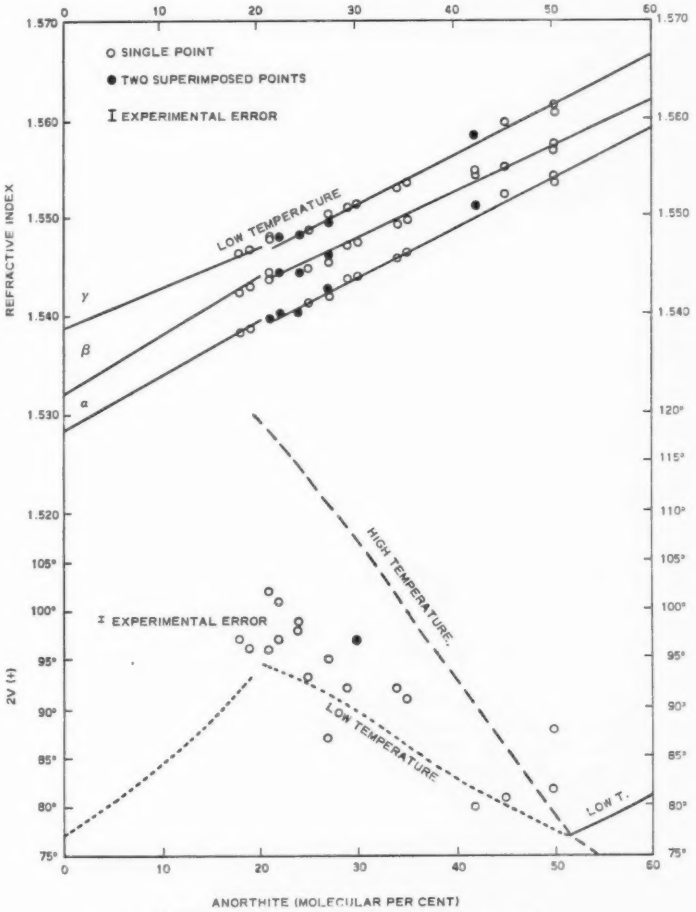

FIGURE 6.—OPTICAL DATA FOR PLAGIOCLASES
Points superimposed on J. R. Smith's graphs (Smith 1956; 1957).

plagioclase. Optic axial angles show wide scatter, hence 2V measurements cannot be used for this purpose.

Plagioclase laths in subophitic metadolerites are more calcic than equidimensional plagioclase in more thoroughly recrystallized metadolerites or in amphibolites. The most calcic plagioclase (An_{50}) is found in two rocks; olivine-metadolerite (R-36) and the fine-grained dike with relict plagioclase laths and augite surphibolites or metadolerites, contain oligoclase. The only markedly porphyroblastic metadolerite in the area (BK-48) has equidimensional oligoclase (An_{18}) in the groundmass and andesine (An_{42}) as porphyroblasts. Even the most calcic lath-shaped plagioclase (An_{50}) is not representative of the composition of plagioclase in normal, unmetamorphosed dolerites (An_{60}-An_{65}). Buddington (1939, p. 271–272; 1952, p. 51) has also found that metadolerites in the

Adirondacks with relict primary ophitic texture have plagioclase which has undergone a change in composition without change in shape. Lath-shaped plagioclase is typically clouded with submicroscopic inclusions and also contains larger inclusions of other metamorphic minerals. Both compositions and clouding of plagioclase are further discussed under petrology.

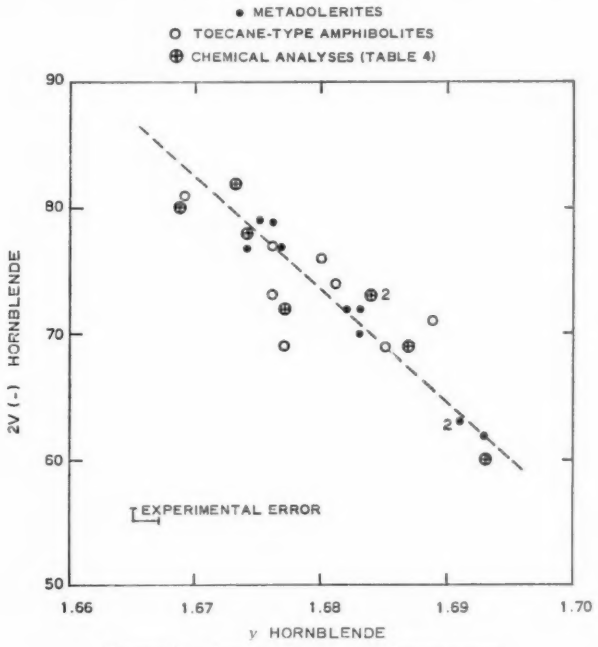

FIGURE 7.—OPTICAL DATA FOR HORNBLENDES

Twinning in plagioclases of the Bakersville-Roan Mountain rocks is complex and irregular. There is a marked difference in twinning of lath-shaped plagioclase and equidimensional crystals. Lath-shaped plagioclase is commonly complexly twinned; twin lamellae thicken and thin, bifurcate, and pinch out in the lath-shaped crystals. In thin section many equidimensional crystals appear to be untwinned, although crystals showing simple or complex twinning are also encountered. In general, the twinned equidimensional crystals have fewer twin lamellae and types of twinning than lath-shaped individuals.

Undulatory extinction is common in both lath-shaped and equidimensional crystals, but zoning is rare and indistinct. The extinction resembles strain shadows so common in quartz and may be due to slight differences in chemical composition resulting from incomplete metamorphic recrystallization, or it may reflect unrelieved strain. Clouding of relict plagioclase does not follow twinning or extinction patterns.

Pyroxenes

CLINOPYROXENE: Large relict augite is subophitic and shows clouding similar to plagioclase. Clouding rarely takes the form of hourglass structure in the augite. More intensely clouded crystals are nearly opaque. Twinning is not common, and zoning is rare. Exsolution lamellae are also rare, but clouding particles and larger inclusions are commonly aligned and form a regular grid under high magnification. Most crystals have sharp extinction, but a few show irregular extinction patterns similar to those exhibited by plagioclase. Compositions of clinopyroxenes are based on curves determined by Hess (1949, p. 634, 637).

As noted, R-57 contains mainly recrystallized pyroxene, but its optical properties are not different from those of the clouded relict augite

TABLE 4.—HORNBLENDE ANALYSES

Taken from the literature. (Analyses recalculated to 100 per cent.)

	1*	2	3	4	5	6	7	A
SiO_2	44.30	44.91	44.49	43.14	43.61	42.24	42.52	43.57
Al_2O_3	12.43	11.59	11.13	12.52	11.33	12.65	10.54	15.26
TiO_2	1.71	1.33	1.77	0.93	2.09	1.48	2.78	1.47
Fe_2O_3	0.18	2.88	2.84	4.36	4.02	4.50	4.06	1.42
FeO	10.28	11.12	12.49	10.95	9.88	11.86	16.17	12.02
MnO	0.18	0.40	0.22	0.15	0.19	0.26	0.28	0.24
MgO	14.27	11.94	11.86	11.40	12.41	10.86	9.28	10.41
CaO	12.48	11.88	11.50	12.10	12.03	11.49	11.30	12.46
Na_2O	1.01	1.46	1.84	1.21	1.38	1.25	1.45	0.45
K_2O	0.30	0.60	0.47	1.50	1.34	1.40	0.90	0.60
H_2O^-	2.86	1.80	1.25	1.68	1.63	1.94	0.72	2.10
F	n.d.	0.16	0.24	0.11	0.16	0.12	n.d.	n.d.
	100.00	100.07	100.10	100.05	100.07	100.05	100.00	100.00
−O for F		0.07	0.10	0.05	0.07	0.05		
		100.00	100.00	100.00	100.00	100.00		
γ	1.673	1.674	1.677	1.684	1.684	1.687	1.693	1.669
2V(−)	82	78	72	73	73	69	60	81

* Numbers refer to authors, as follows:

1.—Miyashiro, 1953, p. 91, no. 1; amphibolite.
2.—Rosenzweig and Watson, 1954, p. 586, no. 35/31; metagabbro.
3.—Rosenzweig and Watson, 1954, p. 586, no. 35/5; metagabbro.
4.—Buddington, 1952, p. 42, no. 4; metagabbro.
5.—Buddington, 1952, p. 42, no. 6; amphibolite.
6.—Buddington, 1952, p. 42, no. 3; amphibolite.
7.—Eskola, 1952, no. 28; metagabbro.
A.—Calculated from mode and analysis of TO-4 (Tables 2, 5).

found in other metadolerites. There may have been a composition change without change of shape in the pyroxenes, similar to that observed in plagioclase. If so, there may not be much difference in composition between the clouded relict augite and associated recrystallized, pale-green pyroxene. Both pyroxenes would be higher in Ca than the original augite (Poldervaart, 1953, p. 262; Howie, 1955, p. 764–765). The clear granules are commonly associated with minute crystals of orthopyroxene, hornblende, garnet, biotite, and magnetite. Clouding of the relict augite probably results from oxidation and ionic diffusion (*c.f.* Muir and Tilley, 1957, p. 252). Walker and Poldervaart (1949, p. 692) similarly noted that in some weathered dolerites, augite may acquire a peculiar dusty appearance where the optic axial angle has increased to 50°–60°.

ORTHOPYROXENE: Few of the metadolerites carry more than trace amounts of orthopyroxene. Optical data are:

Index	2V(−)	γ	Composition (Of)
BK-149	48	.....	47
BK-262	48	.....	47
R-36	82	1.694	18
R-158	51	1.722	44

Two subophitic metadolerites (BK-149 and BK-262) and the mafic Cranberry gneiss (R-158) contain hypersthene. The low values for 2V of the hypersthene indicate that it is a low-temperature pyroxene (Hess, 1952, p. 182). The only other occurrence of orthopyroxene is in the olivine metadolerite (R-36). This rock contains two orthopyroxenes, one a highly pleochroic variety with composition Of_{18}, the other a colorless, fibrous variety,

found in coronas around olivine and inferred to be enstatite.

Hornblende

In Figure 7, data for 2V are plotted against corresponding values for γ. Within the limits of experimental errors, most of the points fall along a straight line. The linear relationship might be taken to indicate that the hornblendes belong to a relatively simple substitution series, but this is not substantiated. Figure 7 includes optical data for seven hornblendes taken from the literature. Analyses of these hornblendes are given in Table 4. The data do not show a regular substitution series but identify the amphiboles as common calciferous hornblendes. The last column of Table 4 shows the calculated composition of hornblende in sample TO-4, computed from the rock analysis and mode. Al_2O_3 is too high in comparison with the other hornblende analyses, whereas Na_2O is too low. Calculations of this type are, of course, not reliable. Composition of plagioclase is not simply related to optical data for coexisting hornblende.

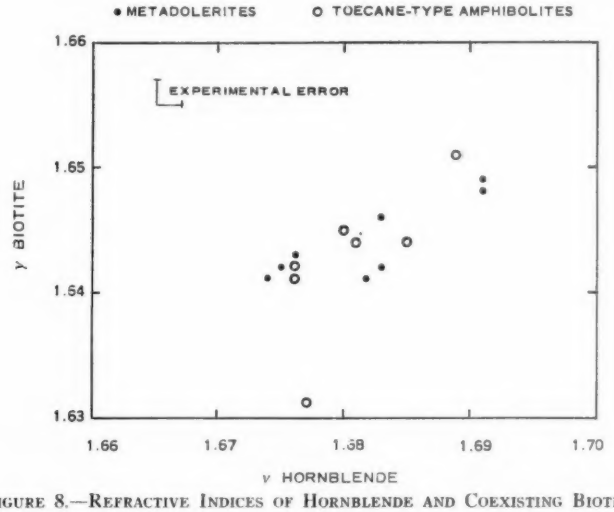

FIGURE 8.—REFRACTIVE INDICES OF HORNBLENDE AND COEXISTING BIOTITE

Biotite

Biotite is an accessory in nearly all the rocks, and it is a major constituent in a few. Values for γ of biotite vary roughly as do those of γ of hornblende (Fig. 8). Samples TO-8 and TO-9 are somewhat anomalous in having biotite with respectively the lowest and the highest γ index. Compositions of plagioclase are not simply related to optical data for coexisting biotite. Biotite is reddish brown in most of the rocks but more definitely brown in a few amphibolites. In foliated rocks, biotite tends to parallel foliation.

Garnet

Levin (1950, p. 528–533) has shown that a garnet may be accurately characterized in terms of the five end members of the group (pyrope, almandine, spessartite, grossularite, andradite) if the refractive index, specific gravity, unit-cell dimensions, and manganese or ferrous iron content are determined. In this study the only properties determined accurately are refractive index and unit-cell dimension (Table 3). They indicate that all garnet in the Bakersville-Roan Mountain metadolerites is of almandine type. Levin (1950, p. 531–533) gives compositions for garnets which have n and a_0 in the same range as those in Table 3, as follows:

Levin No.	B51	B87	RU6	JO2	Levin average	Wright average
PY	31	27	20	25	26	20
AL	44	50	52	53	50	54
SP	2	1	1	1	1	
GR	19	18	25	19	20	21
AN	6	4	2	2	3	

The composition of the four garnets closely approaches that given by Wright (1938, p. 441) for garnet characteristic of amphibolites. Garnet from an alaskite near Spruce Pine has $n = 1.778$, $a_o = 11.595$ Å, and garnet from the parallel cracks. Locally a crack may pass from garnet into adjacent hornblende or plagioclase, but in most cases the cracks are seen only in the garnets. Fracture control of garnet crystallization is seen by garnet trails which crisscross

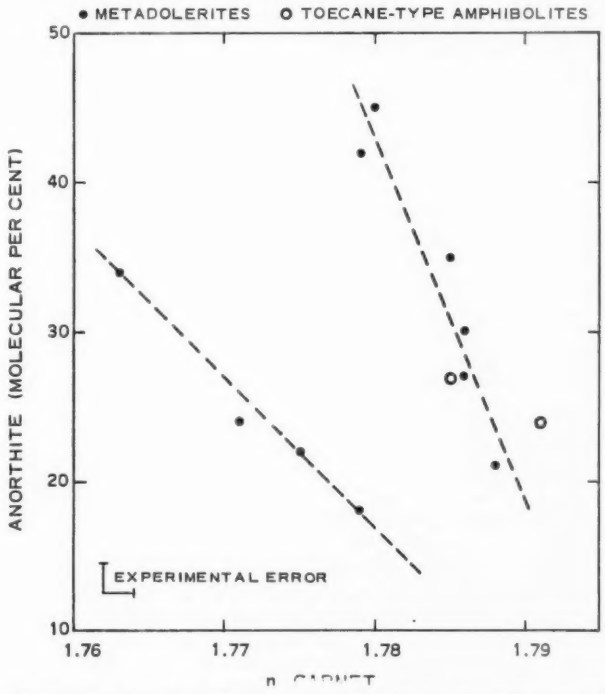

FIGURE 9.—REFRACTIVE INDEX OF GARNET WITH COMPOSITION OF COEXISTING PLAGIOCLASE

Slippery Elm pegmatite has $n = 1.789$, $a_o = 11.612$ Å. These garnets are spessartite-almandine types (*c.f.* Wells, 1937, p. 101, G and H). In Figure 9 the refractive index of garnet is plotted against corresponding plagioclase compositions. The points fall along two distinct lines, but attempts to correlate this with other data have failed, hence the meaning of this grouping of points remains obscure. Many garnets are heavily clouded and choked with inclusions of pyroxene, magnetite, biotite, and in some cases hornblende. In more thoroughly recrystallized rocks, garnet tends to form unclouded, isotropic crystals with fewer inclusions. These crystals are subhedral, with euhedral sides toward plagioclase and anhedral sides toward femic minerals. Garnet completely surrounded by plagioclase is euhedral. In some thin sections all garnets are traversed by exposures of several dikes on Roan Mountain In other outcrops garnet is more uniformly distributed as spots of crystal clusters. Fracture-controlled crystallization of garnet is also well shown in some thin sections by elongated crystals and clusters of crystals which follow healed cracks in the rock (Pl. 3, fig. 4; R-98; $n = 1.782$, $a_o = 11.580$ Å). Although rare, this phenomenon is by no means confined to garnet, and Poldervaart (in preparation) has found the same fracture-controlled crystallization of sillimanite in a few rocks from the Keimoes district, South Africa.

Other Minerals

OLIVINE: Olivine is present in few rocks of the area; it is found in only one of the analyzed rocks (R-36). It has $2V(-)$ 81°, γ1.739, com-

position Fa_{32} (Poldervaart, 1950, p. 1073). The mineral is associated with and commonly surrounded by augite. Where not surrounded by augite, it is almost invariably slightly serpentinized along fractures and rimmed by a double corona of enstatite and amphibole, with or without green spinel.

MAGNETITE: In polished sections ilmenite and magnetite are seen to be intimately mixed as discrete phases and probably also as crystal solutions. In rocks retaining subophitic texture the magnetite is coarsely crystalline and of irregular shape. In granoblastic plagioclase-pyroxene rocks, it is more skeletal or forms small crystals which are scattered uniformly throughout the rock. Continued recrystallization initiates growth of larger magnetites. In foliated amphibolites magnetite may form relatively large, irregular crystals. Sphene in some places forms granular rims around magnetite. Some coarse-grained Toecane-type amphibolites contain sphene scattered uniformly throughout the rock, whereas magnetite is absent.

ACCESSORIES: Calcite is present in some equigranular metadolerites and Toecane-type amphibolites as irregular aggregates, interstitial to other crystals. A few zircons, typical of those found in basaltic rocks (Poldervaart, 1956, p. 522–526), have been recovered from one amphibolite. Abundant zircons have been extracted from the plagioclase-pyroxene granulite (R-158) in Cranberry gneiss. These zircons have unusually smooth, rounded surfaces. Orthoclase is present in some metadolerites. Quartz is also present in places, and in some amphibolites (TO-1) quartz granules are intimately associated with hornblende, suggesting sieve structures. Other accessories include pyrite, epidote or clinozoisite, and apatite.

Chemical Data

Major Elements

Previous work has indicated the desirability of a thorough chemical investigation of associated metadolerites and ortho- and para-amphibolites to determine whether these three rock types are chemically different. The Bakersville-Roan Mountain area is especially suited to such an investigation, because the three rock types are intimately associated and can be identified by their field relationships. The fine interlayering of para-amphibolites with biotite schist and quartzofeldspathic gneiss and schist, seen in several exposures (Pl. 2, fig. 2), leaves no doubt as to the sedimentary origin of these amphibolites. The crosscutting relationships of metadolerite and ortho-amphibolite dikes establish the igneous origin of these two rock types. More problematical examples in which field relationships are not so definitive are also present. Thus this area seemed an opportune place to determine whether or not consistent chemical differences exist between mafic metamorphic rocks of igneous and of sedimentary origin.

Analyses of 22 selected rocks from the Bakersville-Roan Mountain area and the adjoining Spruce Pine district are given in Table 5; modes for 19 of these rocks and optical data for their constituent minerals are listed in Tables 2 and 3. Locations of the samples are shown in Figure 2. Rocks for which modes are given have been described. The three Roan para-amphibolites have been described by Brobst and Kulp (in press).

Tilley (1950, p. 42) showed that alkali basalts and tholeiites may be distinguished by plotting total alkalies against silica. The upper diagram in Figure 10 is such a diagram for the Bakersville-Roan Mountain rocks and identifies them as alkali basalts. Wager (1956, p. 230) found for the Hebridean basalts that separation between plateau basalts and tholeiites could be obtained by plotting Na_2O against SiO_2. This plot is given in the lower diagram in Figure 10 for the Bakersville-Roan Mountain rocks but does not result in clear definition for these rocks. The writers consider the dike rocks typical olivine dolerites (see Table 6).

Wager (1956) has suggested an ingenious method of classifying basalts into four main groups, named early-, middle-, and late-stage basalts, and late differentiates. Basalts in each division are at approximately the same stage of fractionation, but no distinction is made between different magma types. Figure 11 shows the results when this method of classification is applied to the Bakersville-Roan Mountain rocks.

Thornton and Tuttle (1956) suggested plotting oxide weight percentages against the sum of normative quartz, albite, orthoclase, nepheline, leucite, and kaliophilite. This sum, called the differentiation index, expresses numerically the extent to which a rock has approached petrogeny's residua system, and hence also marks the degree of fractionation. A differentiation-index diagram for the Bakersville-Roan Mountain rocks is given in Figure 12. In view of the considerable scatter of points, the curves drawn to indicate differentiation trends

TABLE 5.—CHEMICAL ANALYSES

Index	BK-48*	BK-56*	BK-61*	BK-95*	BK-149*	BK-262*	R-36*	R-57*	R-92*	R-158*	R-163*	TO-1†	TO-2†	TO-3**	TO 4**	TO-5**	TO-7**	TO-8†	TO-9**	SP-5-1†	SP-5-2†	SP-5-3†
SiO_2	53.22	49.70	47.92	46.86	47.11	45.39	45.93	49.27	44.24	47.49	46.94	47.95	47.03	49.37	46.74	45.90	47.01	48.03	51.00	46.63	50.28	49.58
TiO_2	2.73	1.72	2.87	3.15	3.92	2.56	1.06	3.00	4.31	1.96	1.81	3.23	2.56	2.22	1.58	3.01	2.13	2.11	2.74	0.27	0.54	0.99
Al_2O_3	15.29	14.68	13.54	13.68	12.75	15.81	11.95	12.30	13.52	13.36	14.79	16.27	15.16	14.08	16.42	14.76	15.96	15.62	14.90	13.54	16.11	16.11
Fe_2O_3	2.46	3.26	3.25	4.09	4.02	4.20	1.97	4.84	4.85	4.54	2.21	2.23	2.73	2.34	2.15	2.83	2.20	3.52	2.51	2.32	1.46	1.33
FeO	8.73	8.87	12.16	11.50	12.70	11.65	12.01	11.28	12.28	11.43	9.33	10.76	10.91	9.89	9.72	11.98	10.42	8.29	9.97	8.13	8.65	8.42
MnO	0.19	0.21	0.30	0.28	0.28	0.24	0.21	0.30	0.29	0.33	0.26	0.18	0.17	0.18	0.18	0.22	0.18	0.19	0.19	0.19	0.18	0.17
MgO	3.39	6.83	5.41	4.99	5.39	7.14	11.85	4.73	6.05	5.38	9.44	4.66	6.64	5.91	7.86	6.66	6.95	6.51	3.28	14.33	7.76	7.42
CaO	7.32	9.57	8.29	8.23	8.37	9.58	10.36	8.71	9.23	8.86	10.68	9.38	9.25	9.90	10.44	9.34	10.23	9.33	7.47	11.24	9.99	11.47
Na_2O	3.01	2.66	4.04	2.73	3.11	2.17	3.52	3.18	3.10	4.48	2.44	2.73	2.62	3.33	2.42	2.82	2.75	2.88	2.93	1.17	2.94	2.84
K_2O	1.62	0.65	1.54	1.07	1.46	0.35	0.76	1.10	0.84	0.40	0.56	1.10	1.15	0.98	0.45	0.57	0.53	1.61	2.06	0.14	0.45	0.42
P_2O_5	0.52	0.19	0.63	0.57	0.59	0.19	0.24	0.33	0.50	0.34	0.41	0.42	0.30	0.28	0.19	0.34	0.19	0.32	0.71	0.05	0.18	0.19
H_2O^+	0.35	0.30	0.20	0.45	0.27	0.28	0.53	0.12	0.23	0.33	0.51	0.98	1.29	1.15	1.59	1.39	1.37	1.47	1.09	2.08	1.43	0.79
H_2O^-	0.00	0.04	0.07	0.00	0.00	0.06	0.04	0.03	0.02	0.14	0.03	0.04	0.06	0.14	0.11	0.02	0.03	0.08	0.02	0.02	0.09	0.03
CO_2	0.76	0.81	0.00	1.89	0.12	0.00	0.00	0.64	0.84	0.00	0.00	0.13	0.01	0.00	0.00	0.00	0.00	0.01	1.07	0.03	0.00	0.23
S	0.14	0.20	0.21	0.18	0.27	0.16	0.05	0.23	0.21	0.26	0.10	0.07	0.19	n.d.	n.d.	n.d.	n.d.	0.00	n.d.	0.00	0.00	0.11
	99.73	99.69	100.43	99.67	100.36	99.78	100.48	100.06	100.51	99.30	99.51	100.13	100.07	99.77	99.85	99.84	99.95	99.97	99.94	100.14	100.06	100.10
−O for S	0.07	0.10	0.10	0.09	0.13	0.08	0.02	0.11	0.10	0.13	0.05	0.04	0.09									0.06
Total	99.66	99.59	100.33	99.58	100.23	99.70	100.46	99.95	100.41	99.17	99.46	100.09	99.98									100.04

* analyst H. B. Wiik, Helsinki, Finland.
† analyst R. H. Stokes, U. S. Geol. Survey, Denver, Colo.
** analyst L. M. Kehl, U. S. Geol. Survey, Denver, Colo.

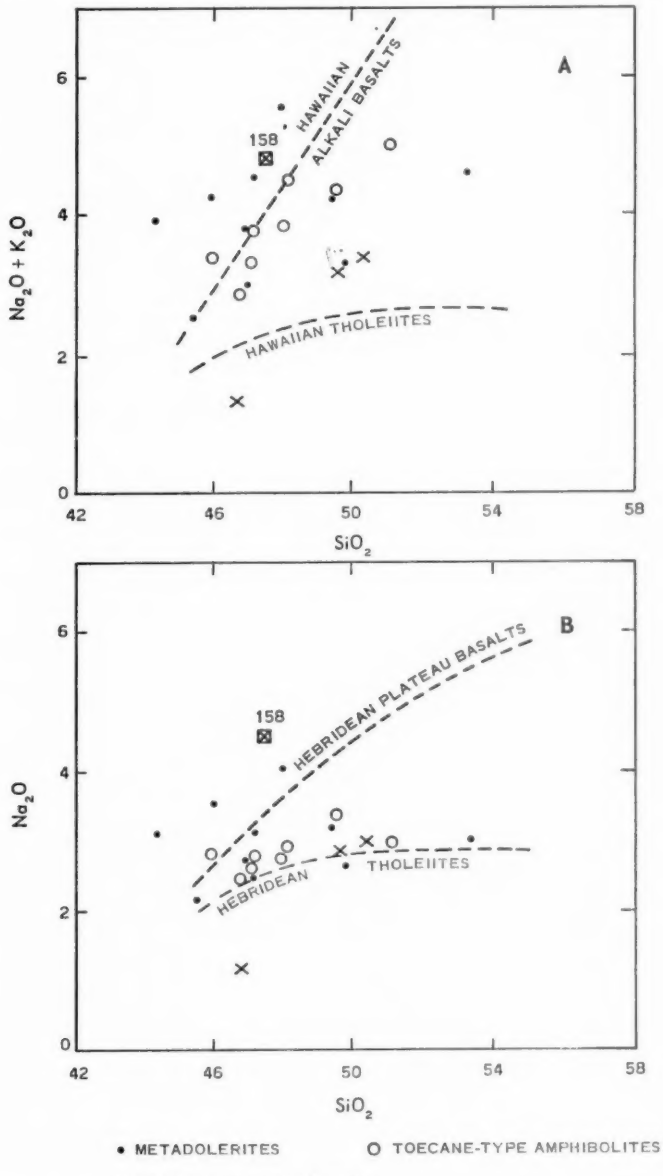

FIGURE 10.—SILICA-ALKALIES DIAGRAM FOR BAKERSVILLE-ROAN MOUNTAIN ROCKS

can only be considered as rough approximations. The peculiar trend of Al_2O_3 is especially suspicious and may not be real. Boundaries for early-, middle-, and late-stage dolerites are approximately at differentiation indices of 20, 30, and 50. When results are compared with those of Figure 11, several anomalies become apparent, especially with respect to the sub-

divisions of each of the main fractionation stages. These subdivisions have therefore been omitted in Figure 12.

Simpson (1954) suggested a diagram in which a mafic index, 100 (FeO + Fe_2O_3)/(FeO + Fe_2O_3 + MgO), is plotted against a felsic index, 100 (Na_2O + K_2O)/(Na_2O + K_2O + CaO), to show the differentiation of suites of basaltic rocks. This diagram, modified to atomic weight percentages, is given in Figure 13 for the Bakersville-Roan Mountain rocks. Divisions into early-, middle-, and late-stages are again shown and follow the divisions for Figures 11 and 12. Several anomalies between these methods of plotting chemical analyses remain.

The differentiation diagrams allow a better understanding of the petrology of the Bakersville-Roan Mountain dike rocks as representatives of basaltic magma. The rocks represent a differentiated suite of olivine basalts. The majority of the rocks belong to the middle and late stages of fractionation, but no late differentiates have been recognized. Except for Al_2O_3, variations in major elements are normal (*c.f.* Nockolds and Allen, 1954), with near-linear increases in SiO_2, TiO_2, Na_2O, and K_2O, and near-linear decreases in MgO and CaO. Variation curves for FeO and Fe_2O_3 are convex upward, indicating moderate iron enrichment and therein resembling the Easter Island basalt series (Nockolds and Allen, 1954, p. 262). The variation of Al_2O_3 is peculiar, but wide scatter of points renders it likely that the variation is more apparent than real.

Table 6.—Averages: Basalts and Amphibolites

Index	A	B	C	1	2	3	4	5	6	7
SiO_2	47.9	48.7	49.7	46.1	47.1	51.2	50.3	50.3	49.9	50.5
TiO_2	2.9	2.4	0.6	2.6	3.0	0.6	1.6	...	...	...
Al_2O_3	14.0	15.7	15.5	14.8	15.1	15.0	15.7	16.6	16.4	16.7
Fe_2O_3	3.8	2.6	1.7	3.2	3.7	2.0	3.6	3.7	3.7	3.7
FeO	11.3	10.4	8.5	8.8	8.1	9.3	7.8	8.9	12.1	7.8
MnO	0.3	0.2	0.2	0.2	0.2	0.2	0.2	...	...	...
MgO	6.4	6.2	10.0	9.4	7.9	8.8	7.0	6.9	6.2	7.2
CaO	9.2	9.6	11.1	10.8	10.9	9.8	9.5	10.0	8.6	10.5
Na_2O	2.9	2.8	2.3	2.7	2.7	2.2	2.9	2.9	2.4	2.9
K_2O	0.9	1.1	0.3	1.0	1.0	0.8	1.1	0.7	0.7	0.7
P_2O_5	0.4	0.3	0.1	0.4	0.3	0.1	0.3	...	...	...
	100.0	100.0	100.0	100.0	100.0	100.0	100.0	100.0	100.0	100.0

A.—Average 8 Bakersville-Roan Mountain metadolerites.
B.—Average 8 Toecane ortho-amphibolites.
C.—Average 3 Roan para-amphibolites.
1.—Average 96 alkali basalts (Nockolds, 1954, p. 1021).
2.—Average Pacific olivine basalt (Green and Poldervaart, 1955, p. 185).
3.—Average 5 Quad Creek para-amphibolites (Eckelmann and Poldervaart, 1957, p. 1252).
4.—Average 200 amphibolites (Poldervaart, 1955, p. 134).
5.—Average 89 amphibolites (Lapadu-Hargues, 1953, p. 161).
6.—Type ortho-amphibolite (Lapadu-Hargues, 1953, p. 161).
7.—Type para-amphibolite (Lapadu-Hargues, 1953, p. 161).

Table 6 lists averages for the rocks. The eight metadolerites averaged do not include BK-48, a porphyroblastic rock; R-36 which contains 12 per cent olivine; and R-158, now known to be country rock. Averages for eight Toecane-type amphibolites and three Spruce Pine amphibolites are nearly identical. For comparison, averages are also listed for amphibolites and olivine-basalts.

There are no essential differences between the analyses of the metadolerites and those of the Toecane-type amphibolites, which in turn closely approach Poldervaart's (1955, p. 136) average amphibolite, except for slightly lower SiO_2 and MgO, and higher FeO. Averages from distinctly bedded para-amphibolites from the Spruce Pine district and the Beartooth Mountains of Montana and Wyoming also resemble

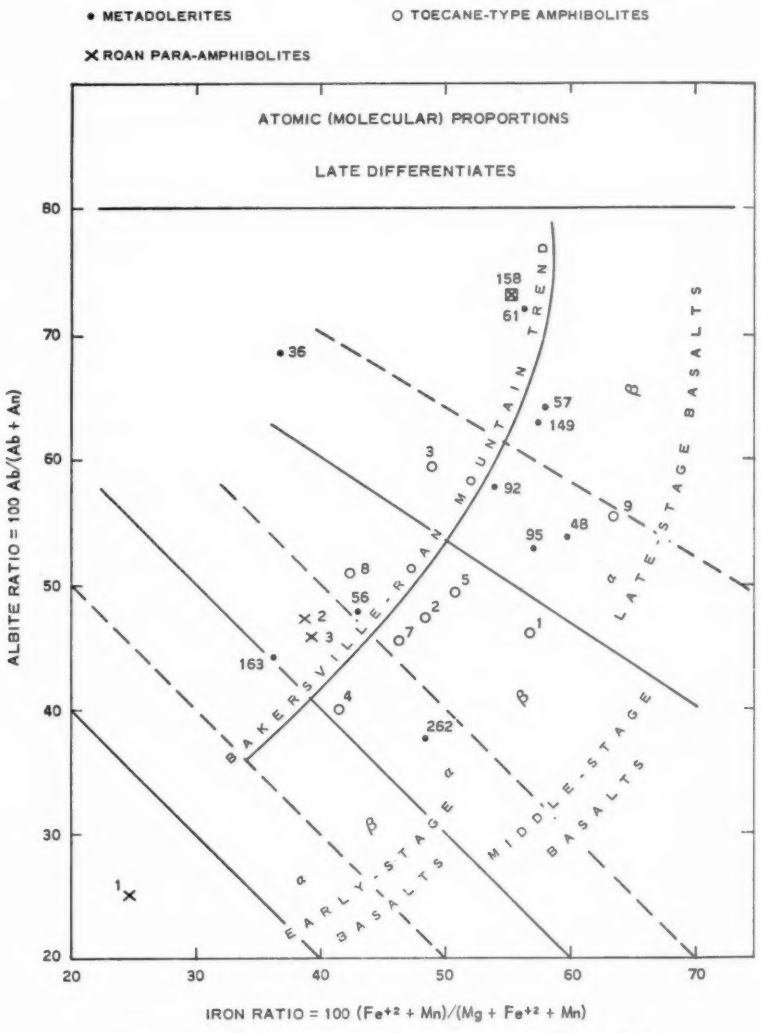

FIGURE 11.—DIFFERENTIATION DIAGRAM AFTER WAGER (1956)

those of the metadolerites and Toecane-type amphibolites. The most consistent difference is in TiO_2 content, which is low in both the Roan and Quad Creek para-amphibolites (0.6 per cent against 2–3 per cent for basaltic rocks and ortho-amphibolites). In view of the well-known variability of TiO_2 in basaltic rocks, it is doubtful that titanium can serve as a general criterion to distinguish ortho- from para-amphibolites. In Figure 14 the 22 analyses have been plotted on superimposed ternary diagrams of Mg-Fe_{total}-(Na + K) and Ca-K-Na. Again it is apparent that the three rock types represented cannot be distinguished by these elements.

Selected Minor Elements

Since no differences could be established between ortho- and para-amphibolites by their bulk chemical compositions, an attempt was made to determine whether the two types of

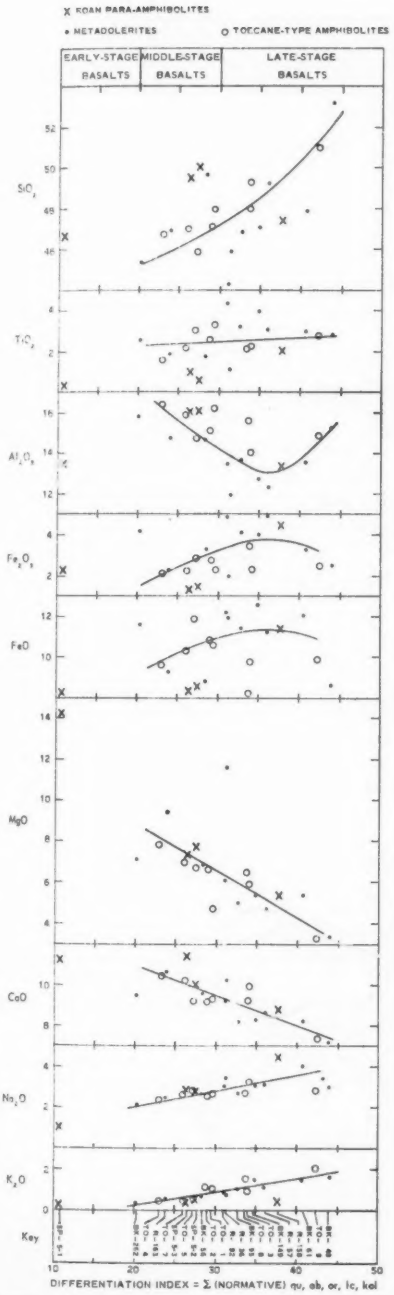

FIGURE 12.—DIFFERENTIATION DIAGRAM AFTER THORNTON AND TUTTLE (1956)

amphibolites can be distinguished by their contents of trace elements. For this purpose the elements gallium, copper, chromium, nickel, cobalt, barium, and strontium were chosen. Two hundred thirty-five metadolerites and amphibolites from the Bakersville-Roan Mountain area were analyzed semiquantitatively for these elements by emission spectrographic techniques. Twenty-three of the rocks were analyzed quantitatively for strontium by an improved spectrographic method (Turekian and Kulp, 1956).

Standard diabase W-1 (Fairbairn *et al.*, 1951) was chosen as one standard (A) for the semiquantitative analyses; the second standard (B) consisted of W-1 plus spikes of other elements. Table 7 gives the two standards.

Spectrographic films have been examined visually, and comparisons were made between sample and the two standards. Six readings are possible for each element: 0, below limits of sensitivity; 1, less than standard A; 2, equal to standard A; 3, between standards A and B; 4, equal to standard B; 5, greater than standard B.

The results of the semiquantitative analyses are listed in Table 8. The number code describes analyses for barium, nickel, cobalt, and chromium, in that order. Copper is absent in all the rocks, and gallium is of constant amount equal to standard A (14 ppm).

Figure 15 is a series of histograms on which abundances of barium, nickel, cobalt, and chromium are plotted against the frequency of samples having these concentrations. Of the 235 samples, 155 are metadolerites, 36 are para-amphibolites from the Roan formation, and the remaining 44 rocks are Toecane-type amphibolites. There is a striking similarity in the frequencies of Ni, Co, and Cr between the three groups of rocks. Frequencies for Ba are more variable. It is clearly impossible to distinguish between the three rock types on the basis of these semiquantitative analyses.

Trace-element results for the analyzed rocks are given in Table 9 in which rocks are listed in the same order as in Table 5. No systematic variation with stage of fractionation can be discerned in these trace-element data. Data given by Nockolds and Allen (1954) also indicate little systematic variation in these trace elements in the equivalent middle- and late-stage basalts studied by them.

Table 10 shows the strontium content for 22 rocks (Turekian and Kulp, 1956, p. 251). A minor error in the Turekian-Kulp paper is the inclusion of R-158 (MD 7, Sr: 254 ppm) in the

Bakersville-Roan Mountain metadolerites. This rock is now known to be mafic Cranberry country rock, and its exclusion from the metadolerites raises the average strontium for this group from 326 to 338 ppm. Statistical comparisons show that the three averages are significantly different from one another at the 1 per cent significance level. The writers do not attach much weight to differences in Sr content between the metadolerites and the Toecane-type amphibolites. This will be discussed further under petrology. However, the lower Sr value shown by the Roan para-amphibolites, as compared with the metadolerites and Toecane ortho-amphibolites, is of considerable interest and raises the question whether ortho- and para-amphibolites can be distinguished by their Sr contents. Turekian and Kulp (1956, p. 267) found a mean Sr content of 465 ppm for basaltic rocks but emphasize the variability of Sr in basaltic rocks. Vinogradov, Ronov, and Ratynski (reviewed by Chilingar, 1957, p. 274) found a mean Sr content of about 40 ppm for Precambrian carbonate rocks of the Russian platform, but the work of Turekian and Kulp (1956) indicates great variations in Sr content of argillites and calcarenites which were deposited in different environments in different ages. These data are encouraging, but considerably more work must be done before Sr contents can be accepted as valid means of distinguishing between ortho- and para-amphibolites. Work on this problem is being continued in the Beartooth Mountains of Montana and Wyoming.

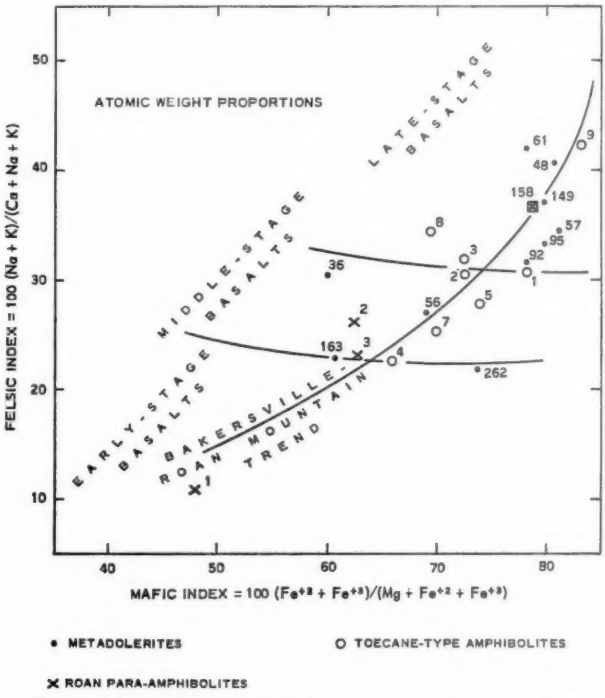

FIGURE 13.—DIFFERENTIATION DIAGRAM AFTER SIMPSON (1954)

PETROLOGY

Metamorphic Clouding

In most of the metadolerites which have relict, lath-shaped plagioclase and relict, subophitic augite, these minerals are clouded. Clouding varies in intensity in different metadolerites, from one crystal to the next in the same rock, and even in different parts of the same crystal. Clouding has been discussed by MacGregor (1931), Poldervaart and Gilkey

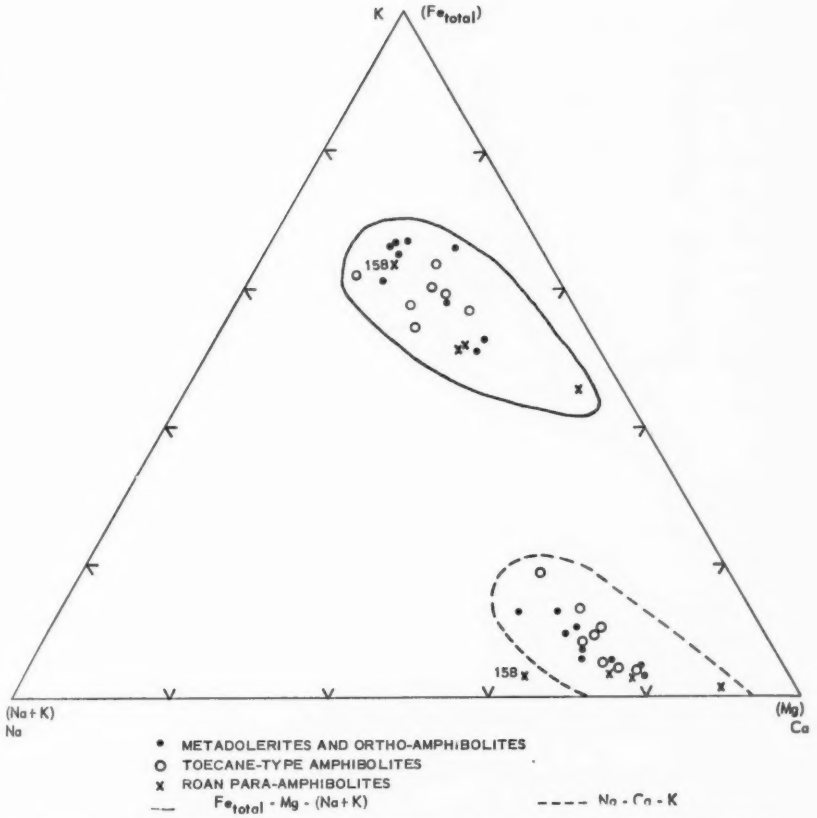

FIGURE 14.—SUPERIMPOSED TERNARY DIAGRAMS OF Fe_{total}-MG-(NA+K) AND NA-CA-K (ATOMIC WEIGHT PER CENT)

TABLE 7.—STANDARDS FOR SPECTROGRAPHIC ANALYSES

Element	A (per cent)	B (per cent)
Ba	0.027	0.27
Ni	0.007	0.067
Co	0.0039	0.064
Cr	0.013	0.100
Ga	0.0014	0.011
Cu	0.012	0.102

(1954), and by Murthy (1958), and has been observed in plagioclase, pyroxene, olivine, garnet, spinel, hornblende, apatite, and other minerals. MacGregor attributes clouding to exsolution upon heating of impurities present in crystal solution in the mineral at the time of its primary crystallization. Poldervaart and Gilkey think it more likely that clouding results from diffusion of ions into the crystals at elevated temperatures and subsequent formation of clouding particles in the host mineral. Buerger's (1948, p. 114) remark that a mineral just below its temperature of recrystallization acts like "a blotter for available atoms" is relevant. As conditions favorable to clouding, Poldervaart and Gilkey (1954, p. 87) list relatively high Fe content of original rocks, long duration of elevated temperatures (probably not lower than 450° C.), and general water deficiency.

The nature of the clouding material is not known, but the particles probably represent a number of phases rather than one mineral. With oil immersion and magnification of 1000×,

TABLE 8.—SPECTROGRAPHIC DATA FOR SELECTED MINOR ELEMENTS

Abundance				Number of Rocks		
Ba	Ni	Co	Cr	Metadolerites	Toecane-type amphibolites	Roan para-amphibolites
1	1	2	2	..	..	2
1	2	2	2	..	..	3
1	2	2	3	..	..	2
1	4	2	3	..	..	1
1	4	2	4	..	..	3
1	4	2	5	..	..	1
2	0	0	2	..	1	..
2	0	1	2	1	..	..
2	0	2	2	..	1	..
2	1	1	2	3	2	..
2	1	2	2	20	5	4
2	1	3	2	..	..	1
2	2	1	2	7	..	..
2	2	1	3	1	..	..
2	2	2	2	42	5	10
2	2	2	3	1	..	..
2	2	2	4	7	1	1
2	2	3	2	7	..	..
2	2	3	3	..	..	1
2	3	2	4	1	..	..
2	4	2	4	1	..	..
2	4	3	2	2	..	..
3	0	0	2	..	1	..
3	0	1	1	2	..	..
3	0	1	2	..	2	..
3	0	2	1	2	..	..
3	0	2	2	..	1	..
3	1	0	0	1	..	..
3	1	1	2	1	..	..
3	1	2	1	3	2	..
3	1	2	2	26	11	1
3	1	3	1	..	1	..
3	1	3	2	2	1	..
3	2	1	2	1	..	..
3	2	2	2	15	5	..
3	2	2	3	3	1	1
3	2	2	4	3	..	..
3	2	3	2	1	..	1
4	0	0	1	..	1	1
4	0	0	2	1	2	..
4	1	0	3	..	..	1
4	1	1	1	..	1	..
4	1	1	2	..	..	1
4	2	2	2	1	..	..
4	2	2	3	..	..	1

regular alignment of the particles within the host mineral is evident, and both opaque and transparent particles are seen. Larger inclusions associated with clouding may be hornblende, pyroxene, magnetite, garnet, biotite, and spinel, but larger inclusions are not necessarily the same phases as the clouding particles. In metadolerites which contain both relict, heavily clouded plagioclase and recrystallized, clear plagioclase, the two feldspars can be separated with a Frantz separator, clouded plagioclase forming the magnetic fraction. X-ray powder photographs of clouded pyroxene and clouded plagioclase have been made. The identity of the clouding material in pyroxene is not resolved by X-ray photographs, but powder photographs of heavily clouded plagioclase indicate that the particles may be rhombic pyroxene. However, no certain identification of clouding material was possible by X-ray methods.

Plagioclases of two samples have been separated, using bromoform and a Frantz separator. One plagioclase (BK-140; An_{42}) is heavily clouded; the other (BK-149; An_{35}) shows slight clouding. The concentrates were checked microscopically; mafic minerals were absent, but a little orthoclase was present in sample BK-149. Chemical analyses of the two samples are given in Table 11; in Table 12 the two analyses are compared with other plagioclases of similar composition. The most conspicuous difference between clouded and unclouded plagioclase is the FeO content which, even in the slightly clouded plagioclase, is higher than in unclouded feldspar. MgO is also higher in clouded plagioclase, but differences with unclouded feldspar are not so marked. All the feldspars have excess alumina, highest in the heavily clouded plagioclase but also quite high in the antiperthitic, unclouded plagioclase No. 6 (Table 12). Silica is either in excess or deficient in these feldspars (*c.f.*, Emmons *et al.* 1953, p. 15).

The data render it likely that clouding results from diffusion of foreign ions into pre-existing crystals during metamorphism and subsequent exsolution of impurities in crystal solution. The high FeO in sample A (Table 11) can scarcely have been present in the original plagioclase since there are no known examples of unmetamorphosed iron-plagioclases. It is likely that diffusion resulted in the plagiclase becoming more sodic without changing its original shape, presumably through emigration of Ca^{+2} ions. The immigration of Fe^{+2} ions, now seen as

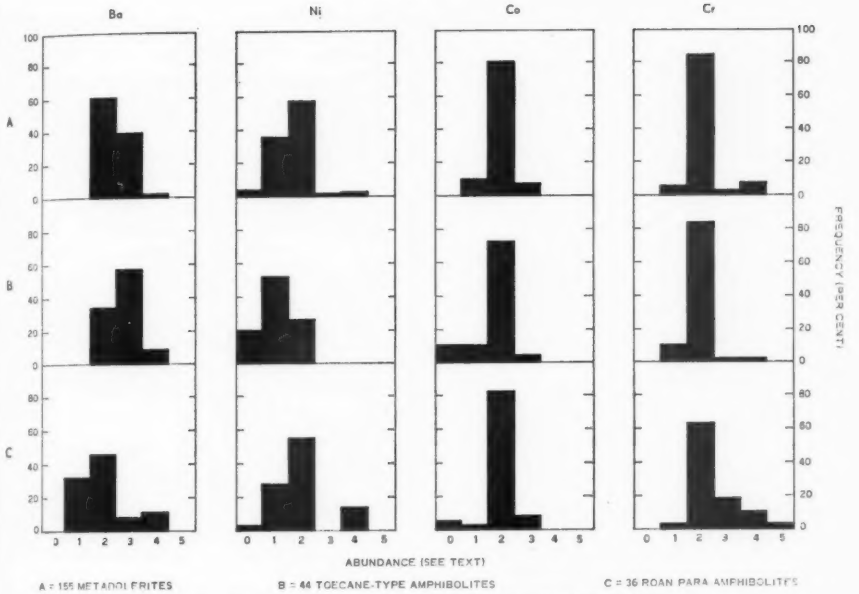

FIGURE 15.—SPECTROGRAPHIC DATA FOR SELECTED MINOR ELEMENTS

TABLE 9.—SPECTROGRAPHIC DATA FOR ANALYZED ROCKS

Index	Abundance			
	Ba	Ni	Co	Cr
BK-48	3	0	1	2
BK-56	2	0	1	2
BK-61	3	1	3	2
BK-95	3	2	3	2
BK-149	3	1	2	2
BK-262	2	1	2	2
R-36	2	4	3	2
R-57	2	1	2	2
R-92	2	2	2	2
R-158	2	1	2	1
R-163	2	2	2	4
TO-1	3	1	2	1
TO-2	3	2	2	2
TO-3	2	1	2	2
TO-4	2	2	2	2
TO-5	2	2	2	2
TO-7	2	2	2	2
TO-8	3	2	2	3
TO-9	3	1	2	1

clouding, is considered part of the same diffusion process which affected plagioclase before its marginal replacement by garnet and hornblende (Poldervaart and Gilkey, 1954, p. 82, Fig. 5).

Ionic diffusion proposed to explain metamorphic clouding is strictly on a scale of a few millimeters. Contacts of metadolerite dikes against chemically contrasted Cranberry gneiss remain knife-sharp, even after Ordovician-Silurian regional metamorphism. The writers consider that this provides strong argument against the large-scale "solid diffusion" advocated by some geologists to explain regional granitization.

The nature of the clouding material remains unknown, but the analyses indicate that the main phase may be an iron-rich rhombic pyroxene (eulite).

Metamorphic Facies

In Figure 16 the analyses have been plotted on an ACF diagram. Corrections for magnetite and ilmenite have been made by estimating proportions of these minerals from the norms and apportioning modal opaque minerals accordingly. Compositions of constituent minerals are also indicated on the diagram.

All the chemically analyzed rocks fall in a relatively small field of the ACF diagram. The metamorphism is clearly amphibolite facies, but no distinction can be made between the staurolite-kyanite subfacies and the sillimanite-almandine subfacies, since all analyses fall in the field plagioclase-hornblende-almandine, which is common to both subfacies. Examination of thin sections of Cranberry-Henderson, Roan, and Carolina gneisses and schists throughout the Spruce Pine district (Eckelmann and Kulp, 1956; Brobst and Kulp, in press) shows that metamorphism is probably of high staurolite-kyanite or low sillimanite-almandine subfacies. Taking mineral assemblages of all the different rock types into account, the writers consider that metamorphic temperatures cannot have been much lower nor much higher than 450°–500° C.

Positions of points within the field plagioclase-hornblende-almandine do not reflect the mineralogy of the rocks, *i.e.*, points nearest almandine do not necessarily contain garnet, and those nearest diopside are not necessarily richest in diopside. However, the olivine metadolerite R-36 is nearest to the F corner of the diagram, whereas rocks with least hornblende fall nearest to diopside. No distinction can be made between amphibolites and pyroxene-hornblende metadolerites, nor between rocks with or without garnet. Both the close association of rocks of different mineralogy and the lack of correlation of mineralogy and position of samples on the ACF diagram indicate that the metamorphic intensity was the same for all the rocks and that their mineralogy was determined not only by temperature but also by water content.

TABLE 10. STRONTIUM ANALYSES (PPM)

Group	Index No.	Turekian and Kulp (1956) Code No.	Sr	Mean	Standard deviation
Metadolerites					
	BK-48	MD-1	384		
	BK-95	MD-2	211		
1	BK-262	MD-3	300	338	112.7
	R-36	MD-4	242		
	R-57	MD-5	370		
	R-92	MD-6	521		
Toecane-type amphibolites					
	TO-1	MD-8	524		
	TO-2	MD-9	606		
	TO-3	MD-10	424		
2.	TO-4	MD-11	445	478	64.8
	TO-5	MD-12	495		
	TO-7	MD-13	397		
	TO-8	MD-14	457		
	TO-9	MD-15	480		
Roan para-amphibolites					
		BK-303	315		
		BK-304	133		
		BK-305	117		
3.		BK-306	56	144	87.0
		BK-307	37		
		BK-308	90		
		BK-309	133		
		BK-310	270		

TABLE 11.—ANALYSES OF CLOUDED PLAGIOCLASE

(Eileen H. Oslund, analyst.)

Index	BK-140*	BK-149†
SiO_2	53.95	58.96
TiO_2	0.16	0.11
Al_2O_3	27.45	24.82
Fe_2O_3	0.27	0.09
FeO	2.02	0.41
MnO	0.02	0.004
MgO	0.25	0.18
CaO	8.81	7.22
Na_2O	5.78	6.52
K_2O	0.58	1.27
P_2O_5	0.05	0.11
H_2O^+	0.13	0.10
H_2O^-	0.01	0.01
CO_2	0.39	0.12
	99.87	99.92

* BK-140 Heavily clouded plagioclase.

† BK-149 Slightly clouded plagioclase, admixed with orthoclase.

Role of Water

Yoder (1955, p. 521–522) has shown that at 1 atmosphere pressure, almandine is stable below 785° C. In the presence of water as a free phase, almandine is stable only below 785° C. and above the stability range of hydrous minerals such as hornblende and biotite, but in the water-deficient region it is stable also at lower temperatures. In this respect the behavior of garnet is similar to that of enstatite (Yoder, 1955, p. 516–518). Most of the Bakersville-

TABLE 12.—PLAGIOCLASE ANALYSES

Index	A	B	1	2	3	4	5	6	7
SiO_2	54.65	59.38	59.87	60.14	59.25	56.16	58.01	59.51	59.95
Al_2O_3	27.80	24.99	25.47	25.28	25.91	27.69	26.39	25.60	24.80
TiO_2	0.16	0.11	0.03	0.02	0.02	0.04	....	....	0.16
Fe_2O_3	0.27	0.09	0.06	0.05	0.05	0.08	0.04	0.26	0.35
FeO	2.05	0.41	0.07	0.06	0.05	0.15	0.15	0.13	0.21
MnO	0.02	....	....	....	....	....	....	0.01	....
MgO	0.25	0.18	0.05	0.02	0.05	0.06	0.03	0.11	0.02
CaO	8.36	6.99	7.02	7.00	7.45	9.71	7.83	6.35	6.64
Na_2O	5.85	6.57	7.18	6.91	6.90	5.49	6.47	6.92	7.53
K_2O	0.59	1.28	0.25	0.52	0.32	0.62	1.10	1.11	0.34
	100.00	100.00	100.00	100.00	100.00	100.00	100.00	100.00	100.00
Qu	*−1.40*	0.83	2.05	2.95	1.88	0.92	*−0.73*	1.25	0.70
Cor	2.34	0.10	0.63	0.63	0.68	0.34	0.33	1.48	0.11
Or	3.48	7.56	1.47	3.07	1.89	3.66	6.49	6.56	2.00
Ab	49.49	55.55	60.73	58.43	58.35	46.43	54.71	58.53	63.69
An	41.47	34.67	34.82	34.72	36.95	48.16	38.83	31.49	32.58
En	0.62	0.45	0.12	0.05	0.12	0.15	0.07	0.27	0.05
Of	3.31	0.50	0.03	0.04	0.02	0.14	0.24	0.04	....
Il	0.30	0.21	0.06	0.04	0.04	0.08	....	....	0.11
Sph	....	....	....	....	....	....	....	....	0.25
Mt	0.39	0.13	0.09	0.07	0.07	0.12	0.06	0.38	0.51
	100.00	100.00	100.00	100.00	100.00	100.00	100.00	100.00	100.00
An (calc)	43.9	35.5	35.9	36.1	38.0	49.0	38.8	32.6	33.2

A.—Strongly clouded plagioclase (An_{42}), sample BK-140.
B.—Lightly clouded plagioclase (An_{35}), sample BK-149.
1.—Emmons *et al.* (1953, p. 18, no. 6), granodiorite gneiss.
2.—Emmons *et al.* (1953, p. 18, no. 7), dacite.
3.—Emmons *et al.* (1953, p. 18, no. 8), granodiorite.
4.—Emmons *et al.* (1953, p. 18, no. 9), anorthosite.
5.—Howie (1955, p. 745, no. 4624A), antiperthitic plagioclase, hypersthene diorite.
6.—Howie (1955, p. 745, no. 2270), antiperthitic plagioclase, intermediate rock.
7.—Howie (1955, p. 745, no. 6436), charnockite.

Roan Mountain metadolerites are garnetiferous, but if these rocks were metamorphosed under water-deficient conditions, garnet could have formed over a wide range of temperatures below 785° C. Toecane-type amphibolites may contain small amounts of garnet, but in general their metamorphism seems to have been effected in the presence of water as a free phase and at temperatures somewhat below the stability range of hornblende. Garnet is exceedingly common in the associated Roan and Carolina schists and gneisses and is a minor constituent in most of the Spruce Pine pegmatites, but this latter is a spessartite-almandine garnet. Rhombic pyroxene has a similar pattern of occurrence and is relatively common in the Bakersville-Roan Mountain metadolerites but exceedingly rare in all other rocks of the Spruce Pine district.

Boyd's (1956, p. 198–200) work allows better understanding of pyroxene-hornblende relationships in igneous and metamorphic rocks. His diagram of the pargasite stability relationships is reproduced in Figure 17. The pargasite field corresponds to the amphibolite facies, the region above boundaries B and C to a magmatic facies, whereas the field bounded by A and B conforms to the pyroxene hornfels or pyroxene

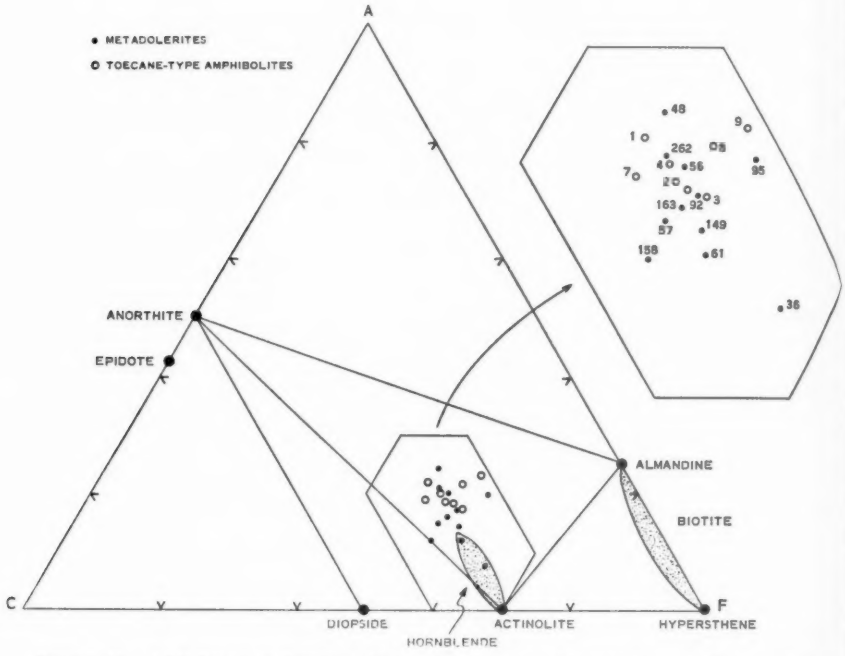

FIGURE 16.—ACF DIAGRAM SHOWING METADOLERITES AND AMPHIBOLITES IN RELATION TO SELECTED MINERALS OF THE AMPHIBOLITE FACIES

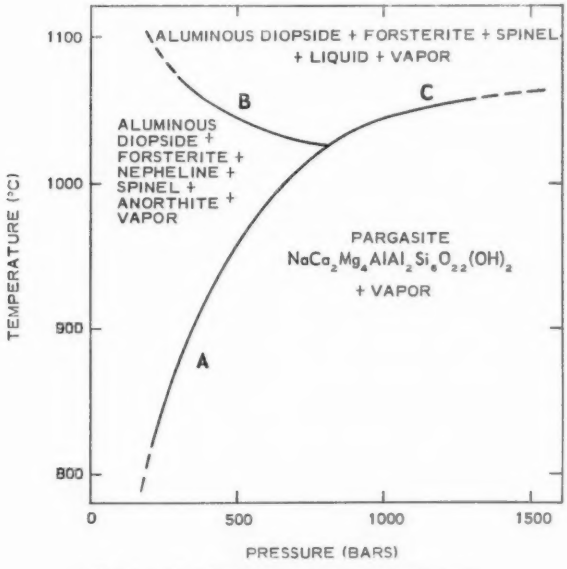

FIGURE 17.—STABILITY FIELD OF PARGASITE
(After Boyd, 1956.)

granulite facies. The two pyroxene facies represent conditions of low water pressure. Boyd (1956, p. 199–200) notes that

> "... the vapor pressure must be less than that of the invariant point ... for a subsolidus pyroxene assemblage to be stable at all."

Figure 17 only shows the effects of temperature and water pressure on the stability of pargasite, and water as a free phase is present throughout. To consider the effects of water content also, arguments similar to those of Yoder (1955, p. 516–518) for the system MgO-SiO_2-H_2O would have to be used, and a water-deficient region postulated in which anhydrous minerals are separated from water as a free phase by a "Yoder umbrella". Combining these observations by Yoder and Boyd, it would seem that at temperatures of 450°–500° C., pyroxene (olivine) assemblages in metamorphosed basaltic rocks are stable in the presence of water as a free phase only at low total pressures, whereas in the water-deficient region these assemblages become stable also at higher total pressures. Considering also the presence of garnet in the metadolerites and its absence in the associated ortho-amphibolites, it becomes apparent that the Bakersville-Roan Mountain metadolerites have been produced by metamorphic recrystallization under water-deficient conditions.

Sutton and Watson (1951) and Poldervaart (1953, p. 263–266) have discussed three different trends in the metamorphism of basaltic rocks, only one of which (Wiseman, 1934, p. 355; Turner, 1948) is regarded as "normal"; the other two are considered "abnormal". The abnormal granulitic trend in which basaltic rocks recrystallize to a plagioclase-pyroxene assemblage (with or without hornblende and garnet) is generally regarded as belonging to the granulite facies, since the mineral assemblage is the same as that of the highest metamorphic facies. Characteristic of the granulitic trend is the partial preservation of original textures, heavy clouding of main constituent minerals, and the partial replacement of original subophitic augite by granoblastic aggregates of minute diopside and hypersthene (hornblende, garnet), and of original lath-shaped plagioclase by granoblastic plagioclase, resulting in a general decrease in grain size of the rocks. Poldervaart (1953, p. 265–266) has pointed out that these features may reflect water-deficient conditions of metamorphic recrystallization, rather than unusually high metamorphic temperatures.

Stages of Recrystallization

Since all the Bakersville-Roan Mountain rocks have apparently been subjected to the same temperature for the same duration, the various stages recognized in their recrystallization evidently represent their response at different water concentrations. With little water present, recrystallization failed to destroy original textures and was presumably effected chiefly by diffusion of ions along crystal boundaries and through crystal lattices—so-called solid diffusion. In the presence of water as a free phase (Toecane-type amphibolites), the rocks were completely recrystallized in the same time and at the same temperatures. The four stages of recrystallization described herein reflect only differences in water content during metamorphism. They are to be considered as four arbitrarily selected points in a continuum, so that all gradations may be encountered between any two successive stages.

STAGE 1. EXTREME WATER DEFICIENCY: Subophitic textures preserved. Plagioclase has become clouded and changed from its original composition to An_{30-45} without change of form. The laths may be somewhat ragged in outline, due to marginal development of small clear granules of plagioclase (An_{15-30}), hornblende, diopside, garnet, and magnetite. Augite has become intensely clouded and changed in composition toward diopside-salite. Marginally the augite is replaced by diopside and hypersthene, or diopside and brown or brownish-green hornblende. Garnet also appears marginal to augite, especially along boundaries with plagioclase. The garnet granules are euhedral toward plagioclase and anhedral toward pyroxene. Minute crystals of magnetite are dusted throughout the rock, and original skeletal magnetite may show numerous protrusions, further emphasizing its irregular shape. Orthoclase and biotite are present in rocks with appreciable potassium.

STAGE 2. WATER DEFICIENT: Subophitic texture partly preserved. Clouded plagioclase is nearly completely replaced by a mosaic of small, clear granoblastic plagioclase An_{15-30}. The mosaics partly preserve outlines of former laths, but boundaries are increasingly irregular. Augite crystals are similarly replaced by granoblastic aggregates of diopside, hypersthene, brownish-green hornblende, and garnet. Slight differential movements or continued mineral growth rapidly destroy all traces of the original texture.

STAGE 3. BORDERLINE EXAMPLES: Subophitic

texture completely destroyed; the rock is medium- to fine-grained and has a uniform, granoblastic texture. Higher water content is indicated by absence of rhombic pyroxene and rapid increase in brownish-green to green hornblende at the expense of diopside, garnet, and plagioclase. Small magnetite crystals, commonly rimmed by sphene, are scattered throughout the rocks. Biotite takes the place of orthoclase in these rocks.

STAGE 4. SMALL EXCESS OF WATER: The rocks are now completely recrystallized and are coarse- to medium-grained, with granoblastic textures. Essential minerals are plagioclase An_{15-30} and green hornblende. Pyroxene is absent. Minor constituents are magnetite, biotite, and sphene, with quartz, garnet and zoisite present in some places. With somewhat larger excess of water the hornblende changes from green to bluish green. Although bluish-green hornblende is characteristic of the epidote-amphibolite facies (Turner and Verhoogen, 1951, p. 462), in the Bakersville-Roan Mountain rocks, its presence is clearly due to higher water content rather than lower metamorphic temperatures.

Amphibolite Problems

Recent field and laboratory work allows better understanding of metabasaltic rocks and the factors contributing to their recrystallization. At the same time new problems have been recognized and older problems have been emphasized. Poldervaart (1953, p. 262–263) has discussed difficulties in establishing the metamorphic origin of basaltic rocks in the granulite facies (or of the granulitic trend in the amphibolite facies), since the mineral assemblage of such rocks is similar to that of their unmetamorphosed equivalents. Probably some occurrences described in the literature as unmetamorphosed are in reality of metamorphic origin. It seems easier to distinguish between relatively rapidly cooled basalts and dolerites and their metamorphosed equivalents than to differentiate between slowly cooled gabbros, especially norites, and corresponding metamorphosed rocks. The present study contributes only to the distinction between hypabyssal basaltic rocks and equivalent metadolerites, but the textural and mineralogical criteria developed may also be applied to volcanic basalts and equivalent metabasalts. However, no criteria have been developed to distinguish plutonic basaltic rocks from metagabbros and metanorites. Further work on this problem is desirable and has many applications, including a better understanding of time relationships in metamorphic regions. Many features ascribed to magmatic crystallization, for example in the Cortlandt Complex (Shand, 1942) and the Baltimore gabbro (Herz, 1951), may prove to result instead from metamorphism.

In their investigation of the system basalt-water, Yoder and Tilley (1956, p. 169–171) have found that basaltic magmas that crystallize to plagioclase-pyroxene assemblages must have little water, since with high water content such magmas would crystallize to amphibolites or hornblendites. This important discovery raises the question whether some amphibolites and hornblendites described in the literature as being of metamorphic origin are not really primarily magmatic features. Thus there is reason for extreme caution, both in regarding plagioclase-pyroxene assemblages as magmatic in origin, and in concluding that plagioclase-hornblende assemblages have resulted from metamorphism.

Amphibolite problems include the controversial issue of para- versus ortho-amphibolites. The literature contains several claims that these two types of amphibolites can be distinguished on the basis of their bulk chemical compositions or trace-element contents (*e.g.*, Lapadu-Hargues, 1953; Engel and Engel 1951). Data presented in this study (*see also* Eckelmann and Poldervaart, 1957, p. 1251) do not substantiate these claims. From 89 amphibolite analyses, Lapadu-Hargues computed compositions for ortho- and para-amphibolites (Table 6) by plotting oxide weight percentages for each element against frequencies. FeO, MgO, CaO, and Na_2O gave bimodal distributions, whereas other constituents showed modal distributions. Lapadu-Hargues' type ortho-amphibolite is higher in FeO and lower in MgO, CaO, and Na_2O than his type para-amphibolite. In checking this work, the writers have found that bimodal peaks for the four oxides used to characterize ortho- and para-amphibolites are not formed by the same rocks. Average olivine basalt of the Pacific (Table 6) is, in terms of these four oxides, identical with Lapadu-Hargues' type para-amphibolite. Continued work by Engel (1956, p. 84–85) resulted in his abandoning earlier suggestions that para- and ortho-amphibolites can be distinguished by their contents of nickel, cobalt, and chromium. This is also the writers' experience (Fig. 15). Thus it seems that the two types of amphibolite cannot be dis-

tinguished chemically by the elements surveyed to date. The possibility that such distinctions can be made on the basis of Ti or Sr contents needs to be explored further.

Para- and ortho-amphibolites are usually distinguished in the field by the former showing intimate interlayering with other rock types and lack of uniformity in the hornblendic bands (Kulp and Poldervaart, 1956, Pl. 1*C*; Eckelmann and Kulp, 1956, Pl. 3), whereas the latter are more homogeneous. The nature of the original material composing the hornblendic bands remains in question. Possibilities are that the bands represent; (1) mafic tuffs, (2) dolomitic shales, or (3) dolomitic graywackes. In view of the close agreement in composition between para-amphibolites and basalts, the first possibility may seem the most likely. However, para-amphibolites of basaltic composition are much more common in metamorphic terrains than are basaltic tuffs in unmetamorphosed formations. The second possibility has been tested by Eckelmann and Poldervaart (1957, p. 1251), who conclude that dolomitic shales have more potassium than sodium, whereas the reverse is true for para-amphibolites. Thus an origin in dolomitic shales necessitates an assumption of widespread Na metasomatism to account for compositions of para-amphibolites. The third alternative (*c.f.*, Engel and Engel, 1953, p. 1023, 1025) may seem the most attractive in view of these difficulties, but the assumption of a greatly enhanced distribution of sodic sediments in the Precambrian places serious strains on the geo-economy of sodium and potassium in the earth's crust (Green and Poldervaart, 1958, p. 105). Until further investigations are carried out with better success, the problem must remain open.

Eckelmann and Poldervaart (1957, p. 1238) note that in large units of well-banded para-amphibolite may be found small lenses of mafic and ultramafic rocks of igneous origin. These are also present in the Bakersville-Roan Mountain area. In the Cranberry gneiss a well-defined dike swarm of metadolerites is found, in which each dike has sharp, crosscutting margins against country rocks. In the transitional zone between Cranberry gneiss and Roan gneiss and schist, along the strike of the dike swarm, there are a few well-defined metadolerite dikes and several exposures of Toecane-type amphibolites which in rare outcrops show poorly defined crosscutting relationships with country rocks, and in one outcrop surround and grade into subophitic metadolerite, similar to the Bakersville-Roan Mountain metadolerites. Farther along the strike of the dike swarm, where country rocks are predominantly Roan gneiss and schist, no exposures of definitely intrusive amphibolite can be found.

There are two alternatives: (1) the dike swarm did not continue into the Roan formation, or (2) it did continue but was subsequently metamorphosed and deformed in such a manner as to become indistinguishable from the hornblendic country rocks. Of these, the writers favor the second, because of the field evidence found in the boundary zone between the Cranberry and Roan formations, and because the dike swarm is so well developed in the Cranberry gneiss, especially near Locust Knob, just before it reaches the Cranberry-Roan boundary zone. Despite statistically significant differences in Sr contents, the writers consider the Toecane-type amphibolites equivalents of the Bakersville-Roan Mountain metadolerites because of the critical exposure on Brush Creek Road near Deyton Bend and the close similarity in MgO contents (Table 6). MgO is an especially sensitive constituent in basalts, and different basaltic provinces are not likely to have the same MgO percentages.

If these considerations are correct, it seems that well-defined metadolerite dikes in quartzofeldspathic gneisses may be sheared out to conformable lenses of amphibolite in formations consisting predominantly of para-amphibolite. The dikes would thereby become indistinguishable from the country rocks, since not only are they both of similar, or even identical mineralogical and chemical composition, but the initial crosscutting relationships between dikes and country rocks are also destroyed by subsequent recrystallization and differential movements. These observations further complicate the problem of ortho- and para-amphibolites. The writers can only stress the need for detailed investigations to solve the riddle of the origin of para-amphibolites and to establish criteria to distinguish between amphibolites of igneous and sedimentary origin.

Summary and Conclusions

The crystalline basement of the Spruce Pine district consists essentially of a synclinorium plunging southwest, of which the core is composed of Roan-Carolina para-amphibolites and mica schists, underlain by paragneisses called Cranberry gneiss on the northwest limb and Henderson gneiss on the southeast limb of the synclinorium. A metadolerite dike swarm in

Cranberry gneiss is exposed between Roan Mountain and Red Hill, North Carolina. In the boundary zone of the Cranberry and Roan-Carolina formations, between Toecane and Green Mountain and along strike of the dike swarm, spotted ortho-amphibolites are in part crosscutting, in part conformable with the country rocks. In one exposure along Brush Creek Road, Toecane-type ortho-amphibolite is associated with and grades into metadolerite. This exposure, and the absence of Toecane-type ortho-amphibolites outside the Toecane-Green Mountain area, are taken as evidence that the ortho-amphibolites are equivalents of the metadolerites. Within the Roan-Carolina core of the Spruce Pine synclinorium no metadolerites or ortho-amphibolites have been identified. Field studies indicate that the dike swarm may well have continued into the Roan-Carolina formations, but that the dike rocks may have completely lost their identity through shearing and metamorphism.

Age determinations show progressive "younging" of the metamorphic rocks, from 860 m. y. in the west at Pardee Point, to 350 m. y. at Spruce Pine and east from there. This indicates superposition of two metamorphic cycles in the area: an Ordovician-Silurian cycle, with its main effects east of Spruce Pine, followed a Precambrian cycle (*ca.* 1 b. y. old), resulting in transitional ages in a narrow zone west of Spruce Pine. Despite metamorphic younging of the rocks eastward, the Cranberry and Roan-Carolina formations east and west of Spruce Pine are clearly Precambrian in age of deposition and first metamorphism.

The metadolerite dikes at Carvers Gap show evidence of having been emplaced at shallow depths. Sharply crosscutting dikes and dikelets and angular thin screens and xenoliths of country rocks indicate that the rocks were relatively rigid and brittle when the dike swarm was intruded. One dike cuts a breccia zone in which angular fragments of Cranberry gneiss are cemented by a dark, iron-rich matrix. Another dike contains ovoidal crystal segregates mainly consisting of plagioclase; these are believed to represent recrystallized amygdules. Several dikes show garnet trails with striking patterns, suggesting fracture-controlled crystallization of garnet along pre-metamorphic joints.

The dikes cut metamorphic rocks of the Cranberry formation, yet are themselves metamorphosed. Field evidence indicates that the dikes were emplaced a considerable time after metamorphism of the country rocks and not during the same metamorphic cycle. Biotites from the metadolerites yield an age of 450 m. y. Since the biotite is moulded on metamorphic minerals such as garnet and pyroxene corona minerals, it is regarded as metamorphic in origin. This suggests that there may have been yet another metamorphic cycle, younger than the ±1 b. y. cycle and older than the 350 m. y. cycle. The Ordovician-Silurian cycle presumably affected the biotite age to some degree, hence 450 m. y. is a minimum age for the intermediate cycle which may be dated at 500-600 m. y.

Thermoremanent magnetic vectors of five pairs of dike rocks and country rocks are not parallel, indicating that metamorphic temperatures were less than 575° C. Susceptibility anisotropy measurements have been made for three pairs of dike rocks and country rocks but results do not lead to conclusions of geologic interest.

Petrographic examinations of thin sections show that the metadolerites exhibit textural relationships indicative of their metamorphism. These textural criteria are: (1) dark clouding of relict plagioclase and relict augite, (2) partial or complete substitution of lath-shaped relict plagioclase by aggregates of granoblastic, clear plagioclase, (3) partial or complete substitution of subophitic relict augite by aggregates of granoblastic pale-green pyroxene, garnet, magnetite, and hornblende, with or without biotite, (4) coronas around olivine, (5) occurrence of pink garnet in rocks of normal basaltic composition; garnets along boundaries of plagioclase and ferromagnesian minerals showing euhedral outlines toward plagioclase and anhedral outlines toward the ferromagnesian minerals, and (6) partial or complete destruction of the original subophitic texture and its substitution by granoblastic textures, attended by decrease in grain size. Mineralogical data confirm the metamorphic recrystallization of the metadolerites. Relict, lath-shaped, clouded plagioclase and granoblastic, clear plagioclase are of low-temperature form. Relict plagioclase has undergone changes in composition without changing its shape. Relict, subophitic, clouded augite has also changed in composition without change of shape and shows compositions similar to the granoblastic, clear, pale-green pyroxene with which it is associated. Pleochroic orthopyroxenes are of low-temperature form. Amphiboles are normal calciferous hornblendes. Garnet is almanditic.

Bulk chemical compositions and their representation on variation diagrams identify the metadolerites and Toecane-type ortho-am-

phibolites as olivine dolerites belonging to the middle and late stages of fractionation of basaltic magmas. Analyses show no differences in major constituents between the metadolerites, Toecane-type ortho-amphibolites and para-amphibolites of the Roan formation. However, TiO_2 is lower in the para-amphibolites than in the metadolerites and ortho-amphibolites, and this difference is shown by data for both the Bakersville-Roan Mountain area and the Beartooth Mountains of Montana and Wyoming. The possibility of distinguishing between ortho- and para-amphibolites on the basis of their TiO_2 contents should be explored further. Semiquantitative data for gallium, copper, chromium, nickel, cobalt, and barium also show no differences between metadolerites, Toecane-type ortho-amphibolites, and para-amphibolites of the Roan formation. However, quantitative data for strontium show that the Roan para-amphibolites have much lower Sr contents than the metadolerites and ortho-amphibolites. Strontium may form a useful criterion to distinguish ortho- and para-amphibolites, but further studies are necessary before this criterion can be accepted generally.

Heavily clouded plagioclase is shown to contain a relatively high percentage of FeO. X-ray studies indicate that the minute particles causing clouding may consist of rhombic pyroxene. It is suggested that comparatively high rates of diffusion during metamorphism resulted in the diffusion of Fe^{+2} ions into pre-existing plagioclase crystals, held in crystal solution at the elevated temperatures. Subsequent cooling caused exsolution of the impurities and crystallization of minute particles of rhombic pyroxene and presumably also other minerals. Conditions favorable to metamorphic clouding are thought to include water deficiency during metamorphism. Heavy clouding of plagioclase is regarded as a criterion of metamorphism of rocks showing this phenomenon.

Considerations of metamorphic facies and mineral assemblages of the rocks of the area indicate temperatures of 450°–500° C. for the metamorphism of the dike rocks. Analysis of garnet and pyroxene (olivine)-hornblende associations indicates that, at these temperatures, the metadolerites in Cranberry gneiss were metamorphosed under water-deficient conditions, whereas ortho-amphibolites in the boundary zone between the Cranberry and Roan-Carolina formations were metamorphosed in the presence of water as a free phase. These differences probably reflect the nature of the country rocks; the Roan-Carolina para-amphibolites and mica schists probably had more water available than the quartzofeldspathic Cranberry gneiss. The petrography of metadolerites is described in four stages in the amphibolite facies, ranging from extreme water-deficient recrystallization to recrystallization in the presence of water as a free phase.

Amphibolite problems are discussed: Water-deficient metamorphism of rocks of basaltic composition may easily escape detection, and the rocks may be regarded as unmetamorphosed. On the other hand, plagioclase-hornblende rocks may be regarded as having resulted from metamorphism, although the rocks may have originated from primary crystallization of water-rich basaltic magmas. The distinction between ortho- and para-amphibolites is presently based only on field evidence and is possible only in exposures where such field evidence is shown clearly and uncontroversially. Claims that ortho- and para-amphibolites can be distinguished by their bulk chemical compositions or contents of Cr, Ni, and Co have been disproved in the present study, but possibly other elements such as Ti or Sr may be used successfully to distinguish between these two types of amphibolites. Para-amphibolites may represent mafic tuffs, dolomitic shales, or dolomitic graywackes. Their identification with one of these rock types is of considerable importance and contributes to knowledge of geologic environment during deposition and subsequent history of the rocks. However, the problem may be complicated by the occurrence of small bodies of ortho-amphibolites in large units of para-amphibolites, the two types of amphibolites being indistinguishable in the field. For instance, the Bakersville-Roan Mountain dike swarm may continue in the Roan-Carolina formations, but the identity of the dike rocks may have been lost in these formations by shearing and metamorphism. In many respects, amphibolite problems are the counterpart of granite problems, and the solution of these problems is essential to understanding of the geology of metamorphic regions.

References Cited

Asami, E., 1956, A paleomagnetic consideration on the remanent magnetism of the basalt lavas at Kawajiri-misaki, Japan: Jour. Geomagnetism and Geoelectricity, v.8, p. 147–155

Balsley, J. R., and Buddington, A. F., 1954, Correlation of reverse remanent magnetism and negative anomalies with certain minerals: Jour. Geomagnetism and Geoelectricity, v. 6, p. 176–181

Benson, W. N., 1926, The tectonic conditions accompanying the intrusion of basic and ultrabasic igneous rocks: Nat. Acad. Sci. Mem. 1, p. 1–90

Blackett, P. M. S., 1956, Lectures on rock magnetism: Jerusalem, The Weizmann Science Press of Israel, 131 p.

Boyd, F. R., Jr., 1956, Amphiboles, p. 153–229 *in* Abelson, P. H., Annual Report of the Director, Geophysical Laboratory: Carnegie Inst. Wash. Yearbook 55

Brobst, D. A., and Kulp, J. L., in press, Geology of the Spruce Pine District, North Carolina: U. S. Geol. Survey Prof. Paper

Buddington, A. F., 1939, Adirondack igneous rocks and their metamorphism: Geol. Soc. America Mem. 7, 354 p.

—— 1952, Chemical petrology of some metamorphosed Adirondack gabbroic, syenitic and quartz syenitic rocks: Am. Jour. Sci., Bowen volume, pt. 1, p. 37–84

Buerger, M. J., 1948, The role of temperature in mineralogy: Am. Mineralogist, v. 33, p. 101–121

Chilingar, G. V., 1957, Review of a paper by A. P. Vinogradov, A. B. Ronov, and V. M. Ratynski (1952), Variation in the chemical composition of carbonate rocks of Russian platform: Geochim. Cosmochim. Acta, v. 12, p. 273–276

Cohen, C. J., 1937, Structure of the metamorphosed gabbro complex at Baltimore, Md.: Maryland Geol. Survey Rept. 13, p. 215–236

Eckelmann, F. D., and Kulp, J. L., 1956, The sedimentary origin and stratigraphic equivalence of the so-called Cranberry and Henderson granites in western North Carolina: Am. Jour. Sci., v. 254, p. 288–315

Eckelmann, F. D., and Poldervaart, Arie, 1957, Geologic evolution of Beartooth Mountains, Montana and Wyoming, Part 1: Archean history of the Quad Creek area: Geol. Soc. America Bull., v. 68, p. 1225–1262

Emmons, R. C., 1943, The universal stage: Geol. Soc. America Mem. 8, 205 p.

Emmons, R. C., *et al.*, 1953, Selected petrogenic relationships of plagioclase: Geol. Soc. America Mem. 52, 142 p.

Engel, A. E. J., 1956, Apropos the Grenville, p. 74–96 *in* The Grenville Problem: Roy. Soc. Canada, Spec. Pub 1.

Engel, A. E. J., and Engel, C. G., 1951, Origin and evolution of hornblende-andesine amphibolites and kindred facies (Abstract): Geol. Soc. America Bull., v. 62, p. 1435

—— 1953, Grenville series in the northwest Adirondack Mountains, New York: Geol. Soc. America Bull., v. 64, p. 1013–1048

Eskola, Pentti, 1952, On the granulites of Lapland: Am. Jour. Sci., Bowen volume, pt. 1, p. 133–171

Fairbairn, H. W., *et al.*, 1951, A co-operative investigation of precision and accuracy in chemical, spectrochemical and modal analyses of silicate rocks: U. S. Geol. Survey Bull. 980, 71 p.

Graham, J. W., 1953, Changes of ferromagnetic minerals and their bearing on magnetic properties of rocks: Jour. Geophysical Research, v. 58, p. 243–260

—— 1954, Magnetic susceptibility anisotropy, an unexplored petrofabric element (Abstract): Geol. Soc. America Bull., v. 65, p. 1257

Green, Jack, and Poldervaart, Arie, 1955, Some basaltic provinces: Geochim. Cosmochim. Acta, v. 7, p. 177–188

—— 1958, Petrochemical fields and trends: Geochim. Cosmochim. Acta, v. 13, p. 87–122

Hertz, Norman, 1951, Petrology of the Baltimore gabbro, Maryland: Geol. Soc. America Bull., v. 62, p. 979–1016

Hess, H. H., 1949, Chemical composition and optical properties of common clinopyroxenes: Am. Mineralogist, v. 34, p. 621–666

—— 1952, Orthopyroxenes of the Bushveld type, ion substitution and changes in unit cell dimensions: Am. Jour. Sci., Bowen volume, pt. 1, p. 173–187

Howie, R. A., 1955, The geochemistry of the charnockite series of Madras, India: Roy. Soc. Edinburgh Trans., v. 62, pt. 3, p. 725–768

Keith, Arthur, 1903, Description of the Cranberry quadrangle, North Carolina-Tennessee: U. S. Geol. Survey Geol. Atlas, folio 90

—— 1905, Description of the Mount Mitchell quadrangle, North Carolina-Tennessee: U. S. Geol. Survey Geol. Atlas, folio 124

—— 1907, Description of the Roan Mountain quadrangle, North Carolina-Tennessee: U. S. Geol. Survey Geol. Atlas, folio 151

King, P. B., 1950, Tectonic framework of southeastern United States: Am. Assoc. Petroleum Geologists Bull., v. 34, p. 635–671

—— 1955, Orogeny and epeirogeny through time, p. 723–740 *in* Poldervaart, Arie, *Editor*, Crust of the earth: Geol. Soc. America Special Paper 62, 762 p.

King, P. B., Hadley, J. B., and Neuman, R. B., 1952, Guidebook of excursion in the Great Smoky Mountains: Carolina Geol. Soc., 60 p.

Kulp, J. L., and Brobst, D. A., 1954, Notes on the dunite and the geochemistry of vermiculite at the Day Book dunite deposit, Yancey County, North Carolina: Econ. Geology, v. 49, p. 211–220

Kulp, J. L., and Poldervaart, Arie, 1956, The metamorphic history of the Spruce Pine District: Am. Jour. Sci., v. 254, p. 393–403

Lapadu-Hargues, Pièrre, 1953, Sur la composition chimique moyenne des amphibolites: Soc. géol. France Bull., 6th ser., v. 3, p. 153–173

Levin, S. B., 1950, Genesis of some Adirondack garnet deposits: Geol. Soc. America Bull., v. 61, p. 519–565

MacGregor, A. G., 1931, Clouded feldspars and thermal metamorphism: Mineralog. Mag., v. 22, p. 524–538

Miyashiro, Akiho, 1953, Progressive metamorphism of calcium-rich rocks of the Gosaisyo-Takanuki district, Abukuma plateau, Japan: Japanese Jour. Geol. Geogr., v. 23, p. 81–107

Muir, I. D., and Tilley, E. C., 1957, Contributions to the petrology of Hawaiian basalts, part 1: The picrite-basalts of Kilauea: Am. Jour. Sci., v. 255, p. 241–253

Murthy, M. V. N., 1958, Coronites from India and their bearing on the origin of coronas: Geol. Soc. America Bull., v. 69, p. 23–38

Néel, Louis, 1955, Some theoretical aspects of rock magnetism: Advances in Physics, v. 4, n. 14, p. 191–243

Nicholls, G. D., 1955, The mineralogy of rock magnetism: Advances in physics, v. 4, n. 14, p. 113–190

Nockolds, S. R., 1954, Average chemical compositions of some igneous rocks: Geol. Soc. America Bull., v. 65, p. 1007–1032

Nockolds, S. R., and Allen, Richard, 1954, The geochemistry of some igneous rock series: Part 2: Geochim. Cosmochim. Acta, v. 5, p. 245–285

Poldervaart, Arie, 1950, Correlation of physical properties and chemical composition in the plagioclase, olivine, and orthopyroxene series: Am. Mineralogist, v. 35, p. 1067–1079

—— 1953, Metamorphism of basaltic rocks; A review: Geol. Soc. America Bull., v. 64, p. 259–274

—— 1955, Chemistry of the earth's crust, p. 119–144 *in* Poldervaart, Arie, *Editor*, Crust of the earth: Geol. Soc. America Special Paper 62, 762 p.

—— 1956, Zircon in rocks; Part 2, Igneous rocks: Am. Jour. Sci., v. 254, p. 521–554

Poldervaart, Arie, and Gilkey, A. K., 1954, On clouded plagioclase: Am. Mineralogist, v. 39, p. 75–91

Rosenzweig, Abraham, and Watson, E. H., 1954, Some hornblendes from southeastern Pennsylvania and Delaware: Am. Mineralogist, v. 39, p. 581–599

Runcorn, S. K., 1955, Rock magnetism—geophysical aspects: Advances in Physics, v. 4, n. 14, p. 244–291

Shand, S. J., 1942, Phase petrology in the Cortlandt complex, New York: Geol. Soc. America Bull., v. 53, p. 409–428

Simpson, E. S. W., 1954, On the graphical representation of differentiation trends in igneous rocks: Geol. Mag., v. 91, p. 238–244

Smith, J. R., 1956, Effects of heating natural plagioclases, p. 188–190 *in* Abelson, P. H., Annual Report of the Director, Geophysical Laboratory: Carnegie Inst., Wash. Yearbook 55

—— 1957, Optical properties of heated plagioclases, p. 216–217 *in* Abelson, P. H., Annual Report of the Director, Geophysical Laboratory: Carnegie Inst., Wash. Yearbook 56

Sutton, John, and Watson, Janet, 1951, Varying trends in the metamorphism of dolerites: Geol. Mag., v. 88, p. 25–35

Tilley, C. E., 1950, Some aspects of magmatic evolution: Geol. Soc. London Quart. Jour., v. 106, p. 37–61

Thornton, C. P., and Tuttle, O. F., 1956, Applications of the differentiation index to petrologic problems (Abstract): Geol. Soc. America Bull., v. 67, p. 1738–1739

Tomita, Toru, 1934, Variations in optical properties according to chemical composition in the pyroxenes of the clinoenstatite, clinohypersthene, diopside, hedenbergite system: Jour. Shanghai Sci. Inst., sect. 2, v. 1, p. 41–58

Turekian, K. K., and Kulp, J. L., 1956, The geochemistry of strontium: Geochim. Cosmochim. Acta, v. 10, p. 245–296

Turner, F. J., 1948, Mineralogical and structural evolution of the metamorphic rocks: Geol. Soc. America Mem. 30, 342 p.

Turner, F. J., and Verhoogen, Jean, 1951, Igneous and metamorphic petrology: N. Y., McGraw-Hill Book Co., 602 p.

Wager, L. R., 1956, A chemical definition of fractionation stages as a basis for comparison of Hawaiian, Hebridean, and other basic lavas: Geochim. Cosmochim. Acta, v. 9, p. 217–248

Walker, Frederick, and Poldervaart, Arie, 1949, Karroo dolerites of the Union of South Africa: Geol. Soc. America Bull., v. 60, p. 591–706

Wells, R. C., 1937, Analyses of rocks and minerals, 1914–36: U. S. Geol. Survey Bull. 878, 134 p.

Wiseman, J. D. H., 1934, The central and southwest Highland epidiorites; A study in progressive metamorphism: Geol. Soc. London Quart. Jour., v. 90, p. 354–417

Wright, W. I., 1938, The composition and occurrence of garnets: Am. Mineralogist, v. 23, p. 436–445

Yoder, H. S., Jr., 1955, Role of water in metamorphism, p. 505–524 *in* Poldervaart, Arie, *Editor*, Crust of the earth: Geol. Soc. America Special Paper 62, 762 p.

Yoder, H. S., Jr., and Tilley, C. E., 1956, Natural tholeiite basalt-water system p. 153–229 *in* Abelson, P. H., Annual Report of the Director, Geophysical Laboratory: Carnegie Inst. Wash. Yearbook 55

Research Division, Humble Oil and Refining Company, Houston 1, Texas
Department of Geology, Columbia University New York 27, New York

Manuscript Received by the Secretary of the Society, November 20, 1957
Penrose Bequest Grant 629-53

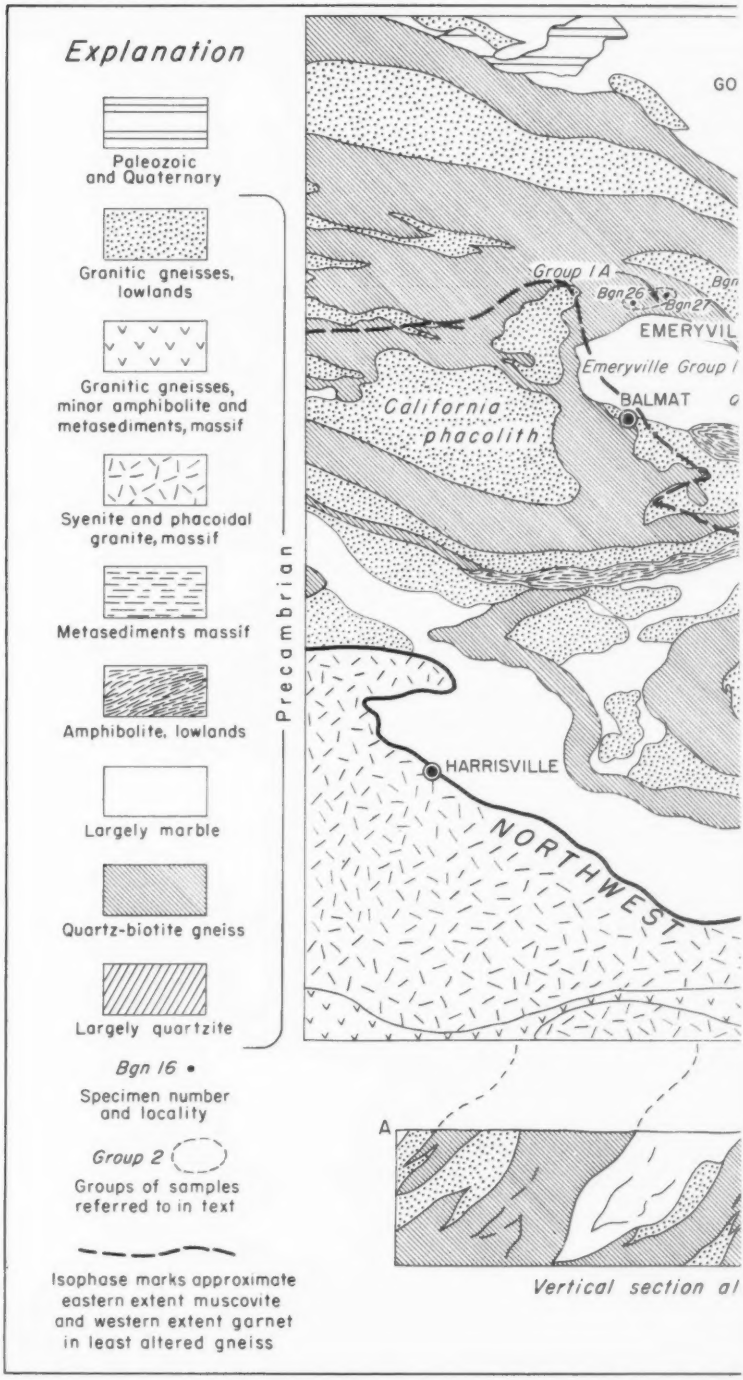

GENERAL GEOLOGIC MAP AND FORM AND DISTRIBUT

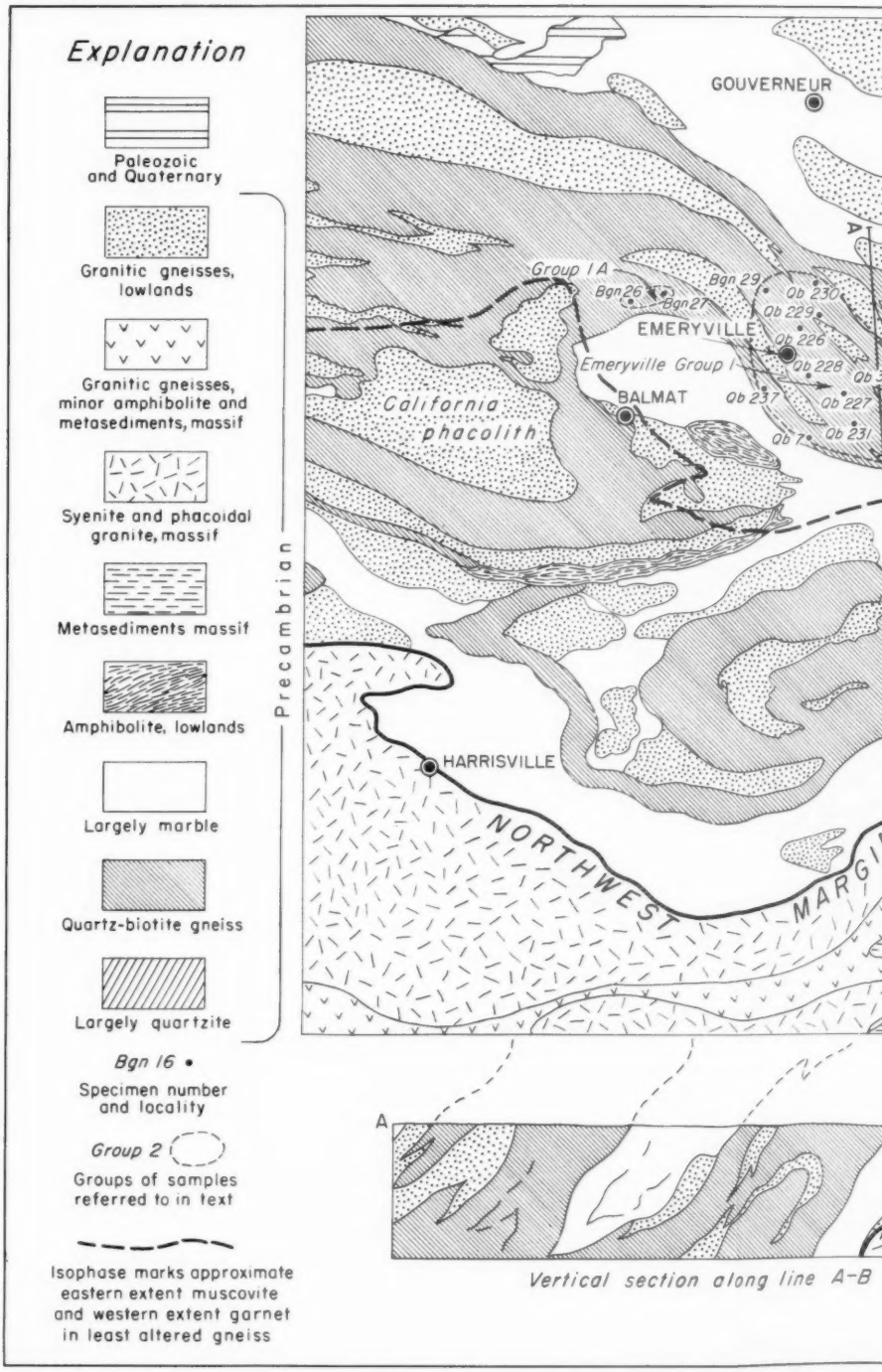

GENERAL GEOLOGIC MAP AND VERTICA
FORM AND DISTRIBUTION OF TI

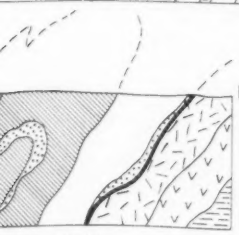

line A-B

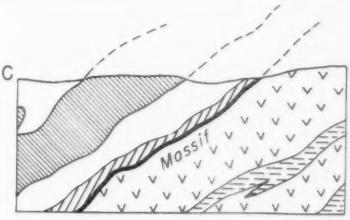

Vertical section along line C-D

ERTICAL SECTIONS OF THE NORTHWEST ADIRONDACK M
N OF THE GNEISS AND LOCATIONS OF THE SAMPLES ST

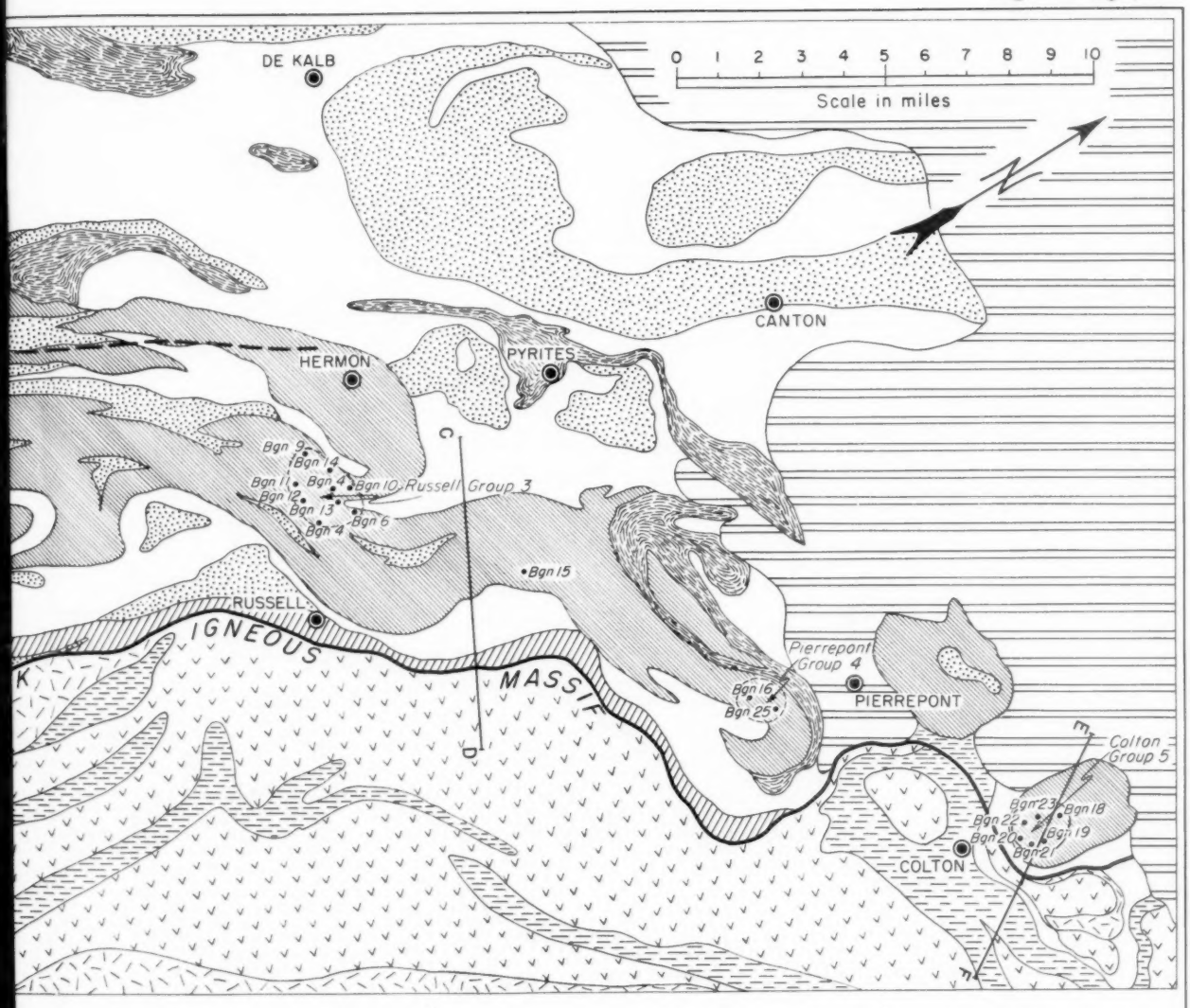

Vertical section along line C–D

Vertical section along line E–F

THE NORTHWEST ADIRONDACK MOUNTAINS SHOWING THE LOCATIONS OF THE SAMPLES STUDIED IN DETAIL

BULLETIN OF THE GEOLOGICAL SOCIETY OF AMERICA
VOL. 69, PP. 1369-1414, 7 FIGS., 4 PLS. NOVEMBER 1958

PROGRESSIVE METAMORPHISM AND GRANITIZATION OF THE MAJOR PARAGNEISS, NORTHWEST ADIRONDACK MOUNTAINS, NEW YORK

PART 1: TOTAL ROCK

BY A. E. J. ENGEL AND CELESTE G. ENGEL

WITH ANALYSES OF TRACE ELEMENTS BY
A. A. CHODOS AND ELISABETH GODIJN

ABSTRACT

The progressive metamorphism and partial granitization of a belt of quartz-mica-feldspar-garnet paragneiss is considered in detail. This paragneiss is traced and sampled along a belt 35 miles long that extends across the Grenville Lowlands into the central massif of the Adirondack Mountains, New York. Geologic thermometers indicate temperatures of metamorphism of about 500° C. at the southwest end of the belt and about 600° C. near the perimeter of the massif.

Minimum temperatures of metamorphism in the gneiss are determined largely from solid solutions of magnesite in dolomite, FeS in sphalerite, paragonite in muscovite, and TiO_2 in magnetite. Maximum temperatures of metamorphism are inferred principally from the absence of wollastonite in closely associated siliceous marbles. The gradient in T is checked by the δO^{18} in quartz and coexisting magnetite in the gneiss.

The composition of the paragneiss and its constituent minerals is determined from 75 new chemical analyses, 50 partial chemical analyses, 400 analyses of trace elements, and modal analyses of approximately 400 rocks.

At the lower-temperature end of the belt the least altered gneiss is a quartz-biotite-oligoclase-muscovite gneiss averaging (weight per cent) 70.25 SiO_2, 0.67 TiO_2, 14.14 Al_2O_3, 0.55 Fe_2O_3, 3.83 FeO, 2.20 CaO, 1.76 MgO, 0.05 MnO, 3.43 Na_2O, 2.40 K_2O, and (in ppm) B, 10; Ba, 600; Co, 8; Cr, 35; Cu, 16; Ga, 11; Ni, 15; Pb, 12; Sc, 12; Sr, 300; V, 56; Y, 50; Yb, 3; Zr, 170. This is inferred to approximate the bulk composition of the parent sedimentary rock.

With increasing temperature of metamorphism of the least altered gneiss, the mineral composition changes as follows: muscovite disappears, garnet appears, plagioclase increases in abundance, and average An content and quartz decrease. Complementary changes in chemical composition include an increase in Al, Fe^{++}, total Fe, Mg, Ca, Cr, Ga, Ni, and V. Amounts of K, Si, Fe^{+++}, H_2O, and Ba decrease.

This "degranitization" or "basification" of the gneiss appears to be a metamorphic process that begins at about 550° C. and is well defined at 600° C. The mobilized Si, K, and H_2O appear to be partly liberated and partly trapped as a venitic migmatite.

Granitization of parts of the gneiss is accompanied by an increase in K feldspar and Ab content of plagioclase and by a decrease in biotite, plagioclase, and quartz. Chemical changes in major elements include an increase in K and a decrease in Ti, Fe^{+++}, Fe^{++}, Mg, Ca, H_2O, and in Na–K ratio. Changes in the amounts of minor elements in granitized parts of the gneiss include increases in Ba and Pb and a decrease in Co, Cr, Ni, Sc, Sr, Ti, V, and Y. All granitizing substances in the gneiss in areas of lower-temperature metamorphism appear to be introduced either laterally or from below. Those in areas of highest-temperature metamorphism are partly introduced, partly derived locally from the gneiss. The implied basic front evolved during granitization of the gneiss may have been large, for the introduced granitizing substances replace one-third of the sedimentary rock throughout a zone over ½ mile thick, 75 miles wide, and more than 40 miles long.

Calculations of the chemical composition of the more even-textured gneiss, from modal analyses and mineral analyses, show about the same deviation from the actual chemical analyses as exists in the 34 analyses of G-1 and W-1 as reported by Fairbairn *et al.* (1951).

CONTENTS

TEXT

	Page
Introduction	1371
Acknowledgments	1371
Scope	1371
Geological setting	1372
Choice and location of rock samples	1376
Preparation of samples	1377
Methods of rock analysis	1377
Introduction	1377
Chemical analyses, major and minor elements	1377
Spectrographic analyses, trace elements	1378
Modal analyses	1379
Calculations of chemical composition from modal analyses	1380
Temperature of metamorphism	1382
Introduction	1382
Geologic evidence of a temperature gradient	1383
Absolute temperatures	1383
Data from magnesian calcites	1383
Thermometric significance of titaniferous magnetite	1384
Temperatures from FeS in sphalerites	1384
Na content of muscovites in the gneiss	1386
Temperature limits implied by wollastonite-free siliceous marble	1386
Temperatures as indicated by the O^{18}–O^{16} ratio in coexisting quartz and magnetite	1386
Presentation of rock analyses	1387
Rock metamorphism	1387
Assumptions	1387
General lithologic features	1388
Least altered gneiss	1393
Introduction	1393
Mineralogy and texture	1394
Chemical composition: major elements	1396
Chemical composition: minor elements	1399
Granitized gneiss	1403
Introduction	1403
Mineralogy and texture	1404
Chemical composition: major elements	1407
Chemical composition: minor elements	1410
Summary	1411
References cited	1412

ILLUSTRATIONS

Figure	Page
1. Generalized plan and vertical section indicating stratigraphy and structure of the Grenville-like rocks in the northwest Adirondack Mountains, New York	1373
2. Curves derived from data in the text indicating maximum, minimum, and probable temperatures of reconstitution of the gneiss complex between Emeryville, New York, and the massif	1374
3. Generalized curves showing interrelationships in the mineralogical, chemical, and textural evolution of the gneiss complex due to granitization	1389
4. Generalized curves indicating changes in mineral and major-element composition of 11 specimens of least altered gneiss studied in detail as traced from Emeryville to Colton, New York	1394
5. Generalized curves indicating changes in mineral and major-element composition of least altered gneiss as traced from Emeryville to Colton, based upon 73 specimens	1398
6. Variations in mineral and chemical composition of specimens in Group 1 resulting from increasing degrees of permeation and replacement of the least altered gneiss by granite-forming substances, especially potassium	1405
7. Graphs showing compositional trends in the gneiss complex at Emeryville and Colton resulting from pervasive and complete granitization of the gneiss	1407

Plate	Facing page
1. Generalized geologic map and vertical sections of the northwest Adirondack Mountains showing the form and distribution of the gneiss and locations of the samples studied in detail	1369
2. Textures of gneiss	1388
3. Migmatite and inequigranular granitized gneiss	1389
4. Detailed geologic map of the Emeryville area showing interrelationships of the rock types within the gneiss and locations of specimens in Group 1	1414

TABLES

Table	Page
1. Duplicate chemical analyses of masked specimens of G-1 and W-1 made with analyses of gneiss and indicative of precision of analytical methods	1378
2. Precision and accuracy of alkali analyses using flame photometer	1378
3. Per cent standard deviations of replicate spectrographic analyses of trace elements	1379
4. Modal analyses of two rocks	1380
5. Data comparing precision of direct chemical analyses and use of modal analyses and physical and chemical properties of minerals in determining chemical compositions of rocks	1381
6. Delta O^{18}–O^{16} ratios for coexisting quartz and magnetite in gneiss at Emeryville and Colton and in hornblende granite gneiss in the adjoining part of the massif	1387
7. Chemical and modal analyses of selected specimens of least altered gneiss between Emeryville and Colton, New York	1390
8. Average chemical and mineralogical compositions, and range in compositions of least altered gneiss in the gneiss complex between Emeryville and Colton, New York	1396
9. Chemical and modal analyses of specimens of granitized gneiss from the paragneiss complex between Emeryville and Colton, New York	1400

Table		Page
10.	Average trace-element composition of least altered gneiss and granitic gneiss compared with that of the Littleton formation	1402
11.	Analyses of trace elements in the Littleton formation	1403
12.	Modal and trace-element analyses of four typical specimens of uniformly granitized gneiss from the Colton area, New York	1406
13.	Average chemical and mineral compositions of least altered and more granitic gneiss from the Emeryville and Colton areas, New York	1408
14.	Average composition of least altered gneiss at Emeryville and compositions of granites in the massif that shred and are contaminated by the gneiss	1410

Introduction

Many, probably most, of the changes in mineral species that occurred during metamorphism of rocks now exposed have been recorded. Unfortunately the exact or even approximate conditions of temperature, pressure, and composition (T, P, X) that pertain as rocks evolve from one metamorphic grade to another remain unknown.

Equally vague is the knowledge of the changes in the physical and chemical properties of the constituent minerals or of the entire rock, as these are a function of changing T, P, or X. With an exception or two, conclusions regarding the extent of isochemical metamorphism and those intriguing threshold conditions at which elements or ichors become mobile are based upon extrapolations from laboratory studies or essentially intuitive inferences from field relationships.

This study attempts to resolve a few more of the uncertainties and to pinpoint some major problems of progressive metamorphism of a graywackelike sedimentary rock under conditions approaching and equivalent to the highest rank of regional metamorphism and incipient magmatism.

Acknowledgments

This study has been possible because of the financial support of the California Institute of Technology, the Geological Society of America, the National Science Foundation, and the U. S. Geological Survey. The manuscript has been read and greatly improved by the constructive comments of Marland Billings, A. F. Buddington, Felix Chayes, B. F. Leonard, and Paul Sims.

Scope

This study complements an earlier paper (Engel and Engel, 1953b). The 1953 paper summarized our initial studies of the regional relationships of an Adirondack paragneiss, its general geological features, and its possible origin. Most of the data were field and petrographic observations complemented by a limited number of chemical analyses of the gneiss complex in the Emeryville-Edwards areas (see southwest part of Pl. 1, this paper).

Regional study of the gneiss complex indicates that two contrasting types of metamorphic rocks are widespread. One type is reconstituted[1] paragneiss with no obvious important additions of substances; although loss or segregation of substances occurs in the reconstituted gneiss in areas of highest-temperature metamorphism, this rock is referred to in this paper as least altered gneiss. The reconstitution of the gneiss offers an example of progressive metamorphism of an initially monotonous belt of clastic sedimentary rock which is like many graywackes in composition. The physical and chemical changes in the least altered gneiss and each of its constituent minerals throughout a 35-mile belt from Emeryville to Colton, New York, are described and related to a gradient in temperature and to other factors in the metamorphism.

The second type of metamorphic rock is granitized[2] paragneiss. The granitized parts are interspersed with least altered gneiss throughout the 35-mile belt. Granitization and reconstitution of the paragniess appear to have proceeded together. In many places the least altered gneiss grades into granitic gneiss; many other contacts between least altered gneiss and granitic gneiss, however, are sharp and well defined. At the sites of transition it is possible to trace the intermediate physical and chemical changes in the gneiss and in constit-

[1] Reconstituted designates what seem to be essentially equilibrium reactions of the metasedimentary constituents.

[2] "Granitized" is used in a purely descriptive sense to indicate the development of granitelike characteristics in the paragneiss, whether by mechanical injection or permeation replacement of metasedimentary rock by magma, fluids from magma, ions, ichors, and so on.

uent minerals induced by the granite-forming processes. Although the origin of the granitizing substances may be very different at Emeryville from that at Colton, many changes induced in the gneiss seem quite similar, despite the differences in temperature between the two places.

Temperatures of metamorphism at Emeryville and for at least 25 miles to the southwest seem to have reached 500°C., and possibly 525° C.; those at Colton 35 miles northeast seem to have reached or slightly exceeded 600°C. These absolute temperatures are based upon (1) solid-solution studies in associated carbonates, ilmenomagnetites, muscovites, and sphalerites; (2) the absence of wollastonite in siliceous marbles; and (3) geologic features and distribution of obviously igneous granite to ambiguous and metamorphic types. The gradient in temperature is substantiated by analyses of the O^{18}–O^{16} ratio in magnetite and quartz in the gneiss.

Inasmuch as certain of the geothermometers employed are pressure sensitive, the depth and rock pressure during metamorphism are estimated, largely from reconstructions of the rock cover and structure extant during metamorphism. These calculations suggest the exposed rocks were metamorphosed at depths of about 8–10 km, with confining pressures of 2500–3000 atmospheres. Probably, however, the pressures were nonhydrostatic, and conceivably the metamorphism occurred at depths as great as 15 km. A more precise piezometer obviously is needed.

Sampling in the southwestern third of the 35-mile segment of gneiss—that metamorphosed under the coolest conditions—was facilitated by the authors' maps (A. E. J. Engel, in press), prepared at a scale of 800 feet to the inch. Information on which sampling of the other two-thirds of the segment could be based was obtained from quadrangle maps by Buddington and Leonard (in press) and from our own field studies. The field data together with petrographic information from about 1000 thin sections were used as a basis for choosing about 35 representative rock specimens for the following detailed studies:

(1) Chemical analyses for major, minor, and trace elements in least altered and incipiently granitized gneiss collected at intervals along the 35-mile segment.

(2) Modes of the rocks.

(3) Analytical studies of the major constituent minerals of the 35 rocks. These minerals are biotite, garnet, plagioclase, K feldspar, muscovite, and quartz. Principal analytical work was focused upon the biotites, K feldspar, and garnet. In the biotites and garnets, chemical compositions, optical data, color, specific gravity, and crystal-structure data have been related to geological occurrence. Two K feldspars have been completely analyzed. Seven other K feldspars and seven muscovites were separated and analyzed for K, Na, and trace elements. Plagioclase compositions were determined by oil-immersion methods.

Partial wet-chemical and spectrographic analyses and optical studies have been made on approximately 200 additional rocks and minerals.

The analytical data on minerals and rocks are related to the inferred geological conditions during metamorphism. Part 1 discusses the metamorphism of the total rock. Part 2, which will follow within several months, is the study of the physical and chemical properties of the component minerals in the gneiss, as these are related to the metamorphism.

Geological Setting

The geology of the northwest Adirondacks has been studied and discussed in recent years by numerous workers, especially Brown (1936), Brown and Engel (1956), Buddington (1939, 1948; 1952; 1957), Buddington and Leonard (in press), A. E. J. Engel (1949; 1956), and A. E. J. Engel and C. G. Engel (1953a; 1953b).

Most pertinent to the ensuing discussion is the paper dealing principally with some of the geological features and the origin of the major paragneiss (Engel and Engel, 1953b). The interested reader is referred to it for a more detailed discussion of the general geology and field relationships.

The paragneiss is the major clastic unit in the Grenville-like[3] metasedimentary sequence of the northwest Adirondack Mountains. The 35-mile segment of paragneiss from which the samples have been obtained extends from Emeryville (northwest of Balmat, New York) northeast to the vicinity of Colton, New York. Plate 1 and Figure 1 are generalized geological maps of this region. This segment of gneiss trends obliquely across the dominantly metasedimentary Grenville Lowlands to the perimeter of the Adirondack igneous massif (Buddington, 1939, p. 5–6; Engel and Engel,

[3] The term Grenville series is deeply intrenched in the literature of the northwest Adirondack Mountains, although the term implies a stratigraphic correlation that is by no means established (A. E. J. Engel, 1956).

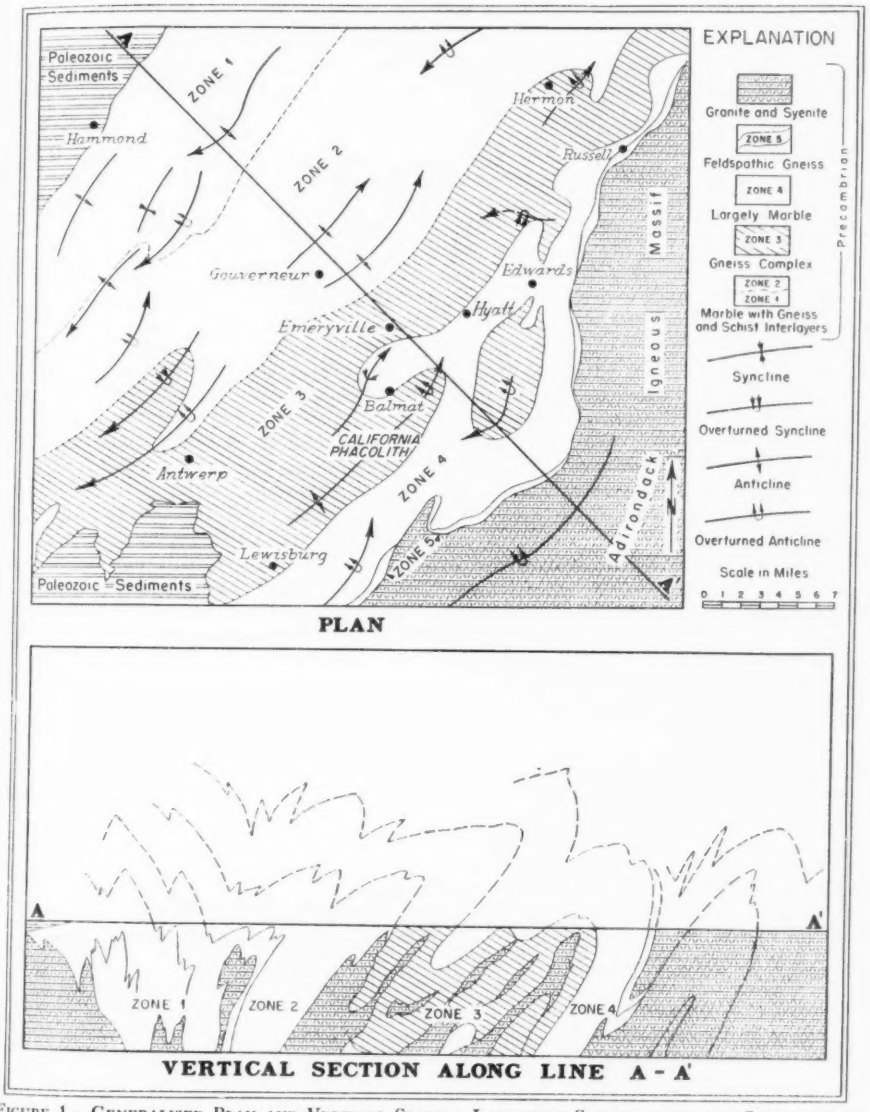

FIGURE 1.—GENERALIZED PLAN AND VERTICAL SECTION INDICATING STRATIGRAPHY AND STRUCTURE OF THE GRENVILLE-LIKE ROCKS IN THE NORTHWEST ADIRONDACK MOUNTAINS, NEW YORK

Gross structure is interpreted to be that of the center and overturned southeast flank of a bulbous anticlinorium. At and near the surface, stratigraphic zone number 5 coincides with the outer edge of the central Adirondack Massif. Note that the dip of the overturned gneiss complex (zone 3) is essentially parallel with the northwest dip of the edge of the massif.

1953b, Fig. 1 and p. 1052). Samples of gneiss discussed in this paper come from a single, originally monotonous formation at least 2000 feet thick.

The gneiss is structurally complex. Its general relationships to other units in the Grenville series and to the Adirondack igneous massif are shown in Plate 1 and Figure 1. The broad

form of the Grenville series throughout the Grenville Lowlands is interpreted to be anticlinorial. The southeastern flank of the anticlinorium is overturned between Emeryville and Colton and dips roughly 45° northwest. Consequently, the present northwest dip of the overturned gneiss throughout the area sampled is roughly parallel to the dip of the outer margin of the igneous massif. The subparallelism in dip of the gneiss and the perimeter of the massif requires emphasis for the following reasons: numerous lines of field evidence (A. E. J. Engel, in press) indicate that these geometrical relationships were approached or existed during final stages in the intermediate- to high-temperature metamorphism and granitization that produced the existing minerals in the gneiss. Under these conditions the geological reconstruction indicates a depth of metamorphism at Emeryville on the order of 5 miles. As noted earlier, however, depth of metamorphism may have been appreciably greater. At Colton the depth of metamorphism is even more difficult to obtain from regional geological considerations. In fact the data seem to conflict. Stratigraphic and structural reconstructions suggest depths no greater than those at Emeryville, but the lithologic features of the metasedimentary and igneous-looking rock types suggest greater depths of metamorphism along and within the massif. For example, both charnokitic syenites and anorthosites appear to have been emplaced as igneous rocks at the present level of erosion.

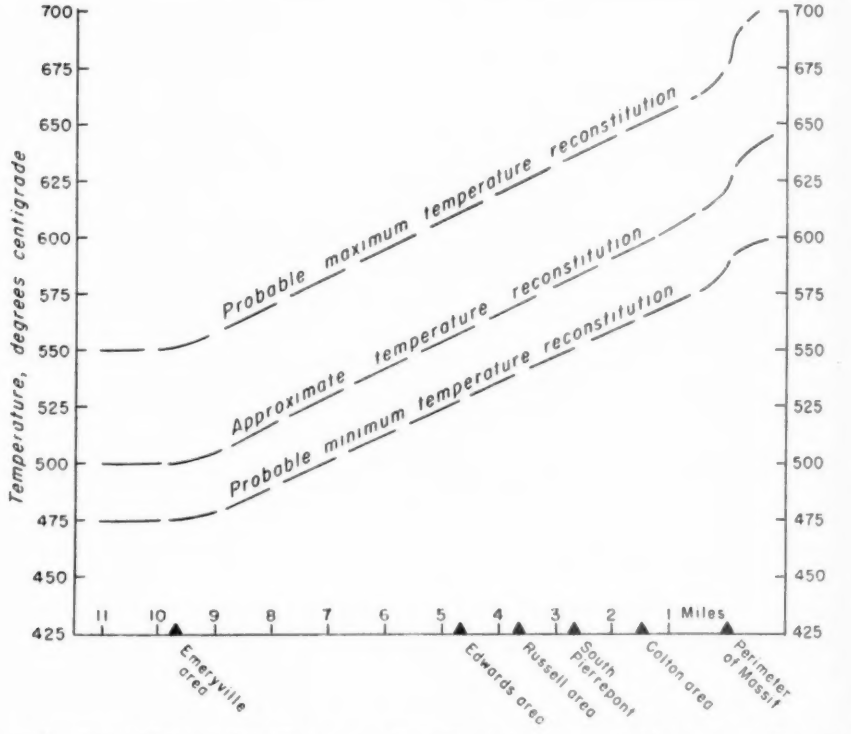

FIGURE 2.—CURVES DERIVED FROM DATA IN THE TEXT INDICATING MAXIMUM, MINIMUM, AND PROBABLE TEMPERATURES OF RECONSTITUTION OF THE GNEISS COMPLEX BETWEEN EMERYVILLE, NEW YORK, AND THE MASSIF

Distances of points from the massif are measured along horizontal lines drawn essentially normal to the trace of the massif. (See Pl. 1.)

The trace of the perimeter of the massif (Pl. 1) seems to represent a line along which temperature was approximately the same during the metamorphism recorded in the gneiss. This

was first noted by Buddington almost two decades ago (1939, p. 326–333). Subsequently, detailed field studies and investigations of the rocks and mineral deposits in the region have confirmed this (Buddington, 1952; A. E. J. Engel, in press). If the depth of metamorphism along this line is assumed to be approximately 5 miles, the maximum temperatures of metamorphism there probably ranged between 600° and 625° C. and could not have exceeded 765° C. Temperatures increased from the perimeter of the massif inward toward the anorthositic core. Outward from the perimeter of the massif along lines essentially at right angles to its trend, temperatures decreased to a calculated 500° C. in the central part of the Grenville Lowlands (Fig. 2.) Field evidence (Engel and Engel, 1953b), studies of solid solution of TiO_2 in magnetites (Buddington *et al.*, 1955), and the data presented in Parts 1 and 2 of this study indicate that isograds of temperatures intermediate between those of the perimeter and those in the center of the lowlands can be drawn as sinuous arcs essentially parallel to the perimeter. It follows that the maximum positive temperature gradient is along a line drawn normal to the southeast overturned side of the gneiss, down to and through the upper surface of the Adirondack igneous massif.

These relationships of increasing temperatures of metamorphism inward from the gneiss to the massif are utilized in the presentation of all data and are explained in a succeeding section.

Two points are of considerable interest with regard to the metamorphic history of the gneiss. The concordance in dip to the northwest of the gneiss and the margin of the massif (Pl. 1) seems to have resulted from the overturning of the gneiss to the southeast (Engel and Engel, 1953b, p. 1054–1059 and Fig. 2, p. 1056). Consequently, the existing systematic metamorphic zonation may be superimposed upon and blot out a very different pattern of largely lower-temperature metamorphic features in the gneiss. At some earlier stage in the formation of the anticlinorium in the Grenville Lowlands, that part of the gneiss now overturned and dipping northwest, nearly parallel to the outward sloping edge of the massif (Fig. 1; Pl. 1), must have dipped in the opposite direction, southeastward toward the trough of a large syncline at the northwest boundary of the massif. This earlier stage in the development of folds in the lowlands seemingly was at the onset of the major epoch of granitic intrusion but subsequent to the emplacement of anorthosites, gabbros, and syenites (Buddington, 1939; 1957, p. 304–305). During this period the rank of metamorphism in the gneiss segment under discussion is presumed to have been lower than that found at Emeryville today.

The line marking the perimeter of the massif (Pl. 1) actually is a zone of intense shearing and displacement. Extensive solid flow as well as discontinuous rupture of the rocks has occurred along the perimeter. Buddington (1939, p. 251–282, Figs. 24, 25; 1952) has presented many geological data that substantiate this conclusion. Our own detailed mapping of local areas indicates an irregular but crude increase in intensity of rock deformation and displacement (plastic tearing-apart) in the metasedimentary rocks as the perimeter of the massif is approached either from the core or from the Grenville Lowlands side. Minimum stratigraphic discontinuities in the metasedimentary sequence along the boundary between the lowlands and the massif probably exceed 1 or perhaps 2 miles. Precise estimates are difficult because of poor exposures of key units, many of which were largely obliterated by the emplacement of the younger granites. The displacements of the metasedimentary units seem to involve both vertical and horizontal motions. Most of the early rock movements (post-syenite, syn-early granite) seem to have involved rolling and thrusting of the metasedimentary rocks of the lowlands southeastward against and possibly over a synclinal perimeter of the massif. This is suggested especially by the subhorizontal axes in the large folds in the syenites and enveloping metasedimentary rocks in this area (Buddington, 1939; 1948, p. 25; A. E. J. Engel, in press). Later rock motions, during and in part after the emplacement of the bulk of the younger granites, seem to have been dominantly strike slip. Rocks of the lowlands were dragged northeast relative to those of the massif, and great cross folds were superimposed upon the pre-existing horizontally folded complex. The evidence for refolding, the relationships of cross folds to pre-existing subhorizontal folds, and the lateral displacement involved are discussed by Brown and Engel (1956) and by A. E. J. Engel (in press).

The intermediate- to high-temperature metamorphic assemblages and textures in the gneiss discussed in this paper evolved during lateral displacements and cross-folding motions in response to the same fundamental cause. These motions have not induced sharp discontinuities

in the pattern of progressive increase in degree of metamorphism as the massif is approached.

Although the curve of rising temperatures (and pressure?) from the Balmat-Emeryville area to Colton appears to have no marked discontinuities or abrupt changes in slope, an abrupt steepening of this temperature curve may occur at the massif (Fig. 2). This change of slope in the temperature curve needs further detailed study. Its clarification is dependent upon either pressure-independent thermometers or more accurate piezometers.

Choice and Location of Rock Samples

The numbers and locations of specimens of gneiss chosen for the more detailed analytical studies are given in Plates 1 and 4. Compositions of the specimens are given in Tables 7 and 9. The primary objective in choice of these samples was to obtain, from intervals along the gneiss belt, specimens that were representative of (1) least altered gneiss, and (2) rocks transitional in composition between the least altered and the migmatitic and granitized gneiss. The specimens are divided into six groups, each representative of a given area and presumably therefore representative of only a very small range of temperature. These groups of specimens are used to evaluate specific chemical and physical changes induced in the gneiss and its component minerals by (1) local temperature gradients; (2) regional temperature gradients; and (3) pervasive lit-par-lit injection and "soaking" of the gneiss by alkali-silicate fluids. Groups of samples of each of the above types, obtained in five areas as shown in Plates 1 and 4, are designated as follows:

EMERYVILLE GROUP 1: Samples in the Emeryville area, at the southwest end of the 35-mile segment of gneiss. The center of the group is approximately 9.7 miles from the nearest margin of the massif (Pl. 1). The group consists of 12 specimens. Four of these, Qb 235M, Qb 230, Qb 228, and Qb 231 are from the cores of the larger areas of least altered gneiss. The remaining eight specimens are examples of gneiss in various stages of granitization and lit-par-lit injection.

GROUP 1A (WEST BALMAT AREA): Consists of only two specimens from the gneiss complex. They were taken just southwest of Group 1 (Pl. 1) between it and the California phacolith. Specimen Bgn 27 is from the core of a large lens of least altered gneiss, whereas Bgn 26 is taken from a zone of subtle transition between this gneiss and equigranular, uniformly feldspathized gneiss. The close proximity of specimens of Group 1 and 1A (Pl. 1) is reflected in the similar textures and compositions. In most respects these two groups may be considered as one and the total number of groups as five.

EDWARDS GROUP 2 (EDWARDS AREA): Consists of four specimens. The center of Group 2 is approximately 4.7 miles from the nearest perimeter of the massif and about 6.7 miles northeast of the center of Group 1; their opposed edges are about 3 miles apart (Pl. 1). Specimen Qb 234 of Group 2 is from the center of the largest body of least altered gneiss in the Edwards area, specimen Qb 100 is inequigranular augen gneiss, and specimens Qb 216 and Qb 233 are equigranular, uniformly feldspathized gneiss.

RUSSELL GROUP 3 (RUSSELL AREA): Nine specimens in Group 3 were studied, four in detail. The center of Group 3 is about 3.7 miles from the massif and about 9 miles northeast of the center of Group 2. The opposed perimeters of these groups are about 8 miles apart as measured along the strike. Specimen Bgn 14 is from the center of a lens of least altered gneiss. The other three specimens studied in detail are from a zone of transition between this gneiss and a faintly foliated, inequigranular granite gneiss.

PIERREPONT GROUP 4 (SOUTH PIERREPONT AREA): Two specimens of gneiss have been studied in detail. This group has its center about 11 miles northeast of the center of Russell Group 3 and about 2.7 miles from the perimeter of the massif. Opposed boundaries of these groups are 10 miles apart. No specimens of least altered gneiss suitable for mineral separations were obtained in the South Pierrepont area. Specimen Bgn 25 represents only incipiently feldspathized gneiss from a zone which merges into equigranular granitic gneiss. Specimen Bgn 16 represents rock intermediate between the incipiently feldspathized gneiss and the inequigranular granite gneiss.

Group 5, from the Colton area, consists of four specimens of least altered gneiss (Bgn 18, 19, 20, and 21) and two specimens of uniformly granitized gneiss (Bgn 22 and 23). The center of this group is about 1½ miles from the Adirondack Massif, and three specimens are within 1 mile of the massif (Pl. 1). The center of Group 5 is about 7 miles northeast of the center of Group 4 near Pierrepont. Time limitations prevented a thorough chemical study of more granitized gneiss from this area, although a limited number of analyses were made (Tables 12, 13, 14).

The irregular distribution of desired rock types and the complexity of the gneiss prevented the use of a more precise sampling pattern. Nevertheless, the spacing of groups and of samples within any group is reasonably uniform along the gneiss segment. There are no great differences in either appearance or composition between the specimens of least altered gneiss in any single group. Systematic differences in texture and composition of least altered gneiss do appear between groups. The maximum differences in composition of least altered gneiss between groups 1 and 5 are inferred to be metamorphic, the product of reconstitution, as amplified in a later section. Major differences in composition in any one group do appear in the specimens of variously granitized gneiss which are closely associated with gneissic granite in the field.

Additional difficulties encountered in sampling were induced by incipient but widespread alteration and cataclasis. More than three-fourths of the samples collected for analysis had to be abandoned after petrographic study because of the patchy retrograde alteration or mortar structure. Neither accurate modal analyses nor clean mineral separations were obtained on specimens with well-developed mortar structure. The retrograde alteration of the gneiss consists largely of chloritization of biotite and sericitization of plagioclase. Alteration varies slightly from specimen to specimen as may be seen from inspection of the modes in Tables 7 and 9. Because of the detailed mapping and collections in the southwest one-third of the gneiss segment, the specimens in Groups 1 1A, and 2 probably are more wisely selected and representative of the desired rock type than specimens from Groups 3, 4, and 5.

Wherever rock exposures permitted, 15–20 pounds of the freshest possible rock was collected. Each sample included two slabs, at least 4 inches across, with flat or slightly rounded faces. The slabs were used as pestle and mortar to crush smaller chips. Far too many sample sites were on glaciated, flat or only gently arched exposures, well removed from the nearest road and air hammer. At these spots sample size was sacrificed rather than location. In several instances the maximum sample obtained was about 5 pounds. We are acutely conscious of limitations in size and quality of the rock and mineral samples, and the 3000 miles between our laboratory and more material.

Preparation of Samples

Commonly four representative rock slices were sawed for thin sections from about 400 to 1000 gms of each sample—depending upon lithologic uniformity and composition—and the remaining sample was then crushed to −100 mesh. This crushing was accomplished by disintegration of rock chips between anvil-like slabs of the same rock specimen. The resulting −100 fraction was quartered down, and about 15 gms was split off for wet-chemical and spectrochemical analyses. All splitting of samples was done with a high purity aluminum microsplitter. About 4 gms of the 15 gm sample was split off and ground to a powder in a mechanical agate mortar for the spectrographic work. Silk screens were used in all sizing operations.

The bulk of the −100-mesh rock sample—350–1000 gms—was used for the separation of the constituent minerals as noted in Part 2 of this study.

Methods of Rock Analysis

Introduction

Analyses of rocks include chemical analyses for major and minor elements, spectrochemical analyses for trace elements, and modal analyses of the volume per cent of mineral constituents in each rock. These analytical methods are discussed in the order named. Unless otherwise specified the chemical analyses of major elements are by Celeste Engel, and the spectrographic analyses of trace elements are by A. A. Chodos and Elisabeth Godijn. In a concluding part of this section the chemical analyses of major constituents in the rock are compared with chemical compositions as calculated from the modal analyses.

Chemical Analyses, Major and Minor Elements

Each sample of gneiss analyzed by C. G. Engel (Tables 7 and 9) was handled as an unknown prepared by A. E. J. Engel. At intervals during the 3 years in which these rock analyses were made, samples of G-1 and W-1 (Fairbairn *et al.*, 1951) were introduced as unknowns along with other specimens of gneiss. The results of these analyses, and the "adjusted" means of G-1 and W-1 (Fairbairn, 1953, p. 146–147) are in Table 1. These indicate reproducibility and any major bias relative to analyses from other laboratories. In the deter-

minations made by C. G. Engel, Al_2O_3 appears to be consistently high by about 2 per cent of the amount determined and SiO_2 slightly low Otherwise no major systematic error is apparent from the analyses of G-1 and W-1.

TABLE 1.—DUPLICATE CHEMICAL ANALYSES OF MASKED SPECIMENS OF G-1 AND W-1 MADE WITH ANALYSES OF GNEISS AND INDICATIVE OF PRECISION OF ANALYTICAL METHODS

	G-1 x̄	G-1*	Mean deviation	W-1 x̄	W-1*	Mean deviation
SiO_2	72.86	72.65	.21	52.69	52.53	.16
TiO_2	.25	.25	.00	1.10	1.10	.00
Al_2O_3	13.94	14.16	.22	14.72	15.20	.48
Fe_2O_3	.93	.85	.08	1.50	1.39	.11
FeO	.99	.90	.09	8.71	8.63	.08
MnO	.027	.03	.003	.165	.16	.00
CaO	1.41	1.35	.06	10.96	11.02	.06
MgO	.39	.36	.03	6.63	6.55	.08
Na_2O	3.25	3.34	.09	2.00	2.04	.04
K_2O	5.42	5.48	.06	.63	.67	.04
H_2O+	.36	.33	.03	.56	.52	.04
P_2O_5	.09	.10	.01	.126	.12	.006
Total	99.92	99.80		99.80	99.93	

* Celeste G. Engel, analyst.

Certain modifications of classical analytical methods were introduced in the rock analyses. These variations in techniques are taken from the methods of "rapid analysis" as formulated by Shapiro and Brannock (1952; 1956). The "main portion" (SiO_2, R_2O_3, CaO, MgO) on all rocks was done by conventional gravimetric methods employing a 1.0000-gm sample. This sample was fused in Na_2CO_3 in a platinum crucible. The fusion was dissolved in HCl, and silica, alumina, total iron, calcium, and magnesia were determined from this fusion. FeO was determined on a 0.5000-gm sample boiled gently in concentrated H_2SO_4 and HF. Crucible and contents were dumped quickly into a dilute solution of phosphoric acid, boric acid, and sulfuric acid and titrated with a standard solution of potassium dichromate.

Total Fe and Fe_2O_3, and MnO, TiO_2, and P_2O_5 were determined on a 0.4000-gm sample, dissolved in a platinum crucible on a steam bath in sulfuric and hydrofluoric acids. The resulting solution was increased to 200-ml volume with water. Aliquots were taken to determine Fe_2O_3, MnO, TiO_2, and P_2O_5 on the Beckman Model B spectrophotometer.[4] In most of the rock analyses another aliquot of this same solution was used to determine Na_2O and K_2O on the Beckman Model DU

TABLE 2.—PRECISION AND ACCURACY OF ALKALI ANALYSES USING FLAME PHOTOMETER

Sample	Date	Flame photometer*		Officially determined concentrations	
		Na_2O	K_2O	Na_2O	K_2O
G-1	1/21/55	3.31	5.48	3.25	5.42
	10/12/56	3.38	5.37	3.25	5.42
W-1	4/16/56	2.16	.67	2.00	.63
N.B.S. Feldspar #70	4/16/56	2.40	12.87	2.38	12.58

* Celeste G. Engel, analyst.

photometer with a flame attachment. This method was used after its precision was established by replicate analyses of G-1, W-1, and of the National Bureau of Standards Feldspar #70. The replications are listed in Table 2. Distinction has been made, however, in the listing of rock analyses (Tables 7 and 9) between those determinations of K_2O and Na_2O by flame photometer and those by the J. Lawrence Smith method.

The plus water (+110° C.) was determined on a 1-gm sample, in a Penfield tube, with a flux of lead oxide. Furnace temperature prior to action of the flux was approximately 850° C.

Spectrographic Analyses, Trace Elements

Trace-element analyses were made emission spectrographically by essentially the same method described by Murata (*in* Gordon and Murata, 1952). Standards were made by mixing either (1) chemically analyzed minerals or (2) pure oxides of the elements into a quartz-feldspar base. Proportions of quartz to feldspar were 6:4. Concentration steps of 10,000, 4640, 2150, and so on down to 2.15 ppm were prepared by dilution with the base. The standards

[4] The analyses of Fe_2O_3 made in this way were checked by five analyses with a silver reductor. In this method iron from the R_2O_3 group, in an HCl solution, was reduced by passing the solution down a column of metallic silver.

and samples were exposed using the following equipment and methods:

Spectrograph:	Jarrell-Ash 3.4 m grating instrument, Wadsworth mount, dispersion, 5.2 Å/mm in the first order.
Excitation:	19-ampere short-circuit D. C. arc from a Jarrell-Ash Varisource. Sample as the anode. Analytical gap, 4 mm magnified 5× and focused on the slit. Central 2 mm used with a slit width of 25 microns; 25-mg samples were burned to completion (90–120 sec.). Total energy method with no internal standardization.
Electrodes:	High purity one-quarter inch graphite rod as the anode. U.C.C. #3417. Pointed one-eighth inch cathode.
Wave-length Range:	2300–4800 Å in the first order.
Plates:	Eastman Kodak III-0.
Processing:	4 minutes in DK-50 developer at 20° C., 20 sec. short stop, 10 min. in acid fix, 20 min. wash.
Plate Calibration:	Selected iron lines after method of Dieke and Crosswhite (1943). Each plate is calibrated.
Densitometer:	Applied Research Laboratories model #2250.

The average sensitivities for the various elements are listed in all tables which include spectrographic data. The sensitivity value represents the average limit of detection and will vary from plate to plate. Each sample was exposed in duplicate; the average was regarded as one analysis. In addition masked duplicates were repeatedly prepared and inserted into the analytical sequence by A. E. J. Engel. Wherever the trace-element data indicated the possibility of a trend, the critical samples were masked and rerun on a single plate. Under these conditions reproducibility is approximately 25 per cent of the amount reported. Detailed data on analytical precision for each element were determined by statistical analyses of the differences between masked samples on the same, and on different plates. The statistical method is described fully by Snedecor (1946, p. 66–68), and the statistical data are summarized in Table 3.

Modal Analyses

All modal analyses of rocks were made from stained sections approximately ¾ by 1 inch in size. For maximum efficiency the sections were cut essentially normal to the strongest foliation, prepared as suggested by Chayes (1952) with hydrofluoric acid as an etching agent and sodium cobaltic nitrate as a stain. In specimens of gneiss devoid of marked lithologic layering, where grain intercepts are less than 0.5 mm and grains average between .05 and 0.3 mm in diameter, calculations indicate that two sections proved adequate if a total of 3000 counts were made. In the coarser-grained and inequigranular layered specimens (Pl. 2, fig. 2), three to four sections were counted, yielding 4500 to 6000 counts per total specimen (Table 4). Number of sections and points counted in more homogeneous specimens was based upon Chayes' replication schedule for maintaining analytical error (Chayes, 1956, p. 79–91,

TABLE 3.—PER CENT STANDARD DEVIATIONS OF REPLICATE SPECTROGRAPHIC ANALYSES OF TRACE ELEMENTS

Element	Per cent standard deviation		Ppm.	
	Same plate	Different plates	Sensitivity	Mean*
B	60	80	10	12
Ba	20	31	1	800
Co	9	16	2	8
Cr	22	20	5	40
Cu	40	50	1	15
Ga	26	24	5	10
La	..	20	80	100
Mn	26	36	2	400
Mo	..	..	3	5
Nb	..	..	15	15
Ni	36	40	2	20
Pb	33	88	10	15
Sc	14	26	2	15
Sn	..	..	5	10
Sr	54	36	2	300
Ti	13	77	2	5000
V	39	20	2	60
Y	13	25	10	50
Yb	15	64	1	4
Zn	24	..	80	80
Zr	18	19	2	200

* This mean value is shown only to indicate that many elements are near the limit of their sensitivity. It represents the mean of only those samples used for statistical analyses.

Fig. 11). Grain counting was done with a point counter (Chayes, 1949) adapted from a Bausch and Lomb mechanical stage. Distance between centers is equivalent to a horizontal traverse of about 0.3 mm. Traverses were spaced at intervals of 500, 1000, and 1500 points (Table 4) indicate the changes in modal analysis in a part of the gneiss devoid of other large garnet clusters. The successive changes in composition at

TABLE 4.—MODAL ANALYSES OF TWO ROCKS

Recorded at counting intervals ranging from 100 to 4500 points to show fluctuations induced by coarse-grained, inequigranular, and irregularly layered gneiss.

	Specimen Bgn 25				Specimen Bgn 21				
	100	500	1000	4500	100	500	1000	1500	4500
Quartz	41.00	23.80	20.00	19.20	28.00	26.60	25.70	31.67	36.27
Plagioclase	38.00	54.30	54.30	48.07	19.00	46.80	53.10	49.63	48.90
K feldspar	4.00	3.40	5.40	10.26	.00	2.00	2.30	2.07	.73
Biotite	17.00	17.60	18.60	19.56	10.00	11.80	11.90	11.27	7.07
Garnet	..	..	.90	2.01	43.00	11.80	5.90	3.93	5.87
Sphene	..	tr	.10	.13	..	..	..	..	..
Apatite	..	tr	.10	.06	..	..	.10	.07	.05
Chlorite	..	.30	.30	.41	..	..	tr	.20	.17
Sericite	..	.40	.20	.18	..	..	.20	.30	.33
Opaques	..	.20	.10	.12	..	1.00	.60	.66	.53
Zircon	..	..	tr	tr	..	..	.20	.20	.08
Total	100.00	100.00	100.00	100.00	100.00	100.00	100.00	100.00	100.00

sites randomly chosen from 10 possibilities within each millimeter. Tabulations were made with a biological counter.

In these specimens the largest analytical errors arise from inadequate areas traversed relative to band width and to the size and distribution of porphyroblasts, especially garnet. Actually the garnet porphyroblasts are not of single crystals but involve either garnet sieved by quartz or a cluster of garnet, quartz, K feldspar, and a little biotite or chlorite, commonly enveloped in a dominantly quartzose sheath. Most feldspar porphyroblasts are sieved with biotite and quartz. Individual grains of garnet and feldspar are both large and small. The presence of very small grains coupled with the polymineral nature of the cluster rules out precise traverses on large polished slabs. The problem is exemplified by modes of two garnetiferous specimens, Bgn 21 and Bgn 25, which have been tabulated in per cent at intervals of 100, 500, 1000, 1500, and 4500 counts (Table 4). In specimen 21, the first traverse crossed a garnet cluster before 100 points were recorded, resulting in an average percentage composition (at 100 points) of 43 garnet, 10 biotite, 19 plagioclase, and 28 quartz, with no K feldspar.

Specimen Bgn 25 shows a reverse relationship in which several of the last traverses went through two clusters, one of garnet, and the other of K feldspar (4500-point column, Table 4).

Very fine-grained alteration products, especially chlorite replacing biotite and sericite replacing feldspar, require high power for adequate resolution and constitute a major source of eye strain and tension if but a minor source of error. Equally fine-grained cataclastic effects compounded the difficulty of getting an unbiased result.

Calculations of Chemical Composition From Modal Analyses

The efforts expended in detailed modal analysis of the gneiss were prompted in part by the desire to calculate a chemical composition of the rock from the mode and to compare this composition with that obtained by conventional wet-chemical analysis. Calculation of the chemical composition of the rock from the mode was attempted on the 24 specimens from which adequate physical and chemical data were available. In each example the chemical

compositions of the total rock, and of biotite and garnet (where present), were determined by chemical analysis. The composition of component K feldspar was obtained by chemical analysis in 8 specimens, and from these data, compositions of the remaining 16 were estimated. Composition of plagioclase was obtained from optical constants and checked independently from the chemical analyses of Ca in the rocks. Analyses were made for Na in seven muscovites. Compositions of accessory sericite, chlorite, and magnetite were estimated.[5] Densities of all garnets were determined directly with a micropycnometer. Densities of plagioclase, biotite, K feldspar, and all accessory minerals were calculated from the compositional data. The detailed mineralogical data will be presented in Part 2 of this paper.

TABLE 5.—DATA COMPARING PRECISION OF DIRECT CHEMICAL ANALYSES AND USE OF MODAL ANALYSES AND PHYSICAL AND CHEMICAL PROPERTIES OF MINERALS IN DETERMINING CHEMICAL COMPOSITIONS OF ROCKS

	Group 1 specimens			Group 5 specimens			Actual chemical analyses		Analyses of G-1 by 34 analysts		
	1	2	$\bar{x}$ 3	4	5	$\bar{x}$ 6	G-1 7	W-1 8	$\bar{x}$ 9	10	11
SiO_2	.26	.65	.26	.40	.61	.10	.21	.16	72.24	.27	1.19
TiO_2	.03	.05	.01	.10	.15	.04	.00	.00	.26	.034	.24
Al_2O_3	.26	.40	.20	.30	51	.01	.22	.48	14.34	.27	1.62
Fe_2O_3	.06	.09	.01	.19	.26	.19	.08	.11	.92	.21	.74
FeO	.25	.46	.25	.27	.50	.26	09	.08	1.01	.09	.31
MnO	.10	.28	.04	.05	.12	.04	.02	.00	.03	007	.021
MgO	.14	.32	.13	.01	.03	.01	.03	.08	.39	.09	.37
CaO	.09	.15	.06	.22	.22	.30	.06	.06	1.40	.10	.50
Na_2O	.19	.35	.09	.14	.20	.05	.09	.04	3.30	.18	.69
K_2O	.05	.09	.00	.15	.23	.15	.06	.04	5.48	.22	1.63
H_2O+	.01	.02	01	.08	.11	.08	.03	.04	.39	.11	1.03
P_2O_5	..	..	..	..	..	..	.01	.006	..	..	..

Columns 1 and 2. Mean and maximum deviations between major-element compositions of 12 specimens in Group 1 as determined by direct analysis and by calculations from modal analyses, using physical and chemical properties of the constituent minerals (specimens are Bgn 26, 27, Qb 236, 235M, 3, 7, 230, 229, 31, 226, 227, 228).

Column 3. Mean deviation between the mean compositions of the specimens in Group 1 cited above, as determined by averaging direct analyses and averaging analyses calculated from modes using physical and chemical properties of the constituent minerals.

Columns 4, 5, and 6. Data from Group 5 analogous to those for Group 1 in columns 1, 2, and 3.

Columns 7 and 8. Mean deviations of chemical analyses of G-1 and W-1 as done by Celeste G. Engel from "adjusted" mean compositions of these rocks (*see* Fairbairn, 1953, Table 1).

Column 9. Average of 34 analyses of the granite G-1 by 34 different analysts working in different laboratories (*see* Fairbairn *et al.*, 1951).

Columns 10 and 11. Mean and maximum deviations between the 34 analysts of the granite G-1 listed in Fairbairn *et al.* (1951).

The results of the calculations of rock composition from the modes exceeded expectations. In the 24 specimens studied, the maximum deviation of each major constituent oxide except MnO and FeO in the gneiss as determined from the mode, from the value of the oxide as determined chemically, is no greater than the maximum deviation in the same oxide in the 34 analyses of the granite W-1, as analyzed by 34 silicate analysts (Fairbairn *et al.*, 1951).

Moreover, calculations from modes of the

[5] Sericite is assumed to have the same composition as muscovite. An intermediate chlorite with equal proportions of antigorite, ferroantigorite, amesite, and daphnite was used (*See* Winchell and Winchell, 1951, p. 381); TiO_2 in magnetite varied from 1.5 at Emeryville to 3.0 at Colton.

composition of 12 of the more equigranular specimens of gneiss (Tables 7 and 9) yield mean and maximum deviations of the major oxides, except MnO, MgO, and FeO, that are less than these deviations in the 34 analyses of W-1, as posted in Fairbairn *et al.* These daat are shown in Table 5. In column 1 of Table 5 are the mean deviations of each major oxide, as computed from the modes of the 12 specimens, from the values of the oxides as determined by wet-chemical analysis. In column 2, Table 5, are the maximum deviations of each oxide, as computed from the mode and mineral analyses, from the value obtained by wet-chemical analyses of the rock. In column 3, Table 5, are the mean deviations of the arithmetic-mean composition of the 12 rocks as computed from the mode, from the arithemetic-mean composition of the 12 rocks as obtained by chemical analyses.

Data on the mean deviations of the 34 wet-chemical analyses of G-1 (Fairbairn *et al.*, 1951) are in columns 10 and 11 of Table 5, along with a computed mean of the 34 analyses (column 9, Table 5).

In columns 7 and 8 are the mean and maximum deviations between the standards G-1 and W-1 as done by C. G. Engel, from the "adjusted" mean compositions of these standard samples (Fairbairn, 1953, Table 1; Table 1, this paper).

The data suggest that, if given an analysis of biotite and garnet from the gneiss together with a careful mode of reasonably homogeneous gneiss within a radius of 2–3 miles of these minerals, the bulk composition of the gneiss can be calculated with about the same precision as the 34 analysts obtained in their work in the granite G-1 (Fairbairn *et al.*, 1951; Fairbairn, 1953). In areas of this size involving the most homogeneous parts of the gneiss where the chemical compositions of more than one biotite and one garnet are known, the precision of such calculations of the concentration of most major elements in the gneiss is greater than that achieved by the 34 analysts of G-1.

Chayes has pointed out repeatedly (*in* Fairbairn *et al.*, 1951; Chayes 1956, p. 1–31) that good modal analyses have not been made often enough, and they have not been adequately exploited by geologists. Work on the gneiss complex seems to confirm that view. For example, if only a couple of chemical analyses were possible during studies of the gneiss complex, these would have been made most profitably on biotite and garnet. In this way the chemistry of not only the parent rock, but of the constituent garnet and biotite as well, could be indicated within or close to the precision of practicing silicate chemists. It has taken about 75 complete chemical analyses of rocks and their constituent minerals to demonstrate this fact but other economically disposed geologists may take note.

The calculations involved in preparation of Table 5 also bring out some interesting and not fully understood sources of error in this work. For example, the values of CaO, FeO, and MgO as calculated from the modal analyses are almost invariably higher than these values obtained by chemical analysis. In contrast Al_2O_3 as calculated from the mode is lower, in about 70 per cent of the examples, than the Al_2O_3 as determined by chemical analysis. The unsymmetrical deviations of CaO and Al_2O_3 values obtained by the differing methods of analysis do not seem attributable to error in identification of plagioclase, for the deviations in Na_2O values are small and uniformly dispersed about the arithmetic means (Table 5). Possibly systematic errors are involved in both modal and chemical analyses. We hope to study this problem further.

The relatively large mean and maximum deviations in determinations of MnO via the two methods in the rocks of Group 1 seem attributable to the big variations in MnO content in specific minerals and in closely spaced specimens of rock. In Group 5 where Mn is more uniformly distributed in each of the constituent minerals, the mean deviation between MnO values obtained by the two methods is almost halved.

The similarity of chemical compositions of rocks obtained through modal analyses with rock compositions obtained by direct chemical analysis seems to justify the use of the former in this study. Accordingly, in demonstrating broad chemical trends, and in miscellaneous other calculations throughout this paper where precision and accuracy are least critical, chemical analytical data have been supplemented with rock compositions derived from modes. Each of these additions is specified. Agnostics may make appropriate allowances.

Temperature of Metamorphism

Introduction

The increase in temperature of metamorphism of the gneiss from Emeryville northeast to the massif (Fig. 2) is demonstrated by numerous lines of evidence. Most data indicate

only a relative increase in temperature. Evidence of this type includes (1) systematic changes in mineralogy and texture of the gneiss and associated metasedimentary rocks; (2) an increase in the abundance of granite and syenite with igneous features as the massif is approached; (3) the crude zonation of essentially contemporary hypogene mineral deposits, from mesothermal types at Emeryville to hypothermal deposits immediately southeast of Colton.

In the search for data on absolute temperatures of metamorphism, solid solutions of one phase in another were studied. Analyses were made of solid solution of $MgCO_3$ in calcite, paragonite in muscovite, TiO_2 in magnetite, and FeS in sphalerite. The data from these studies seem to offer minimal temperatures of the metamorphism. Further bracketing of temperatures was attempted through studies of phase reactions such as the presence or absence of wollastonite in siliceous calcite marbles. Most of these attempts to calculate temperatures of metamorphism are crude because of the uncertainties in regard to the pressures of metamorphism. Consequently the suggested temperatures of metamorphism—about 500°C. at Emeryville and about 600° C. at Colton—may be in error by about 50°.

Geologic Evidence of a Temperature Gradient

The variations in mineral and chemical composition and in texture in the gneiss between Emeryville and Colton, as described in succeeding parts of this paper and in Part 2, are completely consistent with and support the interpretation of a temperature gradient of about 100°C. between Emeryville and Colton during metamorphism.

Between Emeryville and Colton the ratio of granite with igneous characteristics to metasomatic granite increases markedly. In the gneiss of the Emeryville area, only one body of granite has features indicative of magmatic origin. This is the California phacolith (Pl. 1), first recognized and described by Buddington (1929). This phacolith is an equigranular, light-pink, two feldspar-quartz granite. It is enveloped by a narrow, distinctive and markedly disharmonic sillimanite-garnet aureole bearing gneiss formed at temperatures seemingly in excess of 575° C. (A. E. J. Engel, in press). The remainder of the granite lenses and layers are devoid of obvious contact effects. At least half of them are demonstrably metasomatic (Engel and Engel, 1953b, p. 1060–1061; Figure 2 of Plate 3, this paper).

The relative abundance of granite and syenite of probable igneous origin in the vicinity of Colton and near by in the massif has been described and carefully documented by Buddington (1939; 1948; 1957) and by Buddington and Leonard (in press). The regional picture is therefore one of a central, hotter igneous-rich complex, bordered by metasedimentary rocks partly injected and replaced by outward-spreading, highly mobile magma or K- and Si-rich fluids. Within the massif the several igneous-looking rock types are arranged in a crude zonal pattern, including from core to perimeter, (1) anorthosite; (2) gabbroic anorthosite; (3) syenite and syenitic granite; and (4) granite (Buddington, 1939, Pl. 2). Recently Buddington *et al.* (1955) have shown that the amount of TiO_2 in the magnetites of these rocks is directly correlative with their inferred temperatures of solidification from magma. The use of TiO_2 in magnetite as a geological thermometer of metamorphism is discussed in following pages.

The zonation of mineral deposits also has been noted (Buddington, 1939, p. 251–303; Buddington and Leonard, in press) to be sympathetic with the previously described rock and temperature patterns. The anorthositic core of the massif contains concentrations of highly titaniferous magnetite, thought to be segregation deposits. In and near the sheathing granite-syenite complex are numerous much less titaniferous skarns and granite-gneiss magnetite ores (Buddington and Leonard, in press). West of the massif, along the gneiss complex at Edwards and Balmat, important deposits of sphalerite, pyrite, and pyrrhotite, with minor galena, have replaced the marble (Brown, 1936; 1947). In this same area and farther west on the northwest side of the gneiss are large belts of highly pyritic gneiss (Prucha, 1953).

Absolute Temperatures

Data from magnesian calcites.—The amount of magnesium in solid solution in calcite in the magnesian marbles adjacent to the gneiss has been determined by Graf and Goldsmith (1955) and independently by the authors. These analyses suggest the metamorphism of the gneiss in the Emeryville area reached temperatures of at least 475° to 500° C.

Limitations and potentials of this method are noted by Graf and Goldsmith (1955), Goldsmith *et al.* (1955), and Harker and Tuttle (1955). Ideally the calcite should have formed in equilibrium with coexisting dolomite, assuring an

excess of $MgCO_3$ in the system. Even if dolomite was not a coformed phase, the magnesium in solid solution in the calcite may indicate a minimum temperature of metamorphism. The reaction is insensitive to P_{CO_2} and to MgO concentration. Perhaps the most serious difficulty involved in using magnesian calcites as thermometers lies in either (1) finding specimens which seem to have been effectively "quenched" at or near the maximum temperature of metamorphism (2) correctly interpreting whether or not dolomite in or near the calcite has been exsolved during cooling of the marble.

The specimens of calcite analyzed by Goldsmith *et al.* (1955, Table 4, specimens 70 71, and 75) and by the authors are more coarse crystals intergrown with dolomite in the marble about 1000 feet north of Balmat Corners. X-ray and spectrochemical studies indicate the calcites contain respectively about 5.6, 4.1, and 5.4 mol per cent $MgCO_3$ (as corrected, Graf and Goldsmith, 1958) in solid solution in the calcite. The pressure correction (2000–3000 atmospheres) has been investigated by Goldsmith (written communication) and appears to be negligible. Consequently the indicated temperature of metamorphism was about 500° C., possibly 525° C. (Graf and Goldsmith, 1958, Fig. 1). Subsequent search of 500 thin sections of marble in the Emeryville aera revealed three specimens of coarsely crystalline marble in which the calcite crystals contain tiny bleblike dolomite inclusions. In these specimens, coarse crystals of dolomite appear to have formed with the perthitelike magnesian calcites. The perthitelike calcites were carefully separated from the large crystals of dolomite. The sample selected was treated with ferric chloride and ammonium sulphite (Keller and Moore, 1937) to check for dolomite contamination. The concentrate proved to be free of all but the blebs of dolomite in the calcite. Wet-chemical analyses of the three blebby calcites indicate 5.1, 4.8, and 4.7 mol per cent $MgCO_3$. Both calcite and dolomite in the marble are relatively pure, containing less than 0.5 $FeO + Fe_2O_3 + MnO$. If the dolomite blebs were exsolved from the calcite during cooling, a minimum temperature of about 500° C. is indicated for the growth of the parent magnesian calcite crystals. This was presumably during the development of the assemblege quartz, greenish biotite, muscovite, oligoclase in the gneiss near by.

The marbles at the opposite end of the gneiss segment near Colton are poorly exposed and have not been studied in detail. Consequently studies of magnesian calcites from this area have not been attempted.

Thermometric significance of titaniferous magnetite.—Recently Buddington *et al.* (1955) have discussed the variations of titanium content of Adirondack magnetites, as related to the kind, origin, and temperature of formation of various host rocks. Several titanium-bearing phases, especially ilmenite and ulvöspinel, occur as intergrowths in Adirondack magnetites. The textural features and relative abundance of these intergrowths strongly suggest they are of exsolution origin. Buddington's studies show that the amount of titanium present in the exsolved ilmenite or ulvöspinel may reflect the temperature of formation of the specific host rocks—if titanium has been present in the system in excess of that fixed in the magnetite. An excess of titanium is inferred to have existed wherever TiO_2 (ilmenite) is present not only as a solid solution or as exsolved ? blebs in the magnetite, but also in independent grains.

The occurrence of titaniferous magnetite and separate grains of ilmenite in the gneiss and in granitic rocks associated with it offers a possible method of estimating temperatures of growth of the magnetite. Since the magnetite has formed with the silicates under study, the temperature at which they have grown is essentially this value. The TiO_2 content of five magnetites formed with independent ilmenite in rocks of the Emeryville area at the height of metamorphism is approximately 0.75 to 1.7 weight per cent. Two of these magnetites with 1.2 and 1.4 per cent TiO_2 occur in the gneiss; two with 0.97 and 1.7 per cent TiO_2 are in interlayered amphibolites; and one specimen having 0.75 per cent TiO_2 occurs in dominantly if not wholly metasomatic granite. In contrast, five magnetites from the Colton area—three in the gneiss and two in interlayed amphibolites—contain 2.0 to 3.6 per cent TiO_2, averaging about 3.0 per cent. In the youngest granites just southeast of Colton, which were emplaced during reconstitution in the gneiss, the TiO_2 content of three magnetites is slightly higher, averaging 3.9 per cent. These data, as calibrated by Buddington *et al.* (1955, Table 11 and text), suggest that the minerals under study in the gneiss near Balmat formed at about 475°–500° C., whereas those near Colton were developed at about 600° C.

Temperatures from FeS in sphalerites.—A possible minimum temperature of formation of the mineral assembleges in the gneiss in the Balmat-Edwards area may be indicated by the FeS content of sphalerites (Kullerud, 1953;

Barton and Kullerud, 1957). In these areas the sphalerite occurs with abundant pyrite and scattered pyrrhotite in marble and rarely in pyritic gneisses and schists (Brown and Engel, 1956). The use of the sphalerites as indicators of temperatures requires the assumption that the sulfides were emplaced as an integral phase of metamorphism, at essentially the temperature of the enclosing metamorphic rocks. If instead, the sulfides were deposited from localized hydrothermal fluids at very different temperatures, they contribute little to the present discussion.

Three features of the sulfide deposits suggest they may be indicators of the temperatures of metamorphism at the time of their deposition. These features are their (1) form, (2) distribution, and (3) paragenetic relationships to widespread metamorphic minerals. The sphalerite, pyrite, and pyrrhotite are replacement deposits that include not only veins (Brown, 1936) but also diffuse patches and grains disseminated through parts of stratigraphic zones (A. E. J. Engel, 1948). Scattered grains of sulfides occur in marble and in at least two of the metamorphosed clastic beds interlayered in the marble near the paragneiss (Brown and Engel, 1956, p. 1603 and Pls. 1 and 2). Locally, small veins and disseminated masses of pyrite and pyrrhotite occur in the paragneiss with occasional, very tiny crystals of sphalerite and galena. Many sulfide-bearing rocks appear to be devoid of obvious channelways or conduits along which hydrothermal solutions would be localized. In fact the seeming imperviousness of many host rocks has led Brown (1947) to suggest that the sulfides could not be hydrothermal deposits in the conventional sense.

The sulfide mineralization is relatively widespread, although the only known commercial deposits of sphalerite are in the Balmat and Edwards areas. Small veins and disseminated grains of sulfides occur in both marble and schists from Balmat at least to Pyrites, New York. (Pl. 1).

The paragenetic relationships of sulfides to metamorphic minerals also are consistent with an intimate relationship between the sulfide mineralization and the prevailing metamorphic processes. The assemblage diopside-dolomite-calcite-quartz evolved in the marble as the minerals quartz, biotite, plagioclase, and muscovite grew in the gneiss in the Emeryville area (A. E. J. Engel, in press). Subsequently formed retrograde metamorphic assemblages are widespread, although spotty in their development, in both gneiss and marble. The paragenesis in the marble is as follows: diopside → tremolite → anthophyllite → serpentine → talc. The development of these minerals in parts of the marble is paralleled by the appearance of traces of clinozoisite, chlorites, sericite, and albite in parts of the gneiss.

The more iron-rich sphalerites, along with some of the pyrite and pyrrhotite, were introduced during the anthophyllite stage of retrograde metamorphism in the marble. The formation of less iron-rich sphalerites and of iron sulfides continued, however, throughout the period in which serpentine and early talc formed (Brown, 1936; A. E. J. Engel, in press). Much talc postdates all the sulfides.

All these relationships admit but certainly do not prove the possibility that the iron-rich sulfides formed at not only the same time but at the same temperatures as anthophyllite in the marble, and that these temperatures were widespread in the Emeryville area. If this is true, the temperatures recorded in the sphalerites are no higher, and possibly lower, than those at which the quartz, biotite, oligoclase, and muscovite grew in the paragneiss. In effect, temperatures of formation of the sphalerites richest in iron may offer a minimum temperature for the metamorphism of the gneiss.

Analyses of sphalerites coexisting with pyrite in the marble just northwest of Balmat (Pl. 1) have been made by both Brown and Kullerud. It is not clear, however, that these sphalerites grew with coexisting pyrrhotite, hence the values noted may be below actual temperatures of crystal growth (Barton and Kullerud, 1957). These sphalerites contain between 7 and 8.9 weight per cent FeS (Kullerud, 1953, Table 14 and p. 138). Assuming the sulfides were emplaced at approximately 2000 atmospheres, a temperature of formation of at least 350°–375° C. ± 25° C. may be inferred. Mr. Bruce Doe (personal communication) subsequently analyzed specimens of sphalerite intergrown with pyrrhotite at the Balmat number two mine, which is about 4500 feet southeast of the gneiss (*see* Brown and Engel, 1956, Pl. 2). At this writing he has found as much as 10.3 weight per cent FeS in several of the sphalerites. Assuming a pressure of about 2000 atmospheres, the analyses suggest the sphalerites were formed at temperatures of at least 430° C. FeS content of two sphalerites at Edwards (intergrown with pyrite?) analyzed by Kullerud suggests a minimum temperature of growth of 385° ± 25° C. (Kullerud, 1953, Table 14, samples 59, 87). Presumably sphalerites intergrown with pyrrhotite as well as pyrite will indicate

higher temperatures. These data appear entirely consistent with the interpretation of minimum temperatures of metamorphism of at least 450° C. Sphalerites coexisting with pyrrhotite in the gneiss have not been extracted and analyzed, largely because of the formidable problems of concentration and purification. Data from the sphalerites in the gneiss would of course be most valuable in the present context.

Na content of muscovites in the gneiss.—The amount of solid solution of paragonite (Na mica) in muscovite has been shown by Eugster and Yoder (1955, p. 124–125) to be primarily dependent on the temperature of formation of the mica, if the system is saturated in Na. Actually the muscovite in both gneiss and associated pegmatites at Emeryville coexists with an intermediate to calcic oligoclase rather than albite or paragonite. Accordingly the muscovites cannot be expected to contain the maximum amount of Na consistent with their temperature of formation.

Analyses of four muscovites from the gneiss and three from associated pegmatite show a range in mol per cent paragonite from 7.2 to 8.1. The highest value (8.1) indicates that the temperature of metamorphism must have exceeded 400° C. (uncorrected from P_{H_2O} and P_{total}). This is at least 75C.° below temperatures of metamorphism indicated by the other solid-solution geothermometers.

Temperature limits implied by wollastonite-free siliceous marble.—Throughout the Emeryville-Colton region, siliceous calcitic marbles occur on both sides of the gneiss. Quartz-calcite beds and intergrowths in these marbles have been searched for wollastonite. None has been found. In the associated siliceous dolomite layers, diopside is the highest rank silicate present. As much of the quartz and calcite is almost surely of sedimentary origin (A. E. J. Engel, 1949; Brown and Engel, 1956) these two minerals have coexisted without reaction throughout the metamorphism of the gneiss. Assuming (1) the depth of burial of the marble and gneiss at Colton was not in excess of 5 miles and (2) $P_{total} \geq P_{CO_2}$, the temperature of metamorphism of gneiss and marble in the Emeryville-Colton region did not exceed 750° C. This conclusion is based upon the calculated and the experimentally determined invariant equilibrium reaction curve, $CaCO_3 + SiO_2 \rightleftarrows CaSiO_3 + CO_2$ (Harker and Tuttle, 1956; Danielsson, 1950; Weeks, 1956). Probably the weakest assumption involved is that the metamorphism occurred at depths less than 5 miles. If much greater depths were involved the maximum possible temperature of the reactions would be increased. Of course many students of metamorphism assume that during the regional metamorphism $P_{CO_2} \ll P_{total}$ (c Barth, 1952, p. 286–287; Ramberg, 1952, p 155–156). If this is true, the maximum temperature of metamorphism at Colton would b depressed much closer to the 600° C. indicate by the solid-solution data.

Temperatures as indicated by the O^{18}–O^{16} ratio in coexisting quartz and magnetite.—The isotopic compositions of coexisting mineral pairs such as quartz-calcite or quartz-magnetite which precipitate slowly under equilibrium conditions from a water-rich solution have values that depend upon (1) the isotopic composition of the water; (2) the amount of water; and (3) the temperature of growth of the mineral (Clayton and Epstein, 1958). Analyses by Clayton and Epstein of numerous specimens of coexisting quartz and magnetite from suites of metamorphic and igneous rocks indicate isotopic equilibrium commonly is closely approached during mineral formation. These workers show that the δO^{18}–O^{16} ratios for quartz minus δO^{18}–O^{16} values for magnetite indicate a consistent relative temperature of formation of these minerals which is in excellent agreement with geologic data on their origin. The smaller the δ quartz minus magnetite value, the higher the temperature of mineral growth.

During the course of this study Clayton kindly undertook analyses of coexisting quartz and magnetite from the gneiss at Emeryville and at Colton. In addition, analyses were made of coexisting quartz and magnetite from the gneissic hornblende granite just southeast of Colton along the outer margins of the Adirondack Massif. This granite, interpreted to be magmatic in origin, is discussed in a succeeding section of this paper.

The analytical data are listed in Table 6. The decreases in δ quartz minus δ magnetite from 11.1 to 8.2 in the gneiss between Emeryville and Colton is indicative of appreciably higher temperatures of metamorphism at Colton. In general Clayton and Epstein find that δ quartz minus magnetite values of 8 to 8.5 are characteristic of these minerals in plutonic, igneous granites. Values of δ 7 to 8 are recorded for igneous granodiorite and rhyolites.

Although these data are not yet calibrated to a precise temperature scale, they are of special interest for the following reasons: (1) processes of oxygen-isotope fractionation of the

type recorded are strongly temperature dependent but are nearly independent of pressure. In this respect they are superior to some other thermometers used in this study and are good evidence of the temperature gradient between

TABLE 6.—DELTA O^{18}-O^{16} RATIOS FOR COEXISTING QUARTZ AND MAGNETITE IN GNEISS AT EMERYVILLE AND COLTON AND IN HORNBLENDE GRANITE GNEISS IN THE ADJOINING PART OF THE MASSIF

Specimen and Locality	Quartz ‰	Magnetite ‰	Quartz-Magnetite ‰
Paragneiss, Emeryville (Qb 67)	14.8	3.7	11.1
Paragneiss, Colton (Bgn 18)	12.3	4.1	8.2
Hornblende microcline granite gneiss (outer part massif)	11.9	3.3	8.6

Emeryville and Colton; (2) the oxygen-isotope data confirm much geologic evidence (noted in succeeding pages) that the gneiss at Colton was metamorphosed under essentially ultrametamorphic or near-magmatic conditions of T and P; (3) an absolute calibration of the oxygen-isotope data is possible using experimental methods.

PRESENTATION OF ROCK ANALYSES

A standard method of presentation is used to aid rapid comparisons between the analytical data on various figures and tables. Inherent in the method is the conclusion that a positive temperature gradient existed in the gneiss between Emeryville and Colton during metamorphism. The relative temperature of formation of any specimen in this study may be indicated (1) by the relative distance measured along the strike of the gneiss from Colton southwest to the specimen or (2) by the distance of the specimen or group of specimens from the edge of the massif, as measured along a line on the earth's surface drawn normal to the trace of the massif. The last-named measurement is used as a scale (horizontal co-ordinate) and calibrated against an approximation of the temperature of crystal growth (reconstitution) in Figure 2. This scale seems justified by the fact that the outer surface of the massif and the southeast, overturned side of the gneiss are subparallel and dip at moderate angles northwest (Pl. 1). In all tables and figures, therefore, the horizontal co-ordinate is used as a measure of the shortest horizontal distance of the center of each group of specimens from the massif. The vertical co-ordinate represents the property of the rock or mineral being compared as a function of distance and, consequently, relative temperature of formation. The specimens of Group 1 (Emeryville area) are rather uniformly distributed around a point 9.7 miles from the perimeter of the massif, as measured along a line on the map drawn essentially normal to the perimeter (Pl. 1). Specimens in Groups 2, 3, 4, and 5 are distributed around points respectively 4.7, 3.7, 2.7, and 1.5 miles from the perimeter of the massif (Pl. 1). Comparisons are confined for the most part to statistical values of each group rather than those of individual specimens. Consequently, group values for given properties of rocks or minerals in the Emeryville area (Group 1) are plotted at a point on the horizontal co-ordinate 9.7 miles from the right-hand side of graph (perimeter of the massif). Group values for rocks or minerals in the Edwards area (Group 2) are plotted at a point 4.7 miles from the right side (massif), and so on. Considering the complexity of the geology, comparisons of properties of individual rocks or component minerals within any single group simply as a function of slight differences in distance from the massif do not seem justifiable. Hence the relative position of a specimen within the group is not to be regarded as highly significant, although for simplicity the sequence of specimen numbers is kept constant throughout the illustrations.

ROCK METAMORPHISM

Assumptions

Assumptions and errors involved in estimating the temperatures, depth, and pressures of metamorphism have been noted; other critical factors, seemingly impossible to evaluate rigorously, are the extent to which the composition of the gneiss varied from place to place before and during metamorphism and the kind and chemical potential of fluids in the gneiss during its metamorphism. Much geological evidence noted in following passages suggests that the sedimentary parent to the gneiss was compositionally uniform between Emeryville and Colton, and it would be pleasant to assume that the changes recorded in the least altered gneiss are induced largely by temperature. But it would be absurd to argue that the pre-metamorphic composition of the

gneiss was everywhere identical, or that even the small variations were unimportant (*see* Yoder, 1952, p. 615–617).

The data presented on succeeding pages, (see especially Table 13) indicate large volumes of water were expelled from the gneiss and from associated metasedimentary rocks during the metamorphism described. Maximum expulsion of water occurred in areas of most complete granitization. For example the mean H_2O (110° C.+) content of least altered gneiss found at Emeryville is 0.72 weight per cent. In intimately associated gneiss replaced by granite, the water content decreases to 0.32. In the Colton area the least altered gneiss is less hydrous than that at Emeryville, averaging only 0.4 water. Moreover, most granite replacing this gneiss has less than 0.2 per cent water, and numerous bodies of metasomatic (?) granite contain only 0.1 per cent water (Table 13, column 7). Assuming 2–3 per cent water in the gneiss during incipient stages of its metamorphism, it is clear that appreciable water streamed through and out of this metasedimentary rock as metamorphism proceeded.

An enormous volume of CO_2 accompanied the water. The metasedimentary rocks on either side of the gneiss are siliceous magnesian carbonate rocks (Engel and Engel, 1953b, Table 1, p. 1055). The metasedimentary section, including the gneiss, is at least 12,000 feet thick (after metamorphism). Two-thirds of this section is siliceous marble. During the stages of high-rank metamorphism in these siliceous dolomitic marbles, over half the original sedimentary silica reacted with dolomite to produce calcium magnesium silicates, especially diopside. Calculations based upon detailed mapping and analyses indicate CO_2 comprising at least 10 per cent by volume of the early metamorphic marbles was expelled from them (A. E. J. Engel, in press). Much of this CO_2 must have streamed through the gneiss, or at least through more permeable parts of it, as the gneiss was reconstituted and granitized.

If the metamorphism of the gneiss is considered as an isolated problem, there appears to be no way to evaluate the effects of (small ?) variations in composition, or of the chemical potential of CO_2 or H_2O, upon temperatures of metamorphism. At least a crude appraisal of these effects seems possible, however, if studies analogous to this one can be expanded to other terranes. For example, studies could be undertaken of paragneisses most nearly approaching the Adirondack gneiss in "residual" composition. Almost surely, certain conditions of metamorphism—P or T or the kinds and amounts of volatiles—as recorded in the residual system will have been different. An evaluation of temperatures of metamorphism and types of mineral assemblages, together with the properties of constituent minerals, as attempted in succeeding pages and in Part 2, should indicate far more clearly the range of conditions in which a given assemblage may form.

General Lithologic Features

The gneiss has evolved from a monotonous clastic, sedimentary rock into a complex of least altered and variously granitized gneiss. Few exposures of the paragneiss more than 15 or 20 feet thick are devoid of at least thin granitic seams or pegmatitic lenses. In much of the rock described as least altered, these seams do not exceed a foot or two in width or 10 per cent by volume of the gneiss. If the pegmatitic seams are avoided total K feldspar is commonly less than 5 per cent by volume and the K_2O-Na_2O ratio is commonly about 1.3 or more. Exposures of this least altered gneiss in part blend, in part merge abruptly along and across the strike into extensively migmatized or uniformly feldspathized granite gneiss.

The gross interrelationships of form, composition, and texture in the gneiss complex in the Emeryville-Edwards areas are illustrated in Plates 2, 3, and 4 and in Figure 3. Figure 3 is modified from Figure 7 in the paragneiss paper (Engel and Engel, 1953b). Around Emeryville the least altered gneiss is a faintly foliated, equigranular, sodic rock composed of quartz,

PLATE 2.—TEXTURES OF GNEISS

FIGURE 1.—Least altered gneiss near Emeryville (Group 1) with minor pegmatite. The dark massive rock in the lower two-thirds of the photo is the quartz-oligoclase-biotite gneiss with accessory muscovite and K feldspar, inferred to be little changed in bulk composition from its early or pre-metamorphic parent. The lenses of pegmatite are quartz, microcline, and oligoclase, with a little muscovite.

FIGURE 2.—Least altered gneiss near Colton (Group 5). The dark spots are garnet sieved chiefly by quartz. The lighter-colored finer-grained matrix is a quartz-andesine-biotite rock with accessory K feldspar. Grain size of the matrix rock is several times coarser than that in the least altered gneiss at Emeryville (Figure 1).

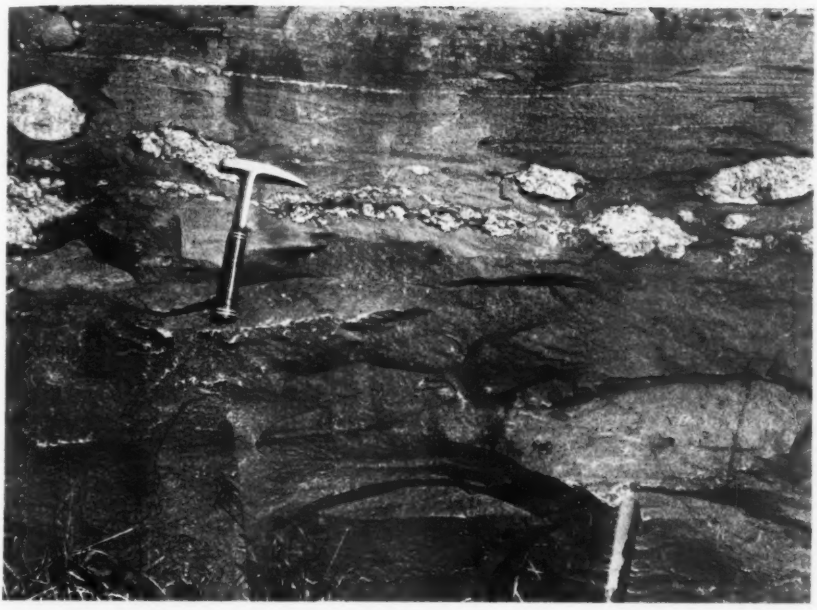

FIGURE 1

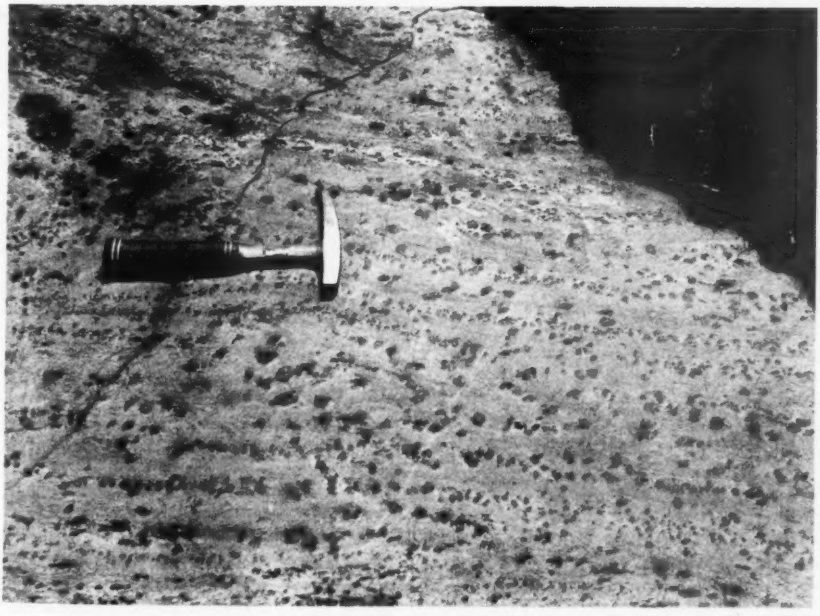

FIGURE 2

TEXTURES OF GNEISS

FIGURE 1

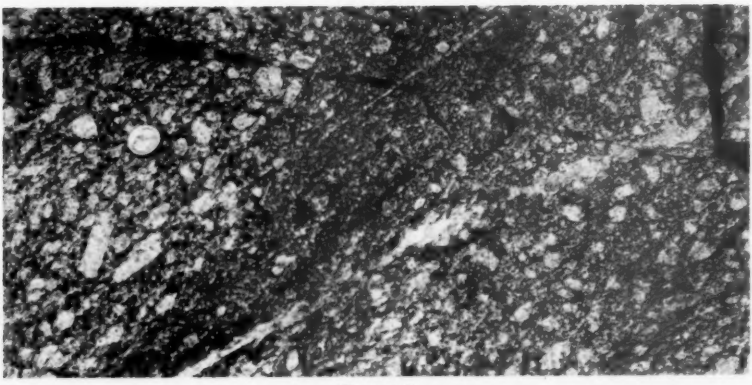

FIGURE 2

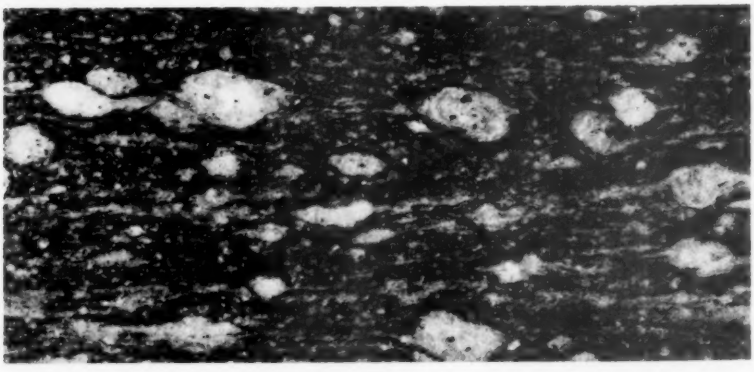

FIGURE 3

MIGMATITE AND INEQUIGRANULAR GRANITIZED GNEISS

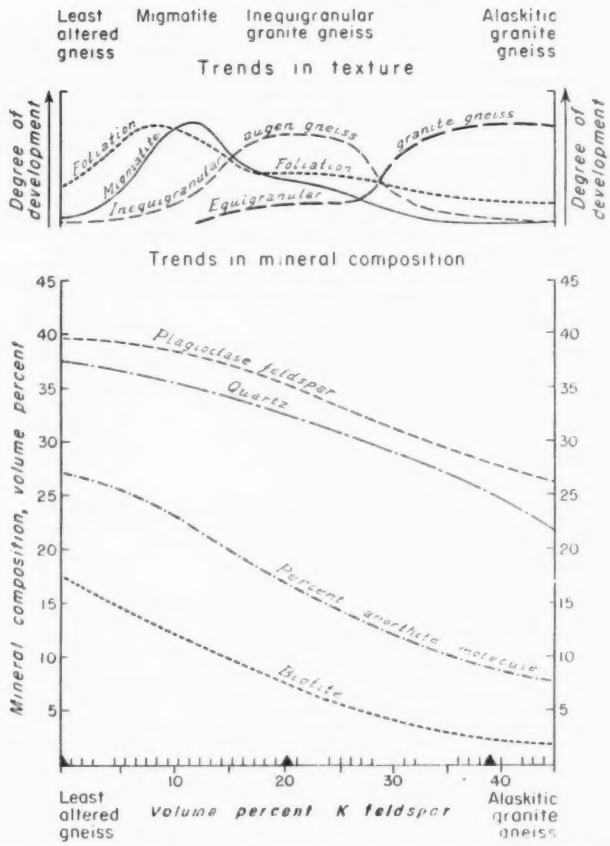

FIGURE 3.—GENERALIZED CURVES SHOWING INTERRELATIONSHIPS IN THE MINERALOGICAL, CHEMICAL, AND TEXTURAL EVOLUTION OF THE GNEISS COMPLEX DUE TO GRANITIZATION

Curves are based upon specimens whose modal analyses are published in Engel and Engel, 1953b, Figures 5, 6, and 7. Each tick on the horizontal co-ordinate indicates a modal analysis. These analyses are arranged from left to right in order of increasing K feldspar content. This order is inferred from field relationships to represent increasing degree of injection and replacement by granite-forming substances. Gaps in the sequence of ticks indicate no specimen of requisite K feldspar composition is available. The darts mark composite specimens analyzed chemically. These chemical analyses appear in columns 1, 3, and 4, Table 13.

PLATE 3.—MIGMATITE AND INEQUIGRANULAR GRANITIZED GNEISS

FIGURE 1.—Crenulated migmatite. The light-colored pegmatitic layers are composed largely of quartz, K feldspar, and oligoclase with scattered muscovite, biotite, and garnet. The darker gneiss has undergone slight to marked feldspathization (K feldspar) and shows a range in composition equivalent to that of specimens in Table 9. The crenulated pegmatite in part follows, and in part cuts across the dominant foliation. About ¾ mile south of Balmat, New York. Note the hammer for scale.

FIGURE 2.—Inequigranular granitic gneiss. The large (up to 2 inches long) anhedral to almost euhedral porphyroblasts are pink microclines, some of which cut or abut against the dominant foliation. They clearly formed by replacement of the groundmass (paragneiss) which now has about the composition of the rock in column 3, Table 13. Note the quarter dollar for scale.

FIGURE 3.—Inequigranular granitic gneiss (augen gneiss). This is the dominant granitic gneiss in the complex. It commonly grades into least altered gneiss and is intermediate in composition between it and more granitic gneiss. The differences between the microcline "eyes" in this rock and the euhedrons in Figure 2 are largely of form, induced by shearing motions during and slightly after the growth of the "eyes" The scale is 6 inches long.

TABLE 7.—CHEMICAL AND MODAL ANALYSES OF SELECTED SPECIMENS OF LEAST ALTERED GNEISS BETWEEN EMERYVILLE AND COLTON, NEW YORK
In chemical analyses, oxides given in weight per cent

	West Balmat Group 1A	Emeryville Group 1					Edwards Group 2	Russell Group 3	Colton Group 5				
	Bgn 27	Qb 235M	Qb 230	Qb 231	Qb 228	$\bar{x}$	Qb 234*	Bgn 14	Bgn 18†	Bgn 20	Bgn 21†	Bgn 19†	$\bar{x}$
SiO_2	67.92	68.24	68.65	70.91	68.12	68.77	68.04	68.85	61.27	65.37	68.63	63.87	64.79
TiO_2	.70	.67	.65	.66	.87	.71	.80	1.02	.78	.67	.52	.57	.64
Al_2O_3	15.53	14.82	15.19	13.88	14.44	14.77	14.80	14.90	17.94	17.83	16.06	17.84	17.42
Fe_2O_3	.77	1.08	.51	.54	.33	.65	.23	.36	.67	.53	1.02	.56	.70
FeO	3.51	3.81	3.90	3.88	4.89	4.00	5.04	4.26	6.81	3.47	.86	6.03	5.04
MnO	.05	.06	.08	.07	.04	.06	.07	n.d	.05	.04	.05	.09	.06
MgO	2.04	1.88	1.86	1.42	2.17	1.87	1.73	2.37	3.01	1.81	1.71	2.63	2.29
CaO	2.22	3.04	2.42	2.24	2.32	2.45	2.76	2.17	3.29	4.35	3.61	3.45	3.68
Na_2O	3.90	3.11	3.84	3.34	3.30	3.50	3.42	3.58	3.51	3.89	3.34	3.53	3.57
K_2O	2.67	2.59	2.09	2.40	2.46	2.44	2.37	1.82	1.93	1.57	1.02	1.04	1.39
H_2O+	.72	.72	.74	.59	.87	.73	.61	.81	.56	.49	.36	.37	.45
P_2O_5	.11	.09	10	.07	.09	.09	n.d	n.d	n.d	n.d	n.d	n.d	..
F	.07	.07	.07	.08	.08	.07	.09	.06	.04	.05	.03	.04	.04
Total	100.21	100.18	100.10	100.08	99.98		99.96	100.20	99.86	100.07	100.21	100.02	

Modes

Volume per cent

Quartz	32.33	34.67	33.89	38.96	32.35	34.44	33.60	34.04	22.58	26.55	36.27	28.40	28.45
Plagioclase	44.37	40.98	45.17	38.92	46.35	43.16	42.63	43.84	46.83	55.05	48.90	49.25	50.00
K feldspar	1.71	4.60	.75	3.71	.67	2.29	4.67	1.20	3.08	3.40	.73	.93	2.04
Biotite	19.97	17.46	18.32	16.05	19.85	18.33	16.81	19.47	15.66	10.08	7.07	7.45	10.06
Garnet	..	..	.13	..	.10	.05	1.94	1.00	9.70	4.40	5.87	12.78	8.19
Chlorite	.47	.72	.27	.96	17	.52	..	.33	.76	.13	.17	.40	.37
Muscovite	.80	.47	1.18	1.10	.01	.71	..	..	..	..	..	..	..
Opaques**	.07	.37	.17	.23	.07	.18	.10	tr	.08	.20	.53	.10	.23
Zircon	.06	.07	tr	.07	.07	.05	tr	tr	tr	tr	.08	.05	.03
Apatite	.16	.12	.12	tr	tr	.08	tr	tr	tr	tr	.05	.11	.04
Sericite	.06	.41	tr	tr	.36	.16	.25	.12	.51	.19	.33	.53	.39
Other		.13[c]	..	..	..	.03	..	..	.80	..	..	..	.20
Total	100.00	100.00	100.00	100.00	100.00	100.00	100.00	100.00	100.00	100.00	100.00	100.00	100.00
Composition of plagioclase	Ab 75	Ab 64	Ab 72	Ab 72	Ab 72	Ab 71	Ab 69	Ab 72	Ab 64	Ab 60	Ab 65	Ab 64	Ab 63
Number of sections	2	2	2	3	2		2	2	3	3	3	3	3
Number of counts	3000	3000	3000	4500	3000		4500	3000	4500	4500	4500	4500	

* Analyses calculated from mode.

† Alkali determinations by J. L. Smith method.

** Chiefly magnetite with hematite, ilmenite and pyrite.

tr Less than .05.

[c] Calcite.

TABLE 7—*Concluded*

Trace Elements
(Parts per million)

		West Balmat Group 1A	Emeryville Group 1					Edwards Group 2	Russell Group 3	Colton Group 5				
		Bgn 27	Qb 235M	Qb 230	Qb 231	Qb 225	x̄	Qb 234*	Bgn 14	Bgn 18†	Bgn 20	Bgn 21†	Bgn 19†	x̄
Element	Sensitivity													
B	10	8	6	10	9	7	8		<10	15	18	12	10	14
Ba	20	1100	620	650	220	375	593		1400	600	400	360	380	435
Co	2	7	7	9	5	8	7		9	9	7	8	12	9
Cr	5	28	32	40	28	38	33		38	45	40	38	60	46
Cu	1	12	18	11	8	40	18		25	3	16	9	12	10
Ga	5	11	12	10	11	8	10		10	20	12	10	15	14
La	80	pt	pt	pt	120	90	pt		pt	125	88	70	90	93
Mn	2	550	350	500	200	135	347		350	140	200	300	550	298
Mo	3	..	..	pt	..	5	..		..	..	..	..	..	..
Nb	15	<10	<10	12	16	pt	pt		<10	10	pt	pt	pt	pt
Ni	2	16	16	20	12	18	16		23	30	15	18	25	22
Pb	10	8	14	9	8	15	11		10	18	6	10	25	15
Sc	2	13	12	14	14	14	13		15	15	22	16	28	20
Sn	5	..	pt	..	7	..	..		..	..	..	pt	pt	..
Sr	2	360	330	340	250	275	311		710	425	350	250	350	344
Ti	2	2500	2000	2400	2200	2600	2340		1350	3500	2800	2500	3300	3025
V	2	65	60	64	50	55	59		62	78	65	42	75	65
Y	10	44	44	35	75	55	51		35	55	35	65	85	60
Yb	1	5	4	3	6	4	4		5	2	2	4	6	3
Zr	2	170	130	175	210	200	177		240	200	180	100	140	155
Number of analyses		4	3	3	2	2	14		2	3	3	3	2	11

pt Approximately at level of sensitivity.

greenish-brown biotite, calcic oligoclase, and a little muscovite. Figure 1 of Plate 2 is a photograph of this gneiss veined by pegmatite. Granite and pegmatite intertongued with and transitional into gneiss include both inequigranular and equigranular varieties, the latter being generally less biotitic, more massive, and highly potassic. Plate 3 illustrates three types of more granitic migmatite and inequigranular granitic gneiss. In the Emeryville-Edwards areas a mappable textural break commonly occurs at or near the mineralogical composition: plagioclase 38 (Ab78), quartz 35, K feldspar 15, and biotite 10 (Fig. 3). This common textural discontinuity is used in field mapping to delineate incipient migmatite and least altered gneiss from more granitized gneiss (called highly granitized gneiss on Pl. 4). Along perhaps three-fourths of the "contacts" of these lithologic types, a slight to obvious compositional discontinuity coincides with the textural break. Along the remaining "contacts" no clearly defined compositional break exists; at many of these localities abrupt variations in textures also disappear. Some of the least altered gneiss and migmatite grade into granite gneiss. Examples of this compositional and textural transition between gneiss and granite gneiss are indicated on Plate 4 by the stippled pattern labeled migmatite and highly granitized gneiss.

As the least altered segments of the gneiss complex are traced northeastward toward Colton (and the massif), grain size increases appreciably (Pl. 2, compare Fig. 1 with Fig. 2). Gross interrelationships of least altered gneiss and incipient migmatite to granite gneiss remain quite similar. The amount and per cent of least altered gneiss may decrease slightly from Emeryville to Colton. Important changes occur in its composition. Granite gneiss also undergoes changes in composition and texture as it increases in abundance and in igneous characteristics toward the massif. These features of least altered gneiss and associated granite gneiss are discussed in the succeeding sections.

Least Altered Gneiss

Introduction.—The properties of 11 specimens of least altered gneiss have been studied in detail. These include five specimens from the Emeryville area—Groups 1 and 1A—as follows: Bgn 27, Qb 235M, Qb 230, Qb 231, Qb 228; one specimen from the Edwards area—Group 2—Qb 234; one specimen from the Russell area—Group 3—Bgn 14; and four specimens from the Colton area—Group 5—Bgn 18, Bgn 20, Bgn 21, Bgn 19. The chemical and mineral compositions of these specimens are listed in Table 7, together with average compositions in the Emeryville and Colton groups. The localities from which the samples came are shown on Plates 1 and 4. The distinction between least altered and incipiently granitized or otherwise altered gneiss is necessarily somewhat arbitrary. The compositions of several other specimens of gneiss that from field and petrographic studies are clearly only slightly altered (granitized) have been listed with the granitized types of gneiss in Table 9. These very slightly granitized specimens are: in the Emeryville area (Group 1), Bgn 29, Qb 236, Qb 7, Qb 229; in the Edwards area (Group 2), Qb 100; in the Russell area, Bgn 9; and in the South Pierrepont area (Group 4), Bgn 29.

Modal analyses of 1500 to 4500 counts each have been made on 62 additional specimens of least altered gneiss. Of these 62 rocks, 19 are in Group 1, 18 in Group 2, 15 in Group 3, and 10 in Group 5. The mineral and chemical compositions of these 62 specimens, together with the compositions of the 11 previously cited specimens are summarized in Table 8 as the mean and the range of compositions of least altered gneiss in Groups 1, 2, 3, and 5. The chemical compositions of the 62 specimens not listed in Table 7 are calculated from the modes by using the mean composition of constituent minerals as determined by the various methods of analysis cited in the introduction. The justification for computing these analyses from the modes has been given in the section on modal analysis of rocks.

Arguments have been presented (Engel and Engel, 1953b, p. 1078–1083) why the chemical composition of least altered gneiss of the Emeryville-Edwards region is thought to approximate the early or pre-metamorphic sedimentary rock. The designation least altered gneiss was made during field mapping. Its composition as determined by either modal or chemical analyses has proved to be as distinctive as its texture or field relationships (Table 7; Table 8, column 1; Fig. 4).

The associated pegmatite and granite gneiss (Fig. 3; Fig. 7) appear to be introduced into the more granitic gneiss of the Emeryville area, rather than partly sweated out of the least granitic parts (Engel and Engel, 1953b, p. 1078–1081).

Least altered gneiss of the Colton area also

seems to be essentially devoid of introduced substances; but either K, Si, and H_2O have been removed from this least altered gneiss, or its sedimentary parent was a more mafic rock.

tion"[6] of the least altered gneiss are many interesting changes in texture and mineral composition. These are discussed with the aid of Tables 7 and 8 and Figure 5, which sum-

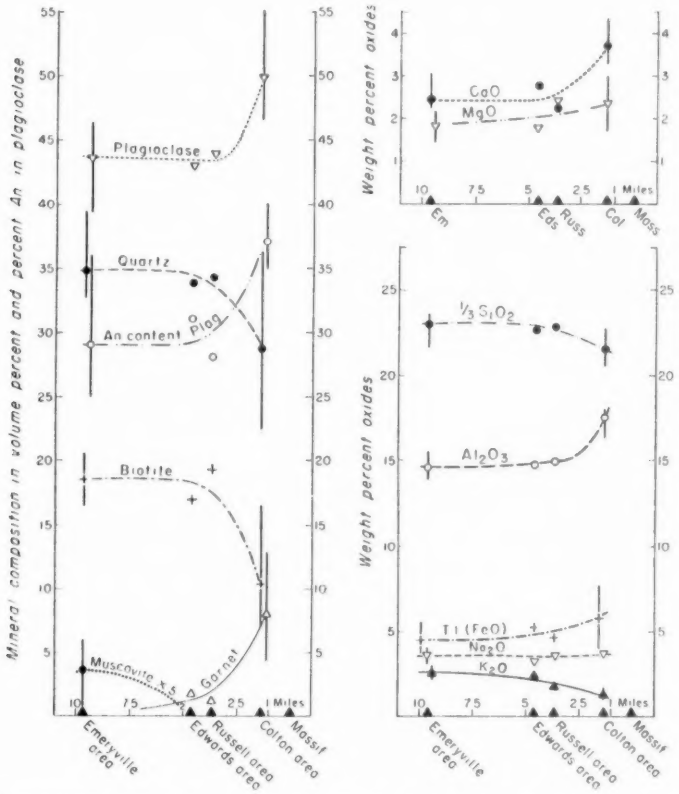

FIGURE 4.—GENERALIZED CURVES INDICATING CHANGES IN MINERAL AND MAJOR-ELEMENT COMPOSITION OF 11 SPECIMENS OF LEAST ALTERED GNEISS STUDIED IN DETAIL (TABLE 7) AS TRACED FROM EMERYVILLE TO COLTON, NEW YORK

Points indicate the mean composition of least altered gneiss in each area or group. The vertical lines through points at Emeryville and Colton indicate the maximum range or dispersion of values from the mean. Distances between areas on the horizontal co-ordinate are measured along horizontal lines drawn normal to the trace of the perimeter of the massif to the center of each area or group (see Pl. 1).

This is clearly shown in Figures 4 and 5, prepared from, respectively, the modal and chemical analyses of least altered gneiss in Tables 7 and 8. Conceivably K and Si were mobilized from the gneiss at Colton and segregated to form some of the more granitic lenses and leaves there, as well as mobile constituents of the "granite" injecting and granitizing the gneiss in the Emeryville area. Complementary to the possible "degranitization" or "basification"[7] of the least altered gneiss are many interesting changes in texture and mineral composition. These are discussed with the aid of Tables 7 and 8 and Figure 5, which summarize the compositional data on specimens of least altered gneiss between Emeryville and Colton.

Mineralogy and Texture.—The assemblage quartz, greenish-brown biotite, oligoclase, and muscovite in least altered gneiss at Emeryville

[6] Terms used by respectively Rosenquist (1952, p. 75) and Ramberg (1951, p. 33) to express the loss of alkali (s) and silica from rocks during extreme metamorphism.

represents the lowest-rank regional metamorphic conditions[7] in the Adirondack orogen. In conventional terms this is presumably upper-middle rank, the highest temperature part of the amphibolite facies of Eskola (1920).

As the least altered parts of the gneiss are traced northeastward to Colton, the following general changes occur: muscovite disappears approximately 10 miles northeast of Emeryville in the Edwards area (Pl. 1; Fig. 4; Fig. 5), and almandite garnet and K feldspar appear consistently through the least altered gneiss. Southwest of Edwards, garnets are confined principally to contacts of pegmatite and gneiss (Engel and Engel, 1953b, p. 1072–1075). As the massif is approached, garnet becomes a major constituent in the least altered gneiss. Sympathetically, the mean plagioclase becomes more calcic. Plagioclase at Emeryville averages Ab 73; that at Colton averages about Ab 67 (Table 8). Biotite changes from greenish brown through successive shades of brown and reddish brown to deep red brown. The quartz content of the gneiss decreases from a mean of about 38 per cent at Emeryville to less than 30 per cent near Colton. Statistical analyses of the data using the "Student's" *t* test (Mood, 1950, Ch. 9) indicate all the cited differences are real. The probability of the differences of the means being due to chance is less than 0.05 in every instance. The changes in the physical and chemical properties of the minerals are discussed in Part 2.

Texturally, most of the least altered gneiss in the Emeryville area is massive, medium-grained (*see* Engel and Engel, 1953b, especially Table 10), and granoblastic. In volume it totals about one-third the gneiss complex. More or less migmatitic and granitized gneiss makes up the other two-thirds. Northeastward, the grain size of the less deformed parts increases several times, and the per cent of least altered gneiss may decrease slightly. The changes noted in least altered gneiss between Emeryville and Colton are accompanied by the appearance of lithologic (segregational ?) banding northeast of Russell. The appearance of bands or layers is a most subtle effect, but their existence is striking if gneiss from opposite ends of the belt is compared directly (Pl. 2, Figs. 1 and 2). The gneissic layers in the Colton area range up to several inches in thickness and are defined by alternations of more or less biotitic and garnetiferous rock. In some of the banded gneiss, grain size varies systematically across the bands from coarse to fine, simulating graded bedding. A good approximation of the bulk composition of the most distinctly layered gneiss requires a sample cut across a foot or more of the rock, normal to the layers. The restriction of these layers to the area of highest-temperature metamorphism, and the fact that individual bands make a most improbable sediment suggest they are due to metamorphic differentiation. Such differentiation is most compatible with the evidence that more felsic constituents are separated from the least altered gneiss.

The detailed patterns of distribution of garnet and muscovite are of interest, in so far as they may reflect the occurrence of an isograd or merely an isoblast or isophase.[8] It is to be recalled that in going northeast garnet first appears throughout the entire gneiss complex in the Edwards area. Southwest of Edwards, in the Emeryville area, garnet is confined largely to contacts of pegmatite and gneiss and is rare or absent in many parts of least altered gneiss (Engel and Engel, 1953b, p. 1072–1076). Muscovite occurs throughout the gneiss complex in the Emeryville area and disappears abruptly from all parts of the gneiss in the Edwards area. The isophase line indicating the disappearance of muscovite is therefore relatively undeflected at contacts of more or less granitic and pegmatite gneiss; but the isophase drawn at the first appearance of garnet is extremely irregular.

The distribution of garnet may be explained in one of several ways. Conceivably garnet was a stable phase in the least altered gneiss around Emeryville and Balmat (that is southwest of Edwards), but the reaction permitting its formation was infinitely slow. The possibilities of sluggish reaction rates in displacing an isophase have been emphasized by Yoder (1952), from his studies of artificial systems. If this interpretation is the correct one, the presence of garnet in the pegmatitic seams may be due to an increased mobility of the reaction in those parts of the gneiss soaked by granitizing and pegmatite-forming fluids.

An obvious alternative is that garnet was not a stable phase in the least altered gneiss

[7] Omitting, of course, the relatively small scale, patchy, retrograde alteration of chlorite, sericite, albite, and so on.

[8] Yoder (1952, p. 621–623) has pointed out possible differences between an isograd and an "isoblast"—a line indicating the appearance of a new phase with increasing metamorphism. The word isophase is used in this paper as synonomous with isoblast.

but was stable at sites of pegmatites because of differences between these different rock systems in temperature, pressure, composition, or chemical potential of a vapor phase. Contrasting possibilities may be imagined, of pegmatites forming along zones of shear in which vapor pressure of volatiles was either relatively high or low. Garnet may have formed along the pegmatites if this site was relatively anhydrous compared to the body of the least altered gneiss. Certainly a marked compositional gradient existed between areas of pegmatization and the cores of least altered gneiss, as is clear from inspection of Figures 3 and 7. Garnet exists principally at sharp contacts of pegmatite and gneiss or in gneissic inclusions and schlieren in the pegmatites. The well-defined pegmatites and granitic layers more devoid of mafic constituents contain no garnets. This is expectable, for wherever the granite- and pegmatite-forming processes have gone well toward completion, an alaskitic leucogranite gneiss is formed (*see* right-hand side of Fig. 7). In this granitic system garnet is not an equilibrium phase.

Chemical composition: major elements.—The major changes in chemical composition in the least altered gneiss between Emeryville and Colton that complement the mineralogical changes are plotted in Tables 7 and 8 and in Figures 4 and 5, alongside the data on mineral composition. Si, K, Fe^{+++}, and H_2O decrease as the massif is approached, whereas total Fe, Al, Mg, and Ca increase. These changes first became apparent in plotting the data from the nine specimens of least altered gneiss studied in detail (Fig. 4; Table 7). From statistical

TABLE 8.—AVERAGE CHEMICAL AND MINERALOGICAL COMPOSITIONS, AND RANGE IN COMPOSITIONS OF LEAST ALTERED GNEISS IN THE GNEISS COMPLEX BETWEEN EMERYVILLE AND COLTON, NEW YORK

Data include the analyses of least altered gneiss in Table 7, plus data from 62 additional specimens added to improve the sampling and clarify trends in composition. In chemical analyses, oxides given in weight per cent.

	Emeryville Area Group 1			Edwards Area Group 2	Russell Area Group 3	Colton Area Group 5		
	1	2	3	4	5	6	7	8
SiO_2	70.25	72.01	66.71	69.61	69.16	65.97	69.92	60.84
TiO_2	.67	.88	.59	.74	.70	.64	.81	.50
Al_2O_3	14.14	16.74	12.01	14.39	15.09	16.83	18.01	15.48
Fe_2O_3	.55	1.51	.33	.47	.33	.36	1.11	.20
FeO	3.83	4.89	2.87	4.35	4.24	4.92	6.81	3.38
MnO	.05	.03	.09	.06	.05	.07	.11	.03
MgO	1.76	2.58	1.26	1.75	1.74	2.25	3.16	1.68
CaO	2.20	3.22	1.55	2.56	2.85	3.41	4.51	2.49
Na_2O	3.43	3.90	2.93	3.45	3.62	3.70	3.96	2.67
K_2O	2.40	2.91	1.84	2.06	1.70	1.46	2.46	1.02
H_2O+	.72	.97	.21	.56	.52	.39	.60	.30
Total	100.00			100.00	100.00	100.00		
Number of specimens	24†			19	16	14*		
Modes Volume per cent								
Quartz	37.86	45.60	30.96	36.50	34.99	29.28	36.27	22.58
Plagioclase	39.86	47.30	32.01	42.00	44.75	48.92	55.10	41.90
K feldspar	3.19	4.60	.23	3.70	2.91	3.17	4.30	.73
Biotite**	17.60	21.96	13.00	14.98	13.85	10.68	16.46	7.07
Garnet	.03	3.00	.00	2.21	3.10	7.38	14.10	.08
Muscovite	.86	1.84	.01	tr	..	..	..	..
Others††	.60	1.63	.37	.61	.40	.57	1.27	.22
Total	100.00			100.00	100.00	100.00		
Composition of plagioclase	Ab 73	Ab 78	Ab 50	Ab 71		Ab 67	Ab 55	Ab 74
Number of specimens	24†	..	..	19	16	14*	..	..

TABLE 8.—*Concluded*

Trace Elements
(Parts per million)

		Emeryville Area Group 1			Edwards Area Group 2	Russell Area Group 3	Colton Area Group 5		
		1	2	3	4	5	6	7	8
Element	Sensitivity								
B	10	10	15	<6	10	10	12	18	<10
Ba	1	612	1200	375	600	650	492	700	280
Co	2	8	12	5	10	8	7	12	4
Cr	5	35	45	25	25	40	56	65	35
Cu	1	16	40	6	12	15	12	20	3
Ga	5	11	15	8	12	12	14	20	10
Mn	2	356	575	135	340	350	341	600	140
Nb	15	pt	16	<10	<10	<10	pt	15	<10
Ni	2	15	20	12	10	12	21	30	15
Pb	10	12	15	<8	10	12	15	25	6
Sc	2	12	16	11	15	15	17	30	8
Sr	2	310	490	225	550	500	304	580	230
Ti	2	2800	3000	2000	3000	2200	3000	3500	2000
V	2	56	65	50	50	65	81	90	42
Y	10	46	75	35	55	40	58	85	25
Yb	1	3	5	2	3	4	3	6	2
Zr	2	171	200	130	180	220	176	200	100
Number of specimens		9†	..	..	4	6	8*	..	..

* Modes and major-element composition based upon 14 specimens, whereas trace-element data are from only 8 of these specimens

† Modes and major element composition based upon 24 specimens, whereas trace-element data are from only 9 of these specimens.

** Includes minor chlorite which replaces biotite.

†† Chiefly apatite, zircon, magnetite, and pyrite.

Description of samples:

Columns 1, 2, and 3 are mean, maximum, and minimum values respectively for 24 specimens of least altered gneiss in the Emeryville area, including the five specimens in Table 7. Composition of major elements in 19 specimens not shown in Table 7 are calculated from modes and chemical analyses of minerals.

Column 4 is the mean of 19 specimens of least altered gneiss in the Edwards area. One of these specimens (Qb 234) is listed in Table 7. Composition of other specimens calculated from the modal data.

Column 5 is the mean of 16 specimens of least altered gneiss in the Russell area. One of these specimens (Bgn 14) is listed in Table 7. Compositions of other specimens calculated from the modal data.

Columns 6, 7, and 8 are mean, maximum, and minimum values respectively for 14 specimens of least altered gneiss from the Colton area, including the four samples in Table 7. Compositions of 10 specimens not shown in Table 7 are calculated from modes and chemical analyses of minerals.

studies using the "Student's" *t* test it was obvious, however, that these trends, based upon only 11 specimens, might be due to chance. Accordingly the additional 62 specimens incorporated in Figure 5 and Table 8 were chosen on the basis of their systematic distribution in the least altered gneiss. All the trends indicated by the limited sampling exist in the larger sample (Fig. 5). The probability that the differences in means of SiO_2, Al_2O_3, Fe_2O_3, MgO, CaO, and H_2O are due to chance is less than 0.05. With the larger sample, definite evidence of "basification" of the gneiss appears about three-fourths of the way from Emeryville to Colton, that is, about 10 miles from the massif (measured along the strike of the gneiss). If the temperature calibration is approximately correct, and the changes are o metamorphic origin, the temperature of incipient degranitization at this point was about 550° C. ± 50° C.

Several questions arise: (1) Is the change in composition of the least altered gneiss metamorphic in origin? (2) Are at least some of the granitic and migmatitic parts of the gneiss complex in the Colton area frozen-in relicts of degranitization-differential anatexis? (Eskola, 1933) (3) Is the potassic injection material that invades the gneiss at Emeryville in part or wholly derived from lateral extensions or underlying parts of the gneiss undergoing ultrametamorphism and degranitization? There appear to be no data definitely opposed to these possibilities. Yet none can be established

definitely. The fact that the changes in composition of the least altered gneiss between Emeryville and Colton coincide with increased temperatures of metamorphism is certainly suggestive of a metamorphic origin. Southwest of Emeryville the gneiss complex can be traced about 20 miles to a point beyond Antwerp and Philadelphia, New York. There it passes beneath the lower Paleozoic sedimentary formations. Throughout this southwesterly segment of the gneiss (not described in this paper) the conditions of metamorphism were essentially those of Emeryville. In the Philadelphia and Antwerp, New York, areas, however, granitized gneiss is more abundant, and least altered gneiss rarer than at Emeryville. The least altered parts of the gneiss complex appear, nevertheless, to be compositionally similar to those present at Emeryville. The least altered gneiss seems, therefore, nearly uniform in composition throughout a distance of about 30 miles, from a point southwest of Antwerp to Edwards. Viewed on this regional scale, the systematic change in composition of the gneiss with increased temperature (and rank) of metamorphism strongly suggests the cause is metamorphic.

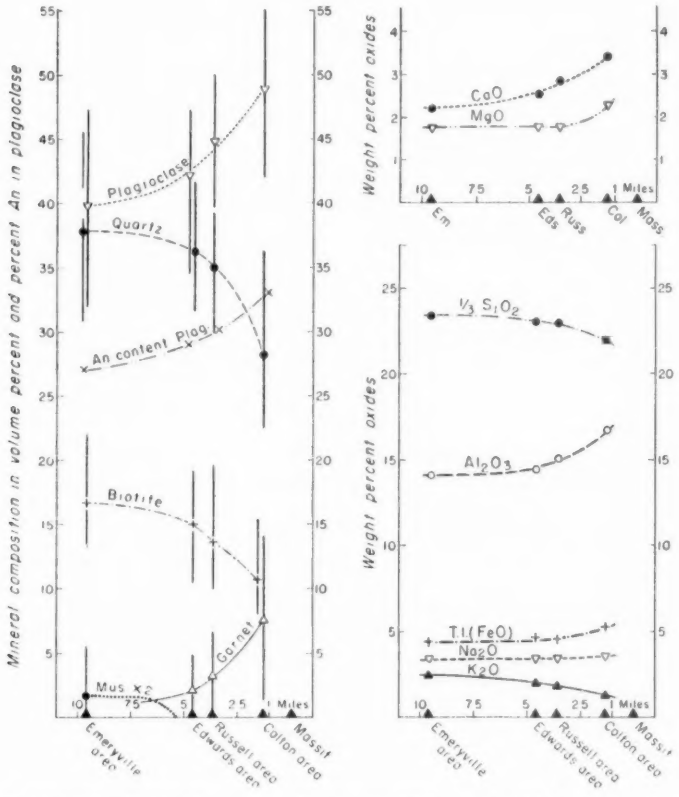

FIGURE 5.—GENERALIZED CURVES INDICATING CHANGES IN MINERAL AND MAJOR-ELEMENT COMPOSITION OF LEAST ALTERED GNEISS AS TRACED FROM EMERYVILLE TO COLTON, BASED UPON 73 SPECIMENS

(See Fig. 4 and Table 8.) Chemical compositions of 62 of the specimens are calculated from modal analyses and from chemical analyses of the constituent minerals in the gneiss.

As noted earlier, the interpretation of a metamorphic origin for the basification of the gneiss in the Colton area seems susceptible to proof. Several metasedimentary units in the Grenville subprovince (A. E. J. Engel, 1956,

p. 77, 81–84) and elsewhere in the world are of about the same composition as the least altered gneiss at Emeryville. Segments of some of these gneiss belts appear to have undergone progressive metamorphism, at about the temperatures recorded in the Adirondack paragneiss. If investigations indicate they also undergo a basification coincident with extremely high-grade metamorphism, a metamorphic origin for the compositional change would seem established.

Apropos of this problem, the work and observations of Ramberg (1951), Shaw (1954), and Lapadu-Hargues (1949) are of considerable interest. Ramberg has studied paragneisses in Greenland that have a bulk composition very similar to the Adirondack gneiss. Ramberg concludes from the samples studied that

> "The main gneiss of the granulite facies is distinctly more basic than the main gneiss of the amphibolite facies area. The former is relatively rich in Mg, Fe^{++}, Fe^{+++}, Ca, Ti and Mn; the latter in Si, Na, K, O, H_2O."

He suggests that the cause of the change is metamorphic. An obvious question is whether Ramberg's sampling and field data are adequate to demonstrate his conclusion.

In contrast Shaw's handling of analyses of the Littleton formation (New Hampshire) indicates no change in the composition of this rock with increased rank of metamorphism, other than minor addition of CaO and Na_2O and loss of H_2O (1956, p. 919–934). Shaw comments (p. 920):

> "It is commonly believed by many petrologists that argillaceous sediments generally do not change in composition during metamorphism (except by loss of volatiles) although exceptions have been recognized in some areas."

As Shaw notes (1956, p. 920), however, there has been essentially no careful work to justify this belief. His studies certainly suggest that only volatiles have been lost during the metamorphism of the Littleton formation. He then concludes:

> "The view that pelitic rocks usually undergo a far-reaching change in composition during regional metamorphism can therefore not be accepted." (1956, p. 931).

Obviously critical differences in metamorphism from region to region may determine whether it is crudely isochemical or not. Presumably temperature is a critical factor. In the paragneisses of Greenland and the Adirondack Mountains, isochemical metamorphism appears to occur up to temperatures of about 550° C. Inasmuch as most regional metamorphism in exposed rocks seems to be at lower temperatures, very approximate isochemical metamorphism may prove to be the rule.

Shaw's concluding comments were taken out of a context in which he reviewed the work of Lapadu-Hargues (1949). In this widely cited work Lapadu-Hargues assembled analyses of metamorphic rocks which seem to indicate a progressive change in composition of clastic metasedimentary rocks with increasing rank of metamorphism. Unfortunately the analyses are of rocks from widely diverse terranes and of very different, commonly not well understood origins. Accordingly their arrangement and interpretation by Lapadu-Hargues is liable to considerable question and error.

There seems to be no great quarrel about the eclectic concept of mobilization and upward migration of silicon, alkalis, and water from deep-seated rocks undergoing extreme metamorphism. The sialic nature of continental masses seems to prove that the process can occur. And if the process occurs, it can be interrupted, leaving a granitic extract in various states of birth and migration. The difficulty is in distinguishing the venitic from the arteritic[9] migmatites (Engel and Engel, 1953b, p. 1079–1080).

Both the data and theoretical considerations are consistent with the idea of degranitization and venitic migmatization of the gneiss at Colton, in contrast to arteritic migmatization and injection of granitic substances in the Emeryville area. These interpretations do not conflict with Buddington's interpretation (1939; 1948; 1957) that much of the granitic rock in the Colton area is of a deeper-seated magmatic origin and is injected into and shredding the gneiss. This magma presumably was frozen in its ascent from deeper, even hotter sources in the orogen.

Chemical composition: minor elements.—The trace-element compositions of the least altered gneiss in the Emeryville-Colton region are shown in Tables 7 and 8. It should be noted that two separate averages are given for gneiss in both the Emeryville and Colton areas. The averages in Table 7 are of the composition of specimens of least altered gneiss given there. The specimens are, for Group 1: Bgn 27, Qb 235M, Qb 230, Qb 231, and Qb 228, and for

[9] Terms suggested by respectively Holmquist (1921) and Sederholm (1923).

TABLE 9.—CHEMICAL AND MODAL ANALYSIS OF SPECIMENS OF GRANITIZED GNEISS FROM THE PARAGNEISS COMPLEX BETWEEN EMERYVILLE AND COLTON, NEW YORK

In chemical analyses, oxides given in weight per cent

	West Balmat Group 1A	Emeryville Group 1								Edwards Group 2			Russell Group 3			South Pierrepont Group 4		Colton Group 5	
	Bgn 26†	Bgn 29*	Qb 236	Qb 237*	Qb 3†	Qb 7†	Qb 229	Qb 226	Qb 227	Qb 233*	Qb 100	Qb 216	Bgn 9	Bgn 4†	Bgn 6	Bgn 25	Bgn 16*	Bgn 22*	Bgn 23*
SiO_2	69.63	68.67	67.83	67.58	70.12	68.75	65.02	69.40	69.51	64.30	61.96	68.89	69.32	67.37	67.12	61.28	66.61	68.89	69.96
TiO_2	.66	.61	.81	.70	.62	.62	.73	.57	.62	.98	1.01	.68	.51	.56	.68	.76	.72	.45	.63
Al_2O_3	14.41	15.25	13.92	14.89	13.79	15.53	16.12	15.22	14.45	14.74	17.23	13.90	15.66	16.89	16.05	18.28	15.56	15.13	14.85
Fe_2O_3	.87	.43	.62	.56	.60	.47	.48	.56	.92	.79	.56	.31	.34	.21	.50	.60	.61	.41	.35
FeO	3.78	3.26	4.49	3.88	3.65	3.89	5.08	2.61	3.35	6.52	5.15	4.55	3.27	2.52	3.01	4.79	4.57	4.10	2.53
MnO	.03	.01	.07	.01	.06	.07	.04	.06	.07	.10	.07	.04	.05	n.d	n.d	n.d	.03	.06	.02
MgO	1.49	1.72	2.79	2.05	1.81	1.62	2.31	1.73	1.61	2.76	2.01	1.94	1.55	1.87	1.46	2.84	2.44	1.65	1.45
CaO	2.38	2.46	1.75	1.95	1.73	2.16	2.33	2.09	1.69	.88	3.81	1.66	2.39	1.43	2.12	2.96	2.35	1.67	1.57
Na_2O	2.76	3.82	2.84	3.29	3.05	3.23	3.54	2.66	3.56	1.74	3.66	2.64	3.63	4.02	3.37	4.23	3.32	3.08	3.17
K_2O	3.32	3.11	3.95	4.27	3.73	3.04	3.36	4.17	3.47	6.39	3.39	4.41	2.71	4.67	5.13	3.45	3.28	4.40	5.29
H_2O+	.59	.61	.84	.76	.78	.71	.91	.70	.73	.78	.79	.68	.48	.58	.59	.74	.59	.23	.33
P_2O_5	.05	n.d	n.d	n.d	.08	.07	.08	.07	.10	n.d	.07	.07	n.d	n.d	n.d	n.d	n.d	n.d	n.d
F	n.d	.05	.08	.06	.04	.06	.10	.05	.06	.08	.13	.10	.04	n.d	n.d	n.d	.06	n.d	n.d
Total	99.97	100.00	99.99	100.00	10.06	100.22	100.10	99.89	100.14	100.06	99.84	99.87	99.95	100.12	100.03	99.93	100.05	100.07	100.15
	Modes, Volume per cent																		
Quartz	35.58	30.26	34.23	29.69	35.64	34.75	28.28	33.91	33.37	27.57	17.25	34.14	32.43	21.25	24.90	19.20	30.38	29.29	28.65
Plagioclase	34.65	42.84	31.83	34.68	32.02	36.10	41.29	33.01	35.93	13.71	44.64	28.03	44.50	20.10	31.47	48.07	37.62	29.99	28.97
K feldspar	11.24	9.43	9.69	16.39	13.86	8.85	6.94	15.22	12.30	31.37	10.73	18.13	8.87	24.70	29.40	10.26	12.15	26.77	30.65
Biotite	16.65	15.61	23.13	18.92	17.01	17.60	21.87	16.09	16.83	21.10	21.54	17.97	10.10	10.35	13.20	19.56	15.03	17.09	9.50
Garnet	..	..	..	..	..	.50	.45	.20	..	5.59	.20	1.22	3.31	.40	.42	2.01	3.92	6.40	1.80
Chlorite	.49	.61	.34	tr	.47	.39	.44	.11	.13	.30	.27	.11	.31	.37	.23	.41	.20	.16	.16
Muscovite	.73	.22	.32	.17	.70	1.30	.44	1.19	.74	..	..	.17	..	..	..	..	..	..	..
Opaques**	.53	.20	tr	tr	tr	tr	tr	.10	.08	.09	.36	tr	.07	.17	.15	.12	.31	.18	.10
Zircon	tr	tr	tr	.07	.04	.07	.09	.05	tr	.08	.07	.11	.05	.07	tr	..	tr	tr	tr
Apatite	tr	tr	.09	.08	.06	.08	.08	.05	.15	.03	.43	tr	tr	.32	tr	.06	tr	tr	tr
Sericite	.13	.74	.37	tr	.20	.36	tr	.07	.40	.16	.73	.12	.26	1.95	.23	.18	.39	.12	.17
Other	tr	.09	tr[a, c]	.13[c]	.10[c]	tr[a]	.12	tr[f, a]	.07	..	3.78[b, c, a]	..	.10[c]	.32[c]	..	.13[a]	..	..	..
Total	100.00	100.00	100.00	100.00	100.00	100.00	100.00	100.00	100.00	100.00	100.00	100.00	100.00	100.00	100.00	100.00	100.00	100.00	100.00
Composition of plagioclase	Ab 68	Ab 73	Ab 73	Ab 74	Ab 74	Ab 70	Ab 72	Ab 68	Ab 77	Ab 74	Ab 68	Ab_{72}^{n}	Ab 72	Ab 76	Ab 75	Ab 68	Ab 70	Ab 76	Ab 76
Number of sections	2	2	2	2	2	2	3	2	2	3	3	2	3	2	2	3	3	3	3
Number of counts	3000	3000	3000	3000	3000	3000	4500	3000	3000	4500	4500	3000	4500	4000	4000	4500	4500	4500	4500

Trace Elements
(Parts per million)

Element	Sensitivity																			
B	10	40	40	24	16	12	15	pt	32	8	6	12	..	..	..	20	<10	<10	<10	<10
Ba	20	125	600	1200	830	750	540	650	2600	1000	980	700	..	400	1000	560	2100	1100	1200	1315
Co	2	8	7	7	8	8	7	6	3	6	10	10	..	5	5	6	10	10	8	4
Cr	5	34	28	34	31	40	30	19	30	28	35	15	..	20	20	25	22	46	21	19
Cu	1	7	44	2	1	7	4	35	3	2	20	7	..	7	10	80	6	47	8	12
Ga	5	7	12	9	9	9	8	12	12	11	17	13	..	15	15	13	25	14	17	14
La	80	..	pt	..	..	..	..	pt	75	pt	..	70	..	70	..	..	..	pt	pt	pt
Mn	2	800	350	380	350	350	650	365	300	370	250	320	..	200	80	240	300	840	520	700
Mo	2	..	..	..	..	pt	..	..	..	..	..	..	..	..	..	pt	..	..	..	..
Nb	15	..	<10	..	..	pt	..	pt	15	10	..	..	..	10	15	..	<10	<10	10	11
Ni	2	18	14	12	16	22	20	12	7	13	18	7	..	10	20	23	16	27	15	11
Pb	10	10	15	7	12	4	2	15	10	18	20	7	..	100	10	13	13	16	15	27
Sc	2	16	15	11	12	13	15	18	15	14	15	15	..	9	8	11	32	18	16	12
Sn	5	pt	..	..	..	..	..	pt	15	..	pt	..	..	..	..	11	..	..	..	..
Sr	2	180	550	500	430	300	310	185	220	470	470	700	..	100	1500	270	250	510	320	390
Ti	2	2700	2000	2500	2500	2500	2600	2300	2800	2600	2600	3400	..	2000	3000	2200	3000	3000	2800	3200
V	2	51	50	45	57	56	41	50	52	48	71	55	..	50	60	50	75	76	50	43
Y	10	61	50	32	44	45	45	65	45	50	54	57	..	40	20	60	58	47	48	52
Yb	1	3	4	2	3	3	3	4	3	3	4	3	..	3	1	4	7	5	5	5
Zr	2	160	160	150	150	170	175	140	200	180	180	200	..	200	200	215	134	175	200	240
Number of analyses		2	4	3	3	3	1	3	1	3	1	1		1	1	1	1	1	1	1

* Analyses calculated from mode.
† Alkali determinations by J. L. Smith method.
** Chiefly magnetite with hematite, ilmenite, and pyrite.
tr less than .05.
[c] calcite.
[s] sphene.
[a] allanite.
[h] hornblende.
[t] tourmaline.
pt approximately at level of sensitivity.

Group 5: Bgn 18, 19, 20, and 21. Inspection of the average values for the elements in these two groups indicates they are very similar. The elements Ba, Co, Mn, Nb, Sc, Sr, Ti, Y, larger group of specimens (nine from Emeryville and eight from Colton) are given in columns 1 and 6 of Table 8. Application of the "Student's" t test to these larger samples

TABLE 10.—AVERAGE TRACE-ELEMENT COMPOSITION OF LEAST ALTERED GNEISS AND GRANITIC GNEISS COMPARED WITH THAT OF THE LITTLETON FORMATION
(*See* Shaw, 1954, pt. 1, Table 15.)

Element	Sensitivity*	Middle-Grade Metamorphism			High-Grade Metamorphism		
		Littleton formation (Shaw 1954)	Least altered gneiss Group 1	Granitic gneiss Group 1	Littleton formation (Shaw, 1954)	Least altered gneiss Group 5	Incipiently granitized gneiss Group 5
		1	2	3	4	5	6
Co	2	19	8	4	18	7	5
Cr	5	113	35	4	109	56	18
Cu	1	23	16	19	13	12	18
Ga	5	16	11	12	20	14	12
Ni	2	64	15	4	57	21	8
Pb	10	16	12	38	27	15	32
Sc	2	11	12	6	16	17	8
Sr	2	524	310	270	760	304	225
V	2	125	56	24	120	81	30
Y	10	39	46	35	52	58	30
Zr	2	191	171	150	203	176	160
Number of specimens		20	9	3	30	8	4

* Sensitivity reported by Chodos and Godijn.

Column 1, average composition of the Littleton formation at middle-grade metamorphism (Shaw, 1954, Table 15).

Column 2, average composition of least altered gneiss in the Emeryville area (from Table 8, col. 1).

Column 3, average composition of more granitic gneiss, Emeryville area (from Table 3, col. 3).

Column 4, average composition of the Littleton formation, at high-grade metamorphism (Shaw, 1954, Table 15).

Column 5, average composition of least altered gneiss in the Colton area (from Table 8, col. 6).

Column 6, average composition of incipiently granitized gneiss in the Colton area (Table 13, col. 6).

Yb, and Zr all lie within two standard deviations. The "Student's" t test shows that for these elements the probability of the means being due to chance is somewhater greater than 0.10. The elements B, Cr, Ga, Ni, Sc, V, and Y may, however, be enriched, and Cu and Ba ? may be depleted in the gneiss at Colton. This is indicated by the fact that there is about 0.10 or less probability that the differences are due to chance.

In an effort to clarify whether real differences in trace-element composition do exist, four additional specimens of least altered gneiss from each area were analyzed. The average trace-element compositions of this of least altered gneiss in the two areas suggests that there are probably real although relatively small increases in Cr, Ga, and V in the gneiss at Colton and possibly small increases in Ni and Y. An increase in these elements at Colton is consistent with the increase in the major elements Fe, Mg, Ca, and Al noted previously. The decrease in Ba and Cu in the gneiss at Colton also appears to be probable. The loss of Ba, sympathetic with the loss of K, is expectable. Almost surely many other changes in trace-element composition could be noted with adequate sampling and highly refined analytical methods. Mn and Pb, for example, probably decrease in the least altered gneiss between

Emeryville and Colton, although present data certainly are not precise enough to demonstrate this.

In Table 10, the average trace-element compositions of least altered gneiss are compared with the trace-element composition of the Littleton formation that has been studied in some detail by Shaw (1954, Part I). In columns 1 and 4 of Table 10 are the average composition of respectively medium- and high-grade paragneisses of the Littleton formation. The average compositions of least altered gneiss from the Emeryville and Colton areas (Groups 1 and 5) are given in columns 2 and 5. A direct comparison is justifiable for most elements, as is indicated by the good reproducibility of analyses between the analysts involved (Table 11). Exceptions should be noted for Sc, Zr, and possibly Sr and V. Shaw's values for Zr are consistently about 30 per cent higher than the values obtained by Chodos and Godijn. His values for Sc are consistently about 50 per cent lower, and his values for V may be lower in most instances. The numbers Shaw reports for Sr are roughly three times higher in two of the three samples run.

The trace-element compositions of the two formations are similar in many respects (Table 10). This is especially true for Zr, Y, Sc, Pb, Ga, and Cu, in which respective concentrations are within or close to the analytical errors between the laboratories. The Littleton formation seems to be richer in Co, Cr, Ni, and V than the gneiss. This is despite the fact that both formations contain approximately the same amounts of Ti, Fe^{++}, and Mg (*see* Shaw, 1956, Part III, p. 924). The principal differences in major-element composition are in Al, Ca, Na, K, and Fe^{+++}. The Littleton is richer in Al, Fe^{+++}, and K and much poorer in Ca and Na than the gneiss. The Na_2O–K_2O ratio in the Littleton is only 0.22; in the least altered gneiss at Emeryville this ratio is about 1.4, and near Colton it increases to more than 2. In terms of the ratio of Na to K the Littleton formation is typical of metasedimentary rocks derived from kaolinitic and illitic sandstones, whereas the gneiss seems to have evolved from a sodic tuff or graywacke-like rock rich in chlorites, montmorillonites, or zeolites (Engel and Engel, 1953b).

TABLE 11.—ANALYSES OF TRACE ELEMENTS IN THE LITTLETON FORMATION

Analyses by Shaw (1954, pt. 1, Table 15) and by Chodos and Godijn are compared to indicate precision between the two laboratories. The analyses L1C-G, L2C-G, and L3C-G were made on the same plates with analyses of gneiss reported in Tables 7, 8, and 9.

Element	L1S 1	L1C-G 2	L2S 3	L2C-G 4	L3S 5	L3C-G 6
Co	11	10	21	15	10	6
Cr	86	96	160	121	93	102
Cu	24	23	59	40	6	14
Ga	31	20	35	19	16	18
Ni	64	65	110	69	46	43
Pb	33	31	1	10	13	10
Sc	11	23	14	25	10	24
Sr	110	130	400	130	350	120
V	68	127	150	115	81	121
Y	36	37	52	40	41	42
Zr	180	140	190	145	260	200

Column 1, trace-element composition of "low grade slate L1" as reported by Shaw (1954, pt. 1, Table 7).

Column 2, trace-element composition of masked sample of L1 by Chodos and Godijn.

Column 3, trace-element composition of "low grade slate" L2 as reported by Shaw (1954, pt. 1, Table 7).

Column 4, trace-element composition of masked sample of L2 as determined by Chodos and Godijn.

Column 5, trace-element composition of "low grade slate" L3 as reported by Shaw (1954, pt. 1, Table 7).

Column 6, trace-element composition of masked sample of L3 as determined by Chodos and Godijn.

Granitized Gneiss

Introduction.—Four general types of more granitic gneiss are distinguished. They are (1) incipient migmatite; (2) migmatite; (3) augen gneiss; and (4) equigranular uniformly granitized gneiss. Examples of types 2 and 3 are shown in Plate 3. Most of the specimens in Table 9 belong to the equigranular, uniformly granitized type of gneiss. The specimens of granitized gneiss studied in greatest detail were largely of this type because of its greater textural uniformity, which in turn enhances the possibility that component minerals have formed in equilibrium and permits more accurate modal and chemical analyses.

Specimens of uniformly granitized gneiss in Table 9 include: Group 1A, Bgn 26; Group 1, Bgn 29, Qb 236, 237, 3, 7, 229, 227; Group 2, Qb 233, 216; Group 3, Bgn 9, 4, 6; Group 4, Bgn 25, 16; Group 5, Bgn 22, 23. Modal

analyses and trace-element composition of four typical specimens of uniformly granitized gneiss from Group 5 are listed in Table 12.

Mineralogy and texture.—The separation between least altered and uniformly granitized gneiss is made on the basis of total K feldspar present. Those specimens of gneiss with less than 5 per cent K feldspar are referred to as least altered gneiss. Those with more than 5 per cent K feldspar are called incipient migmatite. This type of separation is employed purely because of convenience and utility. It is liable to criticism in that (1) some least altered gneiss may be more potassic (2) K feldspar may have formed in the least altered gneiss as a product of the decomposition of muscovite, or at higher temperatures of metamorphism through the transformation of biotite to garnet.

Careful cross check of these possibilities, through studies of the field relationships of the more or less K-rich gneiss and modal analyses indicates that more than about 5 per cent K feldspar is not common in those bodies of gneiss which have not undergone obvious permeation or replacement by granitic material. This is certainly true in the Emeryville-Edwards area, where muscovite and biotite are stable. Farther northeast, in the parts of the gneiss metamorphosed at higher temperatures where K feldspar might normally form, the biotite breaks down very slowly (Fig. 5). With the slow decomposition of biotite, potassium is either abstracted from the least altered gneiss or is largely segregated in the granitic and pegmatitic bands. Finally, as shown below, the use of other compositional indices for granitization such as an increase in total K, or K + Na in the obviously granitized rock, or an increase in the ratio of K to Ca, or of K + Na to Fe + Mg + Ca, and so on also seems to justify essentially the same separations between the least altered and more granitic gneiss.

Marked differences in texture do appear between the several types of more granitic gneiss. The differences in textural types of granitic gneiss are diagrammed in Figure 3, photographed in Plate 3, and described in following pages. The smoothed curves in Figure 3, indicating the changes induced by granitization of the gneiss, are derived largely from modal analyses of the more uniform-textured specimens in the Emeryville area. Each tick on the horizontal co-ordinate of the diagram represents the modal analysis of a specific rock. The three solid darts represent position of rocks whose mineral and chemical compositions are given in columns 1, 3, and 4 of Table 13. The specimens are plotted from left to right in order of increased content of K feldspar. Gaps in the occurrence of ticks indicate no specimens of requisite K feldspar content were available (The modal data from which these curves are obtained are given in Engel and Engel, 1953b, Figs. 5, 6.) The curves indicate the kind of continuous variation in mineral composition between the least altered gneiss and equigranular granitic gneiss, that is, where the most subtle transitions of rock type and texture occur. They also reflect, however, the kinds of mineralogical changes that appear in the transitional contacts between least altered gneiss and any of the more granitic types in the Emeryville area. At the more abrupt contacts of gneiss and granite gneiss, it is obvious that sharp deflections would appear in the curves. The most common and marked deflections coincide with those in the textural curves, at roughly one-third and two-thirds of the distance from left to right. These are the contacts between gneiss and augen gneiss and between augen gneiss and equigranular more alaskitic granite gneiss as mapped (Pl. 4).

Type 1 (incipient migmatite) is especially common southwest of Edwards, where least altered gneiss is relatively most abundant. It consists of lenses and layers of quartz-microcline and quartz-perthite pegmatite and aplite ranging from a fraction of an inch to tens of feet thick, separated by several, up to as much as 30 feet, of least altered gneiss.

Most of the granitic seams contain quartz, microcline, oligoclase, biotite, and scattered muscovite. Southwest of Edwards, almandite garnet borders these seams, but it is not found in the uninjected parts of the gneiss. Many granitic seams are partly crushed, but others are essentially undeformed and appear to postdate all severe cataclasis. Most incipient migmatite in the Emeryville-Edwards areas has about the bulk composition and texture indicated in Figure 3 by the vertical zone just to the right of least altered gneiss and to the left of the area designated migmatite.

Type 2 (migmatite) is common throughout the 35-mile segment of gneiss. Migmatite is a more uniformly and completely "injected" gneiss than Type 1, with lit-par-lit alternations of more granitic and more gneissic layers, each being from a fraction of an inch to several inches or a foot in width. Figure 1 of Plate 3 shows an outcropping of migmatite that has flowed extensively in the solid or semisolid state. Most exposures exhibit very little

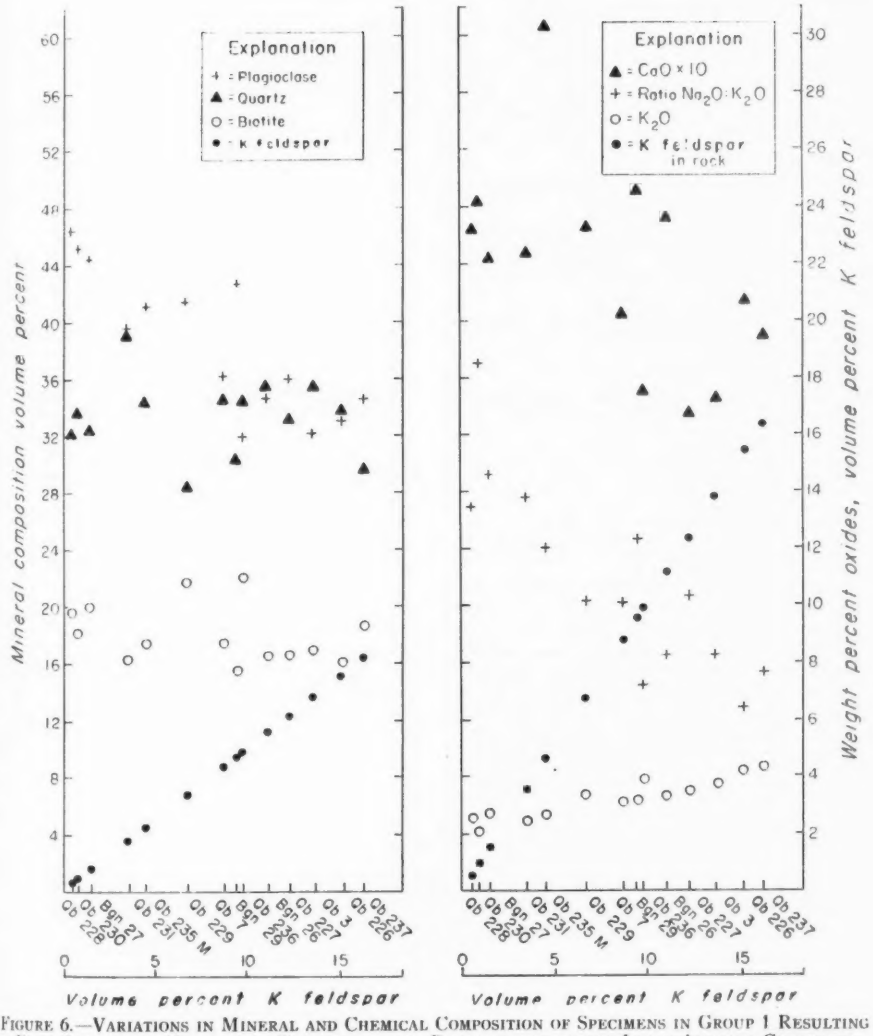

FIGURE 6.—VARIATIONS IN MINERAL AND CHEMICAL COMPOSITION OF SPECIMENS IN GROUP 1 RESULTING FROM INCREASING DEGREES OF PERMEATION AND REPLACEMENT OF THE LEAST ALTERED GNEISS BY GRANITE-FORMING SUBSTANCES, ESPECIALLY POTASSIUM

(See Table 9.) Positions of specimens are indicated by ticks on the horizontal co-ordinate. These are plotted from left to right in order of increasing K feldspar content, which is essentially the same order as increasing K, or decreasing Na_2O–K_2O ratio, CaO, MgO, or FeO. The graph on the left shows the variations in mineralogy, and that on the right shows changes in chemical composition resulting from increasing granitization.

ptygmatic folding, and many appear almost unfolded. Typical bulk compositions and textural features of migmatite in the Emeryville-Edwards areas are shown in the left hand one-third of Figure 3, except that in the more granitic seams the plagioclase may be more sodic than is indicated by the curve.

Type 3 (augen gneiss) consists of inequigranular augen gneiss and porphyroblastic granitic gneiss, in which large crystals and clusters of perthitic microcline, and locally oligoclase, have grown in a more or less pervasively feldspathized groundmass of gneiss. It occurs throughout the gneiss complex as the

commonest type of granite gneiss and is described as the Hermon granite gneiss (Buddington, 1939; Buddington and Leonard in press). Plate 3, Figures 2 and 3 are examples of this type of feldspathization. In the specimen in Figure 2 of Plate 3 the microcline porphyroblasts are remarkably euhedral. This type porphyroblastic gneiss is subordinate to the augen gneiss shown in Figure 3 of Plate 3. Typical textural and compositional features of the augen gneiss in the Emeryville-Edwards areas are shown in the central third of Figure 3

Type 4 (equigranular granitic gneiss) is essentially equigranular, pervasively feldspathized gneiss in which uniformly disseminated, fine- to medium-grained microcline has replaced to varying degrees the plagioclase and biotite of the least altered gneiss. The resulting rock is a faintly to distinctly foliated feldspathic gneiss or granite gneiss (granodiorite to quartz monzonite gneiss). Buddington has published some excellent photographs of this uniformly granitized gneiss (1957, Pl. 1).

The gneiss complex in the Russell-Colton areas has not been mapped in sufficient detail to justify a specific interrelationship of texture and mineral composition between least altered and more granitic gneiss. Approximately the same textural relationships hold, and in a gross way the change in mineralogy is similar. In the northeast segment of the gneiss, of course, the biotite curve (Fig. 3) would be accompanied by a subparallel garnet curve. Sillimanite also appears, commonly in variously granitized parts of the gneiss as Buddington notes (1957, Pl. 1 and p. 297–299). It is only rarely, however, the product of regional metamorphism without granitization. Instead, it appears to be a by-product of complex interaction of potassium-rich? fluids with gneiss (Buddington 1948, p. 36–39; Buddington and Leonard, in press) and is outside the scope of this study.

Additional differences exist in the compositional types of granitic rock associated with the gneiss at and near Colton. The varieties of granitic gneiss described thus far are generally agreed to be in large part, possibly wholly, of metasomatic origin (Buddington, 1957; Gilluly, written communication; Brown, oral communication; Engel and Engel, 1953b, p, 1076–1078). The present authors would add that although this granitic gneiss in the Emeryville area is largely the result of the introduction of granitic constituents, part of the granitic gneiss at Colton may be sweated out of the immediately associated least altered gneiss.

TABLE 12.—MODAL AND TRACE-ELEMENT ANALYSES OF FOUR TYPICAL SPECIMENS OF MORE UNIFORMLY GRANITIZED GNEISS FROM THE COLTON AREA, NEW YORK

Minerals in modal analysis given in volume per cent.

	Bgn 6A	Bgn 1A	Bgn 4A	Bgn 2	Mean
Quartz	30.70	24.60	23.60	24.70	25.90
Plagioclase	26.20	25.10	23.30	22.30	24.23
K feldspar	17.80	35.00	33.10	40.60	31.63
Biotite	9.60	14.00	18.80	11.30	13.42
Garnet	6.50	1.10	.20	.60	2.10
Sillimanite	9.00				2.25
Others*	.20	.20	1.00	.50	.47
Total	100.00	100.00	100.00	100.00	100.00

Trace Elements
(Parts per million)

Element	Sensitivity					
B	10	15	<10	<10	<10	6?
Ba	1	900	1000	1200	2000	1275
Co	2	9	2	5	5	5
Cr	5	20	12	25	17	18
Cu	1	15	25	17	16	18
Ga	5	16	10	12	11	12
Mn	2	360	130	120	110	180
Nb	15	pt	pt	pt	pt	15?
Ni	2	14	4	6	7	8
Pb	10	23	28	41	37	32
Sc	2	12	6	4	10	8
Sr	2	225	245	190	240	225
Ti	2	700	1200	1700	400	1000
V	2	20	35	25	40	30
Y	10	32	25	51	14	30
Yb	1	3	3	3	2	3
Zr	2	100	150	190	200	160

* Chiefly apatite, magnetite, pyrite, zircon, sphene, chlorite.

pt = approximately at the limit of sensitivity.

Looked for but not found: Ag, As, Au, Bi, Cd, Ge, In, La, Mo, Pt, Sb, Sn, Ta, Th, U, Zn.

Two additional types of granite and granitic gneiss occur intimately associated with the gneiss near Colton and along the perimeter of the massif. These are (1) hornblende-microperthite granite and gneissic equivalents and (2) microperthite alaskite granite and gneissic equivalents. Both these granitic rocks, where least deformed, show numerous igneous characteristics, as has been shown by Buddington

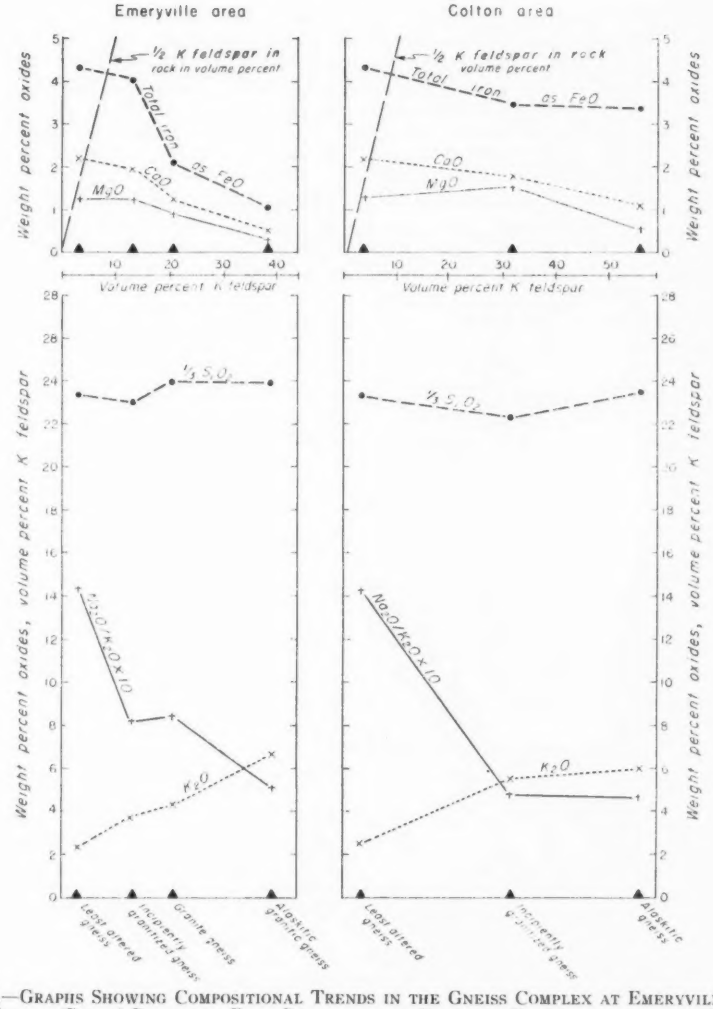

FIGURE 7.—GRAPHS SHOWING COMPOSITIONAL TRENDS IN THE GNEISS COMPLEX AT EMERYVILLE (LEFT) AND COLTON (RIGHT) RESULTING FROM PERVASIVE AND COMPLETE GRANITIZATION OF THE GNEISS

Changes of these types are characteristic of transitional contacts between gneiss and granite. The ticks on the horizontal co-ordinates represent the positions of composite specimens whose detailed compositions are posted in Table 13. Note that the analyses are plotted from left to right in order of increasing content of K feldspar, which is essentially equivalent to plots in order of increasing K_2O, or decreasing Na_2O–K_2O ratio, MgO, CaO, or FeO.

(1939; 1948; 1957) and by Buddington and Leonard (in press).

The hornblende-microperthite granite forms great batholithic masses within the massif where it occupies two-thirds of the area of younger granitic rocks (Buddington 1957, p. 292). It is rare in the Grenville Lowlands. The microperthite alaskite occurs both within the massif and in the Grenville Lowlands, where it forms phacoliths (Buddington 1929; 1957) in the metasedimentary rocks. It is the granite of the California phacolith, west of Balmat, the only obviously igneous granite in or near the Emeryville area.

Chemical composition: major elements.—The continuous to semicontinuous changes in composition between least altered and granitized gneiss are plotted in Figures 6 and 7 and

TABLE 13.–AVERAGE CHEMICAL AND MINERAL COMPOSITIONS OF LEAST ALTERED AND MORE GRANITIC GNEISS FROM THE EMERYVILLE AND COLTON AREAS, NEW YORK

In chemical analyses oxides given in weight per cent.

	Emeryville Area Group 1				Colton Area Group 5		
	1	2	3	4	5	6	7
SiO_2	70.25	69.25	72.31	71.89	65.97	66.93	70.99
TiO_2	.67	.63	.31	.14	.64	.85	.20
Al_2O_3	14.14	14.63	14.76	15.45	16.83	16.32	14.28
Fe_2O_3	.55	.70	.33	.26	.36	.45	1.19
FeO	3.83	3.45	1.76	.85	4.92	3.15	2.30
MnO	.05	.05	.02	.04	.07	.04	n.d.
MgO	1.76	1.74	.79	.36	2.25	1.56	.53
CaO	2.20	1.97	1.40	.58	3.41	1.76	1.12
Na_2O	3.43	3.06	3.57	3.40	3.70	2.67	2.80
K_2O	2.40	3.79	4.27	6.69	1.46	5.57	5.97
H_2O+	.72	.71	.44	.32	.39	.52	.08
P_2O_5	.07	.05	.03	.04	n.d.	n.d.	.09
Total	100.07	100.03	100.00	100.02	100.00	99.82	99.55
Modes (Volume per cent)							
Quartz	37.86	33.62	32.68	25.37	29.28	25.90	24.0
Plagioclase	39.86	34.06	35.50	37.89	48.92	24.23	10.1
K feldspar	3.19	13.80	20.78	38.92	3.17	31.63	56.6
Biotite	17.60	17.10	7.73	2.46	10.68	13.42	..
Garnet	.03	tr	..	..	7.38	2.10	..
Muscovite	.86	.69	1.30	1.73	..	..	..
Sillimanite	..	..	..	..	..	2.25	..
Others†	.60	.73	2.10	2.53	.57	.47	7.8
Plagioclase composition	Ab 73	Ab 72	Ab 81	Ab 91	Ab 67	Ab 74	Ab 90
Trace Elements* (Parts per million)							
Element / Sensitivity							
B 10	10	22	12	6?	12	6?	..
Ba 1	612	750	910	1100	492	1275	..
Co 2	8	7	4	<2	7	5	..
Cr 5	35	16	4	<1	56	18	..
Cu 1	16	4	19	12	12	18	..
Ga 5	11	10	12	16	14	12	..
Mn 2	356	434	260	118	341	180	..
Nb 15	pt	pt	..	<10	pt	15	..
Ni 2	15	12	4	<2	21	8	..
Pb 10	12	21	38	46	15	32	..
Sc 2	12	10	6	<2	17	8	..
Sn 5	7?	7?	..	12	<5	<5	..
Sr 2	310	320	270	96	304	225	..
Ti 2	2800	1800	750	430	3000	1000	..
V 2	56	53	24	10	81	30	..
Y 10	46	49	35	26	58	30	..
Yb 1	3	3	3	4	3	3	..
Zr 2	171	172	150	185	176	160	..
Number of specimens	9	5	3	3	8	4	..

* Looked for but not found: Ag, As Au, Bi, Cd, Ge, In, La, Mo, Pt, Sb, Ta, Th, U, Zn.

† Chiefly apatite, zircon, sericite, magnetite, chlorite, and pyrite.

Description of specimens:

1. Least altered gneiss. Modal analysis is mean of analyses of 24 specimens. Trace-element values are the mean of analyses of 9 of the 24 specimens composing the average mode.

2. Incipiently granitized gneiss. Modal analysis and chemical compositions are averages of analyses of Bgn 26, Qb 3, Qb 226, Qb 227, (Table 7).

(*Continued at foot of page 1409*)

in Tables 12, 13, and 14. The data are specifically for the changes in composition found at transitional contacts between least altered gneiss and equigranular to inequigranular granitic gneiss at (1) Emeryville and (2) Colton. Some variations in composition of the specimens listed in Table 9 are graphed in Figure 6. More comprehensive trends of granitization near Emeryville, as shown by chemical analyses, are listed in columns 1, 2, 3, and 4 of Table 13, and are graphed on the left-hand side of Figure 7. Analyses of rocks from the Colton area are listed in columns 5, 6, and 7 of Table 13 and are graphed on the right-hand side of Figure 7. In Figures 6 and 7, the positions of the analyses on the horizontal co-ordinate are determined by the content of K feldspar in the rock. This ranges from essentially nil to 50 per cent by volume. It is apparent, however, that about the same trends in composition result if the positions of specimens are determined by total iron, Mg, Ca, or K and so on.

Granitization of least altered gneiss as shown in the tables and figures noted involves increases in K and decreases in Fe, Mg, Ca, and in the ratio of Na to K. The specimens of granitized gneiss listed in Table 9, graphed in Figure 6, and studied in detail, represent only incipient stages in the granitization process. The intermediate and end stages of granitization are represented by the right-hand sides of both graphs in Figure 7.

Evaluation of the several possible mechanisms of granitization is beyond the scope of this work, but several implications may be noted briefly. If the gneiss in the Edwards-Emeryville areas and to the southwest is in large part replaced by more granitic rock, and if these granitic (K-rich) constituents are introduced into the gneiss, Fe, Ca, Mg, OH and chemically coherent trace elements are expelled from the gneiss. The segment of gneiss that has undergone this depletion is at least 30 miles long from Edwards southwest to the Paleozoic overlap, southwest of Antwerp and Philadelphia, New York, and appears to have had an early metamorphic thickness of at least 2500 feet. In the Emeryville area detailed mapping suggests that one-fourth to one-third of the gneiss is replaced by granitic gneiss as felsic as, or more felsic than that listed in column 3, Table 13. Reconnaissance of the gneiss southwest of Emeryville, beyond Antwerp and Philadelphia, New York, suggests even greater metasomatism throughout this part of the gneiss. Obviously a very large basic front could be involved. The approximate volume of any such front would be, of course, conditional upon volume changes and upon the amount of gneiss actually replaced. Quantifying these figures will be no mean task for the future.

The significance of the trends in the Colton area is complicated by the fact that some of the granitizing substances seem to have had their origin in the gneiss itself. In indicating trends imparted by granitization near Colton, the composition of least altered gneiss plotted in Figure 7 is that found at Emeryville, not that now found near Colton. This is because the early or pre-metamorphic parent of the least altered gneiss at Colton is assumed to have had about the same composition as that now found at Emeryville. Basification of the least altered gneiss at Colton occurred during this metamorphic differentiation and the development of the intertonguing more granitic gneiss. But in addition to this metamorphic differentiation, granitic magma and K-rich fluids rising from even deeper sources seem to have permeated, shredded, and partly replaced parts of the gneiss at Colton. The extent of metasomatism involved in this last-named granitization in the Russell-Colton region would presumably indicate the volume of mafic constituents expelled there. Data necessary for even a crude estimate are not at hand.

Apropos to the expulsion of iron from the gneiss complex at Colton, Buddington has stressed the fact that much of the magmatic ? granite that has shredded and variously replaced the gneiss along and within the massif is remarkably high in total iron (1957, p. 303, Table 6; Buddington and Leonard, in press). Most of the iron is in the ferric state, largely as magnetite

3. Granitic gneiss. Modal analysis is mean of analyses of three specimens. Chemical analyses are of a mix of equal parts of the powders of the three specimens.

4. Alaskitic granite gneiss. Modal analysis is mean of analyses of three specimens. Chemical analyses are of a mix of equal parts of the powders of the three specimens.

5. Least altered gneiss. Modal analysis is mean of analyses of 14 specimens (Table 8). Trace-element values are the mean of analyses of 8 of the 14 specimens, composing the average mode.

6. Incipiently granitized gneiss. Modal analyses and trace-element compositions are average of analyses of specimens Bgn 2, Bgn 6A, Bgn 1A, and Bgn 4A listed in Table 12. The chemical analysis of major constituents is of a mix of equal parts of the powders of these specimens.

7. Granitic gneiss. Garnet alaskite contaminated with gneiss, Horseshoe Lake, Tupper Lake Quadrangle (with Adirondack Massif). Analyst Lee C. Peck. Quoted from Buddington 1957, p. 298.

and hematite. In much of this granite contaminated by the gneiss, the total iron content may be one-half to three-fourths of that present in least altered gneiss. These possible relationships are indicated by the data in Table 13. Column 1 shows the composition of the least altered gneiss at Emeryville. In columns 6 and 7 are analyses of respectively sillimanite-quartz-microcline granite contaminated with gneiss, and garnet alaskite, also a product of reaction with the gneiss. Both these granites are emplaced within the gneiss near the margin of the massif. In some of these highly granitic rocks which are volumetrically abundant (e.g. the garnet alaskite), a mechanism existed for the formation or retention of relatively large amounts of ferric iron. Whether this iron is in part or wholly from the gneiss at the present level of erosion, or from deeper levels, or of more cryptic magmatic source is not indicated to us by any of our data. Buddington and Leonard (in press) conclude that the bulk of this iron and that in the skarns and iron ores associated with the granites is largely of deep-seated magmatic origin.

The granitization of parts of the gneiss is essentially a potassium metasomatism, not too unlike that known in many terranes in the world (Billings, 1938; Eskola, 1948; and so on). This type granitization of metasedimentary rocks is an interesting contrast to those instances where Na rather than K is the principal element introduced. The migmatites of Sutherland, as described by Read (1931) and Cheng (1943) are a curious case in point. The initial sediments in Sutherland appear to have been rich in potassium and low in Na. With migmitization and granitization the ratio of Na_2O to K_2O is reported to increase greatly. Mineralogically the migmatization is said to be accompanied by an increase in plagioclase and a decrease in muscovite, K feldspar, biotite, garnet, and quartz (Cheng, 1943).

The enormous scale of the K-Si metasomatism in the Adirondack Mountains and its contemporaneity with emplacement of large granitic batholiths seems clearly established. The detailed mechanisms of both processes remain unknown. They represent the final pulse in the evolution of the Adirondack orogen, at approximately 1 billion years ago. All pre-existing rock units are invaded and partly replaced by both granite magma and K and Si ions, atoms, or fluids, producing K feldspar, quartz, and finally sericite. Pre-existing anorthosites, gabbros, syenites, amphibolites, and clastic sediments such as the paragneiss are especially shredded, altered, and injected; but even the orthoquartzites and marbles are enriched in K and Al. Just east of Emeryville more than a cubic mile of marble is replaced by potassic granite gneiss and pegmatite contemporaneous with the granitic gneiss in the gneiss complex.

TABLE 14.—AVERAGE COMPOSITION OF LEAST ALTERED GNEISS AT EMERYVILLE AND COMPOSITIONS OF GRANITES IN THE MASSIF THAT SHRED AND ARE CONTAMINATED BY THE GNEISS

Oxides given in weight per cent.

	Average least altered gneiss 1	Garnet alaskite gneiss 2	Sillimanite-quartz microcline gneiss 3
SiO_2	68.77	70.99	71.44
TiO_2	.71	.26	.65
Al_2O_3	14.77	14.28	14.89
Fe_2O_3	.65	1.19	2.40
FeO	4.00	2.30	1.38
MnO	.06	.09	.03
MgO	1.87	.53	.30
CaO	2.45	1.12	.50
Na_2O	3.50	2.80	1.36
K_2O	2.44	5.97	5.99
H_2O+	.73	.30	.52
P_2O_5	.09	.20	.22
Total	100.04	100.03	99.68

1. Least altered gneiss from Group 1, mean of five chemical analyses from Table 7. Analyst, C. G. Engel.

2. Garnetiferous, inequigranular granitic gneiss 1 mile west of Bear Pond, Tupper Lake quadrangle (from Buddington and Leonard, in press). Analyst, Lee C. Peck.

3. Microcline-rich granitic gneiss, Oswegatchie quadrangle (from Buddington, 1957, Table 4, column 6). Analyst, Lee C. Peck.

This composite wave of K-rich alteration and magmatic injection is by no means confined to the Adirondack segment of the so-called Grenville subprovince (Engel and Engel 1953a; A. E. J. Engel, 1956) of the Canadian Shield. Similar injection and replacement of metasedimentary and older igneous-looking rocks occurs throughout the entire southwest part of the subprovince in southeastern Ontario and southwestern Quebec, a region of about 300,000 square miles (Engel and Engel, 1953a, Fig. 1).

Chemical composition: minor elements.—Trace-element compositions of incipiently granitized gneiss studied in detail between Emeryville and Colton are listed in Table 9 with modal and other chemical data. Concentrations of elements in more completely granitized gneiss, as well as the mean composition of least altered gneiss from Emeryville and Colton, are listed in Tables 12, 13, and 14. An obvious limitation in the data is the small number of specimens analyzed. Despite this limitation certain trends coincident with granitization appear quite real. Specifically Ba and Pb almost surely increase in the more granitic gneiss. Application of the "Student's" *t* test to the data indicates the probability of the differences being due to chance is less than 0.01 for each of these elements.

The apparent decreases in Co, Cr, Mn, Ni, Sc, Sr, Ti, V, and Y in the more granitic gneiss also seem to be real. Trends of the type observed are consistent with empirical data from other rocks and with theoretical conceptions of coherence between minor and major elements.

Summary

The major Adirondack paragneiss extends across the Grenville Lowlands from a point southwest of Antwerp to the perimeter of the central Adirondack igneous massif at Colton, New York. Detailed field and analytical studies have been made of the northeasterly 35-mile segment of the gneiss between Emeryville and Colton. The gneiss seems to have evolved from a monotonous tuff or graywackelike rock into a complex of little altered and variously granitized parts. Two types of metamorphism of gneiss are considered. One is the progressive metamorphism of least altered gneiss, that is, the rock seemingly little altered in bulk composition from the parent sedimentary rock. The second type is the granitization of widely distributed parts of the least altered gneiss.

Geologic thermometers indicate temperatures of both types of metamorphism of the gneiss of about 500° to 525° C. at the southwest end of the belt and about 600° C. near the perimeter of the massif. These data are based upon an assumed depth of metamorphism of about 5 miles, which may be in error by 50 per cent or more. Minimum temperatures of metamorphism are obtained largely from studies of the solid solubility of magnesite in dolomite, FeS in sphalerite, paragonite in muscovite, and TiO_2 in magnetite. These studies indicate temperatures of metamorphism at Emeryville exceeded 475° C. and at Colton exceeded 550° C.

Maximum temperatures of metamorphism are inferred principally from the absence of wollastonite in closely associated siliceous marbles. Assuming a depth of 5 miles, temperatures of metamorphism at Colton did not exceed 750° C. and probably were less than 650° C.

The indicated increases in temperatures of metamorphism between Emeryville and Colton are confirmed by independent lines of evidence, namely (1) the increase in metamorphic rank and grain size in all mineral assemblages, (2) the increase in contemporary granite having igneous characteristics, and (3) the marked decrease in δO^{18} values in quartz minus magnetite that occur as mineral pairs in the gneiss.

At Emeryville the least altered gneiss is a monotonous-appearing, distinctly foliated, medium-grained, quartz-greenish biotite-oligoclase rock with about 1 per cent muscovite. The bulk chemical composition is that of an average graywacke or dacitic tuff with NaO–K_2O ratio of $\sim$ 1.3. This least altered gneiss forms about one-third of the complex at Emeryville and is cut by and transitional into the more granitized parts.

As the least altered gneiss is traced from Emeryville to Colton, muscovite disappears at $\sim$ 525° C., and almandite garnet appears throughout the rock. Sympathetically the average plagioclase becomes more calcic, biotite changes from greenish brown through successive shades of brown, reddish brown, to deep red brown, quartz content decreases, grain size increases, and segregational banding appears in the gneiss.

The changes in texture and mineralogy in least altered gneiss are accompanied by systematic changes in its bulk chemical composition. With increasing temperature of metamorphism the least altered gneiss is enriched in Al, Fe^{++}, total Fe, Mg, Ca, Cr, Ga, Ni, and V. The concentrations of K, Si, Fe^{+++}, H_2O, and Ba decrease. These changes in chemical composition of least altered gneiss are detectable at temperatures of metamorphism of about 550° C. and are well defined at Colton ($\sim$600° C.). The cause of the change is interpreted as a metamorphic "degranitization" or "basification" in which Si, K, and H_2O are mobilized and partly liberated but partly frozen into the rock as venitic migmatite.

Granitization of the gneiss may involve several processes, especially mechanical injection of magma, permeation, and replacement of

the gneiss by magma, by fluids from magma, or by ichors and ions. Granitic rock clearly of igneous origin is not common in or associated with the gneiss complex at Emeryville but is abundant in the Colton area and immediately southeast.

Throughout the gneiss complex the granitic parts include (1) lit-par-lit injection gneiss (migmatite); (2) augen gneiss rich in porphyroblasts (and locally phenocrysts?) of K feldspar; and (3) even-grained uniformly feldspathized gneiss. All these types of granitization of the gneiss are accompanied by an increase in K feldspar and in Ab content of plagioclase and by a decrease in biotite, plagioclase, and quartz. During granitization, K increased and Ti, Fe^{+++}, Fe^{++}, Mg, Ca, H_2O, and Na–K ratio decreased. Changes in the amounts of minor elements in granitized parts of the gneiss include increases in Ba, Pb, and possibly Sn, and decreases in Co, Cr, Mn, Ni, Sc, Sr, Ti, V, and Y.

All granitizing substances in the gneiss in areas of lowest-temperature metamorphism (less than 550° C.) appear to be introduced either laterally or from below. Their source may include ultrametamorphosed parts of the gneiss as well as other parts of the crust or upper mantle.

In the areas of highest temperature of metamorphism studied, the granite-forming constituents appear to be partly introduced and partly sweated out of the associated "basified" gneiss.

Granitization of the gneiss has resulted in the expulsion of large quantities of H_2O, Fe, Mg, and Ca. At least one-third of the gneiss in a zone more than 2500 feet thick, 75 miles wide, and 30 miles long is partly to completely replaced by more anhydrous granitic rock. Exact volume changes are unknown, however, and although there are numerous mafic metamorphic rocks in the region, none can be proved to represent a basic front.

Calculations of the chemical analyses of more even-textured rock in the gneiss complex, from data of modal and mineral analyses, show about the same deviation from actual chemical analyses as exists in the 34 analyses of the standard rocks G-1 and W-1.

References Cited

Barth, Tom, F. W., 1952, Theoretical petrology: N.Y., John Wiley and Sons, Inc., 387 p.

Barton, Paul B., and Kullerud, Gunnar, 1957, Preliminary report on the system FeS-ZnS-S, and implications regarding the use of the sphalerite geothermometer: Geol. Soc. America Bull., v. 68, p. 1699

Billings, M. P., 1938, Introduction of potash during regional metamorphism in western New Hampshire: Geol. Soc. America Bull., v. 49, p. 289–302

Brown, J. S., 1936, Structure and primary mineralization of the zinc mine at Balmat, New York: Econ. Geology, v. 31, p. 233–258

—— 1947, Porosity and ore deposition at Edwards and Balmat, New York: Geol. Soc. America Bull., v. 58, p. 505–545

Brown, J. S., and Engel, A. E. J., 1956, Revision of Grenville stratigraphy and structure in the Balmat-Edwards district, northwest Adirondacks, New York: Geol. Soc. America Bull., v. 67, p. 1599–1622

Buddington, A. F., 1929, Granite phacoliths and their contact zones in the northwest Adirondacks: N. Y. State Museum Bull. 296, 251 p.

—— 1939, Adirondack igneous rocks and their metamorphism: Geol. Soc. America Mem. 7, 354 p.

—— 1948, Origin of granite rocks of the northwest Adirondacks, p. 21–43 *in* Cilluly, James, *Chairman*, Origin of granite: Geol. Soc. America Mem. 28, 139 p.

—— 1952, Chemical petrology of some metamorphosed Adirondack gabbroic, syenitic and quartz syenitic rocks: Am. Jour. Sci., Bowen Volume, p. 37–84

—— 1957, Interrelated Precambrian granitic rocks, northwest Adirondacks, New York: Geol. Soc. America Bull., v. 68, p. 291–305

Buddington, A. F., and Leonard, B. F., Jr., (in press), Precambrian magnetite deposits of St. Lawrence County, New York: U. S. Geol. Survey Prof. Paper

Buddington, A. F., Fahey, Joseph, and Vlisidis, Angelina, 1955, Thermometric and petrogenetic significance of titaniferous magnetite: Am. Jour. Sci., v. 253, p. 497–523

Chayes, Felix, 1949, A single point counter for thin section analysis: Am. Mineralogist v. 34, p. 1–11

—— 1952, Notes on the staining of potash feldspar with sodium cobaltinitrite in thin sections: Am. Mineralogist, v. 37, p. 337–340

—— 1956, Petrographic modal analysis: N. Y., John Wiley and Sons Inc., 113 p.

Cheng, Yu-Chi, 1943, The migmatite area around Bettyhill, Sutherland: Geol. Soc. London Quart. Jour., v. 99, Parts 3 and 4, p. 107–154

Clayton, R. N., and Epstein, S., 1958, The relationship between O^{18}–O^{16} ratios in coexisiting quartz, carbonate, and iron oxides from various geological deposits: Jour. Geology, v. 66, p. 352–373

Danielsson, A., 1950, Das Calcit-Wollastonitgleichgewicht: Geochim. et Cosmochim. Acta, v. 1, p. 55–69

Dieke, G. H., and Crosswhite, H. M., 1943, The use of iron lines as intensity standards: Jour. Opt. Soc. America, v. 33, p. 425–434

Engel, A. E. J., 1948, Diamond drilling in the West Branch area, Gouverneur district, New York: U. S. Geol. Survey prelim. Rept., p. 3–222

—— 1949, Studies of cleavage in the metasedimentary rocks of the northwest Adirondack Mountains, New York: Am. Geophys. Union Trans., v. 30, p. 767–784

—— 1956, Apropos the Grenville, p. 74–98 *in* Thonson, J. E., *Editor*, The Grenville problem: Royal Soc. Canada, Special Pub. No. 1, 285 p.
—— in press, The Precambrian geology and talc deposits of the Balmat-Edwards district, New York: U. S. Geol. Survey Prof. Paper
Engel, A. E. J., and Engel, Celeste G., 1953a, Grenville series in the northwest Adirondack Mountains, New York, Part I, General features of the Grenville series: Geol. Soc. America Bull., v. 64, p. 1013–1047
—— 1953b, Grenville series in the northwest Adirondack Mountains, New York, Part II, Origin and metamorphism of the major paragneiss: Geol. Soc. America Bull., v. 64, p. 1049–1097
Eskola, Pentti, 1920, The mineral facies of rocks: Norsk geol. tidsskr., v. 6 p. 143–194
—— 1933, On the differential anatexis of rocks: Comm. géol. Finlande Bull., v. 17, no. 103
—— 1950, The nature of metasomatism in the processes of granitization: 18th Internat. Geol. Cong., Great Britain, Rept. pt. 3, p. 5–13
Eugster, H. P., and Yoder, H. S., 1955, Micas, p. 124–126 *in* Abelson, P. H., Annual Report of the Director, Geophysical Laboratory (1954–1955): Carnegie Inst. Wash. Year Book. 54, 311 p.
Fairbairn, H. W., 1953, Precision and accuracy of chemical analyses of silicate rocks: Geochim. et Cosmochim. Acta, v. 4, p. 143–156
Fairbairn, H. W., *et al.*, 1951, A cooperative investigation of precision and accuracy in chemical, spectrochemical and modal analysis of silicate rocks: U. S. Geol. Survey Bull. 980, 71 p.
Goldsmith, Julian R., Graf, Donald L., and Joensuu, Oiva, I., 1955, The occurrence of magnesian calcites in nature: Geochim. et Cosmochim. Acta, v. 7, no. 5, p. 212–230
Gordon, M., and Murata, K. J., 1952, Trace elements in Arkansas bauxite: Econ. Geology, v. 47, p. 169–179
Graf, Donald L., and Goldsmith, Julian R., 1955, Dolomite-magnesian calcite relations at elevated temperatures and CO_2 pressures: Geochim. et Cosmochim. Acta, v. 7, nos. 3 and 4, p. 109–128
—— 1958, The solid solubility of $MgCO_3$ in $CaCO_3$, a revision: Geochim. et Cosmochim. Acta, p. 218–219
Harker, R. I., and Tuttle, O. F., 1955, Studies in the system CaO–MgO–CO_2, Part 2, Limits of solid solution along the binary join $CaCO_3$–$MgCO_3$: Am. Jour. Sci., v. 253, p. 274–282
—— 1956, Experimental data on the P_{CO_2}-T curve for the univariant reaction: calcite + quartz wollastonite + carbon dioxide: Am. Jour. Sci., v. 254, p. 234–256
Holmquist, P. J., 1921, Typen and nomenklatur der Adergesteine: Geol. Fören. i Stockholm Förh., v. 43, p. 612–631
Keller, W. D., and Moore George, E., 1937, Staining drill cuttings for calcite-dolomite differentiation: Am. Assoc. Petroleum Geologists Bull. v. 7, p. 949–951
Kullerud, Gunnar, 1953, The FeS-ZnS system, a geological thermometer: Norsk geol. tidsskr., bd. 32, h. 2–3, p. 61–147
Lapadu-Hargues, P., 1949, Contribution aux problèmes de l'apport dans le metamorphisme: Soc. Géol. France Bull., ser. 5, tome 19, p. 89–109
Mood, A. M., 1950, Introduction to the theory of statistics: N.Y., McGraw-Hill Book Co., 325 p.
Prucha, John, 1953, The pyrite deposits of Jefferson and St. Lawrence counties, New York: N. Y. State Sci. Service Rept., Inv. No. 8, 66 p.
Ramberg, Hans, 1951, Remarks on the average chemical composition of granulite facies and amphibolites-to-epidote amphibolite facies in West Greenland: Dansk Geol. Foren. Meddel., bd. 12, p. 27–34
—— 1952, The origin of metamorphic and metasomatic rocks: Chicago, Univ. Chicago Press, 317 p.
Read, H. H., 1931, The geology of central Sutherland: Geol. Survery of Scotland Memoir
Rosenquist, I. T., 1952, The metamorphic facies and the feldspar minerals: Bergens Mus. Årbok, Nat. rekke no. 4, 116 p.
Sederholm, J. J., 1923, On migmatites and associated Precambrian rocks of southwest Finland: Comm. géol. Finlande Bull. no. 58, part 1
Shapiro, Leonard, and Brannock, W., 1952, Rapid analysis of silicate rocks: U. S. Geol. Survey Circ. 165, 17 p.
—— 1956, Rapid analysis of silicate rocks: U. S. Geol. Survey Bull. 1036-C, 56 p.
Shaw, Dennis M., 1954, Trace elements in pelitic rocks, Part I, Variations during metamorphism: Geol. Soc. America Bull., v. 66, p. 1151–1166
—— 1956, Geochemistry of pelitic rocks, Part III, Major elements and general geochemistry: Geol. Soc. America Bull., v. 67, p. 911–934
Snedecor, G. W., 1946, Statistical methods: Ames, Iowa, Iowa State College Press, 351 p.
Weeks, W. F., 1956, A thermochemical study of equilibrium relations during metamorphism of siliceous carbonate rocks: Jour. Geology, v. 64, p. 245–270
Winchell, A. N., and Winchell, Horace, 1951, Elements of optical mineralogy: N.Y., John Wiley and Sons, Inc., 347 p.
Yoder, H. S. Jr., 1952, The MgO-Al_2O_3-SiO_2-H_2O system and the related metamorphic facies: Am. Jour. Sci., Bowen Volume, p. 569–627

California Institute of Technology, Pasadena, California; U.S. Geological Survey, Denver, Colorado

Manuscript Received by the Secretary of the Society, December 17, 1957
Project Grant 622-53
Publication Authorized by the Director, U.S. Geological Survey

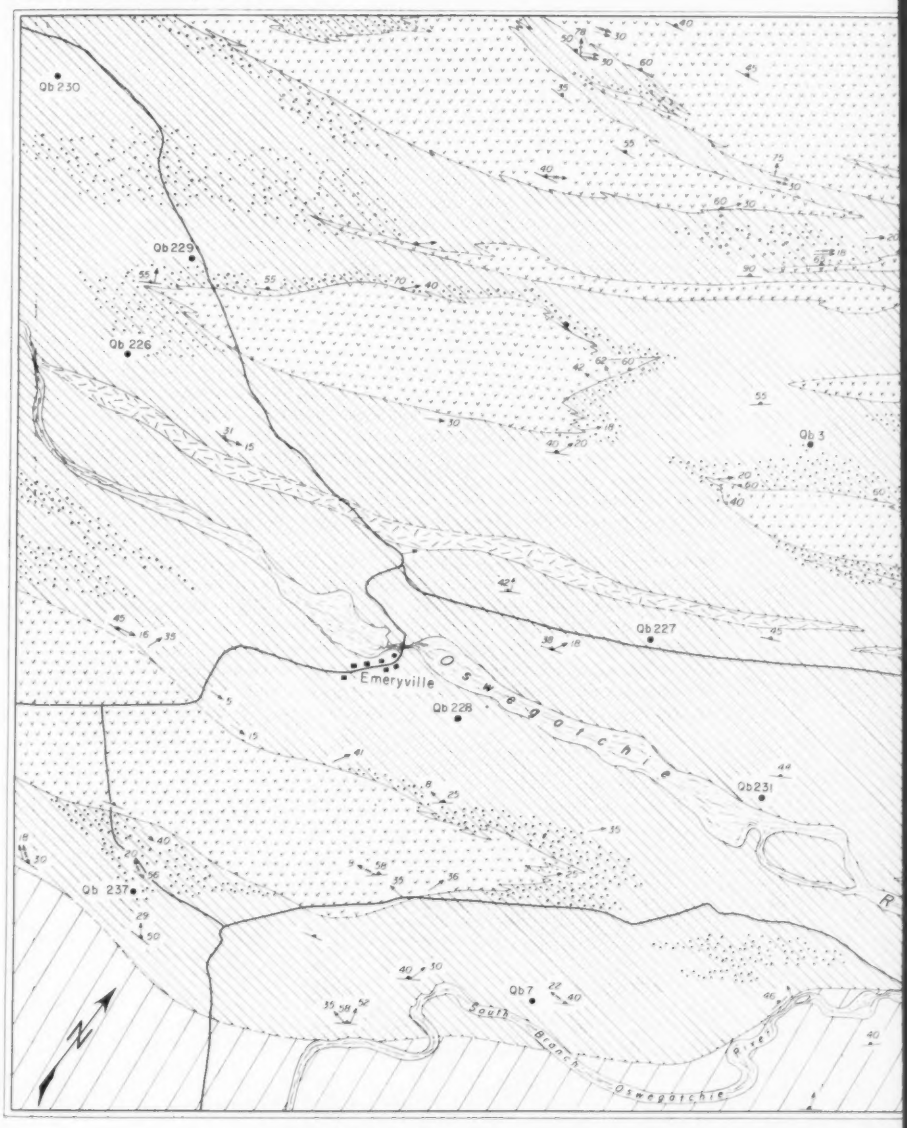

DETAILED GEOLOGIC MAP OF THE EM
ROCK TYPES WITHIN THE

HE EMERYVILLE AREA SHOWING THE INTERRELATIO
N THE GNEISS AND LOCATIONS OF SPECIMENS IN GR

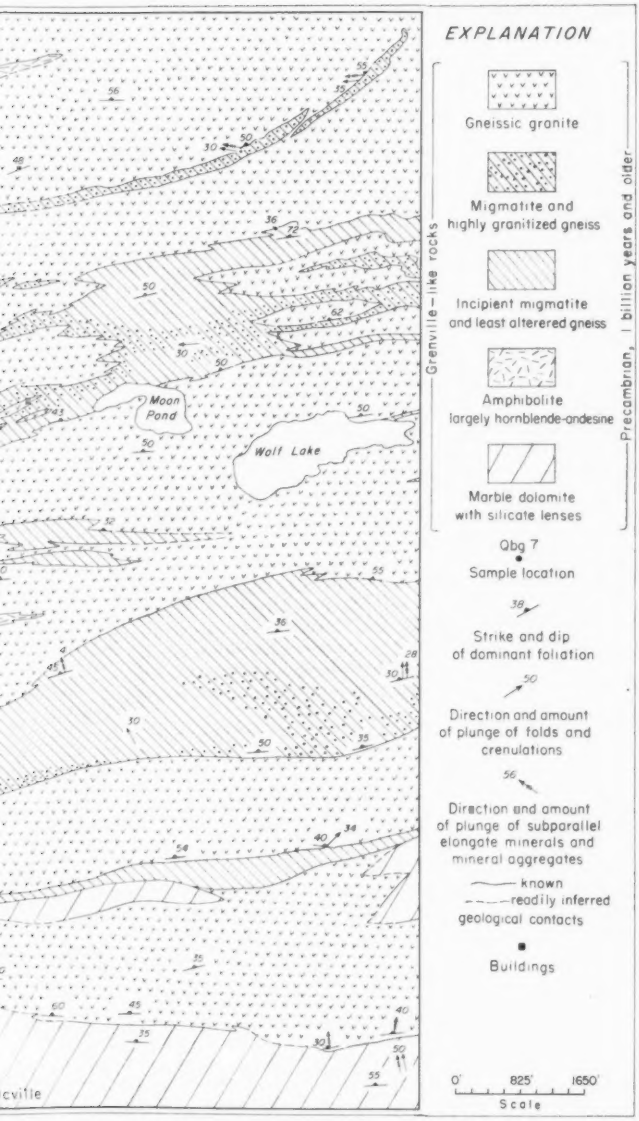

EXPLANATION

Precambrian, 1 billion years and older

Grenville-like rocks

Gneissic granite

Migmatite and highly granitized gneiss

Incipient migmatite and least alterered gneiss

Amphibolite largely hornblende-andesine

Marble dolomite with silicate lenses

Qbg 7
Sample location

38
Strike and dip of dominant foliation

50
Direction and amount of plunge of folds and crenulations

56
Direction and amount of plunge of subparallel elongate minerals and mineral aggregates

known
readily inferred
geological contacts

Buildings

0' 825' 1650'
Scale

ELATIONSHIPS OF THE
IN GROUP 1

BULLETIN OF THE GEOLOGICAL SOCIETY OF AMERICA
VOL. 69, PP. 1415–1430, 1 FIG., 1 PL. NOVEMBER 1958

MINERALIZATION IN THE INTRUSIVE ROCKS IN LITTLE COTTONWOOD CANYON, UTAH

BY BYRON J. SHARP

ABSTRACT

The area described is about 25 miles southeast of Salt Lake City and about 2 miles west of Alta, Utah. Eastward-dipping Precambrian quartzites and argillites have been intruded by a Tertiary pluton called the Little Cottonwood quartz monzonite. Another intrusive body, recognized during this study, is exposed within the borders of the extensive Little Cottonwood pluton. The study has also resulted in the recognition of a widespread scheelite-mineralized zone and the compilation of previously reported molybdenite occurrences, which may be of commercial value. In general, the minerals present in the area are those associated with medium- and high-temperature hydrothermal deposits. Mineralized structures in the intrusive rocks consist of zones of jointing and fracturing which form a concentric pattern around an intensively fractured central zone. The more intense fracture zones are mainly within the exposures of the later and smaller intrusive body. Three stages of mineralization have been recognized. During stage I widespread scheelite, pyrite, and sericite were deposited on joint surfaces of the intrusive rocks. Sparsely distributed scheelite of stage I can be observed over an area of 6 square miles and a vertical range of 3000 feet. During stage II, molybdenite, pyrite, quartz, sericite, galena, sphalerite, and small amounts of scheelite and calcite were deposited in the more intensely fractured zones. Stage III minerals are fluorite and sericite in local zones.

A sample which is possibly representative of much of the 6-square-mile area contained 0.02 per cent WO_3. Assays reported on the molybdenite-mineralized area indicated 0.24 per cent, 0.66 per cent, and 2.14 per cent MoS_2. The tungsten minerals are relatively uniform in distribution, but the molybdenite distribution is erratic. An intensive sampling of the deposit is recommended to determine the economic value of known mineralized zones; the sampling project may also expose other minerals associated with high-temperature deposition. Prospecting for tungsten minerals in other igneous intrusive bodies of the region is also recommended on the basis of this investigation.

CONTENTS

TEXT

	Page
Introduction	1416
History and ore production	1417
Field and laboratory work	1417
Acknowledgments	1417
Geologic setting	1417
Intrusive rocks	1418
General statement	1418
Little Cottonwood quartz monzonite	1419
White Pine leucocratic quartz monzonite	1421
Aplite dikes	1422
Red Pine alaskite porphyry	1422
Lamprophyre dikes	1424
Pebble dike	1424
Sequence of intrusions	1425
Structural zones	1425
General statement	1425
Breccia zone	1426
Stockwork zone	1426
Fringe zone	1426
Mineralization	1426
General statement	1426
Stage I	1426
Stage II	1427
Stage III	1427
Alteration	1427
Comparison with other districts	1428
Economic possibilities	1428
References cited	1429

ILLUSTRATIONS

Figure	Page
1. Index map of Utah showing location of area	1416

Plate	Facing page
1. Geologic map of a part of the Little Cottonwood igneous complex	1430

TABLES

Table	Page
1. Modes of igneous rocks from Little Cottonwood Canyon, Utah	1418
2. Characteristics of igneous rocks from Little Cottonwood Canyon, Utah	1425

Introduction

The writer studied a large mineralized area in the eastern portion of the Little Cottonwood pluton of Utah to determine its extent, characteristics, mineral associations, economic possibilities, and possible origin. The area studied is on the south side of Little Cottonwood Canyon of the Wasatch Mountain range, in southeastern Salt Lake County, Utah, about 2 miles west of Alta (Fig. 1). It includes part of the main canyon and much of Gad Valley, White Pine Fork, Red Pine Fork, and Maybird Gulch, which are southern tributaries of Little Cottonwood Canyon. Road distance from the center of Salt Lake City is about 25 miles, and the nearest railroad is in Salt Lake Valley, 9 miles from the area. The Park City mining district is 10 miles northeast, and the Bingham mining district, in the Oquirrh Mountains, is 20 miles to the west.

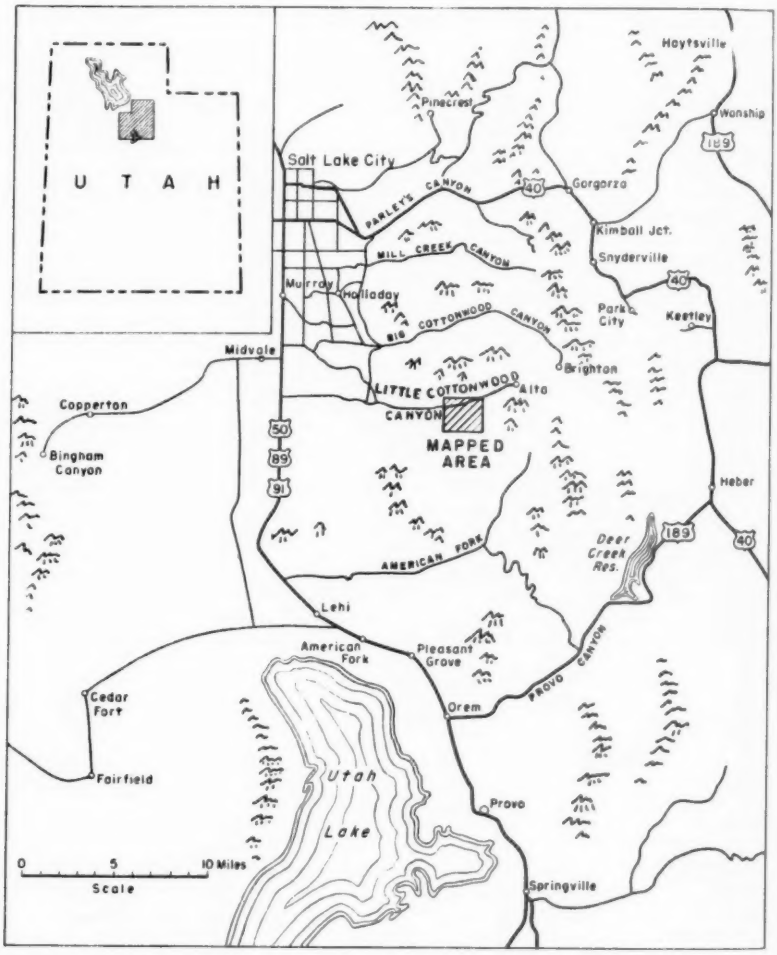

FIGURE 1.—INDEX MAP OF UTAH SHOWING LOCATION OF MAPPED AREA

The elevations in the Little Cottonwood Canyon area range from 7500 to 10,500 feet, and the canyon has been extensively glaciated. Gad Valley, White Pine Fork, Red Pine Fork, and Maybird Gulch are hanging valleys of the main

canyon. Cirques, roches moutonées, and arête ridges are common in the region. Depositional features such as glacial moraines and outwash plains are also conspicuous. Glacial moraines cover most of the tributary valley floors. The main canyon contains moraines on the canyon walls nearly 800 feet above the floor. Extensive talus slopes and alluvium, which represent more recent deposits, together with the earlier glacial deposits, obscure much of the bedrock. About 75 per cent of the surface area is covered with the unconsolidated material. Outcrop areas are shown on the map (Pl. 1.) by toned patterns, and the debris-covered areas by clear patterns.

The climate is somewhat similar to that of Alta, which is now a ski resort. Snow can be expected as early as October and as late as May. Maximum depth of snow, usually reached during April, is about 100 inches. The area contains conifers and aspen in ample quantity for mining operations.

The Little Cottonwood quartz monzonite has been described by Emmons (*in* King, 1878), Giekie (1880), Emmons (1903), Blackwelder (1910), Boutwell (1912), Butler and Loughlin (1915), Butler (1920), Calkins and Butler (1943), and others. Emmons dealt mostly with stratigraphy and the preparation of broad regional geologic maps; he classified the Little Cottonwood quartz monzonite as a Precambrian metamorphic rock. Boutwell (1912), however, found that this and other granitic rocks in the region were intrusive. Emmons (1903) acknowledged that his previous view had been a mistake. Calkins and Butler (1943), in the most comprehensive publication on the area, described the mass in some detail and showed that it contains rocks of several different facies.

History and Ore Production

A mineralized area within the Little Cottonwood intrusive mass attracted the attention of prospectors many years ago and contains a good many old prospect pits and small workings, but no evidence of any recent operations. Production records are not available, but ore was shipped from at least one small high-grade pocket of molybdenite, in the Gladstone mine near the mouth of Gad Valley Gulch. Farther south in Gad Valley, on the fringes of the mineralized area, a little lead and zinc ore can be found on old dumps and in small openings, but these workings cannot have yielded substantial production.

Field and Laboratory Work

A rapid reconnaissance of the area was made in September 1952. Field work was resumed from June to October 1953. Mapping was done with the aid of aerial photographs on a scale of 1/10,000. The information recorded on the photographs was transferred to a modified Soil Conservation Service sheet.

Petrographic studies were made of 54 thin sections from accurately located specimens. The universal stage was used to determine the composition of the plagioclase feldspars, and the Leitz six-spindle integrating stage to measure mineral percentages by the Rosiwal method (Table 1). Orthoclase phenocrysts were etched with hydrofluoric-acid vapor and stained with sodium cobaltinitrite, as suggested by Chayes (1952), to bring out zonal variation in sodium-potassium ratios. Spectrographic analyses were made on minerals separated from a heavy-mineral concentrate of a sample from White Pine Fork, to determine what trace elements they contained. An ultraviolet lamp was first used to examine specimens in the laboratory, but when scheelite was found in many of the specimens a portable lamp was taken into the field, and many observations were made at night to determine distribution and abundance of the mineral.

Acknowledgments

The author is grateful to the University of Utah Research Committee and the Engineering Experiment Station for Research Fellowships granted for this study; to Max P. Erickson for aid and suggestions in the field and laboratory; to Bronson Stringham for aid in the petrographic work and in the preparation of the manuscript; to E. W. Roedder, A. J. Eardley, W. L. Stokes, and S. E. Jerome for valuable criticisms; and to the U. S. Geological Survey for 18 thin sections.

Special thanks are offered to Frank C. Calkins of the U. S. Geological Survey for his suggestions and critical reading of the manuscript for publication.

Geologic Setting

The oldest rocks within the area studied are Precambrian quartzites and argillites, which are exposed on the eastern edge of the area and dip moderately to the east. These form less than 10 per cent of the area, most of which is occupied by what previous authors have called

the Little Cottonwood stock. Since the present study has shown that the eastern part of this mass includes several intrusive bodies, however, it seems more appropriate to call the mass as a whole the Little Cottonwood intrusive complex. The principal rocks in this complex are quartz monzonite, leucocratic quartz monzonite, and alaskite.

A broad arch in the Wasatch Mountains, whose axis trends slightly north of east and plunges about 30° E., is aligned with the Uinta crest. This arch was recognized by Calkins and Butler (1943, p. 3) as an extension of the Uinta arch that contains superimposed complex Laramide and Basin and Range structures. Along the axis of this arch and in line with the Uinta crest are exposed several fairly large intrusive bodies, which are clearly later than the folding and are considered to be of Tertiary age. These are the only large intrusive bodies known in the Wasatch Mountains. The Little Cottonwood igneous complex is the largest and westernmost of these bodies, and Calkins and Butler (1943, p. 34) believe it is the youngest. The Alta stock, a granodiorite with which the ore deposits near Alta are associated, is the central intrusive body. This stock is in contact on the east with the Clayton Peak stock of diorite. Structural evidence along the contact (Calkins and Butler, 1943, p. 35) indicates that the Alta stock is the younger.

TABLE 1.—MODES OF IGNEOUS ROCKS FROM LITTLE COTTONWOOD CANYON, UTAH

	1	2	3	4	5	6	7	8
Quartz	25.1	31.8	44.2	38.1	44.9	10.2	2.0	60.0
Orthoclase	19.4	17.0	17.1	20.2	19.3	....	....	35.0
Plagioclase	42.1	42.3	35.3	40.0	31.4	57.0	60.0	4.0
Biotite	11.8	7.5	3.1	1.5	4.2	18.1	35.0	....
Hornblende	.2	.5	....	....	....	8.5	....	....
Sphene	.9	.6	....	....	....	3.9	....	....
Apatite	.4	.2	.2	.1	.1	.4	1.0	....
Magnetite	.1	.1	.1	.1	.1	1.9	....	.1

1. Little Cottonwood quartz monzonite from top of ridge between White Pine Fork and Gad Valley; mode does not include large orthoclase phenocrysts which make up 5–15 per cent of the rock.

2. Little Cottonwood quartz monzonite from upper White Pine Fork; mode does not include orthoclase phenocrysts, which make up 5–15 per cent of the rock.

3. White Pine leucocratic quartz monzonite from top of ridge between White Pine Fork and Gad Valley; mode does not include orthoclase phenocrysts which make up 10–15 per cent of the rock.

4. White Pine leucocratic quartz monzonite (fine-grained border zone or dike) from upper White Pine Fork; contains almost no large orthoclase phenocrysts.

5. Red Pine alaskite porphyry from middle of Red Pine Fork; mode does not include orthoclase phenocrysts which make up 10–15 per cent of the rock.

6. Little Cottonwood dark inclusions from upper White Pine Fork; mode does not include orthoclase phenocrysts, which make up 3–6 per cent of the rock.

7. Kersantite from lamprophyre dike on ridge between Red Pine Fork and Maybird Gulch (estimated mode).

8. Alaskite aplite dike from White Pine Fork (estimated mode).

All the sedimentary rocks exposed in the mapped area belong to the formation described and referred to as the "Big Cottonwood formation" by Crittenden *et al.* (1952, p. 3), who found that its total thickness is about 16,000 feet.

INTRUSIVE ROCKS

General Statement

By far the most abundant rock is the one here designated as the Little Cottonwood quartz monzonite. A slightly more siliceous rock, here called the White Pine leucocratic quartz monzonite, is exposed in the south-central portion of the mapped area (Pl. 1). It appears to form a cupola intruded into the Little Cottonwood mass and has an oval outcrop about 3 square miles in area, elongated east-west. It is surrounded by the Little Cotton-

wood quartz monzonite. According to Johannsen (1939, p. 155–156), the Little Cottonwood rock would be classified as adamellite and the White Pine rock as leucoadamellite.

Lamprophyre and aplite dikes crosscut both of the major intrusives in a rectangular pattern and generally strike parallel to prominent joint systems. According to Max Crittenden (Personal communication), an aplite dike is cut by a lamprophyre dike on the ridge east of Maybird Gulch.

Small, irregular intrusive bodies with the composition of alaskite are exposed on the ridge east of Red Pine Fork; some samples, however, contain little or no plagioclase and would therefore be classified as kalialaskite (Johannsen, 1939, p. 155). The alaskite and kalialaskite are both porphyritic and are here referred to as the Red Pine alaskite porphyry. On the ridge east of Red Pine Fork, irregular bodies of Red Pine alaskite porphyry contain inclusions of the aplite.

A pebble dike enclosed in the White Pine rock is exposed at stream level in White Pine Fork; it contains pebbles of Little Cottonwood quartz monzonite and of the White Pine leucocratic quartz monzonite.

Little Cottonwood Quartz Monzonite

The Little Cottonwood quartz monzonite constitutes the most extensive igneous body in the central Wasatch Mountains. It is elliptical, elongated east-west, and extends from the mountain front to within a short distance of Alta. The area studied includes an eastern portion of this igneous body. The dominant rock in the Little Cottonwood quartz monzonite (Calkins and Butler, 1943, p. 38) would be classed as adamellite by Johannsen (1939, p. 156). Though its texture is generally granitic, it contains scattered large orthoclase phenocryts that give it a porphyritic appearance. The groundmass has the composition of a granodiorite, but the orthoclase phenocrysts make the orthoclase-plagioclase ratio about 2 to 3.

The fresh unaltered quartz monzonite is light gray, with visible plagioclase, biotite, and quartz and orthoclase phenocrysts about 2–6 cm long which make up about 5–15 per cent of the rock; the average is nearer 5 than 15. Grains of sphene 1–5 mm across can be detected with a hand lens. Only a little hornblende can be observed in the average hand specimen, but zones containing up to 15 per cent hornblende are prominent in the southern part of the mapped area. The Little Cottonwood quartz monzonite contains conspicuous dark rounded inclusions, rather uniformly distributed, which contain biotite, sphene, hornblende, plagioclase, and some orthoclase phenocrysts. The inclusions and the large orthoclase phenocrysts are somewhat more resistant to weathering than the enclosing rock and usually stand out in relief on weathered surfaces. The orthoclase phenocrysts show no conspicuous sodium-rich zones when stained with sodium cobaltinitrite.

The most conspicuous joint system in the Little Cottonwood quartz monzonite trends about N. 60° E. It dips north in the southern part of the mapped area and south in the northern part. Other joint systems trend about N. 85° E. and N. 20° W.; their dips range from vertical to about 50°. The joints are from less than an inch to several feet apart. Veins of introduced material in the joint fissures are generally more resistant to weathering than the quartz monzonite.

Argillite and quartzite inclusions, several inches to several feet across, which display different degrees of assimilation, are common near the eastern contact of the Little Cottonwood quartz monzonite with the sedimentary rocks.

The groundmass of the Little Cottonwood quartz monzonite has a granitic texture and consists of grains 0.5–4 mm in diameter.

The quartz is anhedral and interstitial. Some is in roundish grains up to 4 mm in diameter, some in very irregular grains 0.5–1 mm in diameter. Quartz also appears to have been introduced in small veins. The quartz monzonite contains 25–35 per cent quartz (Table 1). Orthoclase, slightly perthitic, constitutes only about 15–20 per cent of the groundmass, usually in subhedral grains 0.5–1 mm in diameter. The orthoclase phenocrysts show some secondary outgrowth along their borders and generally enclose biotite, quartz, and relict rims of orthoclase.

Plagioclase (An_{30}–An_{32}), generally in euhedral to subhedral grains 0.5–2 mm in diameter, makes up 35–45 per cent of the groundmass.

The most conspicuous ferromagnesian mineral is biotite, in subhedral grains 0.5–3 mm across, which constitutes about 7–13 per cent of the groundmass. Hornblende forms less than 1 per cent of most samples studied. It forms euhedral and subhedral crystals 1–3 mm long.

Sphene is the most prominent accessory mineral and constitutes 0.5–1 per cent of the groundmass of the quartz monzonite. Much of

it is seen in thin sections as euhedral diamond-shaped crystals 0.2–1.5 mm long. Magnetite, which makes up only 0.1 per cent of the rock, occurs as small euhedral crystals generally less than 0.1 mm across. Apatite is about twice as abundant as magnetite; it usually forms hexagonal prisms less than 0.1 mm in diameter. Zircon, in euhedral crystals less than 0.05 mm across, is rather scarce.

Introduced and alteration minerals include hydrothermal sericite, pyrite, and calcite, varying amounts of which can be observed in most thin sections of the quartz monzonite. Sericite constitutes up to 30 per cent of some of the specimens taken from localities where mineralization was rather intense. Pyrite, in euhedral or subhedral cubes 0.5–3 mm across, is usually confined to small veinlets but is also disseminated into the rock a few inches from the veins. Thin stringers of calcite, commonly 0.2 mm wide, have been observed but not in any significant amounts. Chlorite partially or completely replaces the biotite.

Little Cottonwood quartz monzonite on the eastern edge of the mapped area is in contact with argillites and quartzites of the Big Cottonwood series. These beds generally strike north-south, parallel to the intrusive contact, and dip 20°–50°E. In the southeast corner of the area, however, the strike of the bedding turns westward and makes a sharp angle with the contact (Pl. 1). In the eastern part of the area most of the quartz monzonite is in contact with argillite that strikes north. The contact of the argillites and the quartz monzonite is usually sharp, but in some places zones of gradation between the two rocks are as much as 20 feet wide. All observed contacts of intrusive rock with quartzite, on the other hand, are sharp, and the quartzite is not visibly altered at the contact. Megascopically the argillites show very little metamorphic effect at the sharp contacts, but in gradational zones minerals of the intrusive rocks are dispersed in the argillite.

The inclusions in the Little Cottonwood quartz monzonite are of two kinds: inclusions of quartzites and argillites near contacts and dark, rounded inclusions, of igneous texture, scattered throughout the quartz monzonite exposures. Those of the latter kind are generally 5–15 cm in diameter, but a few are as much as 30 cm long. Measured modes of these inclusions are shown in Table 1. Pale-gray orthoclase phenocrysts 0.5–2 cm long, usually visible in the hand specimen, make up 3–6 per cent of the inclusions. Some of the phenocrysts cross the border of the inclusions into the enclosing quartz monzonite. The inclusions are granodiorite according to Johannsen's classification (1939, p. 156), but they are much higher in ferromagnesian and accessory minerals than the typical granodiorite near Alta (Calkins and Butler, 1943, p. 37).

The groundmass of the inclusions is finer-grained than that of the quartz monzonite; its grain size ranges from 0.1 to 2mm, and its texture is lamprophyric. About 10 per cent of it is interstitial quartz, and about 50–60 per cent of it consists of euhedral to subhedral plagioclase (near An_{35}). Abundant biotite (15–20 per cent) and hornblende (6–10 per cent) make the rock dark. Sphene is very conspicuous and makes up about 4 per cent of the groundmass; it usually forms larger and more nearly euhedral grains than it does in the quartz monzonite. Apatite and magnetite are usually more abundant in the inclusions than in the other igneous rocks.

Inclusions within igneous bodies have been studied in many places, and interpretations of their origin have been varied. Balk (1937, p. 12) made the following statement regarding the inclusions in the Sierra Nevada and Coast Ranges and the Idaho and Boulder batholiths:

> "Their origin is controversial; some may represent foreign inclusions, altered to such an extent that their minerals are identical with those of the enclosing igneous rocks, according to Bowen's reaction principle; others may represent accidental accumulations of the normal ferromagnesian minerals in the magma, and they are referred to as segregations or autoliths."

In regard to the inclusions in the Little Cottonwood quartz monzonite, Butler (1920, p. 20) said:

> "Dark inclusions commonly a few inches in diameter, composed of the same minerals as the dominant rock but containing a greater proportion of plagioclase, biotite, hornblende, and accessories, are abundant and conspicuous in the Little Cottonwood stock. They are regarded as representing material which crystallized against the walls of the stock at an early period and was subsequently broken up and scattered through the magma."

The dark inclusions in the Little Cottonwood quartz monzonite probably originated in the manner described by Butler. The uniform textures and sizes of the dark inclusions were probably due to the homogeneous nature of the fine-grained chilled border. The measured modes in Table 1 indicate that the inclusions contain the same minerals as the quartz monzonite but are more basic in composition. Some

argillite and quartzite inclusions surrounded by swarms of dark inclusions show no conspicuous alteration. This fact indicates that the dark inclusions were probably not derived from sedimentary rocks.

The magma from which the Little Cottonwood quartz monzonite was derived was intruded into the Precambrian sediments and partially solidified. The solidified material was then broken up and scattered through the magma in another closely related surge of igneous activity. Stoping was probably a contributing process in the emplacement of the intrusive body, inasmuch as many unoriented xenoliths are enclosed in the quartz monzonite near the sedimentary contacts.

White Pine Leucocratic Quartz Monzonite

The White Pine leucocratic quartz monzonite is exposed in the eastern portion of the Little Cottonwood igneous complex, entirely within the Little Cottonwood quartz monzonite. It is here recognized and described for the first time as a distinct intrusion. It occupies an elliptical area, elongated east and west, that extends about 8000 feet from Red Pine Fork to the west side of Gad Valley. It is about 4500 feet wide in its widest portion, near the middle of White Pine Fork. The White Pine rock would be classified by Johannsen as leucoadamellite. Its texture is granitic, but sparsely scattered large orthoclase phenocrysts give the rock a porphyritic appearance. Plagioclase is more abundant than orthoclase in the groundmass, but the presence of the large orthoclase phenocrysts, generally larger than those in the Little Cottonwood intrusive, makes the total orthoclase content approximately equal to that of the plagioclase.

The White Pine leucocratic quartz monzonite is a light-gray to grayish-brown granitic rock. Large pinkish-brown orthoclase phenocrysts, ranging from 4 to 11 cm across, make up about 10–15 per cent of the rock. In the granitic groundmass, biotite flakes 1–5 mm across are visible but not abundant, rounded grains of quartz up to 8 mm in diameter are very prominent, and plagioclase can be recognized by its white to greenish-white color. Limonite staining, caused by weathering of pyrite, is usually present and makes the White Pine rock difficult to recognize.

Every orthoclase phenocryst from this rock that was stained with sodium cobaltinitrite showed a sodium-bearing zone, up to 1 cm wide, surrounded by a potassic rim about 2 mm wide. The orthoclase phenocrysts of the Little Cottonwood quartz monzonite showed no definite sodium zones.

The White Pine rock differs from the Little Cottonwood rock in that (1) it generally contains less biotite, (2) it contains no inclusions, (3) its orthoclase phenocrysts do not project on weathered surfaces, and (4) its joints are not filled with resistant introduced material that forms raised ridges on weathered surfaces.

Along the southern contact of the White Pine intrusion, a fine-grained granular zone up to 70 feet wide extends east-west for at least a mile. The rock from this zone has an irregular fracture and weathers to a smooth tan surface. A few small flakes of biotite are visible in hand specimens, and some weather out on the surface of the rock, leaving small holes.

Microscopic comparisons indicate that this rock is related to the White Pine rock and is probably a border facies of it (Table 1). It contains no large orthoclase phenocrysts. The fine-grained rock is not present on all contacts, and it may be an acid dike parallel to the southern contact.

The groundmass of the leucocratic quartz monzonite is very similar in microscopic texture to that of the Little Cottonwood quartz monzonite. Its grain sizes range from 1.0 to 8.0 mm. Quartz forms large rounded grains up to 8 mm in diameter and small interstitial anhedral grains about 1.0 mm in diameter. The average specimen of this rock contains 35–45 per cent quartz (Table 1). Subhedral crystals of slightly perthitic orthoclase 0.5–1.5 mm across generally make up 17–21 per cent of the groundmass. The large orthoclase phenocrysts show secondary growth along their borders and make up about 10–15 per cent of the rock. Subhedral plagioclase makes up 35–40 per cent of the groundmass. Its composition ranges from An_{10} to An_{14}, and its grain sizes from 1.0 to 3.1 mm.

The only ferromagnesian mineral in the Pine rock is biotite, in subhedral flakes 1.0–5.0 mm in diameter, which makes up 1–5 per cent of the groundmass.

Apatite, magnetite, and zircon occur as small scarce euhedral and subhedral grains. Sphene, the most conspicuous accessory mineral in the Little Cottonwood quartz monzonite, is not present in this rock.

Hydrothermal pyrite, sericite, and calcite have been introduced into the White Pine rock. Pyrite, in euhedral to subhedral cubes 0.5–3 mm in diameter, is disseminated in the

rock and is also concentrated in small veins. Sericite is present in most samples of this rock and is generally abundant in the plagioclase but scarce in the orthoclase. A few thin stringers of calcite were observed.

The contact of the White Pine leucocratic quartz monzonite with the Little Cottonwood quartz monzonite ranges from "knife edge" to gradational. The width of the gradational zones is difficult to determine, but part of one zone along the north side of the White Pine mass must be hundreds of feet wide (Pl. 1). Sharp contacts are generally limited to the south side of the mass, and the best exposure of the "knife edge" contact is about halfway up the ridge east of Red Pine Fork, about 1¼ miles south of Little Cottonwood Creek. No dikes of White Pine rock in Little Cottonwood quartz monzonite were observed along the contacts, nor any inclusions of quartz monzonite in the White Pine rock.

The writer believes that the White Pine leucocratic quartz monzonite was intruded into the Little Cottonwood quartz monzonite after the solidification of the peripheral shell. The geometric position, shape, and locally sharp but partly gradational contacts of the White Pine intrusion in relation to the Little Cottonwood pluton indicate that it is a younger intrusion and not a true core differentiate of the latter.

Aplite Dikes

The aplite dikes in the mapped area are similar to those described as "alaskite porphyry" by Calkins and Butler (1943, p. 48) in the Cottonwood-American Fork area. Johannsen (1939, p. 155) would term this rock alaskite aplite.

The aplite dikes are found in both the Little Cottonwood and White Pine rocks. Most of them trend northeast, parallel with the major joint systems. Their dips range from vertical to about 70° and in some places do, and in other places do not, coincide with the dips of the major joints. They range in width from a few feet to about 70 feet.

All their observed contacts are very sharp, and most are straight and smooth. Inclusions of country rock were not observed within the dikes or along their contacts.

Two persistent parallel aplite dikes, one about 20 feet wide and the other about 70 feet wide, extend from Maybird Gulch on the west nearly to the mouth of Gad Valley on the east.

The chalky white appearance and somewhat resistant character of these rocks make them easy to recognize in the field. They are very fine-grained and fracture conchoidally. A few small rounded grains of quartz appear dark against the fine-grained white matrix. Very small cubes of pyrite have been observed in some of the specimens, and some of the surface exposures are stained red by the weathering of pyrite.

These rocks consist mainly of grains of quartz and orthoclase 0.05–0.2 mm in diameter. A few larger grains of quartz, orthoclase, and plagioclase (An_{5-10}) up to 1 mm in diameter are scattered throughout the fine-grained groundmass, but they make up only about 2 per cent of the rock. The orthoclase and plagioclase grains are euhedral to subhedral, and most of them contain intergrowths of micropegmatite and myrmekite; most of the quartz grains are rounded and anhedral, and some appear to be fractured. The grains of quartz and orthoclase that make up the groundmass have irregular borders. Very little magnetite is present; the other common accessories are missing. Pyrite occurs in small cubes up to 0.5 mm across. Sericite is scattered throughout the groundmass and enclosed in the larger grains of plagioclase.

The material, rich in potassium and silica, which formed the aplite dikes must have been a late differentiate or residual magma. Some of the larger quartz and plagioclase grains may have begun to crystallize on the walls of the magma chamber at the time of injection and were possibly carried into their present position as solids. The origin of the aplite dikes, together with that of the related Red Pine alaskite porphyry, will be discussed further in the following section.

Red Pine Alaskite Porphyry

The Red Pine alaskite porphyry forms possibly more than two elongated dikelike intrusive bodies between Red Pine Fork and White Pine Fork and about 2 miles south of Little Cottonwood Creek (Pl. 1). Most of the samples contain considerable plagioclase; the others, however, are almost devoid of plagioclase and would be classified by Johannsen (1939, p. 155) as kalialaskite. On the top of the ridge between White Pine Fork and Red Pine Fork, the Red Pine alaskite porphyry contains inclusions of the aplite dike rock. The areal extent of this rock is not known, but the largest body probably extends at least to Red Pine and White Pine creeks, east and west of the ridge, and

at least one small irregular mass of the same material may exist under talus about 300 feet farther south on the east slope of White Pine Fork. All the contacts are obscured by talus, slope wash, and alteration.

Unweathered samples of the Red Pine porphyry were obtained from an old mine dump in Red Pine Fork. Surface exposures are stained red to brown by the weathering of introduced pyrite. The fresh fracture is irregular, and the groundmass of the rock is light gray to white. Orthoclase phenocrysts, mostly pink and 0.5–3.0 cm long, make up 10–15 per cent of the rock. Tests with sodium cobaltinitrite indicated that these phenocrysts have a sodic rim about 1 mm thick. This zoning does not resemble that in the orthoclase phenocrysts of either the White Pine or the Little Cottonwood rocks. Round grains of quartz 0.2–0.5 cm in diameter appear dark gray against the light-colored groundmass. Plagioclase and dark minerals are not visible in the hand specimens. Cubes of introduced pyrite up to 1 cm across are rather uniformly disseminated throughout the rock. The Red Pine porphyry is not conspicuously jointed and contains no dark inclusions.

Under the microscope this rock is strikingly porphyritic. Its composition (Table 1) is that of an alaskite. Most of the groundmass consists of quartz and orthoclase, in rounded and irregular grains 0.01–0.11 mm in diameter. Scattered throughout the groundmass are large rounded grains of quartz (2.0–5.0 mm), subhedral grains of plagioclase (1.0–2.0 mm), and euhedral phenocrysts of orthoclase (5.0 mm–3 cm). Some of the quartz phenocrysts are embayed by resorption. The phenocrysts of orthoclase and quartz usually show a secondary growth into the groundmass along their borders, but those of plagioclase do not. Plagioclase phenocrysts (An_{05}–An_{10}) are nearly as abundant as orthoclase phenocrysts in some samples but almost absent in others. Subhedral flakes of white mica 0.2–0.6 mm in diameter, which make up about 3 per cent of the rock, were probably formed by bleaching of biotite. This is the only indication that any ferromagnesian mineral was originally present.

The rock contains euhedral grains of apatite 0.1–0.4 mm long—much larger than those in the other rock types. Magnetite and zircon are present in some thin sections but are very scarce, and no sphene was found.

The most conspicuous introduced mineral is pyrite, which forms imperfect cubes up to 1 cm in diameter that make up about 2 per cent of the rock. Other minerals, such as quartz, plagioclase, and muscovite, are generally included within the grain borders. Calcite is conspicuous in some specimens. Sericite in flakes 0.1–1.0 mm in diameter is prominent in all specimens, particularly in the groundmass and in the plagioclase phenocrysts. Some thin sections of samples from Red Pine Fork contain fluorite.

Most of the contacts of the Red Pine alaskite porphyry with the Little Cottonwood and White Pine quartz monzonites are obscured by talus and glacial debris, and the surface staining due to the weathering of pyrite makes them hard to locate even in good outcrops. In an outcrop on top of the ridge between Red Pine Fork and White Pine Fork the Red Pine alaskite porphyry contains several inclusions of shattered aplite.

The origin of the Red Pine alaskite porphyry is probably similar to that of the aplite dikes. Under the microscope the groundmass appears almost identical with that of the aplite. The grain size is similar (.01–.1 mm), and each consists mainly of rounded and irregular grains of quartz and orthoclase. The rocks differ in that phenocrysts of quartz, orthoclase, and plagioclase are prominent in the Red Pine rock, but the aplite dikes also contain phenocrysts of plagioclase, orthoclase, and quartz, although they are very scarce and small.

The following theory of origin is proposed for both the aplite dikes and the Red Pine alaskite porphyry. When the late magma, rich in silica and potassium, that was to form these rocks was intruded, some of the partially crystallized material from the walls of the chamber was torn off and carried in the solid state to its present position before the matrix solidified. Since the Red Pine porphyry was intruded later than the aplite dikes, more of this solid material would have been available for it than for the dikes. This fact could also account for the great difference in the amount of plagioclase present in different specimens of the Red Pine rock. In thin section, the large grains of quartz and the orthoclase phenocrysts show secondary growth into the groundmass, but the plagioclase does not. The orthoclase and quartz fragments were similar in composition to the enclosing material and apparently acted as nuclei for the orientation of the adjacent grains of granular quartz and orthoclase that had solidified already in the groundmass. The plagioclase, which had crystallized earlier was more basic than any

constituents in the groundmass and therefore remained unchanged at its borders. Resorption embayments and veins filled with the granular groundmass, in the large quartz grains, indicate that the large grains may have grown before the intrusion.

Lamprophyre Dikes

The term "lamprophyre" is used here as a group name for various dark dike rocks that correspond to Bowen's definition (1928, p. 259):

> "The general character of the group is a richness in ferromagnesian constituents combined with a richness in alkalies, which combination of characters is indeed rather distinctive of lamprophyres in general."

The lamprophyres described here are classified as kersantites, for their essential minerals are biotite and sodic plagioclase. They form dikes ranging in width from a few feet to about 50 feet. One persistent dike, about 50 feet wide, trending slightly west of north and dipping about 30° W., extends southward from Little Cottonwood Creek for about 4000 feet (Pl. 1). Its northern end forms the ridge top between Maybird Gulch and Red Pine Fork. Another dike of the same trend was observed in middle and upper Maybird Gulch.

Observed contacts of the lamprophyre dikes are very sharp and generally smooth. Many inclusions (up to 4 feet in diameter) of the invaded rock are present along the contacts.

The lamprophyre dikes in the area have rounded outcrops and a rusty appearance, apparently because of limonite. On fresh fractures the rock is purplish brown. It contains numerous flakes of black biotite, which are aligned near the contacts and parallel to them.

The lamprophyre is seen in thin section to be somewhat porphyritic and has euhedral crystals of biotite in a groundmass of plagioclase (An_{10}) and accessories. Plagioclase makes up 60–75 per cent of the rock. Its grain boundaries are very difficult to determine because of limonite staining. Undulatory extinction in the plagioclase is common and probably resulted from strain after the material solidified. Euhedral crystals of pale-brown biotite 0.1–1 mm in diameter make up 25–40 per cent of the rock. Euhedral grains of apatite 0.1–0.3 mm long make up about 1 per cent of the rock. Quartz in interstitial grains 0.1–0.5 mm in diameter usually makes up slightly more than 1 per cent of the rock.

Limonite staining is very marked and may obscure other minerals, such as magnetite and zircon.

Pebble Dike

A pebble dike was observed at stream level in White Pine Fork about 1½ miles south of its junction with Little Cottonwood Creek, but its only exposure is only a few feet in length and depth and about 1½ feet wide. The dike pinches out upward in the exposed outcrop. It is almost vertical and appears to strike about east-west; it is surrounded by White Pine rocks. Contacts of the dike with the wall rock are sharp and straight. A substantial amount of float from the pebble dike was found near by, and much of the interpretation below was based on rock that was not in place.

The matrix of the pebble dike is fine-grained and brownish green. The pebbles are rounded to subrounded and up to 15 cm in diameter. Most of the larger pebbles appear to consist of Little Cottonwood quartz monzonite and White Pine leucocratic quartz monzonite, but many small ones are quartz. The rock as a whole has an irregular fracture; it tends to break around the larger pebbles and through some of the brittle quartz pebbles. The presence of pebbles of the Little Cottonwood quartz monzonite in the dike, which is surrounded by the White Pine intrusive rock, indicates that, if the material came from below, the White Pine intrusive body plunges north.

The matrix of the pebble dike consists mainly of fragments of quartz, sodic plagioclase, orthoclase, sericite, and pyrite oriented at random. Some of the sericite and pyrite appears to have formed after the emplacement of the dike. Quartz makes up about 50–60 per cent of the matrix. The quartz fragments have angular to irregular borders and are 0.01 mm–1 cm in diameter. The plagioclase and orthoclase grains are generally subhedral and range from 0.1 to 1 mm. Plagioclase makes up 15–20 per cent of the matrix, and orthoclase 10–12 per cent. Secondary sericite, in euhedral and subhedral flakes 0.01–0.2 mm across, makes up 5–20 per cent. Pyrite forms cubes and subhedral grains 0.05–0.2 mm in diameter. Limonite staining, caused by alteration of pyrite, is conspicuous.

The exposure of the pebble dike is so small that it affords little evidence regarding its origin. Farmin (1934, p. 370) described the pebble dikes at Tintic, Utah, where more data were available. He believes that some of the pebbles were transported from a source more than 6000 feet deep. He referred to the transporting medium as a fluid rather than a liquid or gas, because, under the wide range of pres-

sures involved, it might be a liquid in some places and a gas in others.

The pebble-dike material on White Pine Creek probably moved upward from a deep source. It was intruded later than the first stage of mineralization and earlier than the second.

TABLE 2.—CHARACTERISTICS OF IGNEOUS ROCKS FROM LITTLE COTTONWOOD CANYON, UTAH

Name	Classification	Age	Texture	Essential minerals	Weathering forms	Distinctive features
Lamprophyre	Kersantite	Youngest	Lamprophyric	Plagioclase (An_{10}) Biotite	Rounded	Rusty brown; inclusions of wallrock; irregular fracture, lamprophyric texture; no orthoclase
Red Pine	Alaskite		Porphyritic with aplitic groundmass	Quartz Orthoclase Plagioclase (An_{5-10})	Rounded	Light gray; irregular fracture
Aplite	Alaskite		Aplitic	Quartz Orthoclase Plagioclase (An_{5-10})	Angular Blocky	Chalky white; conchoidal fracture; no inclusions of wallrock; lithoidal texture
White Pine	Leucocratic quartz monzonite		Porphyritic with granitic groundmass	Quartz Orthoclase Plagioclase (An_{10-11}) Biotite	Orthoclase phenocrysts weather the same as groundmass	No inclusions; light gray; irregular fracture; less than 5 per cent dark minerals; limonite staining general
Little Cottonwood	Quartz monzonite	Oldest	Porphyritic with granitic groundmass	Quartz Orthoclase Plagioclase (An_{30-32}) Biotite	Orthoclase phenocrysts and dark inclusions more resistant than groundmass	Dark inclusions abundant; gray; irregular fracture; more than 5 per cent dark minerals; limonite staining local

Sequence of Intrusions

In the regional picture, the Clayton Peak stock of diorite was intruded first, then the Alta stock of granodiorite, and then the Little Cottonwood stock of quartz monzonite—the least silicic first and the most silicic last (Calkins and Butler, 1943, p. 34). In the area described here the least silicic of the granular rocks, the Little Cottonwood quartz monzonite was intruded first, then the White Pine quartz monzonite, then the small aplite dikes and bodies of Red Pine alaskite porphyry, and finally the lamprophyre dikes.

The approximate modes and some other characteristics of the intrusive rocks in the mapped area are shown in Tables 1 and 2.

STRUCTURAL ZONES

General Statement

Three structural zones are defined by the degree of fracturing of the rocks: (1) a central

it is seen in thin sections as euhedral diamond-shaped crystals 0.2–1.5 mm long. Magnetite, which makes up only 0.1 per cent of the rock, occurs as small euhedral crystals generally less than 0.1 mm across. Apatite is about twice as abundant as magnetite; it usually forms hexagonal prisms less than 0.1 mm in diameter. Zircon, in euhedral crystals less than 0.05 mm across, is rather scarce.

Introduced and alteration minerals include hydrothermal sericite, pyrite, and calcite, varying amounts of which can be observed in most thin sections of the quartz monzonite. Sericite constitutes up to 30 per cent of some of the specimens taken from localities where mineralization was rather intense. Pyrite, in euhedral or subhedral cubes 0.5–3 mm across, is usually confined to small veinlets but is also disseminated into the rock a few inches from the veins. Thin stringers of calcite, commonly 0.2 mm wide, have been observed but not in any significant amounts. Chlorite partially or completely replaces the biotite.

Little Cottonwood quartz monzonite on the eastern edge of the mapped area is in contact with argillites and quartzites of the Big Cottonwood series. These beds generally strike north-south, parallel to the intrusive contact, and dip 20°–50°E. In the southeast corner of the area, however, the strike of the bedding turns westward and makes a sharp angle with the contact (Pl. 1). In the eastern part of the area most of the quartz monzonite is in contact with argillite that strikes north. The contact of the argillites and the quartz monzonite is usually sharp, but in some places zones of gradation between the two rocks are as much as 20 feet wide. All observed contacts of intrusive rock with quartzite, on the other hand, are sharp, and the quartzite is not visibly altered at the contact. Megascopically the argillites show very little metamorphic effect at the sharp contacts, but in gradational zones minerals of the intrusive rocks are dispersed in the argillite.

The inclusions in the Little Cottonwood quartz monzonite are of two kinds: inclusions of quartzites and argillites near contacts and dark, rounded inclusions, of igneous texture, scattered throughout the quartz monzonite exposures. Those of the latter kind are generally 5–15 cm in diameter, but a few are as much as 30 cm long. Measured modes of these inclusions are shown in Table 1. Pale-gray orthoclase phenocrysts 0.5–2 cm long, usually visible in the hand specimen, make up 3–6 per cent of the inclusions. Some of the phenocrysts cross the border of the inclusions into the enclosing quartz monzonite. The inclusions are granodiorite according to Johannsen's classification (1939, p. 156), but they are much higher in ferromagnesian and accessory minerals than the typical granodiorite near Alta (Calkins and Butler, 1943, p. 37).

The groundmass of the inclusions is finer-grained than that of the quartz monzonite; its grain size ranges from 0.1 to 2mm, and its texture is lamprophyric. About 10 per cent of it is interstitial quartz, and about 50–60 per cent of it consists of euhedral to subhedral plagioclase (near An_{35}). Abundant biotite (15–20 per cent) and hornblende (6–10 per cent) make the rock dark. Sphene is very conspicuous and makes up about 4 per cent of the groundmass; it usually forms larger and more nearly euhedral grains than it does in the quartz monzonite. Apatite and magnetite are usually more abundant in the inclusions than in the other igneous rocks.

Inclusions within igneous bodies have been studied in many places, and interpretations of their origin have been varied. Balk (1937, p. 12) made the following statement regarding the inclusions in the Sierra Nevada and Coast Ranges and the Idaho and Boulder batholiths:

> "Their origin is controversial; some may represent foreign inclusions, altered to such an extent that their minerals are identical with those of the enclosing igneous rocks, according to Bowen's reaction principle; others may represent accidental accumulations of the normal ferromagnesian minerals in the magma, and they are referred to as segregations or autoliths."

In regard to the inclusions in the Little Cottonwood quartz monzonite, Butler (1920, p. 20) said:

> "Dark inclusions commonly a few inches in diameter, composed of the same minerals as the dominant rock but containing a greater proportion of plagioclase, biotite, hornblende, and accessories, are abundant and conspicuous in the Little Cottonwood stock. They are regarded as representing material which crystallized against the walls of the stock at an early period and was subsequently broken up and scattered through the magma."

The dark inclusions in the Little Cottonwood quartz monzonite probably originated in the manner described by Butler. The uniform textures and sizes of the dark inclusions were probably due to the homogeneous nature of the fine-grained chilled border. The measured modes in Table 1 indicate that the inclusions contain the same minerals as the quartz monzonite but are more basic in composition. Some

argillite and quartzite inclusions surrounded by swarms of dark inclusions show no conspicuous alteration. This fact indicates that the dark inclusions were probably not derived from sedimentary rocks.

The magma from which the Little Cottonwood quartz monzonite was derived was intruded into the Precambrian sediments and partially solidified. The solidified material was then broken up and scattered through the magma in another closely related surge of igneous activity. Stoping was probably a contributing process in the emplacement of the intrusive body, inasmuch as many unoriented xenoliths are enclosed in the quartz monzonite near the sedimentary contacts.

White Pine Leucocratic Quartz Monzonite

The White Pine leucocratic quartz monzonite is exposed in the eastern portion of the Little Cottonwood igneous complex, entirely within the Little Cottonwood quartz monzonite. It is here recognized and described for the first time as a distinct intrusion. It occupies an elliptical area, elongated east and west, that extends about 8000 feet from Red Pine Fork to the west side of Gad Valley. It is about 4500 feet wide in its widest portion, near the middle of White Pine Fork. The White Pine rock would be classified by Johannsen as leucoadamellite. Its texture is granitic, but sparsely scattered large orthoclase phenocrysts give the rock a porphyritic appearance. Plagioclase is more abundant than orthoclase in the groundmass, but the presence of the large orthoclase phenocrysts, generally larger than those in the Little Cottonwood intrusive, makes the total orthoclase content approximately equal to that of the plagioclase.

The White Pine leucocratic quartz monzonite is a light-gray to grayish-brown granitic rock. Large pinkish-brown orthoclase phenocrysts, ranging from 4 to 11 cm across, make up about 10–15 per cent of the rock. In the granitic groundmass, biotite flakes 1–5 mm across are visible but not abundant, rounded grains of quartz up to 8 mm in diameter are very prominent, and plagioclase can be recognized by its white to greenish-white color. Limonite staining, caused by weathering of pyrite, is usually present and makes the White Pine rock difficult to recognize.

Every orthoclase phenocryst from this rock that was stained with sodium cobaltinitrite showed a sodium-bearing zone, up to 1 cm wide, surrounded by a potassic rim about 2 mm wide. The orthoclase phenocrysts of the Little Cottonwood quartz monzonite showed no definite sodium zones.

The White Pine rock differs from the Little Cottonwood rock in that (1) it generally contains less biotite, (2) it contains no inclusions, (3) its orthoclase phenocrysts do not project on weathered surfaces, and (4) its joints are not filled with resistant introduced material that forms raised ridges on weathered surfaces.

Along the southern contact of the White Pine intrusion, a fine-grained granular zone up to 70 feet wide extends east-west for at least a mile. The rock from this zone has an irregular fracture and weathers to a smooth tan surface. A few small flakes of biotite are visible in hand specimens, and some weather out on the surface of the rock, leaving small holes.

Microscopic comparisons indicate that this rock is related to the White Pine rock and is probably a border facies of it (Table 1). It contains no large orthoclase phenocrysts. The fine-grained rock is not present on all contacts, and it may be an acid dike parallel to the southern contact.

The groundmass of the leucocratic quartz monzonite is very similar in microscopic texture to that of the Little Cottonwood quartz monzonite. Its grain sizes range from 1.0 to 8.0 mm. Quartz forms large rounded grains up to 8 mm in diameter and small interstitial anhedral grains about 1.0 mm in diameter. The average specimen of this rock contains 35–45 per cent quartz (Table 1). Subhedral crystals of slightly perthitic orthoclase 0.5–1.5 mm across generally make up 17–21 per cent of the groundmass. The large orthoclase phenocrysts show secondary growth along their borders and make up about 10–15 per cent of the rock. Subhedral plagioclase makes up 35–40 per cent of the groundmass. Its composition ranges from An_{10} to An_{14}, and its grain sizes from 1.0 to 3.1 mm.

The only ferromagnesian mineral in the Pine rock is biotite, in subhedral flakes 1.0–5.0 mm in diameter, which makes up 1–5 per cent of the groundmass.

Apatite, magnetite, and zircon occur as small scarce euhedral and subhedral grains. Sphene, the most conspicuous accessory mineral in the Little Cottonwood quartz monzonite, is not present in this rock.

Hydrothermal pyrite, sericite, and calcite have been introduced into the White Pine rock. Pyrite, in euhedral to subhedral cubes 0.5–3 mm in diameter, is disseminated in the

rock and is also concentrated in small veins. Sericite is present in most samples of this rock and is generally abundant in the plagioclase but scarce in the orthoclase. A few thin stringers of calcite were observed.

The contact of the White Pine leucocratic quartz monzonite with the Little Cottonwood quartz monzonite ranges from "knife edge" to gradational. The width of the gradational zones is difficult to determine, but part of one zone along the north side of the White Pine mass must be hundreds of feet wide (Pl. 1). Sharp contacts are generally limited to the south side of the mass, and the best exposure of the "knife edge" contact is about halfway up the ridge east of Red Pine Fork, about 1¼ miles south of Little Cottonwood Creek. No dikes of White Pine rock in Little Cottonwood quartz monzonite were observed along the contacts, nor any inclusions of quartz monzonite in the White Pine rock.

The writer believes that the White Pine leucocratic quartz monzonite was intruded into the Little Cottonwood quartz monzonite after the solidification of the peripheral shell. The geometric position, shape, and locally sharp but partly gradational contacts of the White Pine intrusion in relation to the Little Cottonwood pluton indicate that it is a younger intrusion and not a true core differentiate of the latter.

Aplite Dikes

The aplite dikes in the mapped area are similar to those described as "alaskite porphyry" by Calkins and Butler (1943, p. 48) in the Cottonwood-American Fork area. Johannsen (1939, p. 155) would term this rock alaskite aplite.

The aplite dikes are found in both the Little Cottonwood and White Pine rocks. Most of them trend northeast, parallel with the major joint systems. Their dips range from vertical to about 70° and in some places do, and in other places do not, coincide with the dips of the major joints. They range in width from a few feet to about 70 feet.

All their observed contacts are very sharp, and most are straight and smooth. Inclusions of country rock were not observed within the dikes or along their contacts.

Two persistent parallel aplite dikes, one about 20 feet wide and the other about 70 feet wide, extend from Maybird Gulch on the west nearly to the mouth of Gad Valley on the east.

The chalky white appearance and somewhat resistant character of these rocks make them easy to recognize in the field. They are very fine-grained and fracture conchoidally. A few small rounded grains of quartz appear dark against the fine-grained white matrix. Very small cubes of pyrite have been observed in some of the specimens, and some of the surface exposures are stained red by the weathering of pyrite.

These rocks consist mainly of grains of quartz and orthoclase 0.05–0.2 mm in diameter. A few larger grains of quartz, orthoclase, and plagioclase (An_{5-10}) up to 1 mm in diameter are scattered throughout the fine-grained groundmass, but they make up only about 2 per cent of the rock. The orthoclase and plagioclase grains are euhedral to subhedral, and most of them contain intergrowths of micropegmatite and myrmekite; most of the quartz grains are rounded and anhedral, and some appear to be fractured. The grains of quartz and orthoclase that make up the groundmass have irregular borders. Very little magnetite is present; the other common accessories are missing. Pyrite occurs in small cubes up to 0.5 mm across. Sericite is scattered throughout the groundmass and enclosed in the larger grains of plagioclase.

The material, rich in potassium and silica, which formed the aplite dikes must have been a late differentiate or residual magma. Some of the larger quartz and plagioclase grains may have begun to crystallize on the walls of the magma chamber at the time of injection and were possibly carried into their present position as solids. The origin of the aplite dikes, together with that of the related Red Pine alaskite porphyry, will be discussed further in the following section.

Red Pine Alaskite Porphyry

The Red Pine alaskite porphyry forms possibly more than two elongated dikelike intrusive bodies between Red Pine Fork and White Pine Fork and about 2 miles south of Little Cottonwood Creek (Pl. 1). Most of the samples contain considerable plagioclase; the others, however, are almost devoid of plagioclase and would be classified by Johannsen (1939, p. 155) as kalialaskite. On the top of the ridge between White Pine Fork and Red Pine Fork, the Red Pine alaskite porphyry contains inclusions of the aplite dike rock. The areal extent of this rock is not known, but the largest body probably extends at least to Red Pine and White Pine creeks, east and west of the ridge, and

at least one small irregular mass of the same material may exist under talus about 300 feet farther south on the east slope of White Pine Fork. All the contacts are obscured by talus, slope wash, and alteration.

Unweathered samples of the Red Pine porphyry were obtained from an old mine dump in Red Pine Fork. Surface exposures are stained red to brown by the weathering of introduced pyrite. The fresh fracture is irregular, and the groundmass of the rock is light gray to white. Orthoclase phenocrysts, mostly pink and 0.5–3.0 cm long, make up 10–15 per cent of the rock. Tests with sodium cobaltinitrite indicated that these phenocrysts have a sodic rim about 1 mm thick. This zoning does not resemble that in the orthoclase phenocrysts of either the White Pine or the Little Cottonwood rocks. Round grains of quartz 0.2–0.5 cm in diameter appear dark gray against the light-colored groundmass. Plagioclase and dark minerals are not visible in the hand specimens. Cubes of introduced pyrite up to 1 cm across are rather uniformly disseminated throughout the rock. The Red Pine porphyry is not conspicuously jointed and contains no dark inclusions.

Under the microscope this rock is strikingly porphyritic. Its composition (Table 1) is that of an alaskite. Most of the groundmass consists of quartz and orthoclase, in rounded and irregular grains 0.01–0.11 mm in diameter. Scattered throughout the groundmass are large rounded grains of quartz (2.0–5.0 mm), subhedral grains of plagioclase (1.0–2.0 mm), and euhedral phenocrysts of orthoclase (5.0 mm–3 cm). Some of the quartz phenocrysts are embayed by resorption. The phenocrysts of orthoclase and quartz usually show a secondary growth into the groundmass along their borders, but those of plagioclase do not. Plagioclase phenocrysts (An_{05}–An_{10}) are nearly as abundant as orthoclase phenocrysts in some samples but almost absent in others. Subhedral flakes of white mica 0.2–0.6 mm in diameter, which make up about 3 per cent of the rock, were probably formed by bleaching of biotite. This is the only indication that any ferromagnesian mineral was originally present.

The rock contains euhedral grains of apatite 0.1–0.4 mm long—much larger than those in the other rock types. Magnetite and zircon are present in some thin sections but are very scarce, and no sphene was found.

The most conspicuous introduced mineral is pyrite, which forms imperfect cubes up to 1 cm in diameter that make up about 2 per cent of the rock. Other minerals, such as quartz, plagioclase, and muscovite, are generally included within the grain borders. Calcite is conspicuous in some specimens. Sericite in flakes 0.1–1.0 mm in diameter is prominent in all specimens, particularly in the groundmass and in the plagioclase phenocrysts. Some thin sections of samples from Red Pine Fork contain fluorite.

Most of the contacts of the Red Pine alaskite porphyry with the Little Cottonwood and White Pine quartz monzonites are obscured by talus and glacial debris, and the surface staining due to the weathering of pyrite makes them hard to locate even in good outcrops. In an outcrop on top of the ridge between Red Pine Fork and White Pine Fork the Red Pine alaskite porphyry contains several inclusions of shattered aplite.

The origin of the Red Pine alaskite porphyry is probably similar to that of the aplite dikes. Under the microscope the groundmass appears almost identical with that of the aplite. The grain size is similar (.01–.1 mm), and each consists mainly of rounded and irregular grains of quartz and orthoclase. The rocks differ in that phenocrysts of quartz, orthoclase, and plagioclase are prominent in the Red Pine rock, but the aplite dikes also contain phenocrysts of plagioclase, orthoclase, and quartz, although they are very scarce and small.

The following theory of origin is proposed for both the aplite dikes and the Red Pine alaskite porphyry. When the late magma, rich in silica and potassium, that was to form these rocks was intruded, some of the partially crystallized material from the walls of the chamber was torn off and carried in the solid state to its present position before the matrix solidified. Since the Red Pine porphyry was intruded later than the aplite dikes, more of this solid material would have been available for it than for the dikes. This fact could also account for the great difference in the amount of plagioclase present in different specimens of the Red Pine rock. In thin section, the large grains of quartz and the orthoclase phenocrysts show secondary growth into the groundmass, but the plagioclase does not. The orthoclase and quartz fragments were similar in composition to the enclosing material and apparently acted as nuclei for the orientation of the adjacent grains of granular quartz and orthoclase that had solidified already in the groundmass. The plagioclase, which had crystallized earlier was more basic than any

constituents in the groundmass and therefore remained unchanged at its borders. Resorption embayments and veins filled with the granular groundmass, in the large quartz grains, indicate that the large grains may have grown before the intrusion.

Lamprophyre Dikes

The term "lamprophyre" is used here as a group name for various dark dike rocks that correspond to Bowen's definition (1928, p. 259):

> "The general character of the group is a richness in ferromagnesian constituents combined with a richness in alkalies, which combination of characters is indeed rather distinctive of lamprophyres in general."

The lamprophyres described here are classified as kersantites, for their essential minerals are biotite and sodic plagioclase. They form dikes ranging in width from a few feet to about 50 feet. One persistent dike, about 50 feet wide, trending slightly west of north and dipping about 30° W., extends southward from Little Cottonwood Creek for about 4000 feet (Pl. 1). Its northern end forms the ridge top between Maybird Gulch and Red Pine Fork. Another dike of the same trend was observed in middle and upper Maybird Gulch.

Observed contacts of the lamprophyre dikes are very sharp and generally smooth. Many inclusions (up to 4 feet in diameter) of the invaded rock are present along the contacts.

The lamprophyre dikes in the area have rounded outcrops and a rusty appearance, apparently because of limonite. On fresh fractures the rock is purplish brown. It contains numerous flakes of black biotite, which are aligned near the contacts and parallel to them.

The lamprophyre is seen in thin section to be somewhat porphyritic and has euhedral crystals of biotite in a groundmass of plagioclase (An_{10}) and accessories. Plagioclase makes up 60–75 per cent of the rock. Its grain boundaries are very difficult to determine because of limonite staining. Undulatory extinction in the plagioclase is common and probably resulted from strain after the material solidified. Euhedral crystals of pale-brown biotite 0.1–1 mm in diameter make up 25–40 per cent of the rock. Euhedral grains of apatite 0.1–0.3 mm long make up about 1 per cent of the rock. Quartz in interstitial grains 0.1–0.5 mm in diameter usually makes up slightly more than 1 per cent of the rock.

Limonite staining is very marked and may obscure other minerals, such as magnetite and zircon.

Pebble Dike

A pebble dike was observed at stream level in White Pine Fork about 1½ miles south of its junction with Little Cottonwood Creek, but its only exposure is only a few feet in length and depth and about 1½ feet wide. The dike pinches out upward in the exposed outcrop. It is almost vertical and appears to strike about east-west; it is surrounded by White Pine rocks. Contacts of the dike with the wall rock are sharp and straight. A substantial amount of float from the pebble dike was found near by, and much of the interpretation below was based on rock that was not in place.

The matrix of the pebble dike is fine-grained and brownish green. The pebbles are rounded to subrounded and up to 15 cm in diameter. Most of the larger pebbles appear to consist of Little Cottonwood quartz monzonite and White Pine leucocratic quartz monzonite, but many small ones are quartz. The rock as a whole has an irregular fracture; it tends to break around the larger pebbles and through some of the brittle quartz pebbles. The presence of pebbles of the Little Cottonwood quartz monzonite in the dike, which is surrounded by the White Pine intrusive rock, indicates that, if the material came from below, the White Pine intrusive body plunges north.

The matrix of the pebble dike consists mainly of fragments of quartz, sodic plagioclase, orthoclase, sericite, and pyrite oriented at random. Some of the sericite and pyrite appears to have formed after the emplacement of the dike. Quartz makes up about 50–60 per cent of the matrix. The quartz fragments have angular to irregular borders and are 0.01 mm–1 cm in diameter. The plagioclase and orthoclase grains are generally subhedral and range from 0.1 to 1 mm. Plagioclase makes up 15–20 per cent of the matrix, and orthoclase 10–12 per cent. Secondary sericite, in euhedral and subhedral flakes 0.01–0.2 mm across, makes up 5–20 per cent. Pyrite forms cubes and subhedral grains 0.05–0.2 mm in diameter. Limonite staining, caused by alteration of pyrite, is conspicuous.

The exposure of the pebble dike is so small that it affords little evidence regarding its origin. Farmin (1934, p. 370) described the pebble dikes at Tintic, Utah, where more data were available. He believes that some of the pebbles were transported from a source more than 6000 feet deep. He referred to the transporting medium as a fluid rather than a liquid or gas, because, under the wide range of pres-

sures involved, it might be a liquid in some places and a gas in others.

The pebble-dike material on White Pine Creek probably moved upward from a deep source. It was intruded later than the first stage of mineralization and earlier than the second.

Table 2.—Characteristics of Igneous Rocks from Little Cottonwood Canyon, Utah

Name	Classification	Age	Texture	Essential minerals	Weathering forms	Distinctive features
Lamprophyre	Kersantite	Youngest	Lamprophyric	Plagioclase (An_{10}) Biotite	Rounded	Rusty brown; inclusions of wallrock; irregular fracture, lamprophyric texture; no orthoclase
Red Pine	Alaskite		Porphyritic with aplitic groundmass	Quartz Orthoclase Plagioclase (An_{5-10})	Rounded	Light gray; irregular fracture
Aplite	Alaskite		Aplitic	Quartz Orthoclase Plagioclase (An_{5-10})	Angular Blocky	Chalky white; conchoidal fracture; no inclusions of wallrock; lithoidal texture
White Pine	Leucocratic quartz monzonite		Porphyritic with granitic groundmass	Quartz Orthoclase Plagioclase (An_{10-14}) Biotite	Orthoclase phenocrysts weather the same as groundmass	No inclusions; light gray; irregular fracture; less than 5 per cent dark minerals; limonite staining general
Little Cottonwood	Quartz monzonite	Oldest	Porphyritic with granitic groundmass	Quartz Orthoclase Plagioclase (An_{30-32}) Biotite	Orthoclase phenocrysts and dark inclusions more resistant than groundmass	Dark inclusions abundant; gray; irregular fracture; more than 5 per cent dark minerals; limonite staining local

Sequence of Intrusions

In the regional picture, the Clayton Peak stock of diorite was intruded first, then the Alta stock of granodiorite, and then the Little Cottonwood stock of quartz monzonite—the least silicic first and the most silicic last (Calkins and Butler, 1943, p. 34). In the area described here the least silicic of the granular rocks, the Little Cottonwood quartz monzonite was intruded first, then the White Pine quartz monzonite, then the small aplite dikes and bodies of Red Pine alaskite porphyry, and finally the lamprophyre dikes.

The approximate modes and some other characteristics of the intrusive rocks in the mapped area are shown in Tables 1 and 2.

Structural Zones

General Statement

Three structural zones are defined by the degree of fracturing of the rocks: (1) a central

breccia zone, surrounded by (2) a stockwork zone, surrounded by (3) a fringe zone whose outer boundary is indefinite (Pl. 1). The breccia and stockwork zones were superimposed on an earlier joint system, which affected all the older igneous rocks and now forms the fringe zone. Surface staining from the weathering of introduced sulfide minerals is much more conspicuous in the breccia and stockwork zones than in the fringe zone.

Breccia Zone

The breccia zone is exposed along the middle part of white Pine Fork, at stream level, and is enclosed within the White Pine leucocratic quartz monzonite. It is roughly oval, about 900 feet east-west by 500 feet north-south. Its peripheral part, 2–20 feet wide, contains angular fragments 1–16 cm in diameter, enclosed in a highly sericitized matrix that contains visible specks of molybdenite. Bull quartz locally surrounds the breccia zone, marking in part its boundary with the stockwork zone.

Stockwork Zone

The stockwork zone differs from the breccia zone mainly in degree of fracturing; the term is used here to indicate a shattered zone interwoven with quartz stringers and veins. Fractures are less numerous in this zone and are oriented at random; they divide the rocks into blocks several centimeters to several meters in diameter. The stockwork zone has an elliptical outcrop elongated east-west. It is about 6600 feet long by 2000 feet wide and extends from Red Pine Fork to the ridge east of White Pine Fork. Its widest part is in White Pine Fork about a mile south of Little Cottonwood Canyon. This zone includes all of the Red Pine alaskite porphyry, most of the White Pine leucocratic quartz monzonite, and a little of the surrounding Little Cottonwood quartz monzonite. Its contact with the surrounding fringe zone is fairly definite on the south, east, and west but is gradational on the north. An area of similarly fractured rocks is exposed on the top of the ridge between Red Pine Fork and Maybird Gulch, along its westward projection. The breccia zone is south of the center of the stockwork zone. Mineralization appears to have been concentrated chiefly in the southern parts of the breccia and stockwork zones. Judging from the relations of the contacts to the topography, the breccia and stockwork zones appear to dip northward like the White Pine mass.

Fringe Zone

The fringe zone consists merely of rocks that are more closely jointed than those that surround it. The joints within this zone have the same trends as those that traverse the entire intrusive complex and probably follow planes of weakness that existed before the formation of the breccia and stockwork zones.

Mineralization

General Statement

Mineralization in the area occurred in three stages. During stage I, scheelite, pyrite, and sericite were deposited in fissures in the Little Cottonwood and White Pine intrusive rocks. During stage II, much quartz, pyrite, molybdenite, sericite, galena, and sphalerite, and a little scheelite and calcite were deposited in the breccia and stockwork zones and also in widespread quartz veins. During stage III, fluorite-bearing sericite zones were formed in the rocks adjacent to intrusive bodies of Red Pine alaskite porphyry, and a little fluorite was disseminated in the Red Pine rock.

The breccia and stockwork zones probably were formed, and the pebble dike injected, between stage I and stage II, for pebbles in the dike contain stage I minerals on joint surfaces, and the matrix contains pyrite of stage II.

Stage I

Scheelite was deposited on joint surfaces of the Little Cottonwood and White Pine intrusive rocks, mainly in the fringe zone. Scheelite is nowhere disseminated through the body of the rock. Pyrite and sericite are found in all the joints that contain scheelite, but scheelite is not always present in the joints that contain pyrite and sericite. A little quartz occurs on some joint surfaces, but it was probably deposited during the second stage of mineralization. Sericite seems to have been deposited first, pyrite next, and scheelite last. Elsewhere scheelite seldom occurs on the joint surfaces of an intrusive rock; it usually occurs in veins or contact replacement deposits. Scheelite is very widespread, however, in this area; it has been recognized through an area

of more than 6 square miles and a vertical range of more than 3000 feet. Its distribution wherever observed is remarkably uniform, but its extent is not fully known.

Scheelite forms grains 0.01–1 cm in diameter, which constitute as much as 2 per cent of some joint fillings. The fillings are 1–5 mm thick. Scheelite is not found in joints of all systems but usually in those of two or three systems in the same outcrop. The number of joints containing scheelite generally increases inward toward the stockwork zone, but the stockwork zone itself contains little visible scheelite. Where scheelite occurs in an outcrop on joints of several systems, it usually favors one system. In the eastern and western parts of the fringe zone, most of the scheelite is in joints of the dominant system, which trends N. 65° E. Locally, however, in the northern and southern parts of the fringe zone, most of it is in joints that strike N. 20° W.

Stage II

Stage II minerals were deposited principally in the breccia and stockwork zones, which were superimposed on the joint systems of the intrusive rocks. Milky quartz occurs in veinlets 0.5–2 cm wide, which form a criss-cross pattern. Vugs 3–15 cm across that contain milky to clear quartz crystals are scattered throughout the central part of the mapped area. Secondary quartz constitutes 3–7 per cent of the total surface area in the breccia zone and 2–5 per cent in the stockwork zone. Molybdenite and pyrite form disseminated crystals and particles and small stringers and veinlets in the breccia and stockwork zones.

Large quartz veins, 10–100 cm wide, 20 feet to several hundred feet long, and variously oriented, are scattered throughout the breccia, stockwork, and fringe zones. These veins appear to cut the smaller quartz veins in the breccia and stockwork zones, but, since they contain similar minerals, they are believed to have been formed late in stage II. Most of the large quartz veins appear to be in the breccia and stockwork zones, but some are in the fringe zone where they cut the joint systems and scheelite of stage I. High-grade pockets of molybdenite associated with pyrite occur in these veins and have been prospected in a few localities. Galena and sphalerite, as well as pyrite, have been observed in the veins in Gad Valley and other areas in the fringe zone. The large quartz veins were apparently formed at the same time as the molybdenite and pyrite found in the central parts of the area. A temperature-zone boundary has been drawn (Pl. 1) in the northern part of the fringe zone to denote the temperature change from molybdenite to sphalerite and galena in the quartz veins. In general, these veins show a similar sequence of mineralization: they are bordered with sericite, which is succeeded inward by quartz, pyrite, molybdenite (or galena and sphalerite in the lower temperature zone), and a little scheelite and calcite.

Weathering of the minerals of stage II yields the most conspicuous surface staining and alteration in the area. Its common products are limonite, hematite, jarosite, and ferrimolybdite, which stain the outcrops and make the mineralized zones recognizable from a distance.

Stage III

Fluorite, pale yellow to purple, has been observed only in and near the Red Pine alaskite porphyry in the stockwork zone. It is generally associated with sericite in rock not otherwise mineralized Disseminated fluorite in grains 2–10 mm in diameter occurs in some specimens of the Red Pine alaskite porphyry. Massive fluorite occurs in the central parts of sericite zones on the ridge between Red Pine Fork and White Pine Fork just north of the Red Pine exposures. These zones, which consist almost entirely of sericite, cut across joint surfaces containing minerals of stage I and also cut quartz veins of stage II. Sericite zones that do not contain fluorite have also been observed in the area. These zones, whether fluorite-bearing or not, are 10–50 cm wide and a few feet to 50 feet long.

Alteration

Surface weathering is a conspicuous process in the area, and unweathered specimens were obtained mainly from old mine dumps. Hydrothermal alteration of the unweathered specimens is attributed to stage II mineralizing solutions. Albitization of plagioclase, introduction of sericite, and quartz are common features in the rocks of the breccia and stockwork zones. A clay mineral that looked like nontronite in thin section (Bronson Stringham, personal communication), occurred in some of the most highly sericitized rocks. In some specimens of the Little Cottonwood quartz monzonite affected by the mineralization of stage II, pseudomorphs of leucoxene

after euhedral sphene were observed in thin section.

Comparison with Other Districts

The general geology, rock types, zonal arrangements, and mineralogical associations in the area studied are similar to those at Climax, Colorado (Butler and Vanderwilt, 1933, p. 220). The host rock at Climax is mainly quartz monzonite[1] intruded into Precambrian sediments. An intensely fractured and silicified central zone in the quartz monzonite contains molybdenite ore on the fringes and within the silicified central zone. Besides molybdenite, other primary minerals at Climax include hübnerite, quartz, pyrite, sericite, sphalerite, fluorite, and topaz. Primary minerals in the Cottonwood area (Pl. 1) include molybdenite, scheelite, quartz, pyrite, sericite, sphalerite, galena, and fluorite. In the Cottonwood area tungsten occurs in scheelite disseminated on joint surfaces of the intrusive rocks, whereas in the Climax district it occurs in siliceous hübnerite veins. Topaz was not recognized in the Cottonwood area, and galena was not recognized at Climax. Secondary minerals such as jarosite, hematite, limonite, and ferrimolybdite occur in both areas. The area of molybdenite-bearing rocks in the Cottonwood region is somewhat larger than the one at Climax but far less rich at the levels exposed.

In the tungsten deposits of the Kiangsi Province in China (Li and Wang, 1947, p. 24) the main tungsten-bearing mineral is wolframite, generally associated with orthoclase, muscovite, molybdenite, cassiterite, arsenopyrite, pyrite, scheelite, chalcopyrite, galena, bismuthinite, beryl, topaz, fluorite, sericite, and chlorite.

The mineral associations in the Cottonwood area are similar to those of the Climax district, and possibly the Cottonwood area could yield a similar type of production at depth.

Economic Possibilities

The minerals most likely to make this area important economically are the scheelite of stage I and the molybdenite of stage II.

Scheelite occurs on joint surfaces of the intrusive rocks associated with pyrite and sericite. The area covered by this mineralization is possibly greater than 6 square miles, and scheelite-bearing rock is exposed through a vertical range of 3000 feet. A sample taken from a talus slope in White Pine Fork in the fringe zone assayed 0.02 per cent WO_3 which may indicate the order of abundance of tungstic oxide in most of the area. The blue-white fluorescence of the scheelite indicates a low molybdenum content in the scheelite crystal structure. The grade is low, but the tungsten exists in a recoverable form and in great quantity. Using the very questionable figure of 0.02 per cent WO_3 and assuming that ore can be mined to a depth of 1000 feet, 36,000,000 units of tungstic oxide is available per square mile.

Weathering of scheelite has been studied in some detail by past investigators, and its economic implications may be summarized as follows:

Campbell (1920, p. 521) observed that sulfuric acid, resulting from the action of oxygenated water on pyrite, attacks scheelite and forms calcium sulfate, which is soluble in water. This decomposition of scheelite takes place with comparative rapidity along cleavage planes and cracks and results in the formation of tungstic hydrate, which is readily dissolved by alkaline carbonates in ground water; secondary scheelite is probably formed by the action of calcium sulfate on alkaline tungstate in an excess of alkaline carbonate solution.

In regard to the possibility of secondary scheelite enrichment in the Cottonwood area, the view summarized by Gannett (1919, p. 78) must be taken into consideration:

"In some deposits, associated minerals other than those containing tungsten dissolve more readily than tungsten minerals and there is enrichment near the surface by removal of valueless material. Tungsten minerals, nevertheless, dissolve rather rapidly, and form soluble salts or colloidal compounds that may remove the tungsten from the outcrop. The tungsten may be leached from its ore bodies without being redeposited below. The facility with which tungsten compounds in solution will hydrolyze and form insoluble compounds, tends to prevent downward migration of tungsten, and there are probably no extensive zones of tungsten minerals like those of copper and silver, although enrichment by solution and reprecipitation probably does occur to a small extent. Ferric sulphate, which increases the solution of copper and silver, slows down or stops the solution and migration of

[1] Butler and Vanderwilt call this rock granite (p. 208), although they indicate that the rock averages 15 per cent plagioclase and on their table (p. 225) show 22 per cent orthoclase and 23 per cent plagioclase.

tungsten. In general, secondary tungsten ores are hübnerite or wolframite rather than scheelite, although secondary scheelite is not unknown."

Secondary enrichment of tungsten is of little economic importance, as far as is known, but it probably does occur. Since the outcrops are leached by weathering, surface samples are probably somewhat lower in grade than samples below the zone of weathering. If any secondary enrichment of tungsten occurred here, the average grade may be considerably higher than surface samples indicate. In the area studied, large-scale operations would probably be necessary in order to make economic production, and a slight increase in grade may make the project feasible. To determine the average grade of the deposit, a drilling project with drill-hole centers spotted on about a 200-foot grid system over the scheelite-mineralized area and drilled to a depth well below the zone of weathering would be necessary.

Most of the molybdenite is concentrated in the breccia and stockwork zones, in which there is little scheelite. There are few high-grade pockets of molybdenite, but this mineral is visible in much of the rock of the central zones. Assays of three samples from this area (Buranek, 1944, p. 5–6) showed 0.25, 0.66, and 2.4 per cent molybdenite, together with traces of gold, silver, and copper. The breccia zone is about 900 feet long by 500 feet wide, and the elliptical stockwork zone is about 6600 feet long by 2000 feet wide. High-grade molybdenite has been observed in quartz veins in the breccia, stockwork, and fringe zones. The main economic problem in mining the molybdenite on a large scale would be the wide variation in grade; large-scale production will depend upon average grade over an extensive area, which can be determined only by careful random sampling of the breccia and stockwork zones. Weathering has not affected the molybdenite to any great extent; surface stains of ferrimolybdite and jarosite are common but apparently thin. Deep holes should also be drilled north of the breccia zone to determine whether any high-temperature minerals occur there and in what quantity.

The mineralized area in the Little Cottonwood igneous complex may have economic significance at some time in the future. It could become so from: (1) increased industrial need for tungsten and molybdenum because of technological advances; (2) government interest in subsidizing development work in order to have a readily available supply of tungsten; (3) curtailing of foreign supplies of tungsten because of international tensions, emergencies, or war (4) presence of other minerals or trace elements that would add to the value of the deposit, and (5) the presence of high-grade localized ore bodies encountered in exploration drilling or prospecting in the vicinity of the breccia and stockwork zones.

The mineral associations in the area suggest the possibility of discovery of other minerals associated with high-temperature deposits containing such metals as tin, chromium, molybdenum, gold, and tungsten.

Minable scheelite may occur in other intrusive bodies of the Alta and Park City districts, and be discoverable by prospecting with the ultraviolet lamp. These intrusive rocks may also contain other tungsten minerals in small amounts, and sampling and tungsten analyses are recommended on the basis of this study.

References Cited

Balk, Robert, 1937, Structural behavior of igneous rocks: Geol. Soc. America Mem. 5, 177 p.

Blackwelder, Eliot, 1910, New light on the geology of the Wasatch Mountains: Geol. Soc. America Bull., v. 21, p. 517–542

Boutwell, J. M., 1912, Geology and ore deposits of Park City District, Utah: U. S. Geol. Survey Prof. Paper 77, 231 p.

Bowen, N. L., 1928, The evolution of the igneous rocks: Princeton Univ. Press, 332 p.

Buranek, A. M., 1944, The molybdenum deposits of White Pine Canyon near Alta, Salt Lake County, Utah: Utah. Geol. Mineral. Survey Circ. 28, 6 p.

Butler, B. S., 1920, Ore deposits of Utah: U. S. Geol. Survey Prof. Paper 111, 672 p.

Butler, B. S., and Loughlin, G. F., 1915, A reconnaissance of the Cottonwood-American Fork mining district, Utah: U. S. Geol. Survey Bull. 620, p. 165–266

Butler, B. S., and Vanderwilt, J. W., 1933, The Climax molybdenum deposit, Colorado: U. S. Geol. Survey Bull. 846-C, p. 195–237

Calkins, F. C., and Butler, B. S., 1943, Geology and ore deposits of the Cottonwood-American Fork area, Utah: U. S. Geol. Survey Prof. Paper 201, 152 p.

Campbell, J. M., 1920, Tungsten deposits of Burma and their origin: Econ. Geology, v. 15, p. 511–534

Chayes, F., 1952, Notes on the staining of potash feldspars with sodium cobaltinitrite in thin section: Am. Mineralogist, v. 37, p. 337–340

Crittenden, M. D., Sharp, B. J., and Calkins, F. C., 1952, Geology of the Wasatch Mountains east of

Salt Lake City, Parleys Canyon to Traverse Range: Utah Guidebook ser. no. 8, p. 1–37

Emmons, S. F., 1903, The Little Cottonwood granite body of the Wasatch Mountains: Am. Jour. Sci., 4th Ser., v. 16, p. 139–147

Farmin, Rollin, 1934, Pebble dikes and associated mineralization at Tintic, Utah: Econ. Geology, v. 29, p. 356–370

Gannett, R. W., 1919, Experiments relating to the enrichment of tungsten ore: Econ. Geology, v. 14, p. 68–78

Giekie, Archibald, 1880, Archean rocks of the Wasatch Mountains: Am. Jour. Sci., 3d ser., v. 19, p. 363–367

Johannsen, Albert, 1939, A descriptive petrography of igneous rocks: Chicago, Chicago Univ. Press, v. 1, p. 1–318

King, C., 1878, Exploration of the 40th parallel: Systematic Geol., U. S. Geol. Survey Rept., v. 1, 803 p.

Li, K. C., and Wang, C. Y., 1947, Tungsten: 2d ed., Am. Chem. Soc. Mon. 94, Reinhold Publishing Corp., New York, 430 p.

3201 Margie Ave., Salt Lake City, Utah

Manuscript Received by the Secretary of the Society, April 12, 1957

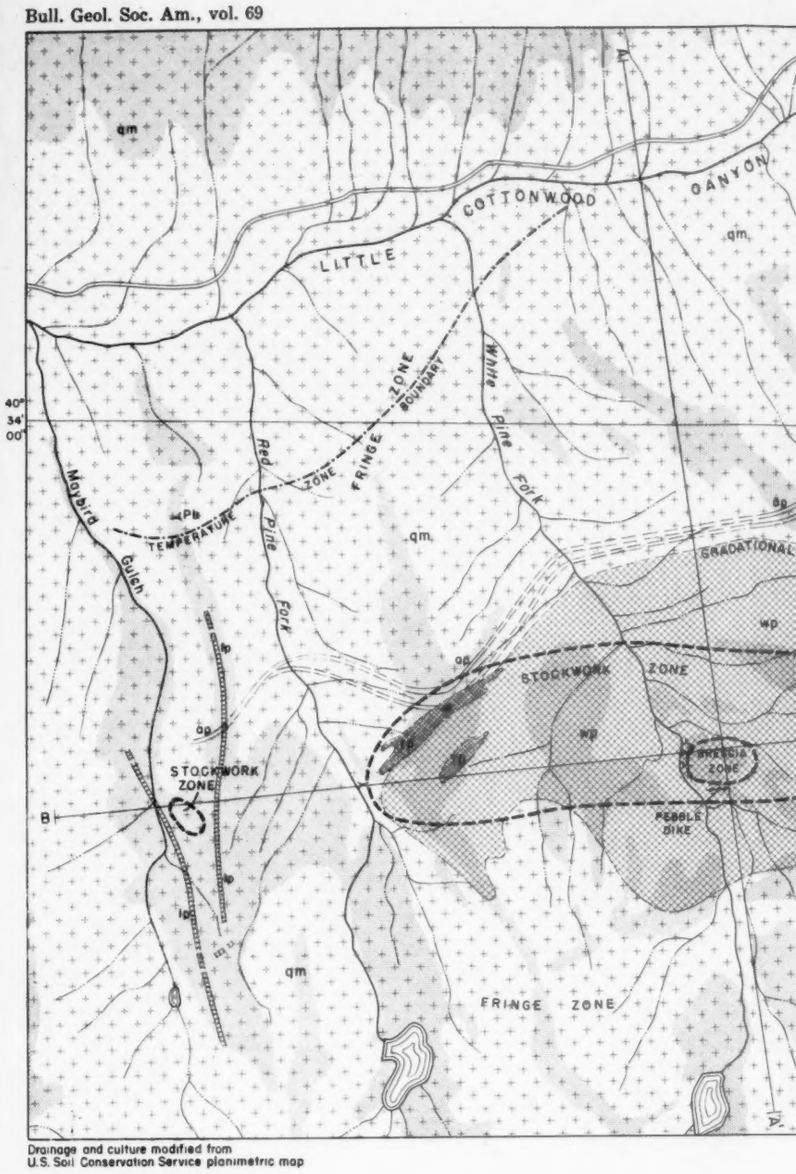

Drainage and culture modified from U.S. Soil Conservation Service planimetric map

1000 0 1000 2000 3000
Scale

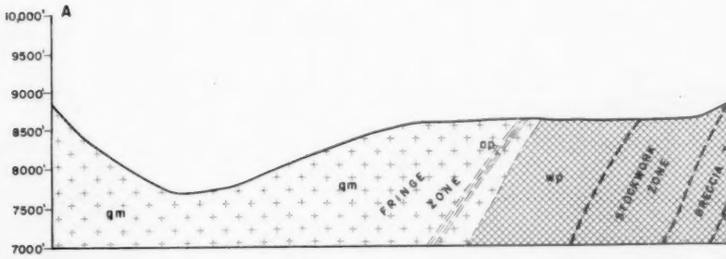

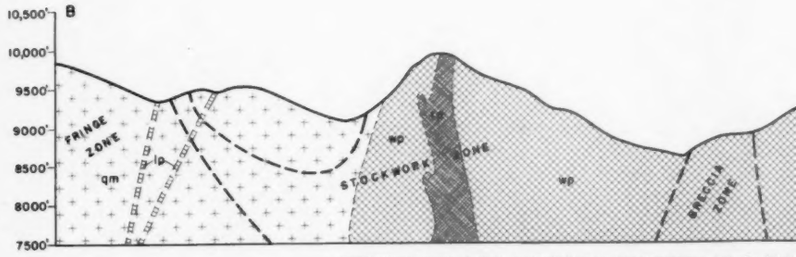

(CONTACTS AND ZONE BOUNDARIES PROJECTED TO PLANE

GEOLOGIC MAP OF A PORTION OF THE LI
IGNEOUS COMPLEX, UTA

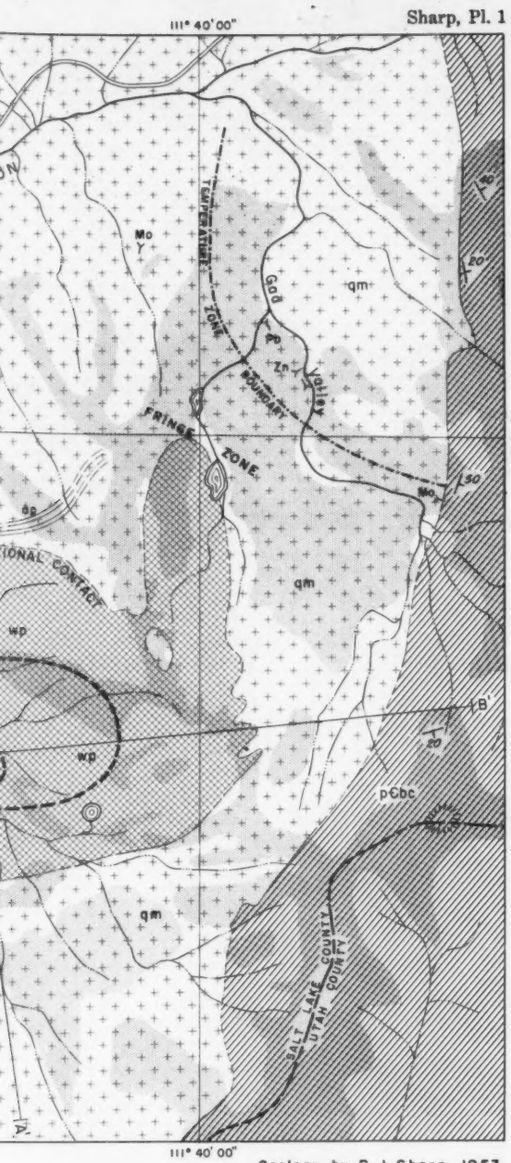

Geology by B. J. Sharp, 1953

EXPLANATION

SEDIMENTARY ROCKS

- pCbc — Big Cottonwood series (PRE-CAMBRIAN)

IGNEOUS ROCKS

- lp — Lamprophyre dikes
- rp, ap — Red Pine alaskite porphyry and aplite dikes
- wp — White Pine leucocratic quartz monzonite
- qm — Little Cottonwood quartz monzonite

(TERTIARY)

Toned pattern represents actual outcrop areas

- Structural zone boundary
- Pb — Mo — Temperature zone boundary
- Observed contact
- Inferred or obscure contact
- 20 — Dip and strike of bedding
- Adits and prospect pits

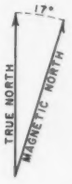

3000 FEET

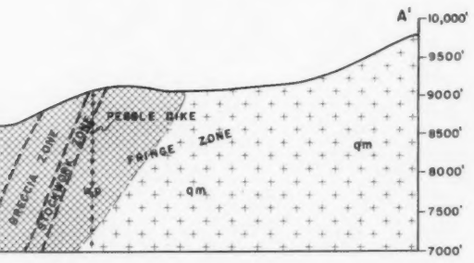

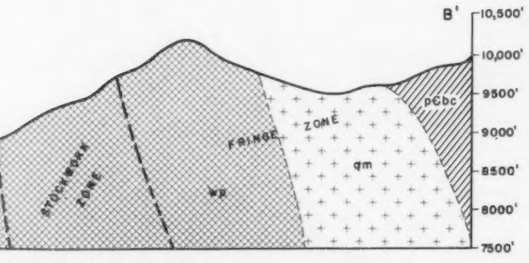

LANE OF CROSS-SECTION)

LITTLE COTTONWOOD
UTAH

BULLETIN OF THE GEOLOGICAL SOCIETY OF AMERICA
VOL 69, PP 1431-1442, 2 FIGS., 2 PLS. NOVEMBER 1958

FAULT PATTERNS IN SOUTHEASTERN ALASKA

BY WILLIAM S. TWENHOFEL AND C. L. SAINSBURY

ABSTRACT

Prominent linear features interpreted as faults were plotted from aerial photographs of southeastern Alaska, and the resultant patterns were analyzed with reference to the literature and to the field relations determined by the writers and other geologists of the U. S. Geological Survey. The faults, as interpreted, seem to belong to a well-defined and widespread system that trends northwesterly and to three ill-defined systems that trend northerly, northeasterly, and easterly respectively. The faults are part of a system of fractures subparalleling the Coast Ranges and the North Pacific coast of British Columbia and Alaska.

Movement on the faults in southeastern Alaska took place during late Mesozoic, Tertiary, and possibly Recent times. A major lineament, the Denali lineament, can be traced for about 1600 miles, from southeastern Alaska northwest along the arcuate Alaskan Range and thence southwest to Bristol Bay.

Most of the hot springs of the area are located on conspicuous faults. Some of the carbonated springs are on linears, but some are not. Sulfur springs seem to be unrelated to linears.

The writers suggest that certain mineral deposits in southeastern Alaska are spatially related to certain faults, particularly those of the northwest-trending system. Data support this thesis for the mineral deposits of the Chichagof-Sitka belt and the Juneau gold belt.

CONTENTS

TEXT

	Page
Introduction	1431
Previous work	1432
Definition of terms	1433
Recognition of linear features	1433
Origin of linear features	1433
Lineaments	1434
Chatham Strait lineament	1434
Clarence Strait lineament	1435
Coast Range lineament	1436
Linears	1436
Northwest-trending linears	1436
Northeast-trending linears	1437
North-trending linears	1437
East-trending linears	1438
Relation of mineral springs to linears	1438
General statement	1438
Hot springs	1439
Carbonated springs	1439
Sulfur springs	1439
Relation of mineral deposits to regional faults	1439
Discussion	1439
Gold deposits of the Chichagof and Sitka belts	1439
Mineral deposits of the Juneau gold belt	1440
Conclusions	1442
References cited	1442

ILLUSTRATIONS

Figure	Page
1. Map of Alaska showing Denali lineament	1432
2. Map showing mineral deposits, linears, and faults, Juneau gold belt	1441

Plate	Facing page
1. Aerial photograph of White Pass and vicinity, Alaska and British Columbia	1434
2. Linear trends in southeastern Alaska	1442

TABLE

Table	Page
1. Mineral springs in southeastern Alaska	1438

INTRODUCTION

We became interested in the fault patterns of southeastern Alaska (Fig. 1) while making a brief study of aerial photographs of an area near Juneau. We realized that linear features, which we interpret as faults or fault zones, are widespread and conspicuous features of the rocks of the Juneau-Skagway area. A subsequent study of aerial photographs indicated that

similar features are widespread throughout southeastern Alaska and adjacent British Columbia. Plate 2 shows the prominent linear features observed on the aerial photographs. This report describes the results of our study.

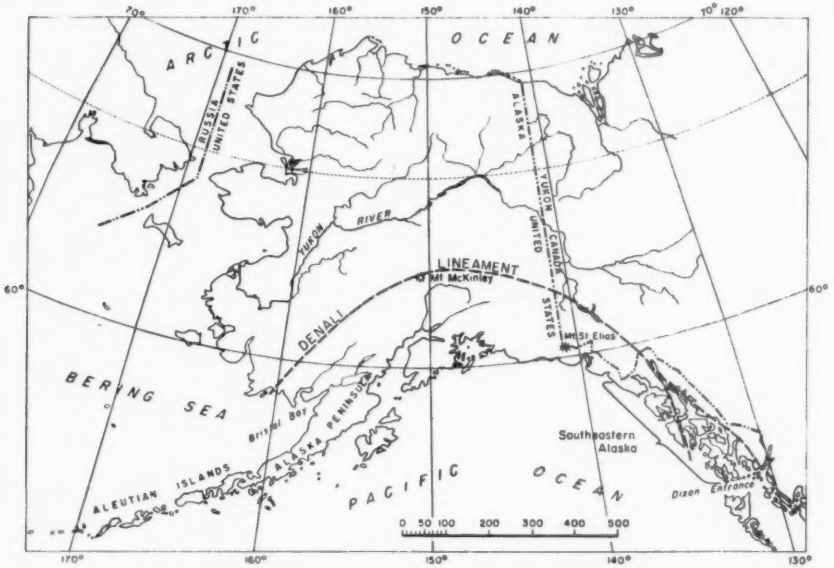

FIGURE 1.—MAP OF ALASKA SHOWING DENALI LINEAMENT

Many unpublished data pertaining to the fault and fracture systems have been gathered by geologists working in Alaska. We are presenting our data with the hope that it will stimulate further interest in the study of this phase of the structure of southeastern Alaska and related regions, and with the hope that several problems of interpretation may be solved in the field.

Much of this report is theoretical and interpretive because of the scarcity of detailed field observations of the faults and related structures and because of the magnitude of the areas involved.

PREVIOUS WORK

Peacock has studied the fiord pattern of the coast of British Columbia and southeastern Alaska by "drawing straight lines in place of all nearly straight fiord reaches, amplified by straight lines representing nearly straight stream valleys, lake shores, and portions of coast" (Peacock, 1935, p 655). As a result of plotting the trends on a map Peacock (1935, p. 656) concluded:

"The fiord pattern of the coastland is, therefore, a complex pattern consisting of a dominant concordant system of longitudinal (concentric) and transverse (radial) lines whose mean trends are N. 50° W. and N: 45° E. respectively, with considerable range due to repeated curving of the pattern in accord with the compound curved plan of the coastland; and a subordinate discordant system which is strongest in the north and weakest in the south, and is composed of lines whose trends differ little from the mean directions: N. 7° W. and N. 84° E."

Peacock ascribes the pattern of the fiords to correspondence with the pattern of folds, joints, and faults in the bedrock, but he confined his studies to the waterways and shore lines.

In their comprehensive report on the geology of southeastern Alaska, Buddington and Chapin (1929, p. 39) noted that faults and fault zones are common in southeastern Alaska; they briefly describe faults observed in the field (Buddington and Chapin, 1929, p. 233–234, 291). However, their geologic maps do not show faults.

Wright and Wright (1908, p. 21) postulated that the position of the Lynn Canal-Chatham

Strait fiord is determined by a fault zone, and Martin and Williams (1924) further elaborated upon this concept. They considered the topographic form of the Lynn Canal-Chatham Strait fiord the result of glacial erosion along a preglacial river whose course was determined by a fault zone.

Reed and Coats (1941) mapped many prominent faults in the Chichagof mining district; they were the first to demonstrate the presence of faults on a large scale in southeastern Alaska.

St. Amand (1957) presented a synthesis of geologic and geophysical data pertaining to the tectonics of Alaska and postulated faults to explain the straight courses of many of the fiords in southeastern Alaska.

Definition of Terms

We use the term linears as originally defined by Wilson (1948, p. 695) to mean "straight or gently curving valleys or scarps, of any origin, conspicuous enough to be seen in air photographs." We use the word lineament in the same sense as used by Wilson (1948, p. 695) to designate a "large zone of many parallel or nearly parallel linears or faults." Nothing in either definition assigns any particular origin to either linears or lineaments.

Recognition of Linear Features

Nearly every aerial photograph of southeastern Alaska reveals linear features: some known from field observations to be bedding and schistosity; others known to be faults, joints, or shear zones; and still others, which have not been observed on the ground, whose cause can only be inferred.

Linear features show up well on aerial photographs of southeastern Alaska for four reasons.

(1) Igneous rocks and well-indurated sedimentary and metamorphic rocks are the dominant bedrocks. Such rocks are very resistant to erosion in contrast to the gouge and sheared rock in fault zones; therefore many linears are the surface expression of fault zones.

(2) Southeastern Alaska was peneplained during Eocene time, uplifted in post-Eocene time, and eroded to a stage of youth prior to Pleistocene glaciation (Spencer, 1903, p. 132). Many of the rejuvenated streams of the uplifted peneplain cut into the softer fault zones and formed many of the larger river valleys. A good example is Lynn Canal-Chatham Strait.

(3) Glaciation, especially the most recent valley glaciation, further deepened and accentuated depressions in gouge and brecciated rock. Where glacier movement paralleled faults and shear zones, depressions were scooped out, and many became lakes and fiords when the ice retreated. Erosion since glaciation has not been sufficient to destroy the lakes, many of which are perched on steep slopes. A notable example is the series of lakes along the linear, known to be a fault, that can be traced for more than 40 miles from the mouth of the Katzehin River on Lynn Canal to the Alaskan border north of Skagway (Pl. 2).

(4) Because of extremely heavy rainfall and steep terrain the streams rapidly erode and incise the faults in the underlying rocks. The resultant alignment of many streams is very noticeable.

Origin of Linear Features

Wilson (1948, p. 699–711) ascribes linear features on aerial photographs to the following seven situations:

(1) Glaciation may produce linear features such as drumlins and glacial grooves.

So far as known the only drumlins in southeastern Alaska are in the valley of the Thorne River on Prince of Wales Island. Glacial grooves have not been recognized on aerial photographs of southeastern Alaska. None of the linears discussed in this report is ascribed to drumlins or glacial grooves.

(2) Many batholiths, stocks, and bosses are foliated, particularly on their borders, and this foliation may appear as a linear feature.

Many of the granitic bodies in southeastern Alaska are gneissic bodies foliated in a northwest direction parallel to the regional structure. Linears of this type generally are relatively short, and we have not shown them on Plate 2.

(3) Dikes, because they generally are straight, well jointed, and are eroded at a rate different from the enclosing rock, may cause prominent linears in many areas.

Linears of this type have been recognized in southeastern Alaska, particularly on the seaward sides of islands exposed to forceful wave erosion, and in areas of massive rocks recently emerged from ice and névé fields. Such dikes generally are not continuous for many miles, and, therefore, few, if any, of the linears shown on Plate 2 are ascribed to erosion along dikes.

(4) Erosion along bedding or geologic contacts may cause linears.

Some of the smaller linears plotted on Plate 2 probably are the result of erosion along bedding and geologic contacts. None of the long and persistent linears is caused by bedding, however, and the linears that cut intrusive rocks cannot be caused by bedding. At a few places, notably at Saginaw Bay on Kuiu Island, and in Kootznahoo Inlet on Admiralty Island, the linears are arranged in a closely spaced parallel system that clearly is caused by bedding. Perhaps a few of the northeast-trending linears on the seaward part of southern Baranof Island are caused by bedding, but we have observed faults in this area that create northeast-trending linears. Many of these linears cross large areas of intrusive rocks and probably are fault-controlled.

(5) Erosion along foliation and schistosity in metamorphic rocks may cause linears.

The strike directions of foliation and schistosity in southeastern Alaska are dominant northwest, and the dips are steep, generally northeasterly. Bedding and foliation generally are parallel, but locally foliation crosscuts bedding. A few of the linears shown on Plate 2 may be caused by foliation or schistosity, but we believe that most of the linears shown are too long and too broad to be related to either foliation or schistosity.

(6) Erosion along joints may produce linears.

In southeastern Alaska joint patterns are easily recognized on aerial photographs in the intrusive rocks above timberline. In other areas the joints are not so apparent, particularly in lowland areas covered by vegetation and muskeg. The linears caused by jointing, however, are too small to be shown on Plate 2, and we are confident that few, if any, of the plotted linears represent joints. Obviously many of the small linears that can be seen in the granitic rocks of Plate 1 are joints, but in our opinion the large linears are faults.

(7) Erosion along faults, fault scarps, and fault-line scarps may create linears easily detected from aerial photographs.

We postulate and assume that the linears shown on Plate 2 are caused principally by erosion along faults. Several facts that give us confidence in postulating a fault origin for the linears are:

(a) The gross pattern of the linears is essentially similar throughout southeastern Alaska. This similarity in pattern can best be ascribed to linears caused by faults.

(b) Most of the plotted linears that have been observed in the field are faults. This suggests that most of the linears plotted on Plate 2 are faults.

(c) Inferences and conclusions (see elsewhere in this report) regarding the origin and age of the inferred faults are compatible with a fault origin.

Lineaments

Chatham Strait Lineament

The Chatham Strait lineament extends from the mouth of Chatham Strait northward beneath Chatham Strait and Lynn Canal to the northern border of southeastern Alaska (Pl. 2). It trends about N. 7° W. and is at least 250 miles long. It is by far the most conspicuous lineament in southeastern Alaska. Early geologists recognized this conspicuous feature, and some postulated an origin by ice erosion along a fault zone (Martin and Williams, 1924). Aerial photographs leave little doubt that this lineament is a fault zone (Pl. 1). Splits from the Chatham Strait lineament apparently controlled erosion that created Chilkoot and White passes, famous from the Klondike gold rush days of 1898.

This lineament is distinctly different from the other major lineaments of southeastern Alaska:

(1) It is especially well developed in the crystalline rocks of the Coast Range batholith which elsewhere are relatively free from linears.

(2) Its trend is transverse to all other major structural trends in southeastern Alaska.

(3) It is a split or extension of the Denali lineament (St. Amand, 1957) that extends northwesterly from Lynn Canal through Canada, then westerly along and parallel to the arcuate front of the Alaska Range in the vicinity of Mt. McKinley, thence southwesterly through the Kuskokwim region into Bristol Bay on the Bering Sea (Dutro and Payne, 1957) (Fig. 1). This great lineament is about 1600 miles long. The Coast Range lineament also

---

Plate 1.—Aerial photograph of White Pass and vicinity, Alaska and British Columbia

The bedrock is part of the Coast Range batholith. Linears appear as topographic depressions aligned in a northerly and northeasterly direction. The White Pass and Yukon Railroad traverses the area from south to north.

AERIAL PHOTOGRAPH OF WHITE PASS AND VICINITY,
ALASKA AND BRITISH COLUMBIA

may be an extension or split from the Denali lineament.

The direction and amount of movement along the Chatham Strait lineament is unknown. Most of the lineament is concealed beneath the waters of Chatham Strait and Lynn Canal, and the rest of the lineament traverses the Coast Range batholith. Throughout most of its length the lineament separates rocks predominantly of Paleozoic age on the west from rocks predominantly of Mesozoic age on the east; this indicates that the west side is upthrown.

In British Columbia and Yukon Territory Bostock (1952, p. 8–9) and Kindle (1949 p. 28) have mapped the Denali lineament, marked by a prominent topographic depression, from the vicinity of Dezadeash Lake northwestward along the front of the Kluane Range to the White River near the 140° meridian. Bostock infers from topographic relations and from the fact that older rocks are on the northeast side and younger rocks are on the southwest side of the fault that the northeast side was uplifted relative to the southwest side. Some evidence, according to Bostock, points to "significant lateral movement."

In the eastern Alaska Range the Denali lineament has been mapped by Moffit (1954, p. 177), who notes that a fault of the lineament separates ancient metamorphic rocks from younger Paleozoic rocks. Moffit states that the north side of the fault is the upthrown side as the older rocks occur on the north side.

In the central Alaska Range Capps (1940, p. 116) mapped the Denali lineament and states, "in the area west of Nenana the fault certainly has a displacement of at least 10,000 feet, and the south side was downthrown." Wahrhaftig (Personal communication) states that the Denali lineament in the Mt. McKinley area dips steeply north with the north side upthrown; his evidence indicates that strike-slip movement is not appreciable.

In the central Kuskokwim region the Denali lineament has been mapped by Cady and others (1955, p. 90–93); the faults associated with it are normal faults, high-angle reverse faults, and a few thrust faults. The northwest side is upthrown along most of the faults.

Although details are lacking the known facts indicate that the principal movement along the Denali lineament has been such that the outer-arc side is upthrown with respect to the inner-arc side. In southeastern Alaska data suggest that the inner-arc side is upthrown relative to the outer-arc side. The only evidence of the amount of movement is in the central Alaska Range where differential vertical movement is at least 10,000 feet (Capps, 1940, p. 116).

St. Amand (1957, p. 1364) suggests, on the basis of topographic offsets and seismic data, that the Denali lineament is a right-lateral fault with many miles of stike-slip movement. The available geologic data indicate a large amount of vertical movement along the Denali fault, but the geologic data neither support nor deny St. Amand's hypothesis of major strike-slip movement.

In southeastern Alaska the Chatham Strait lineament cuts rocks ranging in age from Paleozoic to Cretaceous, inclusive. The lineament and its related splits cut the Coast Range batholith, considered to be Late Jurassic to Early Cretaceous. The latest movement on the fault in southeastern Alaska must, therefore, be Cretaceous or younger.

Elsewhere along the Denali lineament various geologists have dated it as Cretaceous or younger. In Canada Bostock (1952, p. 9) infers that the latest movement is postglacial. In the central Alaska Range Wahrhaftig (1954, p. 1317) states that the faults "have been intermittently active from Cretaceous time to the present." In the eastern Alaska Range much of the movement along the major faults, including the Denali lineament, occurred after the deposition of the Tertiary coal measures, which generally are regarded as early Tertiary (Moffit, 1954, p. 144, 178). In the Kuskokwim region Cady and others (1955, p. 90) have assigned a Quaternary age to most of the faults along the lineament. Some of the faults are still active as indicated by fault scarps in alluvium. Earthquake epicenters along the Denali lineament (St. Amand, 1957, p. 1346) indicate that it is still active.

Thus, the Alaskan lineament and probably its continuation, the Chatham Strait lineament, is active today along its entire length and has been active along its entire length at least since early Tertiary. In the central Alaska Range and possibly elsewhere it has been active at least since Cretaceous time.

Clarence Strait Lineament

The Clarence Strait lineament extends from the mouth of Clarence Strait in Dixon Entrance northwestward along Clarence Strait, probably underlies the Tertiary rocks of Kuiu, Kupreanof, and Admiralty islands,

crosses Chatham Strait and Chichagof Island, and may join a large fault along the southwest side of the Fairweather Range. The Clarence Strait lineament is at least 250 miles long and trends about N. 30°–40° W.

The southern part of the lineament lies beneath the waters of Clarence Strait, and its presence is inferred from the straight course of Clarence Strait. Linears parallel to and probably related to the lineament are exposed on Gravina Island, Cleveland Peninsula, and the northern part of Prince of Wales Island.

The lineament is not apparent in the Tertiary rocks of Kupreanof, Kuiu, and Admiralty islands. It is, therefore, presumed to be covered by these rocks, although the lineament may not be present in this area.

Because the intersection of the Chatham Strait lineament and the Clarence Strait lineament lies beneath the waters of Chatham Strait the nature of the intersection is unknown.

On Plate 2 the Clarence Strait lineament joins the lineament along the southwest side of the Fairweather Range; this interpretation may not be correct as the lineament of the Fairweather Range cuts Tertiary (including Eocene) rocks (D. J. Miller, personal communication), whereas the Clarence Strait lineament on Kuiu, Kupreanof, and Admiralty islands is covered by Tertiary (Eocene) rocks.

Along Clarence Strait the lineament separates Paleozoic rocks on Prince of Wales Island from Mesozoic rocks to the east, thereby suggesting that the west side was upthrown relative to the east side.

Because the lineament cuts the batholithic rocks of Chichagof Island, regarded as Cretaceous (Dutro and Payne, 1956), and does not cut the Eocene rocks on Kupreanof, Kuiu, and Admiralty islands, the principal movement along the Clarence Strait lineament probably took place during Late Cretaceous or Paleocene time.

Coast Range Lineament

The Coast Range lineament extends along the southwest border of the Coast Range batholith from the southern border of southeastern Alaska to Lynn Canal where it either joins or crosses the Chatham Strait lineament. It is at least 370 miles long. Its general trend is N. 30°–40° W.

We have mapped the Coast Range lineament in the vicinity of Juneau, and, in the area between Petersburg and Juneau, Buddington and Chapin (1929, p. 291) note that, "a highly mashed overthrust fault zone is indicated by the cataclastic texture of the rocks in a belt on the mainland adjacent to Stephens Passage from Port Houghton north to Point Astley and to the northwest in the vicinity of Point Arden and Grand Island." Precise data on the amount and type of movement on the faults of the Coast Range lineament are lacking. The topographic expression of the linears suggests that the faults dip steeply.

The relationships between the Coast Range and Chatham Strait lineaments are obscure, principally because the intersection is beneath Lynn Canal. Possibly both lineaments are splits from the Denali lineament.

Linears of the Coast Range lineament are principally confined to the belt of metamorphic rocks along the west side of the Coast Range batholith, but in a few places, in the southern and northern parts of southeastern Alaska, linears cross rocks of the batholith (Pl. 2).

As the youngest rocks cut by the Coast Range lineament are Upper Jurassic–Lower Cretaceous rocks of the Coast Range batholith, the latest movement along the lineament cannot be dated

Linears

Northwest-Trending Linears

Northwest-trending linears are common throughout southeastern Alaska, and many of them are as much as 100 miles long (Pl. 2). They correspond to the longitudinal trends of Peacock's (1935, p. 656) concordant pattern. Available data are summarized as follows:

(1) At a few places, including the Chichagof mining district (Reed and Coats, 1941, p. 63–73), on Admiralty Island west of Juneau, and in the Sitka district, the northwest-trending linears are caused by faults. We believe that most of the northwest-trending linears in southeastern Alaska (Pl. 2) are faults, although a few of them may represent trends of bedding and schistosity.

(2) The linears cross rocks ranging in age from early Paleozoic through Early Cretaceous. None has been observed crossing known Tertiary rocks, although in the Juneau area minor faults of this system of linears offset dikes postulated by Spencer (1906, p. 19) to be Tertiary. Thus the northwest-trending faults cannot be precisely dated, but the fact that the linears do not cut the Eocene rocks of Admiralty, Kuiu, and Kupreanof islands indicates to us that most of the northwest-trending linears are Late Cretaceous or Paleocene.

(3) In the Chichagof mining district the relative movement along the northwest-trending faults is such that the southwest side moved northwestward and upward at about 30° (Reed and Coats, 1941, p. 67). Horizontal displacements of as much as 5000 feet have been measured along northwest-trending faults on Chichagof Island (W. H. Condon, personal communication).

(4) The northwest-trending faults dip steeply, but accurate dips are available only in the Chichagof mining district where the faults generally dip steeply southwest (Reed and Coats, 1941, p. 64).

The similarity in trend and age of the northwest-trending linears with the Coast Range and Clarence Strait lineaments suggests that they are genetically related.

Northeast-Trending Linears

Northeast-trending linears are concentrated in certain areas of southeastern Alaska and are conspicuously absent in other areas. They are prominent features on the mainland north of Cross Sound, on Yakobi Island and adjacent parts of Chichagof Island, on southern Baranof Island, on central Admiralty Island, and on Revillagigedo Island. This type of linear corresponds to the transverse trends of Peacock's (1935, p. 656) concordant pattern.

The most important data and observations relative to the northeast-trending linears are summarized as follows:

(1) Northeast-trending linears are much shorter than the northwest-trending linears; few of them exceed 30 miles in length. Their trend ranges between N. 20° E. and N. 50° E.; the average direction is about N. 30° E. Known faults of this trend dip steeply or are vertical.

(2) Faults cause at least some of the northeast-trending linears: on Chichagof Island near Yakobi Island (Reed and Coats, 1941, p. 63-73), at the northern end of Admiralty Island (personal observation), at the south end of Baranof Island (personal observation), and at Red Bluff Bay on the east coast of Baranof Island (Guild and Balsley, 1942, p. 178). On the basis of these observations we infer that nearly all the northeast-trending linears plotted on Plate 2 represent faults. Support for this inference is the knowledge that the prevailing trend of bedding and schistosity in the rocks traversed by the northeast-trending linears is northwesterly, and, therefore, the linears cannot be traces of bedding or schistosity. However, throughout southeastern Alaska a prominent set of joints in the folded rocks strikes northeasterly (*see* 5 below), and possibly some of the shorter linears trending in this direction are controlled by joints.

(3) Northeast-trending linears cross rocks ranging in age from early Paleozoic through Eocene.

We are unable to arrive at a firm conclusion as to the relative ages of the northeast- and northwest-trending linears. On the basis that a few northeast-trending linears cross Eocene rocks and northwest-trending linears do not, we infer that the movement along the northeast-trending faults is more recent than that along northwest-trending faults. Confirmation of this inference is afforded by the fact that very few northeast-trending linears cross northwest-trending linears; in fact most northeast-trending linears terminate at one end against prominent northwest-trending linears, thereby suggesting that the northwest-trending linears are contemporaneous with, or older than, northeast-trending linears.

(4) No data are available as to the direction and amount of movement along the northeast-trending linears.

(5) The attitude of northeast-trending linears approximately coincides with the attitude (strike N. 30° E., dip 75° NW.) of the most prominent joint system in southeastern Alaska. This joint system is an ac plane approximately perpendicular to fold axes, to lineation, and to stretching in the metamorphic rocks.

North-Trending Linears

North-trending linears are not abundant in southeastern Alaska, but, in the Tertiary rocks of Admiralty, Kuiu, and Kupreanof islands, and in the older rocks of Prince of Wales Island, they are the dominant group of linears. Most of them are less than 40 miles long.

The Chatham Strait lineament also trends north, but only a few north-trending linears occur near it.

The north-trending linears in the vicinity of Kasaan Bay and Thorne Bay on Prince of Wales Island are the expression of throughgoing faults transverse to bedding. We assume most, if not all, of the north-trending linears represent faults as we know of no other bedrock features trending northerly.

North-trending linears correspond in direction to one of the trends of Peacock's (1935, p. 656) discordant system.

Some of the north-trending linears of Kuiu and Admiralty islands cross Eocene rocks. Thus

TABLE 1.—MINERAL SPRINGS IN SOUTHEASTERN ALASKA

Hot springs	Trend of linear
1. Bell Island hot springs	NE
2. Bailey Bay hot springs	No linear observed
3. Unuk River hot springs	NE
4. Saks Cove hot springs	N
5. Shakes hot springs	No linear observed
6. Hot springs on south side of Stikine River	No linear observed
7. Hot springs on north side of Stikine River	No linear observed
8. Vank Island hot springs	No linear observed
9. Baranof hot springs	N
10. Goddard hot springs	NE and N
11. Gut Bay hot springs	NE
12. Fish Bay hot springs	NW
13. Hot springs on north arm of Peril Straits	NW
14. Hoonah hot springs	NW
15. Tenakee hot springs	NW
16. Hot springs near head of Tenakee Inlet	NW
17. Pelican hot springs	NW
18. Mud Bay hot springs	NW
19. Nika Bay hot springs	NW
Carbonated springs	
20. Spring near New Eddystone Rock	N
21. Spring near Unuk River	NE
22. Spring near Soda Bay	No linear observed
23. Spring near Trocadero Bay	NW
24. Spring on north side of Zarembo Island	NW
25. Spring on south side of Zarembo Island	No linear observed
Sulfur springs	
26. Spring on George Inlet	No linear observed
27. El Capitan springs	No linear observed
28. Spring near Mt. Edgecumbe	No linear observed

we assume tentatively that the north-trending linears represent post-Eocene faults.

East-Trending Linears

East-trending linears are common on Dall Island, on the north end of Kupreanof Island, and in the Juneau area. They are the least common of the linears in southeastern Alaska, and most of them are less than 10 miles long.

We have no data on the linears on Dall and Kupreanof islands. In the Juneau area Silverbow fault has been studied in connection with the gold deposits in the area. It is an east-trending fault that joins a northwest-trending fault a few miles east of Juneau. It is nearly vertical, and the north side is displaced westward about 1500 feet and downward at least 1500 feet and possibly more. The precise age of Silverbow fault is not known, but it certainly is post-Coast Range batholith (Jurassic-Cretaceous), and, as the fault cuts dikes thought to be Tertiary, it may be Tertiary or younger.

East-trending linears correspond in direction to one of the trends of Peacock's (1935, p. 656) discordant system.

RELATION OF MINERAL SPRINGS TO LINEARS

General Statement

The mineral springs in southeastern Alaska are described by Waring (1917). He classifies 19 as hot springs, 6 as carbonated springs, and 3 as sulfur springs (Pl. 2). Table 1 lists the springs and the trend of the linear, if any, on which the spring is situated.

Hot Springs

Waring (1917, p. 19) states that the hot springs of southeastern Alaska seem " . . . to be definitely related to intrusive masses of rock, principally of granitic material, in the schists, graywackes, and other more or less altered rocks of the region, and appear to issue along zones of fracturing or faulting in the intrusive rocks."

In the preface to Waring's report (1917, p. 7) A. H. Brooks points out that there is no apparent genetic relation between recent lava flows and hot springs in southeastern Alaska, and that the fissuring of the intrusive rocks probably accounts for the presence of the hot springs. Brooks believed the fissuring took place in pre-Eocene time, but he also indicates that there is some evidence of later movement; he ascribes the presence of the hot springs to this later movement.

Plate 2 and Table 1 show that 14 of the 19 hot springs in southeastern Alaska are definitely on linears large enough to be mapped. Of the 14 hot springs on linears 8 are on northwest-trending linears, and 6 are on northeast- or north-trending linears.

From the available data it seems clear that most of the hot springs in southeastern Alaska are on prominent linears believed to be faults. As previously pointed out by Brooks (Waring, 1917, p. 7) the hot springs are not related to any apparent volcanic activity.

Carbonated Springs

Waring (1917, p, 77–83) describes 6 carbonated springs in southeastern Alaska (Pl. 2; Table 1). Of these, 4 are on prominent linears, and 2 are not on any observed linears. These data are not sufficient to indicate whether or not there is a genetic relationship between linears and carbonated springs. Waring (1917, p. 77) states, "In some places the production of carbon dioxide seems to be associated with the presence of lava of a fairly recent period of effusion, but sufficient information concerning all the localities is not at hand to warrant a general statement to this effect."

Sulfur Springs

Waring (1917, p. 89–91) describes 3 sulfur springs in southeastern Alaska (Pl. 2; Table 1). None is on observable faults or linears, and it therefore seems unlikely that there is any relationship between sulfur springs and linears in southeastern Alaska.

Relation of Mineral Deposits to Regional Faults

Discussion

Prospectors and geologists have long recognized that mineral deposits in southeastern Alaska and adjacent parts of British Columbia tend to be distributed in northwest-trending belts. Within each belt the mineral deposits are characterized by common features of mineralogy, type of mineralization, metal content, and habits of the deposits.

Buddington and Chapin (1929, p. 356–373) have briefly described pertinent features of the mineral belts. They list the following belts: eastern border belt, central Coast Range batholith, western belt of schist and gneiss, Juneau gold belt, Funter Bay-Hawk Inlet belt, Prince of Wales belt, Chichagof gold belt, and Sitka belt. Buddington (1927, p. 158–179) has presented data that relate the belts and types of metalliferous deposit to the various compositions of intrusive masses in southeastern Alaska. He believes the type and position of intrusive rock are possible factors in the localization of the metalliferous belts and the type of mineral deposit.

Most geologists who have studied the ore deposits of southeastern Alaska have postulated a genetic association between ore deposits and the magmas that formed the Coast Range intrusive rocks of Late Jurassic and Early Cretaceous age. However, little direct evidence to confirm this hypothesis has been presented.

We believe it quite possible that magmas may have provided the energy and the mineralizing fluids that created the mineral deposits of southeastern Alaska, but we do not believe the location of most of the mineral deposits was determined by the position of exposed intrusive masses. Instead we postulate that many mineral deposits in southeastern Alaska were localized by regional faults that directed mineralizing fluids into certain belts that are now the metalliferous belts.

To illustrate our thesis, two mining areas that have produced significant amounts of gold are discussed. Each has been described in considerable detail in publications of the U. S. Geological Survey.

Gold Deposits of the Chichagof and Sitka Belts

Reed and Coats have described in detail the gold deposits of the Chichagof mining district. They state (Reed and Coats, 1941, p. 6) in regard to faults:

"It has long been known that the ore bodies in the Chichagof district lie in or on fault zones. Perhaps the most noteworthy results of the investigations of 1938 and 1939 are the recognition of the hitherto unsuspected extent of certain of the faults and the extreme complexity of the fault system. . . . The fault system extends both northwestward and southeastward beyond the limits of the mapped area. Its limits are not known, and the further study and tracing of it offers an attractive geologic problem with a distinct economic slant."

Reed and Coats (1941, p. 81) further state that, "The dikes of the district and the quartz bodies are both believed to be related to the granitic rocks." They indicate that the faults occupied by the gold-bearing veins are younger than the granitic rocks as the faults cut the granitic bodies at several places (Reed and Coats, 1941, Pl. 3).

Reed and Coats (1941, p. 81) state, "The silica-bearing solutions from which the quartz of the veins was deposited apparently traveled upward from depth through the most readily accessible channels. Most of these channels lay along the faults." The faults in the Chichagof mining district were the geologic control that localized the ore-bearing fluids and probably also provided the channelways for the ore-bearing fluids.

In the Sitka belt gold-bearing quartz veins have been prospected in the vicinity of Silver Bay, but only a little gold has been produced. The lodes in general consist of auriferous massive and ribbon quartz in lenses along northwest-trending faults on the east shore of Silver Bay. The deposits are similar in most respects to the deposits in the Chichagof mining district.

In the only published report concerning the gold deposits of the Sitka belt, Knopf (1912b, p. 26–27) states:

"The ore bodies occupy shear zones in graywacke and strike parallel to the stratification of the country rock. The dips are steep—nearly vertical. The lodes form massive outcrops of white quartz up to 15 feet or more in thickness which are apt to show a short lenticular structure along the strike and to split into stringer lodes. They are irregular in shape, bellying out and constricting abruptly. Near the lodes the country rock is much sheared and is penetrated by numerous transverse stringers as well as by veins parallel to the shear planes."

In his conclusions regarding the ore bodies of the Chichagof and Sitka mining districts, Knopf (1912b, p. 31) states:

"The ore bodies of the region show neither in their mode of occurrence or origin any obvious or immediate relation to contacts of dissimilar rocks, to dikes, or to other igneous rocks. The principal mineral belt appears to lie along the edge of the slate-graywacke formation bordering the band of metamorphic rocks that flank the diorite occurring in the central portion of the islands."

Data suggest that faults have been the principal factor in localizing the mineral deposits in the Chichagof and Sitka districts and that the genetic association of the ores with intrusive rocks is a reasonable supposition.

Mineral Deposits of the Juneau Gold Belt

The lode gold deposits of the Juneau gold belt have been described in detail (Spencer, 1906; Knopf, 1911; 1912a). The Juneau gold belt extends for more than 100 miles from just south of Windham Bay to a few miles north of Berners Bay. In general the deposits are confined to a belt of metamorphic rocks about 4 miles wide along the southwestern margin of the Coast Range batholith.

Spencer (1906, p. 26) states:

"One of the most noteworthy features of the Juneau belt is a lode system or complex of veins, which with certain variations in its development, is traceable throughout the greater part of the belt.

"The linear distribution of the mines of this part of southeastern Alaska has been recognized for many years by those interested in the development of the region, and it has been commonly held that a more-or less well defined band exists in which a greater number of auriferous veins are present than in the rocks on either side. The basis of this view is immediately apparent when the positions of the best developed mines of the mainland area are plotted on the map, and they are found to lie almost in a straight line running parallel with the general northwest-southeast course of the adjacent coastal channels."

Knopf (1911, p. 25) describes the gold lodes grouped in or near the Jualin diorite at Berners Bay, on the north end of the Juneau gold belt. He states:

"The Jualin diorite is younger than the Berners formation, which it intrudes, and as it has escaped the dynamic deformation to which the quartz diorite gneiss was subjected, it is an intrusive mass of later age than that of the great body of granitoid rocks which form the backbone of the Coast Range in this latitude. No evidence is at hand to fix any limit to the length of time elapsing between the two periods of intrusion, but so far as our present knowledge of southeastern Alaska geology shows the interval was not great."

In his discussion of the origin of the ore deposits, Knopf states (1911, p. 35):

"The localization of the largest number of ore bodies in the area of the Jualin diorite is the most striking fact in the geology of the region. It suggests a genetic dependence on that rock mass, but what

that genetic relation is can not easily be established."

The lodes of the Juneau gold belt are so similar in mineralogy of the ores and gangue materials, in the wall-rock alterations accompanying the deposition of the vein material, and in the physical characteristcs of the veins and stringer lodes that all geologists who have studied the deposits agree that a common genesis is indicated. In his discussion of the genesis of the ores, Spencer (1906, p. 30) states:

> "The source of the solutions is difficult of determination, because at the best we have here to deal with a problem the elements of which can be only imperfectly known. The fact that the introduction of the veins can be fixed as later than the invasion of the field by the Coast Range diorite suggests a connection between the filling of the veins and the existence of the widely distributed intrusive rocks.
>
> "Though this general connection is here assumed, the relation is manifestly not a direct one, since the diorite itself is sometimes the carrier of simple veins, as in the Berner's Bay district, or the vein networks, as in the Treadwell deposits. The diorites of the Coast Range type must, therefore, have solidified previous to being fractured and it is probable that after their intrusion and consolidation, a long interval elapsed before they were fractured, preparatory to the formation of the veins. It is clear that if the vein waters were derived from igneous rocks, they were not given off by the particular masses of diorite which are found exposed to view."

Spencer points out that a magmatic province as large as the Coast Range batholith must contain a magmatic core that would remain molten long after the upper portions of the batholith solidified, and that this core could furnish the later vein-forming solutions.

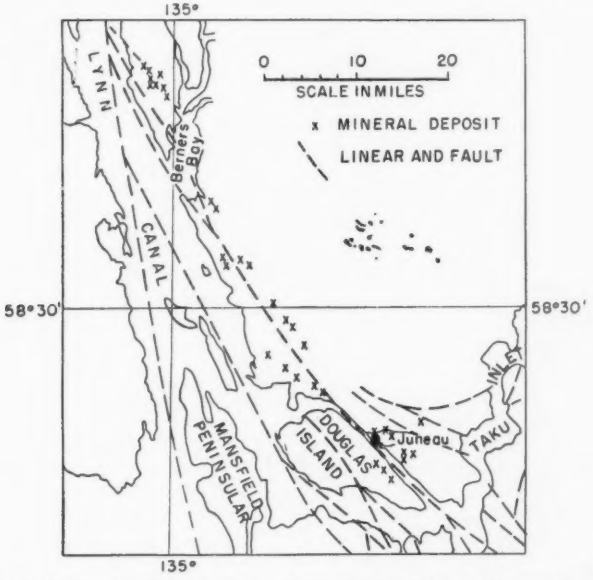

FIGURE 2.—MAP SHOWING MINERAL DEPOSITS, LINEARS, AND FAULTS, JUNEAU GOLD BELT

The larger prospects and mines in the northern part of the Juneau gold belt and the positions of the principal linears and faults are indicated on Figure 2. All the gold deposits are aligned along both sides of a fault zone of the Coast Range lineament; all the deposits are within 3 miles of the fault zone. The deposits are in black slate, graywacke, Jualin diorite, albitized diorite, and greenstone, suggesting that the arrangement of deposits within the Juneau gold belt is not related to the type of host rock, but instead is related to the position of the fault. Similarly the deposits bear no clear-cut spatial relation to outcropping igneous rocks, thereby suggesting to us that igneous rocks cannot be called upon to explain the beltlike distribution of the deposits.

We postulate that the fault zones of the Coast Range lineament were channelways along which mineralizing solutions migrated from depth to the positions of the present mineral deposits. Because the northwest-trending faults clearly are younger than the Coast Range

intrusives, the mineral deposits presumed to be related to the faulting are considered younger than the Coast Range batholith and probably are Late Cretaceous or early Tertiary.

The location near Juneau of two very large gold deposits (the Alaska-Juneau lode system and the Treadwell lode system) may be a consequence of the fact that two large faults, one trending northwesterly and the other trending easterly, intersect in the Juneau area (Fig. 2). At no other place in the Juneau gold belt do two through-going faults intersect at such a large angle.

Conclusions

(1) Linear features are conspicuous on most aerial photographs of southeastern Alaska. These linear features, herein called linears, are interpreted in most cases as faults.

(2) Three large lineaments are recognized: the Clarence Strait lineament, the Chatham Strait lineament, and the Coast Range lineament. The last two may be splits from the Denali lineament extending for 1600 miles from southeastern Alaska along the Alaska Range to Bristol Bay.

(3) Linears in southeastern Alaska may be grouped into a well-defined and widespread system that strikes northwesterly and three ill-defined systems that strike northerly, northeasterly, and easterly.

(4) Most of the hot springs in southeastern Alaska are on conspicuous linears, whereas carbonated and sulfur springs do not seem to be preferentially located on linears.

(5) We believe that the distribution of the mineral deposits in the Juneau gold belt and the Chichagof-Sitka belt is related to the position of regional faults; this hypothesis is worthy of testing in other mineralized districts in southeastern Alaska. We suggest that prospecting and exploration might be profitably guided by such a concept.

References Cited

Bostock, H. S., 1952, Geology of northwest Shakwak Valley, Yukon Territory: Canada Geol. Survey Mem. 267, 54 p.

Buddington, A. F., 1927, Coincident variations of types of mineralization and of Coast Range intrusives: Econ. Geology, v. 22, p. 158–179

Buddington, A. F., and Chapin, Theodore, 1929, Geology and mineral deposits of southeastern Alaska: U. S. Geol. Survey Bull. 800, 398 p.

Cady, W. M., Wallace, R. E., Hoare, J. M., and Webber, E. J., 1955, The central Kuskokwim region, Alaska: U. S. Geol. Survey Prof. Paper 268, 132 p.

Capps, S. R., 1940, Geology of the Alaska Railroad region: U. S. Geol. Survey Bull. 907, 201 p.

Dutro, J. T., Jr., and Payne, T. G., 1957, Geologic map of Alaska: U. S. Geol. Survey

Guild, P. W., and Balsley, J. R., Jr., 1942, Chromite deposits of Red Bluff Bay and vicinity, Baranof Island, Alaska: U. S. Geol. Survey Bull. 936-G p. 171–187

Kindle, E. D., 1949, Dezadeash map-area, Yukon Territory: Canada Geol. Survey Paper 49-24, 33 p.

Knopf, Adolph, 1911, Geology of the Berners Bay region, Alaska: U. S. Geol. Survey Bull. 446, 58 p.

——1912a, The Eagle River region, southeastern Alaska: U. S. Geol. Survey Bull. 502, 61 p.

——1912b, The Sitka mining district, Alaska: U. S. Geol. Survey Bull. 504, 32 p.

Martin, Lawrence, and Williams, F. E., 1924, An ice-eroded fiord; the mode of origin of Lynn Canal, Alaska: Geog. Rev., v. 14, p. 576-596

Moffit, F. H., 1954, Geology of the eastern part of the Alaskan Range and adjacent area: U. S. Geol. Survey Bull. 989-D, p. 63–218

Peacock, M. A., 1935, Fiord-land of British Columbia: Geol. Soc. America Bull., v. 46, p. 633–696

Reed, J. C., and Coats, R. R., 1941, Geology and ore deposits of the Chichagof mining district, Alaska: U. S. Geol. Survey Bull. 929, 148 p.

St. Amand, Pierre, 1954, Tectonics of Alaska as deduced from seismic data (Abstract): Geol. Soc. America Bull., v. 65, p. 1350

——1957, Geological and geophysical synthesis of the tectonics of portions of British Columbia, the Yukon territory, and Alaska: Geol. Soc. America Bull., v. 68, p. 1343–1370

Spencer, A. C., 1903, Pacific Mountain system in British Columbia and Alaska: Geol. Soc. America Bull., v. 14, p. 117–132

——1906, The Juneau gold belt, Alaska: U. S. Geol. Survey Bull. 287, 161 p.

Wahrhaftig, Clyde, 1954, Tectonic history of the central Alaska Range (Abstract): Geol. Soc. America Bull., v. 65, p. 1317

Waring, G. A., 1917, Mineral springs of Alaska: U. S. Geol. Survey Water-Supply Paper 418, 118 p.

Wilson, J. T., 1948, Some aspects of geophysics in Canada with special reference to structural research in the Canadian Shield; Pt. 2, An approach to the structure of the Canadian Shield: Am. Geophys. Union Tr., v. 29, p. 691–762

Wright, F. E., and Wright, C. W., 1908, The Ketchikan and Wrangell mining districts, Alaska: U. S. Geol. Survey Bull. 347, 210 p.

U. S. Geological Survey, Denver, Colo.; Union Carbide Corp., New York, N. Y.

Manuscript Received by the Secretary of the Society, October 28, 1957

Publication Authorized by the Director, U. S. Geological Survey

137°
136°
135°
134°
60°
59°
58°
57°
56°
CHILKOOT PASS
CHILKAT PASS
CHILKAT RIVER
LYNN CANAL
SKAGWAY
DENVER BAY
QUARTZ RANGE
JUNEAU
JUNEAU LINEAMENT
FAIRWEATHER RANGE
CROSS SOUND
YAKOBI ISLAND
CHICHAGOF MINING DISTRICT
CHICHAGOF ISLAND
ADMIRALTY
CHATHAM STRAIT
SITKA
SITKENEK PASSAGE
PT. ARCHER
WRANGELL
WRANGELL ISLAND
KUIU ISLAND
KUIU
REID INLET
REID GLACIER
BAY
FREDERICK SOUND
PORTLAND CANAL
LINEAMENT
NORTH PACIFIC OCEAN
0 10 20 30 40 50 Miles

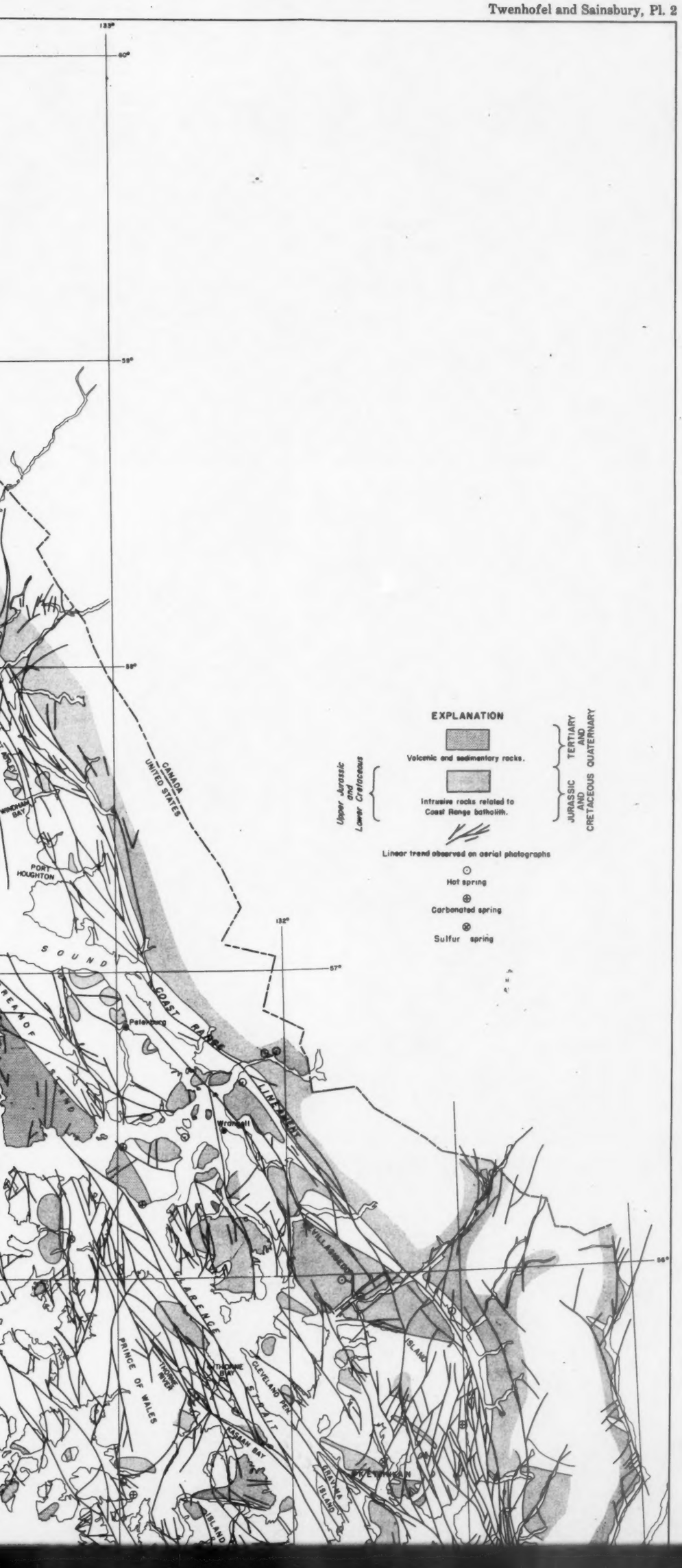
133°
60°
55°
56°
57°
132°
CANADA
UNITED STATES
WINDHAM BAY
PORT HOUGHTON
SOUND
COAST RANGE
LINEMENT
Petersburg
Wrangell
CLARENCE
STRAIT
PRINCE OF WALES
ISLAND
KASAAN BAY
KETCHIKAN
ANNETTE ISLAND
EXPLANATION
Volcanic and sedimentary rocks.
Intrusive rocks related to Coast Range batholith.
Upper Jurassic and Lower Cretaceous
TERTIARY AND QUATERNARY
JURASSIC AND CRETACEOUS
Linear trend observed on aerial photographs
Hot spring
Carbonated spring
Sulfur spring

LINEAR TRENDS IN SOUTHEASTER

Distribution of rocks taken from Buddington and Chapin (1929,
from Tongass National Forest, Alaska, U.S. Dept. Agricultu

ERN ALASKA

(1929, Pls. 1, 2). Base map
iculture, Forest Service

In
A
M
E

R

R

C
I
F

a
r
p
V
i
s

BULLETIN OF THE GEOLOGICAL SOCIETY OF AMERICA
VOL. 69, PP. 1443-1466, 1 FIG., 4 PLS. NOVEMBER 1958

PLASTIC DEFORMATION OF QUARTZ IN NATURE

BY S. W. BAILEY, R. A. BELL, AND C. J. PENG

ABSTRACT

Quartz grains occurring in naturally deformed rocks, irrespective of mode of origin, exhibit a wide variety of deformation features, including undulatory extinction, deformation lamellae, fracturing, and marginal granulation. X-ray studies of individual grains show that most of the quartz has deformed plastically by bend gliding. One of the three crystallographic *a* axes is always the major axis of bending, but no unique glide direction or glide plane has been established. The optical features and the details of the X-ray patterns may be explained and correlated by a theory involving dislocations and polygonization, whereby the bent crystal is transformed into a number of elongate, relatively perfect crystallites inclined to one another at small angles and separated by regions of atomic misfit. Undulatory extinction is explained as the optical expression of the results of bend gliding and polygonization. Deformed crystals show a significant decrease in the frequency of Dauphiné twinning; this is also attributed to the bending process.

CONTENTS

TEXT

	Page
Introduction	1443
Acknowledgments	1444
Materials	1444
Experimental methods	1445
Preparation of samples	1445
Microscopic examination	1445
X-ray diffraction	1445
Results of optical study	1446
General petrography	1446
Classification	1446
Results of X-ray study	1447
Introduction	1447
General features of Laue patterns of imperfect quartz crystals	1447
Asterism	1447
Splitting of Laue spots	1447
Spiralling	1448
Elimination of twinning	1448
Shape of Laue spots as related to crystallographic orientation	1448
Interpretation	1452
Correlation of X-ray study and microscopic observations	1461
Discussion of results	1461
References cited	1464

ILLUSTRATIONS

Figure	Page
1. Explanation of polygonization (schematic)	1453

Plate	Following page
1. Microphotographs of deformation features in imperfect quartz grains	1450
2. Laue patterns of perfect and imperfect quartz grains	1450
3. Shape of Laue spots as related to crystallographic orientation	1450
4. Simulation of bend gliding effects by composite Laue photographs	1450

TABLES

Table	Page
1. Comparison of degree of Laue asterism exhibited by different specimens	1447
2. Frequency of Dauphiné twinning in quartz grains and relationship to the shape of Laue reflections	1449
3. Summary of petrographic and X-ray-diffraction data	1456
4. Correlation of rock origin with quality of Laue reflections	1463

INTRODUCTION

Although the atoms in an ideal crystal are arranged in a lattice array of perfect regularity, most real crystals show some deviation from perfection in the arrangement of their atoms. Various types of imperfections are recognized in most actual crystals, such as vacant lattice sites, interstitial and substitutional impurity atoms, dislocations, mosaic structure and lineage, and twinning. Most of these imperfections are formed during crystal growth, but some are introduced subsequently, for example by deformation.

Crystal imperfections are generally on such a small scale that they are revealed only by the X-ray-diffraction method, or at least most clearly by this method. The Laue tech-

nique is particularly suitable for the study of crystal distortion, for any departure from geometric regularity of the atomic planes is shown by a change of shape of the spots on a Laue photograph. On Laue patterns of deformed metals the imperfections are manifested by such phenomena as asterism and splitting of spots (Barrett, 1953, p. 351; Cahn, 1950, p. 152). Similar features also have been observed on Laue patterns of both artificially and naturally deformed nonmetals, for example rock salt and gypsum (Konobjewski and Mirer, 1932, Figs. 5–9), diamond (Lonsdale, 1945, Pl. 11, figs. 4–5), and ice (Glen and Perutz, 1954, Figs. 12–15).

Much material has been published on imperfections in metals (Seitz, 1952; Read, 1953; Cottrell, 1953), but little information is available on imperfections in minerals. Quartz generally is regarded as forming crystals that are nearly perfect aside from the presence of twinning, lineage structure (Buerger, 1934, p. 203), and the "mosaic structure" recently reported by Frederickson (1955). This belief, however, seems to exist because study has been concentrated on well-formed quartz crystals, such as those found in vugs of hydrothermal veins and pegmatites, rather than on the more common anhedral grains found in massive rocks.

During a study of quartz from various sources, Bell (1953, Ph.D. dissertation, Univ. Wisconsin) noticed that Laue photographs of quartz from certain types of rocks show asterism and in some cases splitting of spots, instead of the well-defined and sharp reflections expected from a relatively perfect crystal. This finding shows the presence of imperfections in quartz and also suggests that the imperfections may give some clue to the natural history of the quartz and therefore of quartz-bearing rocks. This paper gives some of the results of further investigation along the lines of Bell's preliminary study.

Laue asterism produced by quartz was apparently examined first by Berman (*in* Griggs and Bell, 1938, p. 1737) and interpreted as being due to plastic deformation. Although a more extended X-ray study was promised by these authors, none has appeared. The present study not only confirms their interpretation in more detail but also shows that the appearance of Laue reflections produced by a deformed quartz crystal depends upon crystallographic orientation, that the appearance changes with the intensity of deformation a specimen has undergone, and that it correlates with the degree of undulatory extinction exhibited. On the basis of these results, a mechanism of quartz deformation involving dislocation theory is postulated as a contribution to the study of quartz fabrics, some aspects of which have been in controversy for many years. The reader is referred to Fairbairn (1949, Chapt. 9) for a general review of this problem. The proposed mechanism seems to explain the microscopic features of a deformed quartz grain as well as the unusual appearance of its Laue pattern; hence the writers believe that all these phenomena are indications of the presence of dislocations in quartz.

Acknowledgments

This study was supported in part by a grant from the Wisconsin Alumni Research Foundation. Thanks are extended to Dr. R. C. Emmons for suggesting the initial study and for his interest in the course of the research. Drs. R. C. Emmons, R. M. Gates, E. N. Cameron, S. A. Tyler, R. A. Murray, J. B. Jones, T. O. H. Patrick, all of the University of Wisconsin, John Reid, Jr., of Tufts College, and J. J. Prucha of the Shell Development Company kindly supplied specimens used in the investigation. The writers are indebted also to Drs. R. C. Emmons, E. N. Cameron, and S. A. Tyler for critically reviewing the manuscript.

Materials

The quartz crystals used for the present work were obtained from 55 specimens from various geological occurrences, which may be classified as follows:

(1) Massive granitic rocks (both magmatic and metasomatic)	22
(2) Gneissic granites	2
(3) Dikes and sills (granitic or porphyritic)	11
(4) Pegmatites	2
(5) Lava flows	5
(6) Gneisses and schists	6
(7) Quartzites	4
(8) Hydrothermal veins	3

The locality of each specimen is given in Table 3.

In selection of specimens emphasis was given to granitic rocks in the hope that the study might throw new light upon the granite problem. Although the tested specimens represent only a portion of the major quartz-containing rock groups, they were selected be-

cause the origin of many of them is either well established or is at least indicated by field relations. An attempt is made to correlate field data with the results of the laboratory research.

Experimental Methods

Preparation of Samples

Slices about 4.0 by 2.0 by 0.2 cm were cut from each rock specimen and broken into small fragments with a steel mortar and pestle. Quartz grains were hand-picked from the fragments under a binocular microscope. Only those grains were selected for X-ray diffraction that were apparently single optical units, about 0.2 mm across, and free from cracks and inclusions. Standard thin sections were made of each specimen for petrographic work.

Microscopic Examination

Imperfections must be related either to crystal growth or to processes to which a crystal has been subjected subsequently. Some deductions concerning growth features and deformation have been made as a result of optical study to supplement published descriptions for each specimen. Special attention was directed in the thin sections to those petrographic features that might suggest primary crystallization, recrystallization, deformation, and replacement. Each quartz grain to be used for X-ray diffraction was also examined microscopically to detect undulatory extinction and deformation lamellae, generally interpreted as resulting from deformation. Deformation lamellae were not observed in any of the tested grains, probably because the odd shapes and small sizes of the grains made such observation difficult. In thin sections some quartz grains from the same rock specimens did show the lamellae (Pl. 1). These grains were later cut from the sections for X-ray study. Although quartz of any source may show undulatory extinction, the intensity of the effect varies greatly. It is best seen in thin section and may not show up in a thick section. The study of undulatory extinction in individual quartz grains separated from the host rock is difficult and unsatisfactory. Steps or ridges on the broken surface of a grain may produce an apparent irregular extinction, even though an adjacent smooth surface may extinguish uniformly. Because of these complications, undulatory extinction had to be studied mainly in thin sections, with the optical observation of individual grains as a further check.

X-Ray Diffraction

The present study was made chiefly by the Laue method, using unfiltered copper X-radiation. Before taking Laue photographs each quartz grain was oriented optically. The grain was mounted on the tip of a glass fiber on the goniometer head of a cylindrical Unicam camera. Preliminary orientation was made with a Perutz polarizer (Perutz, 1949) attached to the camera in such a way that the grain could be set with its optic axis (*c*) either (1) vertical or (2) horizontal and parallel to the incident X-ray beam. A grain with tabular sides usually can be oriented within a few degrees of the desired position in this manner; wavy extinction, very small grain size, or irregular grain shape may make orientation difficult and less accurate. In this case orientation in an immersion liquid under the petrographic microscope may be necessary. Final orientation was carried out by the X-ray method of Weisz and Cole (1948), using composite 15-degree oscillation exposures. This insures an accurate setting of a selected vertical crystallographic axis. The desired horizontal axis then was rotated to a position parallel to the incident beam by comparison of the orientation Laue patterns with a series of standard patterns of quartz prepared at 5-degree intervals around the horizontal dial. Most grains were oriented either with an *a* axis vertical and the *c* axis parallel to the X-ray beam or with the *c* axis vertical and an *a* or a^* axis (an axis in reciprocal space halfway between any two *a* axes) parallel to the beam. For the purpose of studying the relationship between crystallographic orientation and the shapes of X-ray reflections, series of Laue patterns were taken of a few samples with *c* vertical and with each of the *a* and a^* axes in turn parallel to the incident X-ray beam and then with an *a* axis vertical and successive positions in the zone between a^* and *c* parallel to the beam. Some of the important reflections were indexed by the use of the stereographic projection and curves of constant θ, ρ, and $90 - \phi$ (Henry, Lipson, and Wooster, 1951, p. 108). At least two grains from each specimen were examined by the Laue technique, and as many as nine grains were tested for several specimens. Powder patterns were made of a few selected quartz specimens for the purpose of studying crystallite texture and unit-cell dimensions.

Results of Optical Study

General Petrography

The quartz grains seen in thin sections of the rock specimens show a wide variety of microscopic features, but their appearance generally conforms with the over-all texture of the rock in which they occur. The most common microstructure in the quartz is undulatory extinction. It varies greatly in intensity but is more pronounced and complex in pattern in grains showing cataclastic features, such as granulation and fracturing. In strongly deformed specimens quartz usually develops well-defined, separated zones of undulatory extinction which are invariably parallel to the *c* axes, as reported by previous workers. In a few specimens deformation lamellae, associated with strong strain shadows and other deformation features, were seen in the quartz grains. The lamellae are fine, parallel, slightly bent bands running across a quartz grain but pinching out at both ends (Pl. 1, fig. 1). Those observed were perpendicular to the extinction zones. No lamellae were observed in specimens in which the quartz grains showed normal extinction.

No external indications of deformation, such as mineral elongation or alignment, are evident in the granitic rocks, even if the quartz grains show very strong strain shadows in thin section. Under the microscope all show the typical granitic texture. Quartz in the schists and quartzites is generally in equant grains with subsutured boundaries, but large bands or lenses of quartz are also common in the schists. Typically, such quartz shows little undulatory extinction.

Classification

On the basis of the appearance of the quartz and the general texture of the rocks, the specimens under study may be classified into the following groups.

(1) UNDEFORMED: This group includes the hydrothermal quartz veins, mica schists, quartzites, most of the dikes, sills, and rhyolites, and some of the reportedly magmatic granitic rocks. The texture of the granitic rocks is characteristically granular, porphyritic, or granophyric, whereas the schists are typically granoblastic with parallel mica flakes; some have quartz lenses. The rhyolites are porphyritic and consist of euhedral quartz and feldspar grains in a fine-grained matrix. The quartzites consist of granoblastic aggregates of quartz with some mica and feldspars. Quartz in all these rocks typically shows uniform extinction, but some grains may exhibit weak and broad strain shadows with a variation of extinction angles up to 4°. No deformation features were seen in any other minerals.

(2a) CATACLASTIC; STRAIN SHADOWS DOMINANT: Rocks in which strain shadows are dominant are an intermediate group between groups (1) and (2b). The group is represented by several specimens of reportedly magmatic granitic rocks from widely separated localities, a sheared gneissic granitic dike with associated pegmatite from Golden's Bridge, New York, the rapakivi granites from Tigerton and Waupaca, the granite porphyry from Aurora, and an augen gneiss from Neillsville, all in Wisconsin. All these specimens, except the foliated gneisses, show normal granitic texture. All the quartz shows strain shadows, but the displacement of the *c* axes of the grains varies considerably even in the same thin section, ranging from about 1° to 7°. Most of the extinction bands are broad and straight without any visible fractures between them. Only very rarely are the grains broken along the edges. Slightly bent twinning bands were observed in a few plagioclase grains in a granite from Red Granite, Wisconsin, and faint deformation lamellae were found in some quartz grains in the Neillsville augen gneiss from Wisconsin.

(2b) CATACLASTIC; SHATTERING DOMINANT: The specimens of this group show more intense deformation than those of the preceding group. To this group belong the reportedly metasomatic granites from the Amberg-High Falls area of northeast Wisconsin, from North Chelmsford, Massachusetts, and from Tyson Lake, Ontario, the sheared phase of a magmatic granite from Queensland, Australia, the granites from Quincy, Massachusetts, and from the Montello-Wausau area of central Wisconsin, a rhyolite with "flow structure" from the Thüringer Wald, Germany, a deformed rhyolite from Marquette, Wisconsin, and a deformed quartz porphyry dike from Monterey, Pennsylvania. Most of these specimens are massive granitic rocks. Under the microscope, however, the shattering effects are apparent and pronounced. Most of the quartz develops narrow and in some cases sinuous bands of undulatory extinction with the positions of the *c* axes varying from about 3° to as much as 25°. In some grains the extinction zones are separated by fractures (Pl. 1, fig. 2). Deformation lamellae were seen in several of the specimens (Pl. 1, fig. 1). Many large quartz grains are

broken along the borders and recrystallized into small, less strained fragments, giving rise to a mortar structure. Feldspars also show deformation features, such as bent and offset twinning bands, fractures, and some crushing and undulatory extinction.

TABLE 1.—COMPARISON OF DEGREE OF LAUE ASTERISM EXHIBITED BY DIFFERENT SPECIMENS

Measurements were made on the chart of curves of constant θ, ρ, and $(90 - \varphi)$ (Henry, Lipson, and Wooster, 1951, p. 108). All photographs were taken in cylindrical cameras with unfiltered copper X radiation with the c axis of the crystal vertical and an a^* axis parallel to the X-ray beam. L = length, W = width of reflection.

Laue reflection	Bragg angle		Gray granite; U.S. Highway 141, near Amberg, Wisconsin	Red granite; Montello, Wisconsin	Bluish-gray granite; Quincy, Massachusetts	Red granite; Anderson Brothers quarry, Wausau, Wisconsin	Gray granite; Mundt quarry, Amberg, Wisconsin	Light-gray gneissic granite; North Chelmsford, Massachusetts	Banded red granite; Red Granite, Wisconsin	Gray gneissic granite dike; Golden's Bridge, New York	Rapakivi granite; Tigerton, Wisconsin	Granitic top of sill; Bridgland, Ontario
m $(10\bar{1}0)$	30°	L	7°	7°	6°	6°	4°	5°	2.5°	2°	1.5°	0.5°
		W	5°	3°	1.5°	3°	4°	2.5°	0.8°	1°	0.5°	0.5°
r $(10\bar{1}1)$	30°	L	15°	14.5°	11°	10°	7°	9.5°	4°	3.5°	4.5°	0.5°
		W	5°	5°	2.5°	4.5°	5°	5°	1.5°	1.5°	1.5°	0.5°
$(10\bar{1}3)$	30°	L	23°	17°	17°	16°	13.5°	10°	5.5°	5°	7°	0.5°
		W	5°	3.5°	2.5°	4.5°	7°	5°	1.5°	1.5°	2.5°	0.5°
a $(11\bar{2}0)$	60°	L	4°	5°	3.5°	5°	3.5°	3°	2.5°	2.5°	1°	0.5°
		W	6°	3°	2°	3°	3.5°	2°	1°	1°	2°	0.5°

RESULTS OF X-RAY STUDY

Introduction

Many of the tested quartz grains give normal Laue photographs with sharp, single X-ray reflections (Pl. 2, figs. 1–3). Laue patterns of many other samples, however, are markedly different because of a change of shape of the spots, although the over-all pattern and symmetry remain unaltered. In addition to elongation and splitting of Laue spots, as observed by Bell (1953, Ph.D. dissertation, Univ. Wisconsin), other changes have been noticed. These changes appear to represent stages of development that grade from one to another. They are crystallographic in direction and therefore appear to be the consequence of a directional distortion of the quartz structure.

Somewhat similar changes can be seen on oscillation photographs of the same samples, but the effects usually are less pronounced and not so informative as those seen on the Laue patterns. Despite the fact that sharp Laue photographs are produced by some specimens and diffuse ones by others, the few specimens examined by the powder method, both film and diffractometer techniques, give identical patterns without any noticeable broadening or shifting of lines. This indicates that no fundamental structural changes have been brought about despite the effects noted on the Laue patterns. Minor variations in cell dimensions are expected as a result of impurities (Keith, 1955, p. 532).

General Features of Laue Patterns of Imperfect Quartz Crystals

Asterism.—Asterism is shown on Laue photographs of all imperfect quartz grains examined. The usual sharp reflections are drawn out into long streaks generally pointing toward the center of the film. The ratio of major to minor axis of the streaks is approximately $1/\theta$, and therefore the spots are elongated most at the smaller Bragg angles near the center of the film. Specimens vary considerably in lengths of Laue streaks (Table 1) even from the same atomic planes at the same setting; for any given crystal the reflections from different atomic planes of the same zone are elongated differently (Pls. 2, 3).

Splitting of Laue spots.—Although the Laue patterns of some specimens show only asterism, those of other specimens contain asterism streaks subdivided into striations (Pls. 2, 3). If a Laue reflection has been elongated considerably, it usually also is broken into a large number of subspots or striations, whereas small

Laue streaks generally remain single. This indicates that the subdivision of a single spot into striations takes place only if the effect of asterism has developed to a certain extent. Subdivision must therefore represent an advanced stage of development of imperfections in quartz. This effect is termed polygonization in accordance with metallurgical usage. (*See* section on Interpretation.)

The striations are closely spaced, thin, short lines, each of much weaker intensity than the original Laue spot. In general they are lined up along the major axis of an asterism streak but in certain cases are spread out transversely (Pl. 3). The longer asterism streaks generally contain more striations than the shorter streaks, but the striations are more widely spaced and weaker in intensity in the longer streaks. The striations in some streaks are so widely spread and diffuse that they are almost invisible with the exposure time of 2 hours used in this study. Striations from originally separate but adjacent Laue spots in many patterns coalesce to form an indistinct smudge (Pl. 3, figs. 2, 3).

Another feature related to subdivision of Laue spots is the prominence of high-intensity reflections associated with the polygonized Laue reflections from certain atomic planes. These take the form of dark streaks or spots aligned along the arcs of "powder" rings (Pls. 2, 3). Most of the streaks are subdivided. They do not occupy the exact positions of the associated Laue reflections but are superimposed only upon certain areas of the diffuse Laue spots. When a Laue photograph is taken of the same crystal without exciting the characteristic component of the X-radiation, these extra spots do not show up on the pattern. Evidently they are due to those planes of an imperfect quartz grain which are so oriented that they pick out a characteristic wave length for reflection. Since they appear prominently only where Laue spots are considerably elongated and broken up, their occurrence must also represent an advanced stage in the formation of imperfections in quartz.

Spiralling.—Spots on the left side of the Laue pattern of a normal, relatively perfect quartz crystal oriented with the *c* axis vertical and an a^* axis parallel to the X-ray beam are the mirror images of those on the right side in position, shape, and intensity (Pl. 2, fig. 3). If the reflections are elongated and split into striations the shape symmetry of the spots no longer exists, except in photographs taken at certain unique settings described in the following sections. The over-all pattern, however, remains essentially the same (Pl. 3). This phenomenon is called "spiralling" (Lonsdale, 1945, p. 120).

Elimination of twinning.—Laue photographs given by relatively perfect or slightly distorted quartz crystals oriented with the *c* axis parallel to the X-ray beam show either trigonal (Pl. 2, fig. 2) or pseudohexagonal symmetry (Pl. 2, fig. 1). The latter results from twinning according to the Dauphiné law. However, very few of the samples that produce elongated and subdivided Laue reflections show this type of twinning (Table 2; Pl. 2, fig. 5). In 120 quartz grains from 39 localities specifically examined for twinning by the X-ray technique a progressive decrease in the ratio of twinned to untwinned grains is found as the diffuseness (elongation) of the Laue reflections increases.

Quality of Laue reflections	Number of grains examined	Ratio of twinned to untwinned grains
Sharp	42	23/19 = 1.21
Moderately diffuse	39	14/25 = 0.56
Very diffuse	39	9/30 = 0.30

Since the Dauphiné twin is one of the commonest types of twinning in quartz, its absence in many imperfect quartz crystals of this type is apparently not accidental but is related to the processes causing asterism and polygonization. The other common type of quartz twinning, according to the Brazil law, is not revealed by X-ray study.

Shape of Laue Spots as Related to Crystallographic Orientation

On the Laue photograph of a relatively perfect quartz crystal taken at any setting all spots on the film are uniformly sharp and either round or elliptical (Pl. 2, figs. 1–3). The three crystallographic *a* axes are equivalent in all respects. There is a marked asymmetry of the shape of spots, however, for different reflections on all Laue photographs that show asterism and polygonization. As a consequence of the deformation the three *a* axes are no longer exactly equivalent. The spots on one side of most photographs are elongated and subdivided in a different manner from the corresponding spots on the other side, thus giving rise to a spiralling effect. The following paragraphs give a comparison of Laue photographs of imperfect quartz grains taken at different orientations, showing that one *a* axis and one

TABLE 2.—FREQUENCY OF DAUPHINÉ TWINNING IN QUARTZ GRAINS AND RELATIONSHIP TO THE QUALITY OF LAUE REFLECTIONS

Locality of quartz sample	Type of rock	Number of grains examined	Quality of Laue spots			Dauphiné twinning present	Untwinned
			sharp	moderately diffuse	Very diffuse		
Mundt quarry, Amberg, Wisconsin	Gray granite	5	—	—	5	—	5
Middle Inlet, Wisconsin	Pegmatoid granite	4	—	—	4	—	4
Aurora, Wisconsin	Granite porphyry	3	—	3	—	—	3
Pembine, Wisconsin	Gray granite	4	—	1	3	2	2
Neillsville, Wisconsin	Augen gneiss	2	—	2	—	—	2
Tigerton, Wisconsin	Rapakivi granite	2	—	2	—	—	2
Red Granite, Wisconsin	Red granite	2	—	2	—	—	2
Montello, Wisconsin	Fine-grained red granite	4	—	—	4	—	4
Anderson Bros. quarry, Wausau, Wisconsin	Red granite	4	—	—	4	—	4
Baxter Hollow, Wisconsin	Fine-grained red granite	2	—	2	—	—	2
North Chelmsford, Massachusetts	Gneissic granite	4	—	2	2	1	3
Golden's Bridge, New York	Sheared granitic dike	5	—	5	—	2	3
Golden's Bridge, New York	Pegmatitic phase of granitic dike	1	—	1	—	1	—
Saganaga, Minnesota	Granite porphyry	2	—	2	—	1	1
Quincy, Massachusetts	Bluish-gray granite	3	—	2	1	1	2
Tyson Lake, North Ontario	Gneissic granite	4	—	—	4	2	2
Thüringer Wald, Germany	Rhyolite with flow structure	4	—	—	4	4	—
Cressbrook Creek, Queensland, Australia	Sheared pink granite	3	—	—	3	1	2
Monterey, Pennsylvania	Quartz porphry dike	4	—	—	4	1	3
Marquette, Wisconsin	Rhyolite	2	—	1	1	1	1
Snowbank Lake, Minnesota	Hornblende granite	4	—	4	—	2	2
North Woodbury Quadrangle, Connecticut	Nonewaug granite	4	—	4	—	2	2
New London, Wisconsin	Red granite	1	—	1	—	1	—
Hyde School, Gouverneur, New York	Granitic phacolith	3	2	1	—	2	1
Hyde School, Gouverneur, New York	Pegmatite in phacolith	3	2	1	—	2	1
West Connecticut	Mica-quartz gneiss	10	8	2	—	4	6
Mt. Wright area, Quebec	Quartz rock member of iron formation series	2	2	—	—	1	1
Waupaca, Wisconsin	Gray rapakivi granite	3	2	1	—	1	2
Pigeon Point, Minnesota	Granitic top of diabase sill	2	2	—	—	1	1
Bridgland, Ontario	Granitic top of diabase sill	4	4	—	—	3	1
Summit County, Colorado	Quartz porphyry dike	2	2	—	—	1	1
Annapolis, Missouri	Quartz porphyry dike	2	2	—	—	2	—
Leadville, Colorado	Quartz porphyry sill	2	2	—	—	1	1
Signal Point, Yellowstone Lake, Wyoming	Rhyolite	2	2	—	—	1	1
Red Rock Point, Minnesota	Rhyolite	2	2	—	—	1	1
Sudbury, Ontario	Quartz diorite	1	1	—	—	1	—
Hot Springs, Arkansas	Hydrothermal vein	1	1	—	—	—	1
Siskiyou County, California	Hydrothermal vein	2	2	—	—	1	1
Potosi, Missouri	Quartz-barite deposit	2	2	—	—	—	2
Mellen, Wisconsin	Granitic dike in gabbro	2	2	—	—	1	1
Notre Dame Bay, Newfoundland	Rhyolite	2	2	—	—	1	1

a^* axis are now unique. The features described were found in all imperfect quartz grains examined, regardless of locality or geologic environment.

(1) *c* AXIS VERTICAL AND THE UNIQUE a^* AXIS HORIZONTAL AND PARALLEL TO THE X-RAY BEAM: The Laue reflections on the left side of a photograph taken at this setting are approximately symmetrical to those on the right side in shape as well as in position (Pl. 3, fig. 1). Reflections from planes of the same zone, however, have different shapes. At small Bragg angles the elongation and splitting of the front-reflection Laue spots are mainly in a radial direction, and the length of streak gradually decreases from the center of the film outward, for example from the obtuse rhombohedron reflections $\{h0\bar{h}l\}$ to the prism reflection $(10\bar{1}0)$ along the two most prominent ellipses near the center of the film (Table 1; Pl. 3, fig. 1). The back reflections seen at the edges of the film are less elongated, although more nearly uniformly, in a direction perpendicular to the equator, that is, parallel to the *c* axis.

(2) *c* AXIS VERTICAL AND EITHER OF THE TWO OTHER a^* AXES PARALLEL TO THE BEAM: These two Laue photographs (Pl. 3, figs. 2, 3) show a pronounced spiralling of shape of spots. All reflections on one side of the patterns have corresponding reflections at similar positions on the other side but of different shape. Although these two photographs appear to be alike, the spiralling relationship of spots shown on one is reversed on the other.

One side of each of the two photographs is similar to pattern (1) above in that the asterism streaks on front reflections are elongated considerably and show a gradual decrease in length away from the center of the photograph along the prominent ellipse. But the streaks appear fatter than in case (1) and are oriented nearly vertically, rather than radially from the center of the film. The back reflections are more uniformly distorted and appear contracted.

The most striking differences are found on the other side of each of the two Laue photographs. The spots are in positions that are the mirror images of those on the opposite side, but they are shaped differently. The front reflections are elongated and broken up in a direction nearly tangential to the center of the prominent ellipse. Consequently, the asterism streaks are much shorter, are of more nearly uniform length, and are split into more striae. Owing to the transverse spreading, striae of adjacent spots on very diffuse Laue patterns become merged into an almost continuous ring. The streaks of the back reflections are more nearly uniform in shape, and most are extended vertically.

PLATE 1.—MICROPHOTOGRAPHS OF DEFORMATION FEATURES IN IMPERFECT QUARTZ GRAINS

FIGURE 1.—Bent deformation lamellae in quartz from a red granite, Anderson Brothers quarry, Wausau, Wisconsin. The lamellae are visible only in the immediate vicinity of the undulatory extinction band, normal to the lamellae, which sweeps across the grain on rotation of the stage. × 135.

FIGURE 2.—Same specimen, showing separated zones of undulatory extinction, fractures parallel to the extinction zones, and marginal granulation and recrystallization in quartz. × 135.

PLATE 2.—LAUE PATTERNS OF PERFECT AND IMPERFECT QUARTZ GRAINS

FIGURE 1.—Quartz grain from the granitic differentiate of a diabase sill, Bridgland, Ontario, oriented with an *a* axis vertical and the *c* axis parallel to the incident X-ray beam. The sixfold symmetry (indicated by the circled spots) is due to twinning according to the Dauphiné law. A few reflections have been indexed with symbols for the corresponding crystal faces. Unfiltered Cu radiation, 6 cm diameter cylindrical camera.

FIGURE 2.—Quartz grain from a quartz-rock member of the iron formation series, Mt. Wright area, north Quebec. Same orientation as in Figure 1. Trigonal symmetry and untwinned.

FIGURE 3.—Same grain as in Figure 2, oriented with the *c* axis vertical and an a^* axis parallel to the incident X-ray beam.

FIGURE 4.—Quartz grain from a gray granite, Mundt quarry, Amberg, Wisconsin, oriented with an *a* axis vertical and the unit rhombohedron *r* parallel to the X-ray beam. The individual reflections are elongated and subdivided into multiple striations.

FIGURE 5.—A different quartz grain from the same granite as in Figure 4, oriented with an *a* axis vertical and the *c* axis parallel to the incident X-ray beam. Illustrates case (5) of the section on shape of Laue spots as related to crystallographic orientation, with greatest elongation along one particular a^* axis and least elongation along the *a* axis normal to it. This *a* axis is the axis of bending. Untwinned.

FIGURE 6.—Same grain as in Figure 5, oriented with the *c* axis vertical and the axis of bending parallel to the X-ray beam. Illustrates case (3).

FIGURE 1

FIGURE 2

MICROPHOTOGRAPHS OF DEFORMATION FEATURES IN IMPERFECT QUARTZ GRAINS

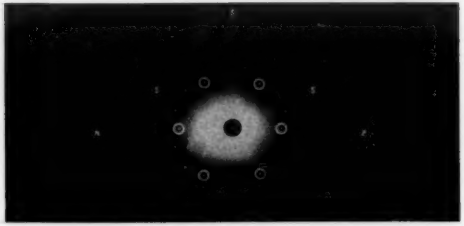

FIGURE 1

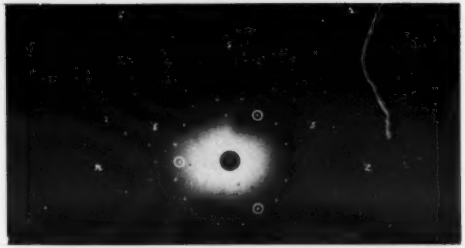

FIGURE 2

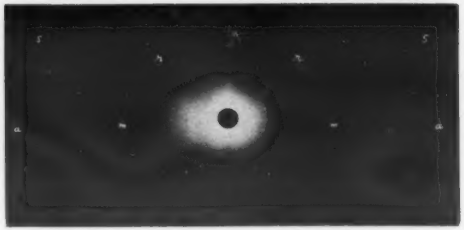

FIGURE 3

FIGURE 4

FIGURE 5

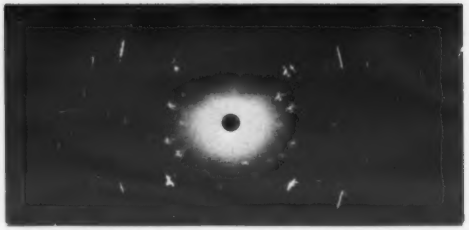

FIGURE 6

LAUE PATTERNS OF PERFECT AND IMPERFECT QUARTZ GRAINS

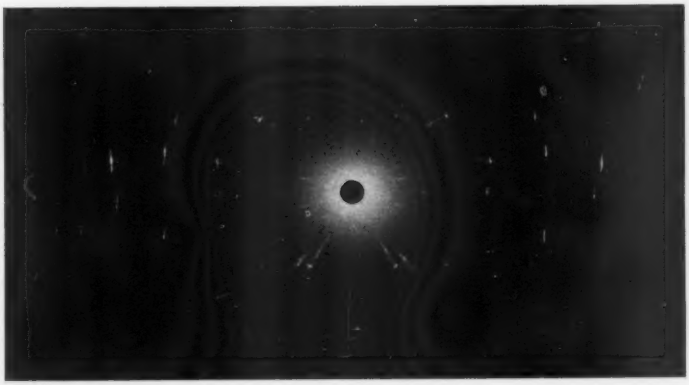

FIGURE 1

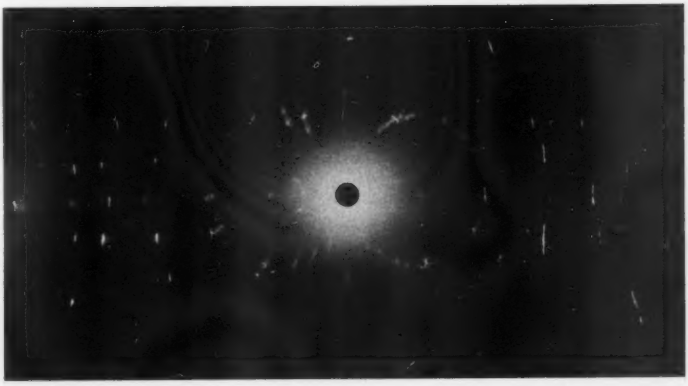

FIGURE 2

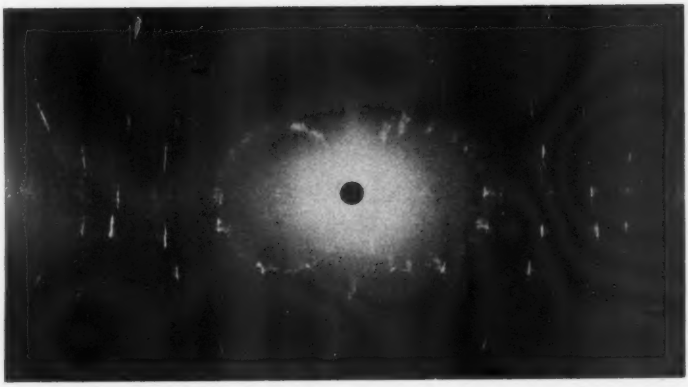

FIGURE 3

SHAPE OF LAUE SPOTS AS RELATED TO CRYSTALLOGRAPHIC ORIENTATION

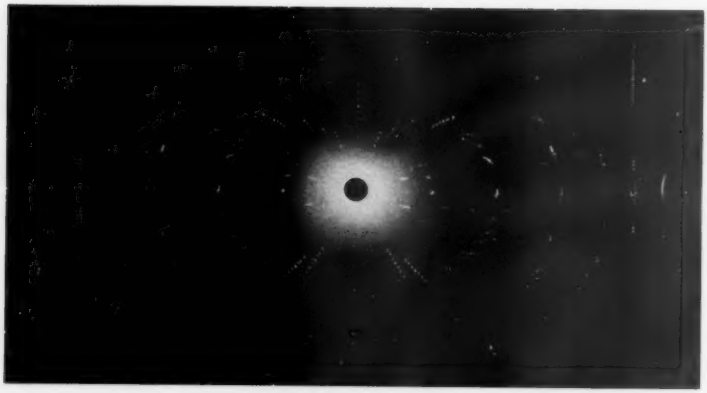

FIGURE 1

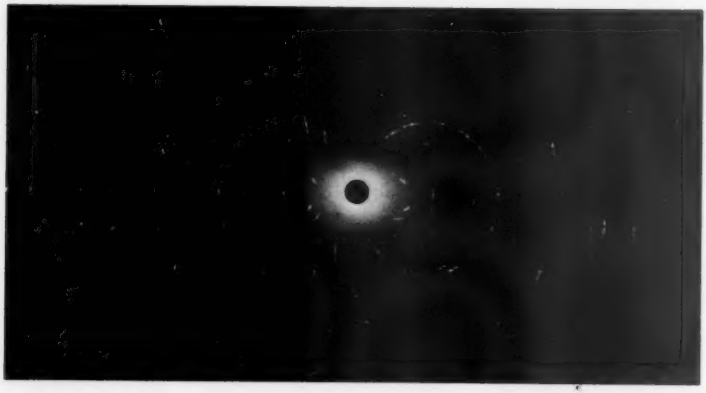

FIGURE 2

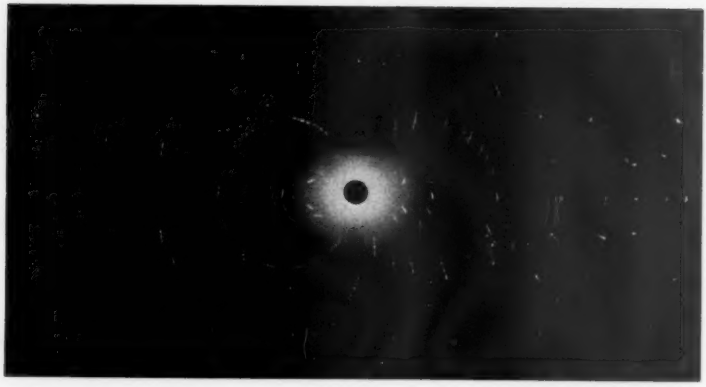

FIGURE 3

SIMULATION OF BEND GLIDING EFFECTS BY COMPOSITE LAUE PHOTOGRAPHS

(3) *c* VERTICAL AND THE UNIQUE *a* AXIS PARALLEL TO THE BEAM: When an imperfect quartz crystal is rotated through 90° about *c* either way from the orientation of case (1), the resulting Laue photograph is different, for one of the *a* axes is now parallel to the beam (Pl. 2, fig. 6). But, as in case (1), reflections on the left and right sides of the film are distorted in a similar manner. Like the a^* axis in the case of (1), this *a* axis must also be unique, since Laue photographs taken with either of the two other *a* axes parallel to the X-ray beam do not show this symmetry of shape of spots.

One of the striking features of this Laue photograph is the nearly uniform shape and size of the distorted spots throughout the film. They are small compared with the spots on the patterns described previously, and many have round to nearly triangular shapes. The front reflections are elongated in a direction tangential to the center of the film. The back reflections are extended perpendicular to the equator.

(4) *c* AXIS VERTICAL AND EITHER OF THE TWO OTHER *a* AXES HORIZONTAL AND PARALLEL TO THE X-RAY BEAM: When the *a* axes on either side of the unique *a* axis in case (3) are set parallel to the X-ray beam, the two Laue patterns reveal spiralling, although the over-all patterns are the same as (3). As in case (2), the spiralling effect shown by one photograph is the opposite of the other. The front reflections on one side of the pattern tend to be extended mainly in a radial direction from the center of the film, whereas the reflections on the other side of the photograph tend to be elongated perpendicular to the equator.

(5) *c* AXIS PARALLEL TO THE X-RAY BEAM: On the Laue photograph of a relatively perfect quartz crystal taken at this orientation, the shape of spots is uniform throughout (Pl. 2, figs. 1, 2). Laue patterns of imperfect quartz grains that show strong asterism and polygonization, however, show reflections that are elongated most along the unique a^* axis and then decrease in length gradually in both directions toward the unique *a* axis perpendicular to it (Pl. 2, fig. 5). As in most transmission Laue patterns, the central area of the photograph of a good quartz grain taken at this setting is devoid of spots, even if it shows slight asterism (Pl. 2, figs. 1, 2). If the distortion of reflections is strong, a short streak occurs near the center of the film directed along that a^* axis upon which the spots are drawn out the most; some smaller streaks are found on the two other a^* axes and still weaker streaks on one or two of the *a* axes (Pl. 2, fig. 5). Since the angle of deviation from the direct beam for these reflections is less than 5°, they must come from planes parallel to the prisms. Normally such reflections should not occur, for the prisms are parallel to the incident X-ray beam. Their appearance must be due to distortion of these planes, and their occurrence mainly on one par-

---

PLATE 3.—SHAPE OF LAUE SPOTS AS RELATED TO CRYSTALLOGRAPHIC ORIENTATION

FIGURE 1.—Quartz grain from gray granite, Mundt quarry, Amberg, Wisconsin, oriented with the *c* axis vertical and the unique a^* axis parallel to the X-ray beam. Illustrates case (1) of the section on shape of Laue spots as related to crystallographic orientation, with the axis of bending horizontal and perpendicular to the X-ray beam. The two prominent ellipses are approximately symmetrical. Compared to Figure 3 of Plate 2 and Figure 1 of Plate 4 the Laue reflections are much more diffuse and tend to blend into the background. Elongated Bragg reflections are now prominent.

FIGURE 2.—Same grain. Illustrates case (2), with a second a^* axis brought parallel to the X-ray beam by a 60-degree clockwise rotation of the horizontal dial. Reflections in the two prominent ellipses are elongated i different fashion and reveal a marked spiralling effect.

FIGURE 3.—Same grain. Oriented with the third a^* axis parallel to the X-ray beam by a 60-degree counterclockwise rotation of the horizontal dial from the position of Figure 1.

PLATE 4.—SIMULATION OF BEND GLIDING EFFECTS BY COMPOSITE LAUE PHOTOGRAPHS

FIGURE 1.—Composite Laue photograph of a normal quartz grain oriented with its *c* axis vertical but tilted through an arc of 7°, by 1-degree intervals, about an *a* axis that is horizontal and perpendicular to the X-ray beam. This photograph is comparable to that from the imperfect grain illustrated in Figure 1 of Plate 3.

FIGURE 2.—Same grain, but with the *a* axis of bending rotated 60° clockwise from the orientation of Figure 1. Comparable to Figure 2 of Plate 3.

FIGURE 3.—Same grain, but with the *a* axis of bending rotated 60° counterclockwise from the orientation of Figure 1. Comparable to Figure 3 of Plate 3.

ticular a^* axis further indicates that the distortion is strongest along that direction.

The above study shows that the shapes of reflections on Laue photographs of an imperfect quartz grain vary systematically with crystallographic orientation. A Laue photograph will show the most elongated asterism streaks only if it is taken with the c axis vertical and a particular a^* axis parallel to the X-ray beam, and the streaks will be spread most transversely if the a axis at 90° from that unique a^* axis is set parallel to the incident beam. All Laue photographs taken with any of the other a or a^* axes parallel to the beam are intermediate and show radially elongated streaks on one side of the film and transversely spread streaks on the other side.

Interpretation

Elongation of Laue reflections in the form of asterism is generally regarded as indicating that portions of the structure are distorted because of plastic deformation (Taylor, 1952, p. 240; Schmid and Boas, 1950, p. 195–198). As a crystal is deformed plastically by bend gliding (axial translation), curvatures develop in the crystal and give rise to streak-shaped Laue spots (Bragg, 1949, p. 202). This phenomenon is revealed commonly on Laue photographs of cold-worked metals.

If a crystal is subdivided into slightly disoriented small crystallites or blocks by plastic deformation, in many cases accompanied or followed by annealing, its Laue pattern also shows asterism. The asterisms now appear as elongated streaks split into a number of striae which correspond to reflections from the individual crystallites. The subdivision of a deformed crystal into subgrains of this type is known in metallurgy as polygonization (Cahn, 1950, p. 156) or as recrystallization *in situ* (Crussard, 1944, p. 120–121). Lacombe (*in* Cahn, 1950, p. 157) suggested that slightly different meanings be given to these two terms: polygonization refers to the very fine subgrains that can be detected only by a special X-ray focusing technique (Guinier and Tennevin, 1950, p. 177–179), whereas recrystallization *in situ* describes later developed, larger blocks that can be detected in ordinary Laue photographs, as in the present study. This latter term is unwieldly, however, and has not been widely used. It is somewhat misleading to geologists, since the effect is produced before the "primary recrystallization" familiar to them in metamorphic processes. Polygonization is used throughout this paper.

The deformed quartz Laue patterns in this study show a striking similarity to Laue patterns of polygonized metals that have been cold-worked in the laboratory and then annealed at some temperature below the primary recrystallization temperature. An insight into the history of these quartz grains may be gained, therefore, by a consideration of the mechanics of the simpler metallic systems. Experimental evidence in metals indicates that polygonization is usually associated with recovery (Cahn, 1950, p. 168; Burke and Turnbull, 1952, p. 220). The strained, high-energy state produced by deformation is partly relieved on annealing by the formation of strain-free blocks separated by higher-energy sub-boundaries within the gross crystal.

The fragmentation of a deformed metal can be given a physical explanation in terms of the theory of dislocations. The term dislocation can be applied to certain regions of atomic misfit, such as may arise through plastic bending of a crystal or slip of one row of atoms relative to another row, where the dislocation forms the boundary between slipped and unslipped parts. It is convenient to describe an arbitrarily oriented dislocation in terms of edge and screw sections, which have slip directions perpendicular and parallel to the dislocation respectively. Most natural crystals contain many such regions of atomic misfit as a result of growth processes, as evidenced by growth spirals and mosaic or lineage structures. Gay, Hirsch, and Kelly (1953, p. 317), using a microbeam X-ray technique, computed the number of dislocations along surfaces of misorientation at 10^6 to 10^8 per sq. cm in unworked metal crystals. Shear applied to such crystals results in plastic deformation because of the migration and multiplication of the dislocations. Gay, Hirsch, and Kelly measured dislocation densities of 10^{10} to 10^{11} cm^{-2} in the more imperfect regions of a number of cold-worked metals.

According to Cottrell (1949, p. 94), Cahn (1950, p. 157–159), and Guinier (1952, p. 428–429), if a crystal is deformed plastically, for example by bending, it will contain a large number of edge dislocations, predominantly of one sign,[1] randomly distributed along the glide planes (Fig. 1*a*). If the bent crystal is

[1] The sign of a dislocation is arbitrarily designated positive or negative depending on whether the atomic misfit creates an extra row of atoms above or below the plane of slip.

annealed at a temperature below the recrystallization point, the dislocations can migrate through the structure and tend to come together, either annihilating one another or combining to form fewer dislocations, so that the crystal will have an over-all lower strain energy. The energy per dislocation is also reduced by forming an orderly array of dislocations in walls normal to the slip direction. The driving force for this process is believed to be the elastic interaction energy of attraction of dislocations (Read, 1953, p. 125–127; Cottrell, 1953, p. 43–51), but thermal energy is required to enable the dislocations to climb from one atomic plane to another in forming the polygonization walls. The over-all structure of the resulting crystal is the same as before annealing, but the crystal consists of a number of relatively perfect crystallites which, inclined to each other at small angles, are separated by arrays of dislocations as sub-boundaries (Fig. 1*b*). Thus, in general, the Laue pattern of a deformed metal crystal first shows asterism because of bending of the atomic planes. After annealing, its Laue asterisms are subdivided because of polygonization. Recent work (Hirsch, 1956, p. 315) suggests that annealing is not a prerequisite in all cases for the formation of dislocation boundaries of this type.

Polygonization can be brought about by other methods of deformation, for example by tension or compression, but with more difficulty than by simple bending, because the necessary lattice curvatures are produced much more readily by bending (Cahn, 1950, p. 155–157; Guinier, 1952, p. 429–430). The rate of polygonization increases, in general, with increase in the temperature at which the deformation has been carried out (Crussard *et al.*, 1950, p. 198; Cahn, 1950, p. 165; Guinier and Tennevin, 1950, p. 180). It also increases with the amount of distortion of the lattice and hence with the intensity of deformation. "Primary recrystallization" takes place at higher temperatures than those required for polygonization and results in removal of the polygonized crystallites and creation of a strain-free, relatively perfect crystal. Deformed and polygonized crystals recrystallize at significantly lower temperatures than do more nearly perfect crystals (Buerger and Washken, 1947, p. 305–307; Guinier and Tennevin, 1950, p. 185–187).

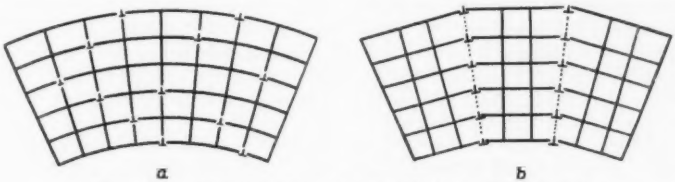

FIGURE 1.—EXPLANATION OF POLYGONIZATION (SCHEMATIC)

a. Random distribution of dislocations of the same sign in a bent crystal. The dislocations are represented by ⊥ symbols.

b. Assembly of the dislocations into walls normal to the bent planes, producing elongate crystallites. Notice that the crystallites are relatively free of dislocations, thus becoming more perfect, while the boundaries between them are discontinuities of orientation. After Cottrell (1949, p. 94).

Because of the similarity of the Laue photographs of the quartz grains under study to those given by many metals and by a number of nonmetallic crystals deformed plastically in the laboratory, these quartz grains have undoubtedly undergone plastic deformation in nature. Examination of the evidence presented above in terms of the dislocation theory indicates that the splitting of Laue spots shown by the specimens can be explained as being due to polygonization of the crystal. In metal crystals the polygon boundaries are in many cases observable after etching, and the distribution of striations within individual Laue reflections can be changed by further annealing treatments (Guinier and Tennevin, 1950, p. 180). In the present study a number of deformed quartz grains were etched, but etching did not reveal recognizable sub-boundaries. Heat treatments ranging from 200° to 900°C. for 100 hours caused a slight sharpening of the striations within Laue streaks at the higher temperatures, but the effect is minor compared to that possible in metals. This is not surprising in view of the differences involved in structure and bonding.

The problem now is to define the mechanism of the deformation. In theory (Berg, 1934, p. 591), if a crystal is bent about an axis perpendicular to the incident X-ray beam, the front reflections will be elongated radially most

along the glide direction and least along the axis of bending. The back reflections will be drawn out about equally and nearly uniformly perpendicular to the axis of bending. Bending around the X-ray beam as an axis, however, will cause Laue reflections to be extended in a tangential direction with respect to the center of the film, in both the front and back reflection regions. The elongation is smaller than that produced by bending around an axis perpendicular to the beam. This analysis is in almost perfect agreement with the observations made in this study; hence the plastic deformation of quartz in nature must proceed in the form of bend gliding (axial translation).

X-ray results show that the Laue reflections produced by a deformed quartz grain show the greatest radial elongation only if the photograph is taken with the unique a axis perpendicular to the beam and have a smaller tangential spreading only if the photograph is taken with that same a axis parallel to the beam. Laue patterns made at any other orientation reveal a marked asymmetry of shape of the distorted spots. This unique a axis, therefore, must be the axis of bending. The axis of bending has been determined in this manner on 41 quartz grains taken from 24 localities scattered over North America. Most of the grains were taken from massive granitic rocks, which have given more diffuse Laue patterns, in general, than any of the other rock types here investigated. Axes of bending also can be determined from Laue patterns which are only slightly or moderately diffuse. These patterns were given by quartz from quartzites, dikes and sills, and schists. In all cases one of the a axes is the major axis of bending. A more detailed analysis of the patterns reveals that many quartz grains show, in addition, small components of bending about the other two a axes; a few grains show components of bending about one or more of the a^* axes as well as about the unique a axis. These consistent results for quartz from different geologic environments indicate the crystallographic control of the quartz structure over the plastic deformation.

The direction of gliding must be at right angles to the axis of bending. Reflections should tend to be elongated most along the glide direction; this suggests that in the deformed quartz grains studied the unique a^* axis normal to the a axis of bending (cases 1 and 5) must be the glide direction. Elongation is greatest along this a^* direction in the Laue patterns described, but not all directions normal to the axis of bending have been observed because of the limited number of orientations used. All directions in the zone between the a^* and c axes are normal to the unique a axis and thus are possible glide directions. For this reason additional Laue photographs were taken of a few grains exhibiting a well-defined a axis of bending. The grains were oriented first with the axis of bending vertical and different directions in the a^*-c zone perpendicular to the X-ray beam, and then with the axis of bending parallel to the beam and the a^*-c plane perpendicular to the beam. The results, however, are not clear-cut, and it is not yet possible to assign a unique glide direction. Equal elongation apparently is given by several directions in this zone; this suggests multiple glide directions. All these glide directions lie within 45° on either side of a^*, and they can probably be restricted to a zone between the basal pinacoid and the unit rhombohedron.

This study is confined to naturally deformed quartz grains from massive rocks and does not include single crystals deformed under controlled conditions. The writers believe, however, that the mechanism discussed above can be applied equally well to both cases, since similar deformation features on a small scale have been reported to occur in artificially deformed single crystals of quartz (Griggs and Bell, 1938, p. 1737). Plastic deformation of a polycrystalline quartz aggregate must be more complex, since it involves not only intragranular bending but also intergranular movements, as shown by the cataclastic features described above. Hence the stress distribution of the system may be greatly affected by the movements between individual grains, and the final deformation will result from the combined effects of the two types of movements. This may explain the possible existence of multiple glide directions in the tested grains and the observed small components of bending about other horizontal axes in addition to the unique a axis. Since the three a axes are crystallographically equivalent, any one of them should be equally qualified as the axis of bending, and the ultimate selection must depend on the directional relation of the axes to the distribution of stresses during deformation.

The mechanism of deformation defined here has been tested in the following way. A normal quartz grain was oriented on the goniometer with c vertical and an a^* axis placed horizontally and parallel to the X-ray beam. A Laue photograph was taken with an exposure time of 30 minutes. Then, to approximate the mechanism of bend gliding, the grain was tilted 3° on

each side of this position, 1° at a time, by means of the north-south adjusting arc. After each 1-degree tilt the grain was recentered, and another exposure was made on the same film for 10 minutes. This gave a composite X-ray pattern which simulates that given by a crystal bent by 7° around an *a* axis normal to the beam. The same procedure was repeated with different a^* axes successively brought parallel to the beam, and composite photographs were made at each setting. For these latter patterns the axis of bending (*a*) remains the same but is not perpendicular to the X-ray beam. A comparison of this series of Laue photographs (Pl. 4) with that produced by a naturally deformed quartz grain (Pl. 3) shows that the two are remarkably similar.

On the Laue photographs taken by tilting the specimen through 7°, 1° at a time, every Laue reflection is replaced by seven sharp, discrete subspots, each the image of the crystal, as if the crystal had been subdivided into seven differently oriented (1°) crystallites. Since the Laue reflections produced by many of the naturally deformed quartz grains are split similarly, each of them must be made of subgrains; that is, they are polygonized. This experiment offers further support of the conclusion already reached after comparing the splitting of Laue spots shown by these specimens with the splitting shown by cold-worked metals. But each of the subdivided Laue asterisms shown by an actually deformed crystal consists of numerous closely spaced, fine striations, indicating that the crystallites are very small and have lattice orientations that commonly differ only by a few minutes of arc or less.

For the deformed crystals strong asterism and polygonization effects are accompanied on the film by intense reflections due to characteristic radiation. These reflections are split into subspots and extended along the arcs of powder rings; this is additional evidence for the fragmentation and misorientation of the structure. With the *c* axis of the crystal vertical the maximum vertical extension of these reflections was 12° in the specimens of this study. In addition, there is a horizontal component of misorientation, since the same plane will reflect the characteristic wave length over a considerable horizontal rocking angle. A grain from the Amberg, Wisconsin, granite (Mundt quarry) was selected as representative of the more imperfect quartz specimens, and a grain from the granitic differentiate of the Bridgland sill, Ontario, was selected as representative of nearly perfect quartz. The Amberg sample gave a horizontal rocking angle of 11° with CuKα radiation for the reflection from the rhombohedron *r*, as contrasted to 1° for the Bridgland sample. These values compare favorably with the measured elongation of the Laue reflection from the same plane for these samples, as recorded in Table 3. The occurrence of a large number of characteristic reflections on the Laue patterns of distorted quartz grains is a direct consequence of the considerable angle over which these reflections can take place as a result of the distortion.

Although quartz is almost universally twinned according to the Dauphiné law, few of the quartz grains having strong Laue asterism show this type of twinning (Table 2). They may have been untwinned in the process of plastic deformation by bend gliding. The adjacent elements or domains of a Dauphiné twin are joined together on the plane $(10\bar{1}0)$ and may be imagined as being derived from an original single crystal by rotation of the Si—O—Si bond between groups of linked SiO_4 tetrahedra to produce a buckling of these groups in opposite directions across the composite plane with only a small atomic displacement. A twinned crystal deformed in the manner established by the present study, by bending around an *a* axis lying in the twin plane, might have its twinned parts buckle in the same direction, thus giving rise to a single crystal of α quartz. Hall (1954, p. 62) reported that metallic specimens of tin and zinc can be twinned or untwinned at will in a similar manner by bending. The observations made by Wooster *et al.* (1947) and by Thomas and Wooster (1951) on the experimental elimination of Dauphiné twinning in quartz oscillator plates by the application of stress, for example by bending, compression, or torque under moderate temperatures, lend support to this explanation.

One theory of origin attributes the formation of Dauphiné twins to passage through the β-α transition on cooling as a consequence of the difference in symmetry of β and α quartz (Frondel, 1945, p. 450). An alternative explanation of the paucity of Dauphiné twinning in the deformed quartz grains, therefore, might be that these grains crystallized below the β-α inversion (about 573°C.). This view finds some support in the fact that many of the deformed crystals in this study have come from those granitic bodies which petrologists have been most likely to call "granitized", *i.e.*, formed at relatively low temperatures by metamorphism of previously existing rocks. Table 2, however, shows that the reduction in

TABLE 3.—SUMMARY OF PETROGRAPHIC AND X-RAY-DIFFRACTION DATA

Specimen	Locality	Geologic origin and reference	Number of quartz grains tested	Petrographic data (U. E. = range of undulatory extinction in quartz)	Quality of Laue pattern (r = length of asterism from the unit rhombohedron)
Quartz crystals SWB-1	Crystal Mountains, Hot Springs, Arkansas	Hydrothermal (Engel, 1952)	4	Quartz shows uniform extinction	Sharp pattern
Quartz-gold vein 17144	Siskiyou County, California	Hydrothermal (Lindgren, 1895)	3	Quartz shows uniform extinction	Slight asterism $r = 1.5°$
Quartz-barite deposit	Hornsey Bros. barite mine, Potosi, Missouri	Epigenetic aqueous (Tarr, 1918; Bastin and Behre, 1939)	2	Quartz shows uniform extinction	Sharp pattern
Quartz porphyry sill A-19-9	Leadville, Colorado	Magmatic (Emmons *et al.*, 1927)	2	Embayed quartz phenocrysts show uniform extinction	Slight asterism $r = 1.5°$
Quartz porphyry dike A-15-6	Annapolis, Missouri	Magmatic (Haworth, 1895)	2	Quart shows variable U.E. 1°–4°	Slight asterism $r = 1$–$3°$
Quartz-feldspar porphyry dike SWB-2	Notre Dame Bay, Newfoundland	Magmatic	2	Quartz shows variable U.E. 1°–2°	Slight asterism $r = 2°$
Quartz porphyry dike B-13-22	Summit County, Colorado	Magmatic (Ransome, 1911)	2	Euhedral quartz phenocrysts with uniform extinction	Sharp pattern
Granitic dike in gabbro 38-20	Mellen, Wisconsin	Magmatic (Emmons and Gates, 1943)	2	Coarse-grained with feldspars dominant, interstitial and graphic quartz with weak to moderate U.E. 1°–4°	Sharp pattern
Granitic top of diabase sill SWB-3	Bridgland, Ontario	Magmatic (Emmons, 1927)	4	Feldspars heavily sericitized and chloritized; embayed quartz shows uniform extinction	Sharp pattern
Granitic top of diabase sill M-12	Pigeon Point, Minnesota	Magmatic (Grout, 1928)	3	Granophyric; quartz shows uniform extinction	Sharp pattern
Quartz diorite EDK-9-11	Sudbury, Ontario	Magmatic (Collins and Kindle, 1935)	3	Delicate granophyric texture; quartz shows uniform extinction	Sharp pattern
Rhyolite A-17-9	Red Rock Point, Minnesota	Volcanic (Irving, 1883)	2	Euhedral quartz with uniform extinction	Sharp pattern
Rhyolite SWB-4	Notre Dame Bay, Newfoundland	Volcanic	2	Quartz shows slight U.E. 1°–2°	Slight asterism $r = 2°$
Rhyolite A-16-2	Signal Point, Yellowstone Lake, Wyoming	Volcanic (Iddings, 1899)	2	Broken euhedral quartz grains with uniform extinction	Sharp pattern
Granitic dike E-44-26	Wausau, Wisconsin	Magmatic*	8	Coarse quartz with variable extinction, uni-	Patterns variable from sharp

Granitic dike E-44-26	Wausau, Wisconsin	Magmatic*	8	Coarse quartz with variable extinction, uniform to moderate U.E. 1°–6°; sericitized feldspar in irregular pattern with quartz in fine mosaic texture	Patterns variable from sharp to slight asterism $r = 1°–3°$
Granitic dike P-1, 2	Golden's Bridge, New York	Magmatic (sheared)	5	Even granular, foliated; quartz often shows weak to moderate U.E. 1°–5°	Slight to moderate asterism and polygonization $r = 2°–3°$
Pegmatite in granitic dike P-3	Golden's Bridge, New York	Magmatic	2	Slightly bent twinning lamellae in plagioclase; quartz shows U.E. 1.5°–6°	Slight asterism and polygonization $r = 2°$
Hartland mica-quartz schist H-722	Central New Preston quadrangle, Connecticut	Metamorphic (Gates and Bradley, 1952)	3	Well-developed orientation; quartz has uniform extinction	Weak asterism $r = 1°–2°$
Waramaug mica-quartz gneiss H-707 matrix	North-central New Preston quadrangle, Connecticut	Metamorphic (Gates and Bradley, 1952)	4	Well-developed orientation; quartz has uniform extinction	Sharp pattern
Waramaug gneiss quartz lenses in H-707	North-central New Preston quadrangle, Connecticut	Metamorphic (Gates and Bradley, 1952)	4	Uniform extinction	Sharp pattern
Mica-quartz gneiss H-775 matrix	SE Woodbury quadrangle, Connecticut	Metamorphic (Gates, 1954)	2	Well-developed orientation with some graphic intergrowths of quartz and feldspar; quartz extinction sharp to slight U.E. 2°–3°	Sharp pattern
Quartz lenses in H-775	SE Woodbury Quadrangle, Connecticut	Metamorphic (Gates, 1954)	2	Uniform extinction	Sharp pattern
White quartzite immediately above intrusive syenite SWB-5	Wausau, Wisconsin	Metamorphic,* (show-some hydrothermal effects)	5	Interstitial perthite, microcline, and plagioclase; quartz has subsutured borders, U.E. 1°–2.5°	Sharp pattern
White quartzite SWB-6	Rib Mountain, Wausau, Wisconsin	Metamorphic, (heavily veined by quartz) (Emmons, 1940)	7	Muscovite present; quartz has uniform extinction to U.E. 1°–2.5°	Sharp pattern
Mississagi quartzite SWB-7	North Lake Huron, Ontario	Metamorphic (Collins, 1925)	2	Quartz has U.E. 3°–6°	Moderate asterism and polygonization $r = 5°$
Quartz rock member of iron formation series SWB-8	Mt. Wright area, north Quebec	Uncertain	4	Uniform extinction	Sharp pattern
Granitic phacolith E-52-9	Hyde School, Gouverneur, New York	Magmatic (Buddington, 1939)	6	Quartz extinction uniform to weak U.E. 2°–3°	Slight asterism $r = 0.5°–3°$

* R. C. Emmons, based on unpublished field work.

TABLE 3.—*Continued*

Specimen	Locality	Geologic origin and reference	Number of quartz grains tested	Petrographic data (U. E. = range of undulatory extinction in quartz	quality of Laue pattern (r = length of asterism from the unit rhombohedron)
Pegmatite in granitic phacolith E-52-9a	Hyde School, Gouverneur, New York	Magmatic (Buddington, 1939)	6	Graphic texture; quartz shows weak U.E. 1.5°–3°	Sharp pattern r = 0.5°–2°
Fine-grained red granite BH-39-3	Baxter Hollow, Wisconsin	Magmatic (Gates, 1942)	4	Even granular; quartz mainly with uniform extinction but some grains with U.E. 3°–5°	Slight asterism r = 1°–3°
Gray-green granite porphyry A-3-9	Saganaga Lake, Minnesota	Magmatic (Grout, 1929)	4	Plagioclase shows slightly bent and offset twin lamellae; quartz in clusters of grains with angular and subsutured borders, U.E. 3°–4°	Slight asterism r = 3°
Nonewaug white granite H-492	North Woodbury Quadrangle, Connecticut	Magmatic (Gates, 1954)	4	Equigranular quartz - feldspar - muscovite; quartz extinction mainly uniform with some U.E. 1°–4°	Moderate asterism and polygonization r = 2°–7°
Pink hornblende granite A-3-14	Snowbank Lake, Minnesota	Magmatic (Sanders, 1929; Balk and Grout, 1934)	4	Equigranular quartz - feldspar - hornblende; quartz has moderate U.E. 2°–7°	Moderate asterism and polygonization r = 2°–7°
Light-red granite, slightly banded GP-32	Red Granite, Wisconsin	Uncertain*	3	Porphyritic with some quartz showing weak to moderate U.E. 1°–5°	Moderate asterism and polygonization r = 1.5°–4°
Light-red granite GP-36	New London, Wisconsin	Uncertain*	3	Fine-grained with sutured borders; quartz shows moderate U.E. 3°–5°	Slight asterism r = 1°–2°
Gray rapakivi granite SWB-9	Waupaca, Wisconsin	Metasomatic* (granitized greenstone)	7	Porphyritic with myrmekite around perthite and plagioclase; large quartz grains with U.E. 4°–6°	Patterns variable from fairly sharp to moderate asterism and polygonization r = 2°–4°
Red granite HF-16	High Falls, Wisconsin	Metasomatic* (feldspathized sandstone)	4	Heavily sericitized feldspars with U.E.; quartz of two types, small grains with interlocking borders and uniform extinction, larger grains with U.E. up to 13°	Moderate asterism and polygonization r = 4°–6°
Granite porphyry SWB-10	Near Aurora, Florence County, Wisconsin	Metasomatic (Bradley and Lyons, 1953)	3	Large grains of microcline with quartz inclusions; myrmekite around feldspars; quartz with moderate U.E. 3°–5° with slight granulation and fracturing	Moderate asterism and polygonization r = 2°–6°

Gray granite 4553-11	On U.S. Highway 141 north of Pembine, Wisconsin	Metasomatic* (granitized greenstone)	4	Feldspars are zoned and sericitized; quartz with strong strain shadows U.E. 1°–9°	Moderate asterism and polygonization $r = 2°–6°$
Coarse granite 49-8	Athelstane, Wisconsin	Metasomatic* (granitized greenstone)	2		Moderate asterism $r = 2°–5°$
Pink siliceous granite with relict cross-bedding N-10, 11	Neillsville, Wisconsin	Metasomatic*	2	Fine- and even grained with aggregates of large grains; feldspars slightly bent; quartz with weak to moderate U.E. but large grains with U.E. up to 8°	Moderate asterism and polygonization $r = 2°–6°$
Augen gneiss SWB-11	Neillsville, Wisconsin	Metasomatic*	8	Biotite-quartz-feldspar gneiss with large lenses of aggregates of quartz or feldspar; quartz with weak to moderate U.E. 2°–6° and a few faint deformation lamellae	Moderate asterism and polygonization $r = 1°–6°$
Rapakivi granite SWB-12	Tigerton, Wisconsin	Metasomatic* (associated with pegmatite dikes)	4	Porphyritic with myrmekite; feldspars with slightly bent twin lamellae; quartz with moderate U.E. 3°–6° but with many grains of uniform extinction	Moderate asterism and polygonization $r = 2°–6°$
Pegmatoid granite SWB-13	Middle Inlet, Wisconsin	Metasomatic* (associated with hydrothermal effects)	6	Plagioclase with severely bent twin lamellae; quartz with zones of strong U.E. 3°–7° and mortar texture	Strong asterism and polygonization $r = 5°–9°$
Gray granite 49-6	On U.S. Highway 141 near Amberg, Wisconsin	Metasomatic* (granitized greenstone transected by pegmatites)	5	Myrmekite around plagioclase, bent twin lamellae in feldspars; quartz with zones of strong U.E. 3°–11°, mortar texture, and deformation lamellae	Strong asterism and polygonization $r = 5°–15°$
Fine-grained dark-red granite SWB-14	Montello, Wisconsin	Uncertain*	9	Some areas with granophyric texture; quartz shows zones of strong U.E. 2°–10°; marginal granulation and a few deformation lamellae; feldspars show bent twin lamellae and inclusions of aggregates of quartz along fractures	Strong asterism and polygonization $r = 6°–15°$
Red gneissic granite SWB-15	Southeast shore of Tyson Lake, north Ontario	Metasomatic (Quirke and Collins, 1930)	4		Strong asterism and polygonization $r = 7°–10°$

* R. C. Emmons, based on unpublished field work.

TABLE 3.—*Concluded*

Specimen	Locality	Geologic origin and reference	Number of quartz grains tested	Petrographic data (U. E. = range of undulatory extinction in quartz)	Quality of Laue pattern (r = length of asterism from the unit rhombohedron)
White gneissic granite SWB-16	Fletcher Bros. quarry, North Chelmsford, Massachusetts	Metasomatic (Currier, 1937; 1947)	7	Feldspars with bent twin lamellae and containing aggregates of quartz along fractures; quartz with strong U.E. 3°–11° and mortar texture; mica with wavy bands and U.E.	Moderate to strong asterism and polygonization r = 6°–10°
Gray granite SWB-17	Mundt quarry, Amberg, Wisconsin	Metasomatic* (granitized greenstone)	9	Plagioclase zoned and has bent twin lamellae; mortar texture in quartz and feldspar; quartz with zones of strong U.E. 2°–10° and deformation lamellae	Strong asterism and polygonization r = 9°–15°
Bluish-gray granite SWB-18	Quincy, Massachusetts	Magmatic (LaForge, 1932; Chute, 1940)	8	Perthite dominant; quartz shows zones of moderate to strong U.E. 2°–9°	Moderate to strong asterism and polygonization r = 5°–11°
Red granite SWB-19	Anderson Bros. quarry, Wausau, Wisconsin	Uncertain* (probably metasomatic)	9	Perthite dominant, plagioclase with bent twin lamellae and U.E.; quartz with zones of mortar texture, deformation lamellae, and U.E. 5°–14°	Strong asterism and polygonization r = 9°–14°
Red granite SWB-20	Wausau granite company quarry, Wausau, Wisconsin	Uncertain* (probably metasomatic)	5	Similar to above with crushing in feldspars; marginal granulation, deformation lamellae, and strong U.E. 6°–10° in quartz	Strong asterism and polygonization r = 7°–11°
Pink granite R14962	Cressbrook Creek near Crow's Nest, Queensland, Australia	Magmatic (sheared phase)	2	Quartz has U.E. 15°–25°, mortar texture, lies in fine-grained fault gouge of quartz-feldspar-mica	Strong asterism r = 7°–15° with incomplete polygonization
Rhyolite A-22-18	Noble's quarry, Marquette, Wisconsin	Volcanic (Chamberlin, 1877).	2	Rounded quartz and feldspar phenocrysts in fine-grained matrix; quartz has U.E. 5°–9° and fractures	Moderate to strong asterism and polygonization r = 5°–9°
Quartz porphyry dike A-14-10	Monterey, Franklin County, Pennsylvania	Magmatic (Bascom, 1896)	4	Rounded quartz and feldspar phenocrysts in fine-grained matrix; quartz has U.E. 8°–15°	Strong asterism and polygonization r = 13°–15°
Rhyolite A-14-6	Thüringer Wald, Germany	Volcanic (flow structure) (Johs, 1933)	5	Rounded and elongated quartz and feldspar phenocrysts in flow structure; quartz is fractured, has U.E. 12°–22°, some recrystallization within grains	Strong asterism and polygonization r = 10°–15°

* R. C. Emmons, based on unpublished field work.

twinning is just as great in deformed magmatic quartz-bearing rocks as in the metasomatic types, which emphasizes the more general influence of the deformation as the cause of the elimination of the twinning.

Correlation of X-ray Study and Microscopic Observations

A close correlation exists between the petrographic features and the X-ray-diffraction patterns. Quartz grains from rock specimens that do not show deformation features give sharp Laue patterns. The first group of the preceding petrographic classification falls into this category. As undulatory extinction develops and becomes stronger, the degree of Laue asterism increases correspondingly, as demonstrated in rocks of the second group. If specimens show strong undulatory extinction and marginal granulation in quartz and bent twinning lamellae in feldspars, the quartz grains give Laue photographs that exhibit both greatly elongated and polygonized asterism streaks. Table 3 summarizes the optical and X-ray results for all samples. This table shows that a particularly good correlation exists between the degree of undulatory extinction and the degree of elongation of the Laue reflection from the unit rhombohedron. These data indicate that undulatory extinction is the optical expression of the effects of plastic deformation.

In terms of the dislocation theory, the crystallites created in a deformed quartz by bend gliding and polygonization are inclined to each other at small angles. This must result in a relative displacement of the optic axes of the subgrains, and the extinction position of the "mother" crystal will therefore vary from one area to another, which accounts for the familiar wavy extinction seen under the microscope. This extinction will sweep across the field of view on the rotation of the microscope stage if the quartz grain is oriented with the axis of bending vertical. For other orientations the sweeping effect will be less noticeable, and the variation in extinction angles will be smaller. Since the misorientation of the crystallites is very small, the bands of undulatory extinction should be, as they are, subparallel to each other, but the departure from this relationship increases with increasing deformation. As the deformation increases in intensity, the extinction bands become regular, narrow, and pronounced. The writers believe that this is a consequence of the greater concentration of the dislocations into walls normal to the bent glide planes, creating elongate polygonized zones or crystallites (Fig. 1*b*). The minute fractures found between the extinction zones in some places may have developed along certain of these sub-boundaries of the crystallites. According to the hypothesis advanced by Sander (1930, p. 175) and later supported by Griggs and Bell (1938, p. 1735), quartz tends to fracture into needlelike fragments during deformation. The crystallite sub-boundaries, which are arrays of dislocations, are potential loci of easy rupture and may be involved in this process. Fracturing and displacement along faults complicate the extinction patterns created by bending and polygonization.

The association of deformation lamellae and strong strain shadows in quartz is in accord with the view of previous investigators (Fairbairn, 1941, p. 1266; Ingerson and Tuttle, 1945, p. 96) that the lamellae occur only in deformed but unrecrystallized rocks. Many of the lamellae are nearly perpendicular to the extinction bands. These may be traces of translation glide planes (Mügge, 1896, p. 769–770; Sander, 1930, p. 178; Hietanen, 1938, p. 34; Fairbairn, 1941, p. 1272–1273). In an attempt to ascertain whether this is the case, two grains from different localities, showing deformation lamellae, were cut from thin sections for X-ray study. The Laue patterns are somewhat more distorted than others from the same rocks, but no evidence indicates whether or not the lamellae represent glide planes. The grains show well-developed *a* axes of bending but no unique glide direction or plane. Fairbairn (1941, p. 1269) and Ingerson and Tuttle (1945, p. 102) state as a result of statistical studies that deformation lamellae have variable orientations relative to the *c* axes of individual grains. The relationship of this irrational orientation of the lamellae to the lack of unique glide direction found in this study is not clear. Possibly the macroscopic lamellae are composed, on an atomic scale, of packets of nonparallel glide planes. If the lamellae do represent such glide surfaces, it may mean that the bending axis is the controlling feature of the deformation and that gliding can occur along a number of directions normal to that axis.

Discussion of Results

Many people have postulated from petrographic evidence that quartz must deform plastically in nature, but attempts to prove it experimentally have not succeeded (Griggs

* R. C. Emmons, based on unpublished field work.

TABLE 3.—SUMMARY OF PETROGRAPHIC AND X-RAY-DIFFRACTION DATA

Specimen	Locality	Geologic origin and reference	Number of quartz grains tested	Petrographic data (U. E. = range of undulatory extinction in quartz)	Quality of Laue pattern (r = length of asterism from the unit rhombohedron)
Quartz crystals SWB-1	Crystal Mountains, Hot Springs, Arkansas	Hydrothermal (Engel, 1952)	4	Quartz shows uniform extinction	Sharp pattern
Quartz-gold vein 17144	Siskiyou County, California	Hydrothermal (Lindgren, 1895)	3	Quartz shows uniform extinction	Slight asterism $r = 1.5°$
Quartz-barite deposit	Hornsey Bros. barite mine, Potosi, Missouri	Epigenetic aqueous (Tarr, 1918; Bastin and Behre, 1939)	2	Quartz shows uniform extinction	Sharp pattern
Quartz porphyry sill A-19-9	Leadville, Colorado	Magmatic (Emmons *et al.*, 1927)	2	Embayed quartz phenocrysts show uniform extinction	Slight asterism $r = 1.5°$
Quartz porphyry dike A-15-6	Annapolis, Missouri	Magmatic (Haworth, 1895)	2	Quart shows variable U.E. 1°–4°	Slight asterism $r = 1$–$3°$
Quartz-feldspar porphyry dike SWB-2	Notre Dame Bay, Newfoundland	Magmatic	2	Quartz shows variable U.E. 1°–2°	Slight asterism $r = 2°$
Quartz porphyry dike B-13-22	Summit County, Colorado	Magmatic (Ransome, 1911)	2	Euhedral quartz phenocrysts with uniform extinction	Sharp pattern
Granitic dike in gabbro 38-20	Mellen, Wisconsin	Magmatic (Emmons and Gates, 1943)	2	Coarse-grained with feldspars dominant, interstitial and graphic quartz with weak to moderate U.E. 1°–4°	Sharp pattern
Granitic top of diabase sill SWB-3	Bridgland, Ontario	Magmatic (Emmons, 1927)	4	Feldspars heavily sericitized and chloritized; embayed quartz shows uniform extinction	Sharp pattern
Granitic top of diabase sill M-12	Pigeon Point, Minnesota	Magmatic (Grout, 1928)	3	Granophyric; quartz shows uniform extinction	Sharp pattern
Quartz diorite EDK-9-11	Sudbury, Ontario	Magmatic (Collins and Kindle, 1935)	3	Delicate granophyric texture; quartz shows uniform extinction	Sharp pattern
Rhyolite A-17-9	Red Rock Point, Minnesota	Volcanic (Irving, 1883)	2	Euhedral quartz with uniform extinction	Sharp pattern
Rhyolite SWB-4	Notre Dame Bay, Newfoundland	Volcanic	2	Quartz shows slight U.E. 1°–2°	Slight asterism $r = 2°$
Rhyolite A-16-2	Signal Point, Yellowstone Lake, Wyoming	Volcanic (Iddings, 1899)	2	Broken euhedral quartz grains with uniform extinction	Sharp pattern
Granitic dike E-44-26	Wausau, Wisconsin	Magmatic*	8	Coarse quartz with variable extinction, uniform to moderate U.E. 1°–6°; sericitized	Patterns variable from sharp to slight asterism $r = 1°$–

Granitic dike E-44-26	Wausau, Wisconsin	Magmatic*	8	Coarse quartz with variable extinction, uniform to moderate U.E. 1°–6°; sericitized feldspar in irregular pattern with quartz in fine mosaic texture	Patterns variable from sharp to slight asterism $r = 1°–3°$
Granitic dike P-1, 2	Golden's Bridge, New York	Magmatic (sheared)	5	Even granular, foliated; quartz often shows weak to moderate U.E. 1°–5°	Slight to moderate asterism and polygonization $r = 2°–3°$
Pegmatite in granitic dike P-3	Golden's Bridge, New York	Magmatic	2	Slightly bent twinning lamellae in plagioclase; quartz shows U.E. 1.5°–6°	Slight asterism and polygonization $r = 2°$
Hartland mica-quartz schist H-722	Central New Preston quadrangle, Connecticut	Metamorphic (Gates and Bradley, 1952)	3	Well-developed orientation; quartz has uniform extinction	Weak asterism $r = 1°–2°$
Waramaug mica-quartz gneiss H-707 matrix	North-central New Preston quadrangle, Connecticut	Metamorphic (Gates and Bradley, 1952)	4	Well-developed orientation; quartz has uniform extinction	Sharp pattern
Waramaug gneiss quartz lenses in H-707	North-central New Preston quadrangle, Connecticut	Metamorphic (Gates and Bradley, 1952)	4	Uniform extinction	Sharp pattern
Mica-quartz gneiss H-775 matrix	SE Woodbury quadrangle, Connecticut	Metamorphic (Gates, 1954)	2	Well-developed orientation with some graphic intergrowths of quartz and feldspar; quartz extinction sharp to slight U.E. 2°–3°	Sharp pattern
Quartz lenses in H-775	SE Woodbury Quadrangle, Connecticut	Metamorphic (Gates, 1954)	2	Uniform extinction	Sharp pattern
White quartzite immediately above intrusive syenite SWB-5	Wausau, Wisconsin	Metamorphic,* (showsome hydrothermal effects)	5	Interstitial perthite, microcline, and plagioclase; quartz has subsutured borders, U.E. 1°–2.5°	Sharp pattern
White quartzite SWB-6	Rib Mountain, Wausau, Wisconsin	Metamorphic, (heavily veined by quartz) (Emmons, 1940)	7	Muscovite present; quartz has uniform extinction to U.E. 1°–2.5°	Sharp pattern
Mississagi quartzite SWB-7	North Lake Huron, Ontario	Metamorphic (Collins, 1925)	2	Quartz has U.E. 3°–6°	Moderate asterism and polygonization $r = 5°$
Quartz rock member of iron formation series SWB-8	Mt. Wright area, north Quebec	Uncertain	4	Uniform extinction	Sharp pattern
Granitic phacolith E-52-9	Hyde School, Gouverneur, New York	Magmatic (Buddington, 1939)	6	Quartz extinction uniform to weak U.E. 2°–3°	Slight asterism $r = 0.5°–3°$

* R. C. Emmons, based on unpublished field work.

TABLE 3.—*Continued*

Specimen	Locality	Geologic origin and reference	Number of quartz grains tested	Petrographic data (U. E. = range of undulatory extinction in quartz	quality of Laue pattern (r = length of asterism from the unit rhombohedron)
Pegmatite in granitic phacolith E-52-9a	Hyde School, Gouverneur, New York	Magmatic (Buddington, 1939)	6	Graphic texture; quartz shows weak U.E. 1.5°–3°	Sharp pattern r = 0.5°–2°
Fine-grained red granite BH-39-3	Baxter Hollow, Wisconsin	Magmatic (Gates, 1942)	4	Even granular; quartz mainly with uniform extinction but some grains with U.E. 3°–5°	Slight asterism r = 1°–3°
Gray-green granite porphyry A-3-9	Saganaga Lake, Minnesota	Magmatic (Grout, 1929)	4	Plagioclase shows slightly bent and offset twin lamellae; quartz in clusters of grains with angular and subsutured borders, U.E. 3°–4°	Slight asterism r = 3°
Nonewaug white granite H-492	North Woodbury Quadrangle, Connecticut	Magmatic (Gates, 1954)	4	Equigranular quartz - feldspar - muscovite; quartz extinction mainly uniform with some U.E. 1°–4°	Moderate asterism and polygonization r = 2°–7°
Pink hornblende granite A-3-14	Snowbank Lake, Minnesota	Magmatic (Sanders, 1929; Balk and Grout, 1934)	4	Equigranular quartz - feldspar - hornblende; quartz has moderate U.E. 2°–7°	Moderate asterism and polygonization r = 2°–7°
Light-red granite, slightly banded GP-32	Red Granite, Wisconsin	Uncertain*	3	Porphyritic with some quartz showing weak to moderate U.E. 1°–5°	Moderate asterism and polygonization r = 1.5°–4°
Light-red granite GP-36	New London, Wisconsin	Uncertain*	3	Fine-grained with sutured borders; quartz shows moderate U.E. 3°–5°	Slight asterism r = 1°–2°
Gray rapakivi granite SWB-9	Waupaca, Wisconsin	Metasomatic* (granitized greenstone)	7	Porphyritic with myrmekite around perthite and plagioclase; large quartz grains with U.E. 4°–6°	Patterns variable from fairly sharp to moderate asterism and polygonization r = 2°–4°
Red granite HF-16	High Falls, Wisconsin	Metasomatic* (feldspathized sandstone)	4	Heavily sericitized feldspars with U.E.; quartz of two types, small grains with interlocking borders and uniform extinction, larger grains with U.E. up to 13°	Moderate asterism and polygonization r = 4°–6°
Granite porphyry SWB-10	Near Aurora, Florence County, Wisconsin	Metasomatic (Bradley and Lyons, 1953)	3	Large grains of microcline with quartz inclusions; myrmekite around feldspars; quartz with moderate U.E. 3°–5° with slight granulation and fracturing	Moderate asterism and polygonization r = 2°–6°

				slight granulation and fracturing	
Gray granite 4553-11	On U.S. Highway 141 north of Pembine, Wisconsin	Metasomatic* (granitized greenstone)	4	Feldspars are zoned and sericitized; quartz with strong strain shadows U.E. 1°–9°	Moderate asterism and polygonization $r = 2°–6°$
Coarse granite 49-8	Athelstane, Wisconsin	Metasomatic* (granitized greenstone)	2		Moderate asterism $r = 2°–5°$
Pink siliceous granite with relict cross-bedding N-10, 11	Neillsville, Wisconsin	Metasomatic*	2	Fine- and even grained with aggregates of large grains; feldspars slightly bent; quartz with weak to moderate U.E. but large grains with U.E. up to 8°	Moderate asterism and polygonization $r = 2°–6°$
Augen gneiss SWB-11	Neillsville, Wisconsin	Metasomatic*	8	Biotite-quartz-feldspar gneiss with large lenses of aggregates of quartz or feldspar; quartz with weak to moderate U.E. 2°–6° and a few faint deformation lamellae	Moderate asterism and polygonization $r = 1°–6°$
Rapakivi granite SWB-12	Tigerton, Wisconsin	Metasomatic* (associated with pegmatite dikes)	4	Porphyritic with myrmekite; feldspars with slightly bent twin lamellae; quartz with moderate U.E. 3°–6° but with many grains of uniform extinction	Moderate asterism and polygonization $r = 2°–6°$
Pegmatoid granite SWB-13	Middle Inlet, Wisconsin	Metasomatic* (associated with hydrothermal effects)	6	Plagioclase with severely bent twin lamellae; quartz with zones of strong U.E. 3°–7° and mortar texture	Strong asterism and polygonization $r = 5°–9°$
Gray granite 49-6	On U.S. Highway 141 near Amberg, Wisconsin	Metasomatic* (granitized greenstone transected by pegmatites)	5	Myrmekite around plagioclase, bent twin lamellae in feldspars; quartz with zones of strong U.E. 3°–11°, mortar texture, and deformation lamellae	Strong asterism and polygonization $r = 5°–15°$
Fine-grained dark-red granite SWB-14	Montello, Wisconsin	Uncertain*	9	Some areas with granophyric texture; quartz shows zones of strong U.E. 2°–10°; marginal granulation and a few deformation lamellae; feldspars show bent twin lamellae and inclusions of aggregates of quartz along fractures	Strong asterism and polygonization $r = 6°–15°$
Red gneissic granite SWB-15	Southeast shore of Tyson Lake, north Ontario	Metasomatic (Quirke and Collins, 1930)	4		Strong asterism and polygonization $r = 7°–10°$

* R. C. Emmons, based on unpublished field work.

TABLE 3.—*Concluded*

Specimen	Locality	Geologic origin and reference	Number of quartz grains tested	Petrographic data (U. E. = range of undulatory extinction in quartz)	Quality of Laue pattern (r = length of asterism from the unit rhombohedron)
White gneissic granite SWB-16	Fletcher Bros. quarry, North Chelmsford, Massachusetts	Metasomatic (Currier, 1937; 1947)	7	Feldspars with bent twin lamellae and containing aggregates of quartz along fractures; quartz with strong U.E. 3°–11° and mortar texture; mica with wavy bands and U.E.	Moderate to strong asterism and polygonization r = 6°–10°
Gray granite SWB-17	Mundt quarry, Amberg, Wisconsin	Metasomatic* (granitized greenstone)	9	Plagioclase zoned and has bent twin lamellae; mortar texture in quartz and feldspar; quartz with zones of strong U.E. 2°–10° and deformation lamellae	Strong asterism and polygonization r = 9°–15°
Bluish-gray granite SWB-18	Quincy, Massachusetts	Magmatic (LaForge, 1932; Chute, 1940)	8	Perthite dominant; quartz shows zones of moderate to strong U.E. 2°–9°	Moderate to strong asterism and polygonization r = 5°–11°
Red granite SWB-19	Anderson Bros. quarry, Wausau, Wisconsin	Uncertain* (probably metasomatic)	9	Perthite dominant, plagioclase with bent twin lamellae and U.E.; quartz with zones of mortar texture, deformation lamellae, and U.E. 5°–14°	Strong asterism and polygonization r = 9°–14°
Red granite SWB-20	Wausau granite company quarry, Wausau, Wisconsin	Uncertain* (probably metasomatic)	5	Similar to above with crushing in feldspars; marginal granulation, deformation lamellae, and strong U.E. 6°–10° in quartz	Strong asterism and polygonization r = 7°–11°
Pink granite R14962	Cressbrook Creek near Crow's Nest, Queensland, Australia	Magmatic (sheared phase)	2	Quartz has U.E. 15°–25°, mortar texture, lies in fine-grained fault gouge of quartz-feldspar-mica	Strong asterism r = 7°–15° with incomplete polygonization
Rhyolite A-22-18	Noble's quarry, Marquette, Wisconsin	Volcanic (Chamberlin, 1877)	2	Rounded quartz and feldspar phenocrysts in fine-grained matrix; quartz has U.E. 5°–9° and fractures	Moderate to strong asterism and polygonization r = 5°–9°
Quartz porphyry dike A-14-10	Monterey, Franklin County, Pennsylvania	Magmatic (Bascom, 1896)	4	Rounded quartz and feldspar phenocrysts in fine-grained matrix; quartz has U.E. 8°–15°	Strong asterism and polygonization r = 13°–15°
Rhyolite A-14-6	Thüringer Wald, Germany	Volcanic (flow structure) (Johs, 1933)	5	Rounded and elongated quartz and feldspar phenocrysts in flow structure; quartz is fractured, has U.E. 12°–22°, some recrystallization within grains	Strong asterism and polygonization r = 10°–15°

* R. C. Emmons, based on unpublished field work.

twinning is just as great in deformed magmatic quartz-bearing rocks as in the metasomatic types, which emphasizes the more general influence of the deformation as the cause of the elimination of the twinning.

Correlation of X-ray Study and Microscopic Observations

A close correlation exists between the petrographic features and the X-ray-diffraction patterns. Quartz grains from rock specimens that do not show deformation features give sharp Laue patterns. The first group of the preceding petrographic classification falls into this category. As undulatory extinction develops and becomes stronger, the degree of Laue asterism increases correspondingly, as demonstrated in rocks of the second group. If specimens show strong undulatory extinction and marginal granulation in quartz and bent twinning lamellae in feldspars, the quartz grains give Laue photographs that exhibit both greatly elongated and polygonized asterism streaks. Table 3 summarizes the optical and X-ray results for all samples. This table shows that a particularly good correlation exists between the degree of undulatory extinction and the degree of elongation of the Laue reflection from the unit rhombohedron. These data indicate that undulatory extinction is the optical expression of the effects of plastic deformation.

In terms of the dislocation theory, the crystallites created in a deformed quartz by bend gliding and polygonization are inclined to each other at small angles. This must result in a relative displacement of the optic axes of the subgrains, and the extinction position of the "mother" crystal will therefore vary from one area to another, which accounts for the familiar wavy extinction seen under the microscope. This extinction will sweep across the field of view on the rotation of the microscope stage if the quartz grain is oriented with the axis of bending vertical. For other orientations the sweeping effect will be less noticeable, and the variation in extinction angles will be smaller. Since the misorientation of the crystallites is very small, the bands of undulatory extinction should be, as they are, subparallel to each other, but the departure from this relationship increases with increasing deformation. As the deformation increases in intensity, the extinction bands become regular, narrow, and pronounced. The writers believe that this is a consequence of the greater concentration of the dislocations into walls normal to the bent glide planes, creating elongate polygonized zones or crystallites (Fig. 1*b*). The minute fractures found between the extinction zones in some places may have developed along certain of these sub-boundaries of the crystallites. According to the hypothesis advanced by Sander (1930, p. 175) and later supported by Griggs and Bell (1938, p. 1735), quartz tends to fracture into needlelike fragments during deformation. The crystallite sub-boundaries, which are arrays of dislocations, are potential loci of easy rupture and may be involved in this process. Fracturing and displacement along faults complicate the extinction patterns created by bending and polygonization.

The association of deformation lamellae and strong strain shadows in quartz is in accord with the view of previous investigators (Fairbairn, 1941, p. 1266; Ingerson and Tuttle, 1945, p. 96) that the lamellae occur only in deformed but unrecrystallized rocks. Many of the lamellae are nearly perpendicular to the extinction bands. These may be traces of translation glide planes (Mügge, 1896, p. 769–770; Sander, 1930, p. 178; Hietanen, 1938, p. 34; Fairbairn, 1941, p. 1272–1273). In an attempt to ascertain whether this is the case, two grains from different localities, showing deformation lamellae, were cut from thin sections for X-ray study. The Laue patterns are somewhat more distorted than others from the same rocks, but no evidence indicates whether or not the lamellae represent glide planes. The grains show well-developed *a* axes of bending but no unique glide direction or plane. Fairbairn (1941, p. 1269) and Ingerson and Tuttle (1945, p. 102) state as a result of statistical studies that deformation lamellae have variable orientations relative to the *c* axes of individual grains. The relationship of this irrational orientation of the lamellae to the lack of unique glide direction found in this study is not clear. Possibly the macroscopic lamellae are composed, on an atomic scale, of packets of nonparallel glide planes. If the lamellae do represent such glide surfaces, it may mean that the bending axis is the controlling feature of the deformation and that gliding can occur along a number of directions normal to that axis.

Discussion of Results

Many people have postulated from petrographic evidence that quartz must deform plastically in nature, but attempts to prove it experimentally have not succeeded (Griggs

* R. C. Emmons, based on unpublished field work

and Bell, 1938, p. 1732, 1735). As far as the authors are aware, the present investigation provides the first conclusive X-ray evidence of the plastic deformation of quartz. It also shows that the deformation takes place by bend gliding and polygonization and that one of the *a* axes is always the major axis of bending. No unique glide direction has been found.

Fairbairn (1939a, p. 357) suggested from study of the quartz structure that the horizontal edge [*m:r*] parallel to the *a* axis was the most probable glide line in quartz, because of the presence of rows of oxygen atoms running parallel to this direction, and that no glide plane could be assigned. The results of the present study show that the *a* axis is perpendicular, rather than parallel, to the possible glide lines. Griggs and Bell (1938, p. 1740) pointed out that there is a prominent sheeting of SiO_4 tetrahedra of relatively wide spacing and weak bonding parallel to the unit rhombohedron, and a less prominent one parallel to the basal plane. Hence, gliding along any of these planes in quartz may be structurally possible. These observations have been confirmed by the present authors on a packing model of quartz. Although rows of oxygen atoms parallel the *a* axes, as observed by Fairbairn, the atoms in the rows are arranged in a zigzag pattern rather than in a colinear pattern. This arrangement could offer a barrier to glide parallel to the *a* axis and, indeed, might better function as a hinge line about which bending could take place. There are several parallel chains of oxygen atoms which might serve as easier glide directions. Two such sets of chains look promising, since both are normal to an *a* axis and lie in nearly coplanar sheets of atoms. The most promising direction lies in the unit rhombohedron $\{10\bar{1}1\}$ and the other in the obtuse rhombohedron $\{10\bar{1}2\}$. Gliding along either of these planes would be further facilitated by the sets of channels, parallel to the *a* axes and to the directions [*r:r*], which transect the structure immediately above and below these sheets of atoms.

One of the characteristic features of many metamorphic rocks containing quartz is a high degree of preferred orientation of the *c* axes of the quartz grains. A number of hypotheses proposed to interpret this phenomenon are discussed in detail by Fairbairn (1939b; 1949). Several of these hypotheses call upon plastic deformation in some form as the mechanism responsible for the orientation (Mügge, 1896; Schmidt, 1927; Hietanen, 1938; Anderson, 1948), even though there has been no clear proof of the plastic deformation of quartz before the present study. The evidence presented in this paper for the bend gliding of quartz and its universal presence in rocks of all degrees of deformation short of primary recrystallization must emphasize the possible role of gliding in creating orientation, either directly or indirectly through its influence on the fracturing patterns. As noted previously, strong bend gliding is normally accompanied by polygonization, creating elongate crystallites separated by walls of dislocations which could serve as loci of easy rupture. These directions of rupture would lie perpendicular to the actual glide planes, as yet unknown, and may be additional to those postulated from the structure by Fairbairn (1939a, p. 361) and found experimentally by Anderson (1945, p. 426), Borg and Maxwell (1956, p. 76), and Bloss (1957, p. 218–219). The several glide hypotheses, therefore, may not be independent of the fracture hypothesis. This suggests that a re-evaluation of the various hypotheses of quartz fabrics may be in order, to ascertain whether the mechanism of bend gliding can be integrated with the tendency of quartz to fracture into needles, as postulated by Sander (1930). This re-evaluation should take into account any changes necessary in the glide hypotheses to incorporate gliding perpendicular, rather than parallel, to the *a* axis. Since the present study has been restricted largely to massive granitic rocks with little dimensional orientation (lattice orientation was not studied), it offers little concerning the details of such orientation other than the behavior of quartz under what appear to be less rigorous stress conditions.

A future study of interest would be the determination of the bend axes from oriented quartz sections for which petrofabric diagrams are available. Such a study would have to be restricted to cases where the deformation had stopped short of recrystallization, which would eliminate all trace of the previous bending. Recrystallization has taken place in many of the rocks upon which petrofabric analyses have been made, and there appears to be no way of correlating the resulting lattice orientation with the process of bend gliding, even though there may be a direct relationship. Another factor is that of more than one period of deformation, or of deformation continuing beyond the stage of recrystallization. Turner (1948, p. 566), for example, suggested that a number of examples of observed deformation lamellae in quartz represent only the latest deformation involved and may not be related to the deformation

that brought about the lattice orientation. The same reasoning can be applied to bend axes relative to lattice orientation.

An interesting correlation exists between the reported geologic origins of the rock specimens used in this study and the quality of the X-ray patterns as estimated from the degree of elongation of the Laue reflection from the unit rhombohedron ($10\bar{1}1$) for quartz grains from each rock (Table 3). Of the 55 samples studied, 49 may be assigned a tentative origin on the basis of published and unpublished information.

TABLE 4.—CORRELATION OF ROCK ORIGIN WITH QUALITY OF LAUE REFLECTIONS

Reported origin	Number of samples	Quality of Laue reflections (r = length of asterism from the unit rhombohedron)		
		sharp r = 0°–3°	moderately diffuse r = 4°–6°	very diffuse r = 7°–15°
Metasomatic granites	13	0	8	5
Magmatic granites	7	3	2	2
Other rocks crystallized from a fluid (includes dikes, sills, lava flows, hydrothermal veins, and pegmatites)	21	18	0	3
Recrystallized rocks (includes quartzites, gneisses, and schists)	8	7	1	0

Table 4 indicates that quartz grains from rocks crystallized from fluids tend to give sharp Laue patterns, as would be expected from the mode of origin. The exceptions to this generalization are a quartz porphyry dike near Monterey, Pennsylvania, and two rhyolites, one from Marquette, Wisconsin, and the other from Thüringer Wald, Germany. The deformation of the latter is apparent in the banded structure and elongation of grains. The other two rocks apparently have not been studied in detail, but Gram (1947) has shown that other lava flows of similar Precambrian age in the same area as the Marquette, Wisconsin, rhyolite have been folded intricately subsequent to emplacement. Since the quartz grains of 10 other dikes and sills and 3 other rhyolites give sharp Laue patterns, the 3 exceptions can be accepted as due to the effects of deformation.

Recrystallized metamorphic rocks should also give sharp Laue patterns, since recrystallization obliterates any prior strain in the structure. The 1 exception out of 8 specimens is a facies of the Mississagi quartzite of Ontario which has undergone very little recrystallization.

The quartz grains of 7 probable magmatic granites give Laue patterns with variable degrees of asterism which correlate well with the known structural histories of the rocks. An alaskitic granite phacolith at Hyde School near Gouverneur, New York, is reported by Buddington (1939, p. 292) to show no evidence of cataclastic deformation. The quartz Laue patterns are sharp or show only slight asterism. A fine-grained red granite at Baxter Hollow, Wisconsin, is described by Gates (1942, p. 711) as being introduced late in the history of a cupola which had earlier been involved in folding. The quartz Laue patterns show only slight asterism. Grout (1929, p. 571, 576) reports little indication of dynamic action in the Saganaga granite of Minnesota, but that the whole region has suffered later deep-seated deformation. The Laue asterism is slight to moderate. Moderate asterism is shown by the quartz of both the Nonewaug granite, Connecticut, and the Snowbank Lake granite, Minnesota. Gates (1954, p. 18) believes that repeated movements of varying magnitudes along the fault zone occupied by the Nonewaug granite account for some of the observed textures. This would also account for the moderate asterism. Balk and Grout (1934) mapped the structural features of the Snowbank Lake stock in considerable detail and characterized the intrusion as aggressive with intense deformation and thrusting to make room for itself. They conclude that the dynamic period must have ended about the time of intrusion of the granitic phase of the stock. This presumably explains why the quartz shows only moderate asterism. Extreme asterism is shown by quartz grains from a granite at Cressbrook Creek in Queensland, Australia, and from a granite at Quincy, Massachusetts. The Australian granite was sampled in the shear zone of a fault. The quartz elsewhere in the granite shows uniform extinction. The Quincy granite, as well as the rest of the rocks of the Boston district, was subjected to the severe folding and compressive forces which closed the Paleozoic era in the New England States (LaForge, 1932, p. 72).

The quartz grains of the 13 probable metasomatic granites sampled all show either moderate or extreme asterism. Since deformation is believed to be a part of the metasomatic process

this result may seem expected, but recrystallization is also a part of the same process. Since these rocks are now granites they must have undergone recrystallization to be truly metasomatic. Deformation features found in the quartz may be a result of deformation later than recrystallization or of deformation concurrent with and continuing beyond the state of recrystallization. Quirke and Collins (1930, p. 107) believe that the Tyson Lake, Ontario, gneissic granite underwent deformation both concurrent with and later than the metasomatism. Currier (1937, p. 261) believes that deformation was concurrent in the formation of the North Chelmsford, Massachusetts, gneissic granite, but the relationship to later deformation is still unsolved (Currier, 1947, p. 85). In the cases of the several massive Precambrian granites of north-central and northeast Wisconsin deformation is believed to be largely concurrent with metasomatism, but the detailed deformational history is complex (R. C. Emmons, private communication).

The listing of a granite as metasomatic or magmatic is a controversial issue. The origins given here are based on published and unpublished information available to the writers, without field observations in most cases but with some attempt at discrimination as evidenced by the choice of specimens studied. Enough data have been listed from deformed rocks other than granites, however, to emphasize the point that the experimental data of this paper, both X-ray and optical, are measures of deformation, perhaps aided by temperature, and should not be construed as necessarily dependent on any particular mode of origin of the rock.

Sedimentary petrologists have used the degree of undulatory extinction in quartz as one criterion among others to differentiate clastic quartz grains of igneous versus metamorphic derivation (Gilligan, 1919, p. 260–261; Krynine, 1940, p. 13–20; Siever and Potter, 1956, p. 318). The results of this paper have shown that both igneous and metamorphic quartz can exhibit sharp extinction and that both can exhibit undulatory extinction, depending on the natural history of the rock. The statement commonly found in papers and textbooks on sedimentary petrology that in general the quartz of metamorphic rocks is characterized by marked wavy extinction is of doubtful validity, since theoretically and in practice recrystallized quartz grains have ideally sharp extinction. Marked wavy extinction is characteristic only of deformed rocks, irrespective of mode of origin of the rock. The quartz structure is apparently sensitive to deformation, and wavy extinction cannot be assumed to be a result of regional deformation in the metamorphic sense. The deformation may be regional or local, in the form of stresses during emplacement of an igneous body or of later faulting. There seems to be little justification in using quality of extinction as a criterion of origin.

References Cited

Anderson, E. M., 1948, On lineation and petrofabric structure, and the shearing movement by which they have been produced: Geol. Soc. London Quart. Jour., v. 104, p. 99–132

Anderson, J. L., 1945, Deformation planes and crystallographic directions in quartz: Geol. Soc. America Bull., v. 56, p. 409–430

Balk, R., and Grout, F. F., 1934, Structural study of the Snowbank stock: Geol. Soc. America Bull., v. 45, p. 621–636

Barrett, C. S., 1943, Structure of metals: N. Y., McGraw-Hill Book Co., Inc., 567 p.

Bascom, Florence, 1896, The ancient volcanic rocks of South Mountain, Pennsylvania: U. S. Geol. Survey Bull. 136, 124 p.

Bastin, E. S., and Behre, C. H., Jr., 1939, Origin of the Mississippi Valley lead and zinc deposits, p. 121–143 *in* Bastin, E. S., *Editor*, Contribution to a knowledge of the lead and zinc deposits of the Mississippi Valley region: Geol. Soc. America Special Paper 24, 156 p.

Berg, W. F., 1934, Laue diagrams of deformed crystals: Zeitschr. f. Krist., v. 89, p. 587–593

Bloss, F. D., 1957, Anisotropy of fracture in quartz: Am. Jour. Sci., v. 255, p. 214–225

Borg, I. Y., and Maxwell, J. C., 1956, Interpretation of fabrics of experimentally deformed sands: Am. Jour. Sci., v. 254, p. 71–81

Bradley, C., and Lyons, E. J., 1953, A mode of evolution of a granitic texture, p. 101–110 *in* Emmons, R. C., *Editor*, Selected petrogenic relationships of plagioclase: Geol. Soc. America Mem. 52, 142 p.

Bragg, W. L., 1949, The crystalline state. V. 1, A general survey: London, G. Bell and Sons, Ltd., 352 p.

Buddington, A. F., 1939, Adirondack igneous rocks and their metamorphism: Geol. Soc. America Mem. 7, 354 p.

Buerger, M. J., 1934, The lineage structure of crystals: Zeitschr. f. Krist., v. 89, p. 195–220

Buerger, M. J., and Washken, E., 1947, Metamorphism of minerals: Am. Mineralogist, v. 32, p. 296–308

Burke, J. E., and Turnbull, D., 1952, Recrystallization and grain growth, p. 220–292 *in* Chalmers, B., *Editor*: Progress in metal physics, V. 3: London, Butterworths Sci. Pubs., 334 p.

Cahn, R. W., 1950, Internal strains and recrystallization, p. 151–176 *in* Chalmers, B., *Editor*: Progress in metal physics, V. 2: London, Butterworths Sci. Pubs., 213 p.

Chamberlin, T. C., 1877, Geology of eastern Wisconsin, p. 91–405 *in* Geology of Wisconsin: Wis. Geol. Survey, v. 2, 769 p.

Chute, N. E., 1940, Preliminary report on the geology of the Blue Hill quadrangle, Mass.: Mass. Dept. Public Works Bull. 1, 52 p.
Collins, W. H., 1925, North shore of Lake Huron: Geol. Survey Canada Mem. 143, 160 p.
Collins, W. H., and Kindle, E. D., 1935, The life history of the Sudbury nickel irruptive. Pt. 2. Intrusion and deformation: Royal Soc. Canada Trans., 3rd ser., v. 29, p. 27–47
Cottrell, A. H., 1949, Theory of dislocations, p. 77–126 *in* Chalmers, B., *Editor*: Progress in metal physics, V. 1: London, Butterworths Sci. Pubs., 401 p.
——1953, Dislocations and plastic flow in crystals: Oxford, Clarendon Press, 223 p.
Crussard, C., 1944, Etude du recuit de l'aluminium (à suivre): Revue de Métallurgie, v. 41, p. 111–121
Crussard, C., Aubertin, F., Jaoul, B., and Wyon, G., 1950, Polygonization in strongly deformed metals, p. 193–202 *in* Chalmers, B., *Editor*: Progress in metal physics, V. 2: London, Butterworths Sci. Pubs., 213 p.
Currier, L. W., 1937, The problem of the Chelmsford, Massachusetts, granite: Am. Geophys. Union Trans., v. 18, p. 260–261
——1947, Granitization and its significance as a regional metamorphic process in New England: Wash. Acad. Sci. Jour., v. 37, p. 75–86
Emmons, R. C., 1927, Diabase differentiation: Am. Jour. Sci., 5th ser., v. 13, p. 73–82
——1940, The contribution of differential pressures to magmatic differentiation: Am. Jour. Sci., v. 238, p. 1–21
Emmons, R. C., and Gates, R. M., 1943, Plagioclase twinning: Geol. Soc. America Bull., v. 54, p. 287–304
Emmons, S. F., Irving, J. D., and Loughlin, G. F., 1927, Geology and ore deposits of the Leadville mining district, Colorado: U. S. Geol. Survey Prof. Paper 148, 368 p.
Engel, A. E. J., 1952, Quartz crystal deposits of western Arkansas: U. S. Geol. Surv. Bull. 973-E, 260 p.
Fairbairn, H. W., 1939a, Correlation of quartz deformation with its crystal structure: Am. Mineralogist, v. 24, p. 351–368
——1939b, Hypotheses of quartz orientation in tectonites: Geol. Soc. America Bull., v. 50, p. 1475–1492
——1941, Deformation lamellae in quartz from the Ajibik formation, Michigan: Geol. Soc. America Bull., v. 52, p. 1265–1277
——1949, Structural petrology of deformed rocks: Cambridge, Mass., Addison-Wesley Press, Inc., 344 p.
Frederickson, A. F., 1955, Mosaic structure in quartz: Am. Mineralogist, v. 40, p. 1–9
Frondel, C., 1945, Secondary Dauphiné twinning in quartz: Am. Mineralogist, v. 30, p. 447–460
Gates, R. M., 1942, The Baxter Hollow granite cupola: Am. Mineralogist, v. 27, p. 699–711
——1954, The bedrock geology of the Woodbury quadrangle: Conn. State Geol. and Nat. History Survey Quadrangle Rept. 3, 23 p.
Gates, R. M., and Bradley, W. C., 1952, The geology of the New Preston quadrangle: Conn. State Geol. and Nat. History Survey Misc. Ser. no. 5, 46 p.
Gay, P., Hirsch, P. B., and Kelly, A., 1953, The estimation of dislocation densities in metals from X-ray data: Acta Metallurgica, v. 1, p. 315–319
Gilligan, A., 1919, The petrography of the Millstone grit of Yorkshire: Geol. Soc. London Quart. Jour., v. 75, p. 251–292
Glen, J. W., and Perutz, M. F., 1954, The growth and deformation of ice crystals: Jour. Glaciology, v. 2, p. 397–403
Gram, O. E., 1947, Tectonic features of the Utley meta-rhyolite: Jour. Geology, v. 55, p. 427–438
Griggs, D., and Bell, J. F., 1938, Experiments bearing on the orientation of quartz in deformed rocks: Geol. Soc. America Bull., v. 49, p. 1723–1746
Grout, F. F., 1928, Anorthosite and granite as differentiates of a diabase sill on Pigeon Point, Minnesota: Geol. Soc. America Bull., v. 39, p. 555–577
——1929, The Saganaga granite of Minnesota-Ontario: Jour. Geology, v. 37, p. 562–591
Guinier, A., 1952, Substructures in crystals, p. 402–440 *in* Shockley, W., *Editor*: Imperfections in nearly perfect crystals: N. Y., John Wiley & Sons, Inc., 490 p.
Guinier, A., and Tennevin, J., 1950, Researches on the polygonization of metals, p. 177–192 *in* Chalmers, B., *Editor*: Progress in metal physics, V. 2: London, Butterworths Sci. Pubs., 213 p.
Hall, E. O., 1954, Twinning and diffusionless transformations in metals: London, Butterworths Sci. Pubs., 181 p.
Haworth, E., 1895, Crystalline rocks of Missouri, p. 81–224 *in* Keyes, C. R., Annual Report for 1894: Mo. Geol. Survey, v. 8, 405 p.
Henry, N. F. M., Lipson, H., and Wooster, W. A., 1951, The interpretation of X-ray diffraction photographs: London, Macmillan and Co., Ltd., 258 p.
Hietanen, A., 1938, On the petrology of Finnish quartzites: Geol. Comm. de Finlande, v. 21, no. 122, 118 p.
Hirsch, P. B., 1956, Mosaic structure, p. 236–339 *in* Chalmers, B., *Editor*: Progress in metal physics, v. 6: London, Pergamon Press, Ltd., 354 p.
Iddings, J. P., 1899, The rhyolites, p. 356–432 *in* Geology of the Yellowstone National Park: U. S. Geol. Survey Mon. 32, pt. 2, 893 p.
Ingerson, E., and Tuttle, O. F., 1945, Relations of lamellae and crystallography of quartz and fabric directions in some deformed rocks: Am. Geophys. Union Trans., v. 26, p. 95–105
Irving, R. D., 1883, The copper-bearing rocks of Lake Superior: U. S. Geol. Survey Mon. 5, 464 p.
Johs, M., 1933, Der Granitporphyr von Thal-Heiligenstein im Thüringer Wald: Mineral. u. Petr. Mitt., v. 43, p. 283–318
Keith, H. D., 1955, Lattice spacings in clear crystalline quartz and their variability: Am. Mineralogist, v. 40, p. 530–534
Konobejewski, S., and Mirer, I., 1932, Die röntgenographische Bestimmung elastischer Spannungen in gebogenen Kristallen: Zeitschr. f. Krist., v. 81, p. 69–91
Krynine, P. D., 1940, Petrology and genesis of the third Bradford sand: Pa. State Coll. Min. Industries Expt. Sta. Bull. 29, 134 p.
LaForge, L., 1932, Geology of the Boston area,

Massachusetts: U. S. Geol. Survey Bull. 839, 105 p.

Lindgren, W., 1895, Characteristic features of California gold-quartz veins: Geol. Soc. America Bull., v. 6., p. 221–240

Lonsdale, K., 1945, The shape of reflections on X-ray, single-crystal photographs: Mineralog. Mag., v. 27, p. 112–125

Mügge, O., 1896, Der Quarzporphyr der Bruchhaüser Steine in Westfalen: Neues Jahrb. f. Mineralogie, Beil.-Band 10, p. 757–787

Perutz, M. F., 1949, Polarizing attachment for the microscope of a single crystal X-ray goniometer: Jour. Sci. Instruments, v. 26, p. 127–128

Quirke, T. T., and Collins, W. H., 1930, The disappearance of the Huronian: Geol. Survey Canada Mem. 160, 129 p.

Ransome, F. L., 1911, Geology and ore deposits of the Breckenridge district, Colorado: U. S. Geol. Survey Prof. Paper 75, 187 p.

Read, W. T., Jr., 1953, Dislocations in crystals: N. Y., McGraw-Hill Book Co., 228 p.

Sander, B., 1930, Gefügekunde der Gesteine: Vienna, J. Springer, 352 p.

Sanders, C. W., Jr., 1929, A composite stock at Snowbank Lake in northeastern Minnesota: Jour. Geology, v. 37, p. 135–149

Schmid, E., and Boas, W., 1950, Plasticity of crystals: Trans. from German by F. A. Hughes and Co., Ltd., London, 353 p.

Schmidt. W., 1927, Untersuchung über die Regelung des Quarzgefüges kristalliner Schiefer: Fort Min., Krist. u. Petrographie, v. 11, p. 29–31

Seitz, F., 1952, Imperfections in nearly perfect crystals: a synthesis, p. 3–76 *in* Shockley, W., *Editor:* Imperfections in nearly perfect crystals: N. Y., John Wiley & Sons, Inc., 490 p.

Siever, R., and Potter, P. E., 1956, Sources of basal Pennsylvanian sediments in the Eastern Interior Basin. 2. Sedimentary Petrology: Jour. Geology, v. 64, p. 317–335

Tarr, W. A., 1918, The barite deposits of Missouri and the geology of the barite district: Univ. Mo. Studies, v. 3, 111 p.

Taylor, A., 1952, An introduction to X-ray metallography: London, Chapman and Hall, Ltd., 400 p.

Thomas, L. A., and Wooster, W. A., 1951, Piezocrescence—the growth of Dauphiné twinning in quartz under stress: Royal Soc. London Proc., ser. A, v. 208, p. 43–62

Turner, F. J., 1948, Note on the tectonic significance of deformation lamellae in quartz and calcite: Am. Geophys. Union Trans., v. 29, p. 565–569

Weisz, O., and Cole, W. F., 1948, An improved technique for setting single crystals from zero layer-line photographs: Jour. Sci. Instruments, v. 25, p. 213–214

Wooster, W. A., Wooster, Nora, Rycroft, J. L., and Thomas, L. A., 1947, The control and elimination of electrical (Dauphiné) twinning in quartz: Jour. Inst. Elec. Engineers, v. 94, p. 927–938

DEPARTMENT OF GEOLOGY, UNIVERSITY OF WISCONSIN, MADISON 6, WIS.

MANUSCRIPT RECEIVED BY THE SECRETARY OF THE SOCIETY, MARCH 4, 1958

Short Notes

BULLETIN OF THE GEOLOGICAL SOCIETY OF AMERICA
VOL. 69, PP. 1467-1468, 2 PLS. NOVEMBER 1958

THREE-DIMENSIONAL LIESEGANG RINGS BY DIFFUSION IN A COLLOIDAL MATRIX, AND THEIR SIGNIFICANCE FOR THE INTERPRETATION OF GEOLOGICAL PHENOMENA

BY JAMES D. CARL AND G. C. AMSTUTZ

The phenomenon of periodic precipitation was discovered by the German chemist and photographer R. E. Liesegang in 1896. In his classical experiments a chemical reaction was allowed to take place in a gelatin between potassium dichromate and silver nitrate; silver dichromate was precipitated in concentric rings, separated by areas of no precipitate. These rings form during gradual diffusion of one salt through the gelatin which holds a solution of the other salt. Named after their discoverer, the rings and the processes of their formation appear in the literature as the Liesegang phenomenon.

Liesegang himself, noting the similarity between limonitic banding on weathered rocks and his artificially produced rings, postulated that the modes of formation might be similar (Liesegang, 1913). A mathematical treatment of the Liesegang phenomenon was recently published by Packter (1956). The following experiment was to determine whether or not the same type of ring formation would take place in a colloidal medium (gelatin) which constitutes only a matrix or intergranular film throughout an inactive granular substance (sand grains in this experiment).

The writers followed Liesegang's original instructions in producing the rings in a thin layer of gelatin on glass plates. The most successful experiment of this type was produced by dissolving 1.4 gm of commercial gelatin in 0.06 gm of $K_2Cr_2O_7$ in 60 ml of boiling distilled water. A portion of this solution was poured onto a glass plate and allowed to solidify for about 45 minutes. After solidification, one drop of a solution of 1.7 gm of $AgNO_3$ dissolved in 20 ml of distilled water was carefully placed in the center of the gel, and the glass plate then placed in a closed container. The gel was thus prevented from drying out by creation of a moist atmosphere above it.

Immediately after the drop of silver-nitrate solution was placed on the gelatin, a faint gray corona appeared around the red area formed by the drop and spread out ahead of the slowly developing Liesegang rings. Microscopic examination showed the halolike film to be composed of minute white secondary rings among which the larger primary Liesegang rings arranged themselves in a periodic order. A larger reddish Liesegang ring had the width of three or four secondary rings and was separated from another primary ring by five or six of the secondary ones. Farther from the initial seeding point, the primary rings became less distinct and formed in the secondary rings more or less at random. The secondary rings were whitish and differed in composition from the reddish ones. The coexistence of the two orders of rings has been reported in the literature by several authors and was ascribed to impurities in the gelatin. The formation of Liesegang rings, their width, and rate of formation can be controlled by changing the viscosity of the gel or some other parameter.

Three-dimensional bodies of gelatin were next produced by pouring the gelatin solution containing $K_2Cr_2O_7$ into a mold (a 50-ml beaker) and placing the mold in a pan of cold water to speed solidification. After about 2 hours, the beaker was dipped into hot water, and the gel globule about 4 cm in diameter and 2 cm high was readily removed. This globule was placed in a beaker of silver-nitrate solution (8.5 gm $AgNO_3$ to 100 ml water) and remained there for 26 hours. The beaker was covered to prevent reduction of the silver. At the end of this time the globule had sunk to the bottom of the beaker and was removed, slices cut, and photographs taken (Pl. 1, fig. 1). Perfect layering of the silver dichromate rings was observed, closely resembling the structure of banded agates, jaspers, etc. After obtaining the rings

in completely gelatin bodies, the authors proceeded to determine whether or not these rings would form in three-dimensional globules in which the gel was merely a matrix material.

In this experiment, only the concentration of the gelatin was varied (to 6 gm), and clean, pure quartz sand from St. Peter sandstone was added to the gelatin solution in the mold. This rocklike body consisted of about 80–90 per cent quartz grains and 5–10 per cent gelatin. After solidification, a small sand block was removed and suspended in the silver-nitrate solution with a string to facilitate diffusion on all sides. The same result was obtained as in the colloidal body consisting completely of gelatin; however, the rings were either terminated at the grain boundaries (seen on the two-dimensional section) or, in some cases, deviated around the grains. These observations correspond to observations made on natural rocks, in which the weathering rings of limonite stop at the mineral grains or wave around them (Pl. 1, fig. 2; Pl. 2).

This suggests that weathering rings may actually be caused by the same process: diffusions and periodic precipitation in a colloidal matrix or intergranular film.

The periodic rings in rocks consist commonly of limonite. It is not yet known however whether an iron compound is the diffusing agent or whether something else is migrating and possibly causing a periodic pH change that leads to a strong decomposition of the iron-bearing minerals. A study of many outcrops of exfoliated igneous, sedimentary, and metamorphic rocks and of some 50 examples mentioned in the literature showed that the same periodic rings as pictured in Figure 2 of Plate 1 always accompany exfoliation. A good example of true exfoliation is shown in Plate 2. A forthcoming paper will show in detail and by mathematical treatment (Amstutz and Rivers, 1958) that the Liesegang diffusion phenomenon offers a perfect explanation for true multiple exfoliation and that the old weathering pressure theory has to be abandoned. The terms exfoliation, spheroidal weathering, and spalling are redefined, and it is explained that a pre-existing or a newly growing pressure in a rock can produce only spalling or grain by grain disintegration but not periodic exfoliation.

After the completion of these experiments and the manuscript it was found that Kieslinger (1932) had suggested that exfoliation may be caused by the Liesegang phenomenon. No experiments and no clear division between spalling and exfoliation was found in his or any other papers, however.

References Cited

Amstutz, G. C., and Rivers, J. L., In press, On rock exfoliation and spheroidal weathering

Kieslinger, A. (1932) Zerstörungen an Steinbauten, ihre Ursachen und ihre Abwehr: Leipzig und Wien, p. 57

Liesegang, R. E., 1913, Geologische Diffusionen: Dresden u. Leipzig, Steinkopf, 180 p.

Packter, A., 1955–1956, The Liesegang phenomenon: Jour. Colloid Sci., v. 10, p. 46–62; v. 11, p. 96–106, 150–157

Missouri School of Mines and Metallurgy, Rolla, Mo.

Manuscript Received by the Secretary of the Society, February 20, 1958

Plate 1.—LIESEGANG RINGS

Figure 1.—Silver dichromate layers in gelatin; section through a three-dimensional body. The same layering was reproduced in a gelatin matrix between sand grains making up 80–90 per cent of the body.

Figure 2.—Limonite banding in a weathered volcanic rock, Zona de Carbonera, Peru (sample from Mr. B. Mabire)

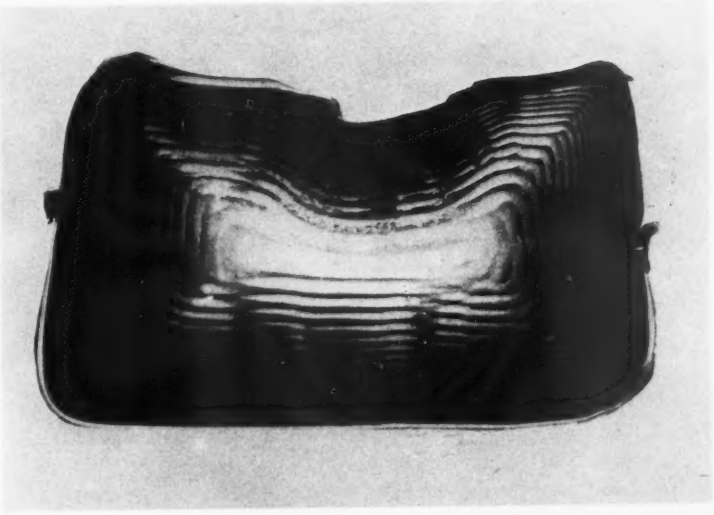

FIGURE 1

FIGURE 2

LIESEGANG RINGS

TRUE EXFOLIATION
Massive granite, 20 miles southeast of Huaraz, Peru. Scale given by grass sheaves

BULLETIN OF THE GEOLOGICAL SOCIETY OF AMERICA
VOL. 69, PP. 1469-1474, 2 FIGS. NOVEMBER 1958

AGES OF MINERALS FROM THE BALTIMORE GNEISS NEAR BALTIMORE, MARYLAND

BY G. R. TILTON, G. W. WETHERILL, G. L. DAVIS, AND C. A. HOPSON

The Baltimore gneiss is generally considered to represent the Precambrian basement upon which the metasediments of the Glenarm series were deposited (Knopf and Jonas, 1929). A recent paper by Wasserburg, Pettijohn, and Lipson (1957), however, indicates a Paleozoic age for biotite from the gneiss. The present work deals with the discovery of Precambrian as well as Paleozoic ages for minerals in the rock.

The Baltimore gneiss domes lie along the axis of most intense metamorphism and injection of the Appalachian orogenic belt. These domes have cores of gneiss and migmatite (Baltimore gneiss) mantled by metasedimentary rocks (Glenarm series) (Fig. 1). Granitic stocks (Woodstock granite, Ellicott City granite) and pegmatite dikes transect the domes and the metasedimentary mantle.

Foliation in the Baltimore gneiss everywhere parallels the contact with the mantle; yet it has been inferred that a major unconformity once existed between them, mainly because of the "much greater deformation and igneous injection of the gneiss as compared with the Glenarm series" (Broedel, 1937, p. 162). Metamorphism and doming of the sedimentary cover were thought to have obliterated the original basement structures and produced a new concordant foliation.[1] If the unconformity existed, two periods of tectonism are implied, one prior to Glenarm sedimentation and another following it. If the unconformity did not exist, a single period of deformation, metamorphism, and injection can explain observed relationships. All previous investigators of the domes favor existence of the unconformity (Knopf and Jonas, 1929; Cloos, 1937; Broedel, 1937), but conclusive proof is lacking.

Eskola concluded that two orogenies are necessary for the formation of mantled gneiss domes. Mantled gneiss domes near Baltimore, Maryland, were cited as implying two orogenies in the central Appalachian region (Eskola, 1949, p. 470). If this hypothesis is true, then the time at which these events occurred would be of great importance in reconstructing the history of the Appalachian orogenic belt, but lack of diagnostic geologic and fossil evidence has made dating uncertain. The later (Glenarm) metamorphism has been regarded as Appalachian (late Paleozoic) but may be much earlier, possibly Taconic (Hess, 1939; 1955). The age of the postulated older orogeny is actually unknown, except that it is probably Precambrian.

The time of the later metamorphism has been clarified by recent investigation of radiogenic (A^{40}/R^{40}) ages of metamorphic minerals in the Glenarm series. Micas from the Setters quartzite, Cockeysville marble, and also from the Baltimore gneiss average 330 million years (Wasserburg, Pettijohn, and Lipson, 1957). Unmetamorphosed pegmatites transecting the Glenarm metasediments give similar ages, thus setting an age of about 300–350 million years for the Glenarm metamorphism.

Rock Description

The sample locations are given in Figure 1. The detailed locations are:

B-2, Towson dome: Roadcut on Charles Street Avenue, Towson, between Malvern and Chesapeake Avenue

B-4, Phoenix dome: Channel change on Piney Creek next to the new U. S. Highway 111, 0.5 mile southwest of Verona. Contact of the gneiss with the Setters quartzite is exposed approximately 200 feet north of where the sample was collected.

B-7, Woodstock dome: Railroad cut a quarter of a mile west of Woodstock (Md. Route 125) along the Baltimore and Ohio railroad.

Samples B-2 and B-4 are fine-grained, foliated, biotite-rich rocks typical of much of the Baltimore gneiss. It is not clear whether this rock, weakly migmatitic at both localities, is of igneous or sedimentary derivation. It is not the distinctly bedded variety considered metasedimentary by Knopf and Jonas (1929, p. 147–150). Both samples consist of granoblastic oligoclase (An_{20}), microcline, quartz, and brown biotite, with accessory apatite, sphene,

[1] This process has recently been shown for the Green Mountain anticlinorium, near Rutland, Vermont (Brace, 1958).

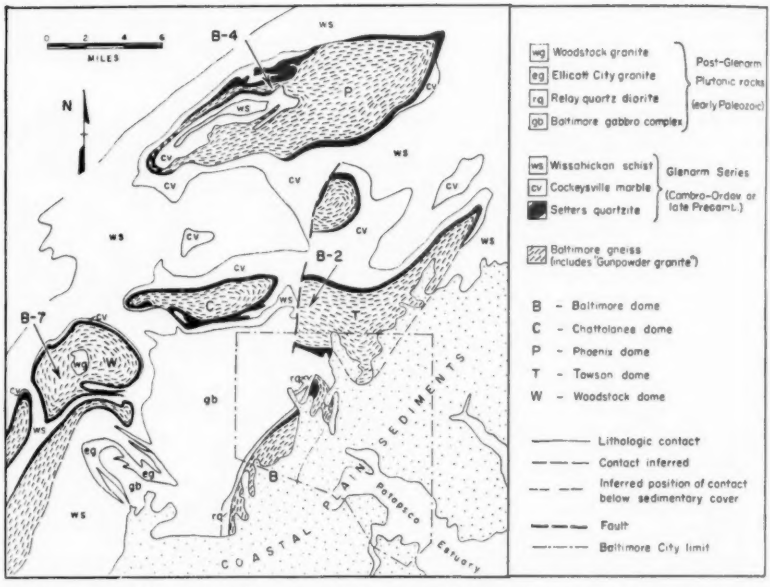

FIGURE 1. GNEISS DOMES NEAR BALTIMORE, MARYLAND, SHOWING LOCATION OF SAMPLES STUDIED

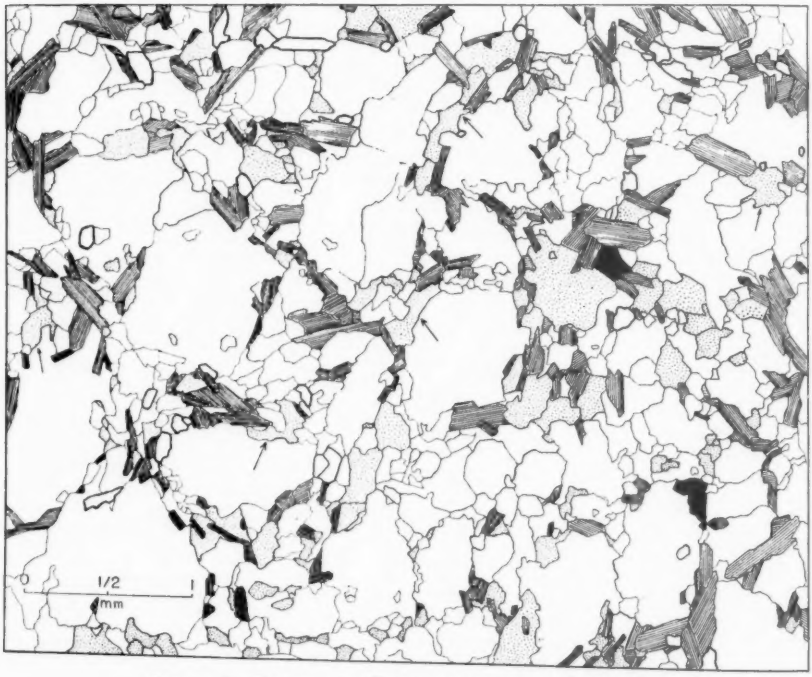

FIGURE 2.—DRAWING OF PHOTOMICROGRAPH OF SAMPLE B-4

Biotite-microcline-quartz-oligoclase gneiss from Phoenix dome, showing textural relations of the microcline. The microcline grains, many having irregular shape and some with delicate projections interlocking with other enclosing minerals, are clearly not detrital relics. Arrows indicate five such grains. Many crystals, shown as a single grain in the drawing, are bent or broken and appear as several smaller grains in the photomicrograph. Microcline shown stippled; biotite ruled; oligoclase and quartz open; magnetite black; and accessory clinozoisite, apatite, and sphene open with heavy outlines. Potassium feldspar grains were identified by staining.

TABLE 1.—ANALYTICAL DATA FOR ZIRCON

Location	Concentration in ppm				Atom per cent abundance			
	U	Th	Pb	Pb^{206}	Pb^{204}	Pb^{206}	Pb^{207}	Pb^{208}
Towson dome	369	134	65.0	55.0	0	100	7.60	10.39
Phoenix dome	678	100	104	91.6	0	100	7.62	5.45

TABLE 2.—ANALYTICAL DATA FOR MICAS AND FELDSPARS

Location	Mineral	Concentration in ppm*				Radiogenic Sr^{87} / Total Sr^{87}
		K^{40}	Radiogenic A^{40}	Rb^{87}	Radiogenic Sr^{87}	
Towson dome	biotite	9.54	0.207	103.6	0.442	0.52
	microcline	15.0	0.293	38.3	0.4	0.008
Phoenix dome	biotite	9.54	.....	188	0.813	0.71
	microcline	14.9	.....	67.4	1.12	0.073
	microcline	15.9	.....	73.3	1.16	0.068
Woodstock dome	biotite	9.26	.....	94.7	0.424	0.46
	microcline	14.58	.....	46.4	0.67	0.023

* The following isotopic abundances were used: $K^{40} = 1.22 \times 10^{-4}$ g/gK; $Rb^{87} = 0.283$ g/gRb; Normal strontium: $Sr^{87}/Sr^{88} = 0.0841$.

TABLE 3.—MINERALS AGES FROM THE BALTIMORE GNEISS

Location	Mineral	Age in million years					
		$\frac{U^{238}}{Pb^{206}}$	$\frac{U^{235}}{Pb^{207}}$	$\frac{Pb^{207}}{Pb^{206}}$	$\frac{Th^{232}}{Pb^{208}}$	$\frac{Rb^{87}}{Sr^{87}}$	$\frac{K^{40}}{A^{40}}$
Towson dome	zircon	1040	1070	1120	940	.....	.....
	biotite	.....	.....	.....	.....	305	339
	microcline	.....	.....	.....	.....	.....	309
Phoenix dome	zircon	960	1020	1120	1100	.....	.....
	biotite	.....	.....	.....	.....	310	.....
	microcline	.....	.....	.....	.....	1190*	.....
	microcline	.....	.....	.....	.....	1130*	.....
Woodstock dome	biotite	.....	.....	.....	.....	305	.....

* For discussion of errors, *see* text.

clinozoisite, allanite, zircon, and magnetite. Biotite forms 20–25 per cent of the rock by volume, and the accessories total less than 3 per cent.

Sample B-7 is a strongly foliated biotite gneiss from the Woodstock dome. Again there is no conclusive proof of either igneous or sedimentary derivation, although the locally abundant garnet would seem to favor the latter. The rock has a seriate granoblastic texture and consists of microcline, oligoclase (An_{14}), quartz, myrmekite, and brown biotite, with accessory

garnet, apatite, sphene, allanite, zircon, and magnetite. Unlike B-2 and B-4 microcline greatly exceeds oligoclase.

The texture of all three samples is clearly metamorphic, with biotite segregated into layers and streaks (not apparent in Figure 2, showing a biotite-rich layer) and quartz into coarse pods or lenses. If the rocks were once igneous they bear no trace of it now: no relict minerals are recognized, no order of magmatic crystallization (based on order of mineral idiomorphism) can be established, and the plagioclases are unzoned. If the rocks were once sedimentary no trace of original detrital grains remains; the feldspar and quartz have delicate interlocking boundaries (Fig. 2) which clearly are not overgrowths.

The status of the zircons is less certain. Knopf and Jonas separated zircons from Baltimore gneiss at two localities and found them to be "rounded and well-worn . . . suggestive of waterborne material" (1929, p. 147–148). These were inferred to be clastic relics in paragneiss. Zircons in thin sections and separates of B-2, B-4, and B-7 mostly have crystal faces, but none has sharp terminations. The rounding may indicate relict detrital grains or metamorphic zircons with poorly developed crystal form.

Results

Age determinations were made on zircon, biotite, and microcline. The analytical data and age results appear in Tables 1–3. The decay constants used in calculating the mica ages are: $\lambda(Rb^{87}) = 1.39 \times 10^{-11}$ yr^{-1} (Aldrich, Wetherill, *et al.*, 1956), $\lambda_\beta(K^{40}) = 4.72 \times 10^{-10}$ yr^{-1} and $\lambda_\epsilon(K^{40}) = 0.583 \times 10^{-10}$ yr^{-1} (Wetherill, 1957). The decay constants used for the uranium and thorium ages are those which are in common use, namely U^{238}, 1.54×10^{-10} yr^{-1}; U^{235}, 9.72×10^{-10} yr^{-1}; Th^{232}, 4.99×10^{-11} yr^{-1}. A value of 137.8 was used for the ratio U^{238}/U^{235}.

The zircon procedures were identical with those described by Tilton *et al.* (1957), and the same uncertainties apply. The isotopic ratios are accurate within 1 per cent, the uranium, thorium, and lead concentrations within 1 or 2 per cent as far as mass spectrometer errors are concerned. As mentioned by Tilton *et al.* there may be a loss of up to 10 per cent of the lead in a zircon to the platinum during fusion. All or part of the discordance in the lead ages in Table 3 may be due to this effect. The Pb^{204} found in the zircon was within the range to be expected from the blanks of 0.3 to 0.5 microgram observed in previous work; therefore, all the Pb^{204} was assumed to be due to contamination, and no Pb^{204} is reported in the zircon in Table 1. The Pb^{206}/Pb^{204} ratios actually observed in the runs were 1100 for B-2 and 2400 for B-4.

The procedures for the determination of rubidium, strontium, potassium, and argon were similar to those described elsewhere (Aldrich, Davis, *et al.*, 1956). The analytical errors in the concentrations of these elements are 1–2 per cent.

Discussion

The biotite in the three gneiss samples has an age of 300–350 m.y. Greatest reliance is placed on the rubidium-strontium ages, giving a probable age of 310 ± 10 m.y. for the mineral. This figure agrees with the potassium-argon ages reported by Wasserburg *et al.* (1957) for mica from the Cockeysville marble, Setters quartzite, and Baltimore gneiss. The ages given by Wasserburg *et al.* were calculated with different decay constants from those used here so that their values must be reduced by 15 m.y. in order to compare them with the present work. The mica-age values clearly date the last recrystallization of these rocks, presumably the time of metamorphism of the Glenarm sediments.

The zircon is definitely older than the biotite. The two uranium-lead ages may be considered concordant for the Towson dome zircon, and slightly discordant for the Phoenix dome zircon. Although the Pb^{207}-Pb^{206} ages agree at 1120 m.y., this is not necessarily the best age value. The half-life of U^{235} is given by Fleming, Ghiorso, and Cunningham (1952) as 7.13 ± 0.16 m.y. The error may be even larger. This uncertainty in the half-life produces an uncertainty of ±25 m.y. in the Pb^{207}-Pb^{206} age. However, an age of 1050–1100 m.y. is favored for the zircon for several reasons. The U^{235}-Pb^{207} age is 1070 m.y. for the Towson zircon, and the Phoenix zircon has a Th^{232}-Pb^{208} age of 1100 m.y. The uncertainty in the U^{235} half-life affects the U^{235}-Pb^{207} age by only ±2 m.y. Thorium-lead ages tend to be too low when they are in error (Tilton *et al.*, 1957). Also the existence of zircon with ages of around 1100 m.y. has been established in other parts of the Appalachian Mountains without resort to the Pb^{207}–Pb^{206} age (Table 4).

Rubidium-strontium age measurements were made on microcline from each dome. Unfor-

tunately, the radiogenic Sr^{87} constituted but a small percentage of the total Sr^{87} in all samples. The Sr^{87} was about 1 per cent radiogenic at Towson, 2 per cent radiogenic at Woodstock, and 7 per cent radiogenic at the Phoenix dome.

m.y. crystallization in the Maryland Piedmont. Two interpretations could be given: (1) The gneiss was crystallized or recrystallized 1000–1100 m.y. ago. (2) The gneiss was originally a clastic sediment metamorphosed 300–350 m.y.

TABLE 4.—MINERAL AGES OF PRECAMBRIAN GNEISSES

Location	Mineral	Age in million years					
		$\frac{U^{238}}{Pb^{206}}$	$\frac{U^{235}}{Pb^{207}}$	$\frac{Pb^{207}}{Pb^{206}}$	$\frac{Th^{232}}{Pb^{208}}$	$\frac{Rb^{87}}{Sr^{87}}$	$\frac{K^{40}}{A^{40}}$
Bear Mountain, N. Y.							
Canada Hill gneiss	zircon	1140	1150	1170	1030	....	....
	biotite	....	....	....	....	900	780
Storm King granite	zircon	960	990	1060	850	....	....
	biotite	....	....	....	....	930	....
Shenandoah National Park, Virginia							
Gneiss, Mary's Rock Tunnel	zircon	1070	1100	1150	1110	....	....
	biotite	....	....	....	....	890	840
Hibernia, N. J.							
Gneiss (dark)	biotite	....	....	....	....	920	....
Gneiss (light)	biotite	....	....	....	....	760	....

The Phoenix dome Sr^{87} is sufficiently radiogenic to permit an accurate age calculation, providing the correction for common Sr^{87} is known. Analytical errors produce an uncertainty of ± 100 m.y., excluding uncertainties in the common strontium correction. Although the radiogenic Sr^{87} in the Towson dome sample is too low to permit a meaningful age calculation, it is of great value in placing a limit on the error which could result from an improper common strontium correction in the Phoenix dome sample. The value used for common strontium ($Sr^{87}/Sr^{86} = 0.709$) cannot be in error by more than 0.8 per cent, and the age cannot be high by more than 100 m.y. because of this uncertainty. The rubidium-strontium age for the Phoenix microcline is fixed at $1200 + 100$ or -200 m.y. This is significantly greater than the age of the biotite and is in agreement with the zircon age. The rubidium-strontium age of the microcline from the Woodstock dome, 1040 m.y., is also greater than that of the biotite, although the strontium is not sufficiently radiogenic for the result to be of much significance.

The zircon and the rubidium-strontium microcline ages evidently record a 1000–1100 m.y. ago, and the zircon and microcline were relict detrital grains eroded from a terrain 1000–1100 m.y. old. The first interpretation is favored, chiefly because of the nonclastic character of the microcline grains. Their irregular shapes, with delicate projections and interlocking contacts with other minerals, were clearly formed during crystallization of the gneiss. Possible detrital origin for the zircon cannot be excluded, although if this were the case a greater age than that of the microcline might be expected. It is concluded that the microcline and the zircon probably record a 1000–1100 m.y. crystallization in the Baltimore gneiss, while biotite records a second crystallization 300–350 m.y. ago. It should be noted that these conclusions allow either a sedimentary or igneous origin for the gneiss.

The lower age of the biotite accords with textural relations in the gneiss. Some feldspar grains, but not all, in the rock display bent and partly obliterated twin lamellae, which evidently record a deformation not completely effaced by recrystallization. All biotite flakes, on the other hand, are unstrained. Penetrative rock deformation normally deforms the delicate mica flakes more readily than the feldspar; it

seems unlikely that rock movement deforming the feldspar would leave the mica unaffected. Where undeformed biotite accompanies bent feldspar grains, as in the Baltimore gneiss samples, the mica flakes were probably completely recrystallized at the time the feldspar grains were chiefly just deformed. If, during formation of the gneiss domes at the time of the Glenarm metamorphism 300–350 million years ago, deformation was so intense that a new foliation formed in the gneiss parallel to its contact with the mantle, then it is surprising that the microcline did not lose its radiogenic strontium.

The potassium-argon age for the Towson dome microcline is 308 m.y., much less than the rubidium-strontium age of the Phoenix dome microcline, and indicates that the mineral lost its argon at the time of Paleozoic metamorphism. This is perhaps to be expected since it is known that feldspars have lost argon even in granites and pegmatites that do not bear evidence of metamorphism since the time of crystallization (Wetherill *et al.*, 1955).

The data presented here substantiate the assignment of the Baltimore gneiss to the Precambrian basement complex and are consistent with Eskola's hypothesis for the origin of these mantled gneiss domes. It is pertinent that in three gneisses and a granite from other locations in the Appalachian Mountains mica gives rubidium-strontium ages of 900 m.y., although the potassium-argon ages are somewhat less. Zircon, where measured, gives nearly concordant age values which indicate an age of 1000–1100 m.y. These age measurements are given in Table 4. The analytical data for these minerals will be published later in an expanded discussion of Appalachian age work. These ages indicate that crystalline rocks with ages of at least 900 m.y. do exist in the Appalachian region. The rubidium-strontium age of 760 m.y. for the biotite from the light gneiss at Hibernia, New Jersey, may indicate that a 900–1100 m.y. old mica lost only part of its radiogenic strontium during Paleozoic metamorphism. The Baltimore gneiss would appear to be a member of this group of rocks, but it was more strongly metamorphosed during the Paleozoic era, causing the biotite to take on a new age.

References Cited

Aldrich, L. T., Davis, G. L., Tilton, G. R., and Wetherill, G. W., 1956, Radioactive ages of minerals from the Brown Derby Mine and the Quartz Creek granite near Gunnison, Colorado: Jour. Geophys. Res., v. 61, p. 215–232

Aldrich, L. T., Wetherill, G. W., Tilton, G. R., and Davis, G. L., 1956, Half-life of Rb^{87}: Phys. Rev., v. 103, p. 1045–1047

Brace, W. F., 1958, Interaction of basement and mantle during folding near Rutland, Vermont: Am. Jour. Sci., v. 256, p. 241–256

Broedel, C. H., 1937, The structure of the gneiss domes near Baltimore, Maryland: Md. Geol. Survey, v. 13, p. 151–187

Cloos, E., 1937, The application of recent structural methods in the interpretation of the crystalline rocks of Maryland: Md. Geol. Survey, v. 13, p. 27–100

Eskola, P. E., 1949, The problem of mantled gneiss domes: Geol. Soc. London Quart. Jour., v. 104, p. 461–477

Fleming, E. H., Jr., Ghiorso, A., and Cunningham, B. B., 1952, The specific alpha-activities and half-lives of U^{234}, U^{235}, and U^{236}: Physics Rev., v. 88, p. 642–652

Hess, H. H., 1939, Island arcs, gravity anomalies and serpentinite intrusions: 17th Intern. Geol. Cong. Moscow, 1937, Rept. 17, v. 2, p. 263–283

—— 1955, Serpentines, orogeny and epeirogeny, p. 391–408 *in* Poldervaart, Arie, *Editor*, Crust of the earth: Geol. Soc. America Special Paper 62, 762 p.

Knopf, E. B., and Jonas, A. I., 1929, Geology of the crystalline rock: Md. Geological Survey, Baltimore County, p. 97–199

Tilton, G. R., Davis, G. L., Wetherill, G. W., and Aldrich, L. T., 1957, Isotopic ages of zircon from granites and pegmatites: Am. Geophys. Union Trans., v. 38, p. 360–371

Wasserburg, G. J., Pettijohn, F. J., and Lipson, J., 1957, A^{40}/K^{40} ages of micas and feldspars from the Glenarm series near Baltimore, Maryland: Science, v. 126, p. 355–357

Wetherill, G. W., 1957, Radioactivity of potassium and geologic time: Science, v. 126, p. 545–549

Wetherill, G. W., Aldrich, L. T., and Davis, G. L., 1955, A^{40}/K^{40} ratios of feldspars and micas from the same rock: Geochim. et Cosmochim. Acta, v. 8, p. 171–172

GEOPHYSICAL LABORATORY, CARNEGIE INSTITUTION OF WASHINGTON, WASHINGTON, D. C.; DEPARTMENT OF TERRESTRIAL MAGNETISM, CARNEGIE INSTITUTION OF WASHINGTON, WASHINGTON, D. C.; GEOPHYSICAL LABORATORY, CARNEGIE INSTITUTION OF WASHINGTON, WASHINGTON, D. C.; DEPARTMENT OF GEOLOGY, THE JOHNS HOPKINS UNIVERSITY, BALTIMORE, MARYLAND

MANUSCRIPT RECEIVED BY THE SECRETARY OF THE SOCIETY JUNE 25, 1958